# Application of unmanned aerial systems for crop discrimination in smallholder farms

**by**

**Pride Mafuratidze**

A thesis submitted to the College of Agriculture, Engineering and Science, at the University of KwaZulu-Natal in fulfilment of the academic requirements of Doctor of Philosophy in Environmental Sciences, under the School of Agricultural, Earth and Environmental Sciences.

Academic Supervisor: Professor Onisimo Mutanga

Professor Mhosisi Masocha

Pietermaritzburg, South Africa

August 2025

## ABSTRACT

Agriculture is the cornerstone of global food security, serving as humanity's principal source of sustenance and the primary supplier of critical crops. A crucial challenge facing society is ensuring food security for a rapidly growing population, projected to exceed nine billion by 2050. With limited opportunities to expand arable land, improving agricultural productivity has become indispensable to meet escalating global food demand. Thus, there is a need for robust, precise, holistic agricultural intelligence systems to monitor and optimise crop production. This is particularly so, in regions characterised by heterogeneous smallholder farming systems dominated by mixed cropping. The ability to identify and monitor individual crop types is fundamental for optimising resource allocation, informing targeted interventions, and ultimately enhancing agricultural productivity. Unfortunately, the use of traditional ground-based methods for crop identification has been deemed labour-intensive, time-consuming, and spatially limited, rendering them inadequate for large-scale or frequently updated crop assessments. Thus, the efficacy of remote sensing technologies has been proven in acquiring synoptic and multi-temporal data that is crucial for agricultural monitoring and management.

Among the suite of remote sensing platforms, unmanned aerial systems (UASs) have garnered significant attention due to their capacity for near-real-time data acquisition at high spatial resolutions. Equipped with increasingly sophisticated yet miniaturised and lightweight sensors, UAS offers a flexible and cost-effective alternative to traditional aerial and satellite imagery, particularly for localised agricultural applications. The advancements in geospatial technologies have facilitated critical data collection on various farm tasks, with crop discrimination and classification as key focus areas. However, despite the evident potential of UAS in agriculture, several bottlenecks have been identified, including lack of comprehensive information regarding optimal UAS configuration, sensor characteristics tailored for specific crop discrimination, and robust data processing and analytical methodologies applicable across diverse cropping systems. Given this background, this study sought to (i) systematically review the current state, challenges and opportunities in the application of unmanned aerial systems for crop discrimination, (ii) determine the optimal field parameters, specifically the number of crop species and crop row widths, that facilitate accurate crop discrimination and (iii) develop techniques that distinguish crop types in a mixed cropping setting, owing to the flexibility and cost-effectiveness of UASs particularly for localised agricultural applications.

This thesis addresses the overarching challenge of achieving accurate and reliable crop discrimination, explicitly focusing on the prevalent mixed-cropping system of maize (*Zea mays*) and soybean (*Glycine max*), which are of significant economic and nutritional importance in regions of sub-Saharan Africa. The thesis focused on multiple investigations employing a range of remote sensing data modalities and analytical techniques to tackle the complexities inherent in distinguishing spectrally and structurally similar crops within heterogeneous agricultural environments. The first objective was to systematically review the current state, challenges and opportunities in the application of unmanned aerial systems for crop discrimination. This was followed by examining the spectral separability of maize and soybean across different growth stages using hyperspectral data. Thirdly, the thesis evaluated the utility of spectral, textural and morphological features derived from UAS-based RGB imagery to distinguish maize and soybean from other objects. This was followed by developing a novel technique for shadow detection in RGB datasets. Lastly, the thesis developed a hybrid approach by integrating segmentation and pixel-based classification to provide a comprehensive understanding of effective remote sensing strategies for enhanced crop discrimination in mixed-cropping systems. The ultimate goal is to contribute to advancing precision agriculture practices, particularly in resource-constrained settings, where accurate and timely information on crop distribution is paramount for sustainable agricultural development.

This explores different facets of crop discrimination in mixed-cropping systems, which are a characteristic of smallholder farming systems in most developing countries. The second objective sought to investigate the spectral separability of maize and soybean at different phenological stages based on field experiments. To achieve this, hyperspectral data spanning the visible to near-infrared spectrum (400–1100 nm) were employed to evaluate the spectral signatures of these two crops across five critical growth stages. The integration of statistical analysis (ANOVA), distance (Jeffries-Matusita distance) and divergence metrics (Transform Divergence, Kullback-Leibler Divergence), and machine learning algorithms (Partial Least Squares-Discriminant Analysis (PLS-DA)) provided a robust framework for optimising band selection and identifying critical phenological stages for discrimination. The key findings of this study revealed that peak spectral separability occurred during the reproductive stages (85–110 days after planting), with the red spectral region (600–700 nm) exhibiting maximum divergence, attributed to differences in chlorophyll dynamics. Notably, PLS-DA achieved near-perfect classification accuracy (100% F1-score) at the mid-grain filling stage (DAP 85), highlighting the efficacy of leveraging red-edge (680–750 nm) and near-infrared (700–1100 nm) bands during this period. Conversely, minimal separability was observed during early vegetative stages due to spectral overlap. This research underscores the need to consider phenological timing and specific spectral regions for effective crop discrimination using hyperspectral data, offering valuable insights for designing targeted remote sensing surveys.

The third objective leveraged the increasing accessibility and affordability of UAS-based RGB imagery to evaluate the utility of spectral, textural, and morphological features for distinguishing maize and soybean in a mixed-cropping environment. High-spatial-resolution RGB images were captured during the tasselling stage of maize (48 days after planting) using a DJI Matrice 300 drone. Due to persistent cloud cover and rainfall during the summer, data acquisition was constrained; consequently, only DAP48 observations were obtained during the reproductive and maturity stages. By extracting a comprehensive set of 26 variables encompassing spectral indices, textural features, and morphological transformations, the study employed a random forest (RF) algorithm for supervised classification. The results emphatically demonstrated the superior performance of morphological features, achieving the highest classification accuracy (0.93) and F1-score (92%), followed by a combination of textural and morphological features. Spectral features alone proved to be the least effective. Morphological features, capturing canopy structure and plant geometry, outperformed spectral and textural traits, highlighting the limitations of spectral-only approaches in mixed-cropping systems. Although these features focusing on the structural and geometrical features of maize and soybean were successful, the results revealed that RGB datasets in smallholder farms were compromised by shadows, which disproportionately increase spectral overlap.

To address the problem of shadows that are prevalent due to mixed cropping with varying plant heights, particularly in smallholder farming systems, the fourth objective developed a novel hue-intensity-green-blue (HIGB) difference technique. The performance of this new technique was rigorously compared against established methods ($C_3$ and normalised saturation-value difference index) using RGB datasets from experimentally manipulated maize and soybean mixtures. The HIGB technique, based on the differences between hue and intensity and the green and blue channels, consistently outperformed the benchmark models ($C_3$ and NSVDI) across various shadow conditions, achieving overall accuracies ranging from 77% to 95%. This robust performance, even in scenarios with dark or obscured shadows, underscored the practical utility of the HIGB technique for improving the reliability of crop discrimination efforts using RGB imagery. The HIGB technique performs robustly under varying lighting conditions, underscoring its value as a critical preprocessing tool for improving crop discrimination. Furthermore, the thesis proposed an alternative light intensity ratio-based (LIRB) approach for shadow removal using RGB imagery. This method is applicable in areas where shadow pixels are sparse; however, it did not fully meet expectations. The approach struggled to reconstruct or eliminate dense shadows, resulting in the introduction of blurry artefacts. These artefacts significantly compromised the overall objective of accurately detecting actual crop acreage within a mixed cropping system.

By understanding the limitations of LIRB, the last chapter focused on developing a hybrid classification framework integrating region-based segmentation and pixel-based machine learning. This approach was proposed to tackle the spectral and structural complexity of heterogeneous agro-ecological landscapes by focusing on vegetation pixels only. This method leverages simple linear iterative clustering (SLIC) superpixels to group spectrally similar pixels into meaningful and targeted regions, followed by extracting texture and structural features from these segments. These multi-faceted features were then used to train robust machine learning classifiers: Random Forest and Extreme Gradient Boosting. The experimental results demonstrated remarkably high detection accuracy, with precision, recall, and F1-scores exceeding 0.98 for both classifiers. Feature contribution analysis revealed that mean intensity and standard deviation features derived from SLIC were the most influential, followed by textural and morphological traits. Integrating diverse features substantially reduced error rates from 8% (SLIC-only) to 1% with multi-feature integration, demonstrating the synergistic benefits of combining segmentation, feature fusion, and ensemble learning. This research strongly suggests the benefits of employing such a robust hybrid approach, combining the strengths of segmentation and pixel-based methods and advanced machine learning classifiers to achieve scalable and high-resolution crop mapping in complex agricultural environments.

In conclusion, these findings provide actionable strategies for mapping and monitoring crops in smallholder systems, where technical and financial constraints limit multispectral adoption. By prioritising accessible RGB sensors, simple algorithms, and phenological timing, this work supports scalable precision agriculture in developing countries, ultimately aiding food security and sustainable land management. The research highlights the importance of considering the phenological stage and leveraging specific spectral regions, as demonstrated by the hyperspectral analysis. It also underscores the significant role of morphological features derivable from UAS-based RGB imagery for effective crop differentiation. Finally, the

proposed hybrid segmentation-classification approach showcases the potential for integrating diverse features and advanced machine learning algorithms for achieving high accuracy in heterogeneous landscapes. The collective insights from these investigations contribute significantly to precision agriculture, offering valuable methodologies and findings that can be further developed and implemented for improved crop monitoring and management, especially in resource-constrained agricultural systems prevalent in regions like sub-Saharan Africa (SSA) and similar environments worldwide. Future research should focus on translating these ground- and UAS-based insights to satellite platforms, enabling broader regional scalability while maintaining accuracy in complex cropping systems. Further research could also focus on integrating these diverse approaches, exploring the transferability of these techniques across different crop types and geographical locations, and developing user-friendly tools for practical implementation by agricultural stakeholders.

Keywords: Spectral overlaps; heterogeneous agro-ecological landscapes; feature extraction; classification accuracy; multi-feature integration

## PREFACE

The research contained in this thesis was completed by the candidate while based in the Discipline of Environmental Sciences, School of Agricultural, Earth and Environmental Sciences of the College of Agriculture, Engineering and Science, University of KwaZulu-Natal, Pietermaritzburg, from January 2021 to May 2025, under the supervision of Professor Onisimo Mutanga and Professor Mhosisi Masocha.

The contents of this work have not been submitted in any form to another university and, except where the work of others is acknowledged in the text, the results reported are due to investigations by the candidate.

Pride Mafuratidze:…… [redacted] ………… Date: 29/08/2025 …………………………….

As the candidate's supervisor, I certify the above statement and have approved this thesis for submission.

Prof. Onisimo Mutanga:……………………… Date: …………………………….

## DECLARATION 1: PLAGIARISM

I, Pride Mafuratidze, declare that:

(i) the research reported in this thesis, except where otherwise indicated or acknowledged, is my original work;

(ii) this thesis has not been submitted in full or in part for any degree or examination to any other university;

(iii) this thesis does not contain other persons' data, pictures, graphs or other information, unless specifically acknowledged as being sourced from other persons;

(iv) this thesis does not contain other persons' writing, unless specifically acknowledged as being sourced from other researchers. Where other written sources have been quoted, then:

a) their words have been re-written but the general information attributed to them has been referenced;

b) where their exact words have been used, their writing has been placed inside quotation marks, and referenced;

(v) where I have used material for which publications followed, I have indicated in detail my role in the work;

(vi) this thesis is primarily a collection of material, prepared by myself, published as journal articles or presented as a poster and oral presentations at conferences. In some cases, additional material has been included;

(vii) this thesis does not contain text, graphics or tables copied and pasted from the Internet, unless specifically acknowledged, and the source being detailed in the thesis and in the References sections.

[redacted]

Signed: Pride Mafuratidze

Date: August 2025

## DECLARATION 2: PUBLICATIONS AND MANUSCRIPTS

1. **Mafuratidze, P.,** Mutanga, O., and Masocha, M. (2024). Application of unmanned aerial systems for crop discrimination in smallholder farming systems: a systematic review of trends, technical challenges and opportunities. *Transactions of the Royal Society of South Africa*, 1–22. https://doi.org/10.1080/0035919X.2024.2409629.

2. **Mafuratidze, P., Mutanga, O, Masocha, M. (in review).** Spectral separability of maize and soybean using hyperspectral data, *Computers and Electronics in Agriculture.*

3. **Mafuratidze, P**, Mutanga, O, Masocha, M and Chivasa, W. (2025). Discriminating maize and soybean in mixed cropping systems using an unmanned aerial systems dataset and random forest. A book chapter (*Springer Nature*).

4. **Mafuratidze, P.,** Mutanga, O., Masocha, M., Dube, T., & Sibanda, M. (2025). Enhancing target crop discrimination: a novel shadow detection technique for RGB datasets in mixed agricultural environments. *Journal of Spatial Science*, 1–16. https://doi.org/10.1080/14498596.2025.2544143

5. **Mafuratidze, P., Mutanga, O., and Masocha, M. (in review).** Enhancing Mixed-Crop Classification in Heterogeneous Agricultural Landscapes by Leveraging Multi-Feature Integration, *ISPRS Journal of Photogrammetry and Remote Sensing.*

[redacted]

Signed: Pride Mafuratidze

Date: August 2025

## DEDICATION

*To the departed soul of my late mother, Rosemary Mafuratidze*

## ACKNOWLEDGMENTS

First and foremost, to God Be the Glory, as I honour You, God Almighty, for taking me this far with all the hardships and trials I have endured to complete my PhD thesis.

As a point of departure, I would like to express profound gratitude to my colleagues, supervisors, friends, and academic and non-academic staff whose guidance, expertise, patience, and unwavering support throughout this energy-sapping research process have been invaluable. Your timely, insightful, and constructive feedback and dedication have shaped this project into a comprehensive and coherent work. This research work coincided with demanding tasks that required utmost attention, but your guidance made the process plausible. I am truly grateful for your mentorship and for pushing me to achieve my best. The support I have received from various individuals and institutions cannot be thanked enough. Without these people's contributions and efforts, this thesis's preparation would not have been possible.

Firstly, I want to thank my PhD supervisors, Prof. Onisimo Mutanga (University of KwaZulu-Natal) and Prof. Mhosisi Masocha (University of Zimbabwe), for invaluable supervision, scientific guidance, critical comments, moral support and the helpful discussions during my PhD journey. Without your fruitful scientific discussions and teaching on how to do science, my scientific reasoning would have been difficult. One aspect I hold dearly from one of your comments *You are just throwing issues that are not directly linked to your findings. Are you on a fishing expedition*? Such statements would encourage me to think before I send any draft to you critically. I am also grateful to the University of KwaZulu-Natal for allowing me to study on one the great universities in Africa.

My deep gratitude also goes to my colleagues at the University of Zimbabwe in the Department Geography Geospatial and Earth Observation: Aldridge Mazhindu, Dr Isaiah Gwitira, Dr Munyaradzi Davis Shekede, Dr Fadzai Zengeya, Dr Tagwireyi, Dr Samuel Kusangaya, Ratidzo Mapfumo, Patience Zirota, Mark Zvidzai, Mathias Ndoro, Beven Mafoko, and homeboy Never Mujere. I must admit that even non-academic staff played an important role, especially when preparing for field work. Special thanks to Felix Chinembiri, Richard Nyambodza, Jacob Funani Rebecca and Mai Matsiya. Thank you, guys, for organising fuel, transport and other logistics related to my field work for data collection.

I am very grateful to all the staff and post-graduate students from the School of Agricultural, Earth and Environmental Sciences (SAEES) and Higher Degrees Office, University of KwaZulu-Natal. This includes Andile Mshengu for all the assistance, especially during registration and other critical assignments I troubled her with. Special thanks to Dr Dadirai Matarira for the encouragement and your moral support. My deep gratitude also goes to friends and post-graduate students in the department: Dr Henry Ndaimani, Dr Terrence Mushore, Dr Collins Matiza, Prof Timothy Dube, Dr Rowan Naicker, Dr Godfrey Mutowo, Dr Walter Chivasa and Dr Mbulisi Sibanda.

Most of this work could not have been possible without the appropriate data. I am grateful to the Department of Research Specialist and Services under the Ministry of Lands, Agriculture, Fisheries, Water and Rural Development, Zimbabwe, especially to Dr Chiduwa and Dr Dhliwayo, for sponsoring all the inputs and a space to conduct our field experiments. I would also want to thank Mr Clever Zvarova, Mr Sibanda, Mrs Zaranyika, Mr Garutsa and Miss Nziramasanga of Panmure Research Station, who assisted with extensive knowledge in agricultural trials and experiments. Acknowledgements are also given to the Zimbabwe National Geospatial and Space Agency, particularly Colonel Gweme, Mr Keen Marozva and Nyasha Siziba for their generous sponsorship of unmanned aerial systems as well as for their contribution to data collection during the conduct of this study.

Finally, I want to thank my relatives, friends, and those I did not mention by name for their patience and moral and mental support during this study.

## TABLE OF CONTENTS

# LIST OF TABLES

**Table** **Page**

# LIST OF FIGURES

**Figure** **Page**

# CHAPTER 1 : GENERAL INTRODUCTION

## 1.1 Introduction

Agriculture is an important driver of economic growth, particularly in developing countries, through the creation of employment and serving as a primary source of income and food production (Onyeaka et al., 2024; Pawlak & Kołodziejczak, 2020; Rafael, 2023; Runganga & Mhaka, 2021; Woodhill et al., 2022). In most developing regions, food systems are heavily reliant on a limited number of staple crops that account for approximately 75% of human caloric intake. Key examples include maize, soybean, rice, and wheat, which are cereal crops that not only serve as dietary staple foods across various global regions but also constitute major sources of calories. In sub-Saharan Africa (SSA) and Latin America, maize (*Zea mays*) is one of the most grown crops, accounting for nearly 60% of total crop production and energy requirements. Similarly, leguminous crops such as soybean, cowpea, mung bean, lima bean, faba bean, etc., are essential because they enhance soil nitrogen content and simultaneously improve farm-level economic returns. These crops are thus indispensable components of smallholder agricultural systems across diverse agro-ecological landscapes.

In most developing countries, a major future challenge is ensuring food security for a continuously expanding global population. With rising population pressures and fragmented landholdings, the potential for cropland expansion remains extremely limited. Consequently, the growing demand for food must be met by improving agricultural productivity rather than expanding farmland. Crucially, this challenge must be addressed within the context of smallholder farming systems, which dominate the agricultural landscape in various developing regions. Smallholder farmers represent over 60% of the rural population (Gebregergis, 2016; Shoko et al., 2015). This is particularly true in nations like Zimbabwe, where smallholder farming is the backbone of the rural economy.

Globally, smallholder farms contribute more than 70% of the world's food supply while occupying less than 30% of agricultural land (Mutanga et al., 2017; Rahman, 2014; Stutsel et al., 2021). In SSA, Latin America and parts of Asia, smallholder farms underpin the livelihoods of approximately 2.5 billion people, many of whom rely primarily on subsistence agriculture to meet daily nutritional needs. Despite their critical contribution to food security, smallholder agricultural activities are constrained by limited access to capital, poor infrastructure, retained seed use, inadequate mechanisation, erratic climatic conditions, pest and disease outbreaks, and minimal access to advanced agricultural technologies. Moreover, with rising population pressures and fragmented landholdings, the potential for cropland expansion remains extremely limited. Consequently, the growing demand for food must be met by improving agricultural productivity rather than expanding farmland.

These persistent challenges threaten the broader societal objectives of improving food, income, and nutrition security (Makate et al., 2016; Scoones et al., 2011). In response, smallholders in Zimbabwe have adopted various resilience strategies, including mixed farming, agroforestry, crop rotation, the cultivation of drought-resistant crops, and mixed/intercropping systems (Wolmer and Scoones, 2000; Mwanyumba et al., 2010; Slingerland, 2000; Moyo, 2011). Such adaptive strategies reflect a pragmatic response to biophysical and socio-economic constraints and highlight the cleverness of smallholder systems in confronting complex agricultural challenges.

## 1.2 Mixed cropping systems in smallholder farms

Given the dual pressures of a persistently rising global population and increasingly restricted opportunities for expanding arable land, mixed cropping systems are anticipated to play a progressively vital role in bolstering global food production in developing regions. Within the context of smallholder farming, two predominant cropping strategies are frequently adopted: mixed cropping and inter-cropping (FAO, 2017; Gebregergis, 2016; Handique et al., 2020; Maurice et al., 2015; Richard et al., 2017). For the purpose of this study, both systems will be collectively referred to as mixed cropping. It is defined as the simultaneous cultivation of two or more crop varieties or species on the same land area within a specific period (Figure 1-1) (Gebregergis, 2016; Lobell, 2013). This agricultural practice presents a sustainable and effective strategy for enhancing soil productivity, managing pests and diseases, minimising reliance on chemical inputs, mitigating the risks associated with single crop failure, and stabilising income variability (Lin, 2013). By optimising the utilisation of physical space and temporal resources, mixed cropping maximises production per unit area over time, concurrently enhancing both crop yield and quality (Ndakidemi, 2006). Furthermore, it offers a significant degree of insurance against crop failure and can provide lodging resistance to vulnerable crops. Makate et al. (2016) observed that mixed cropping systems exhibit greater agronomic stability and resilience, notably through the reduction of weed and insect pressures.

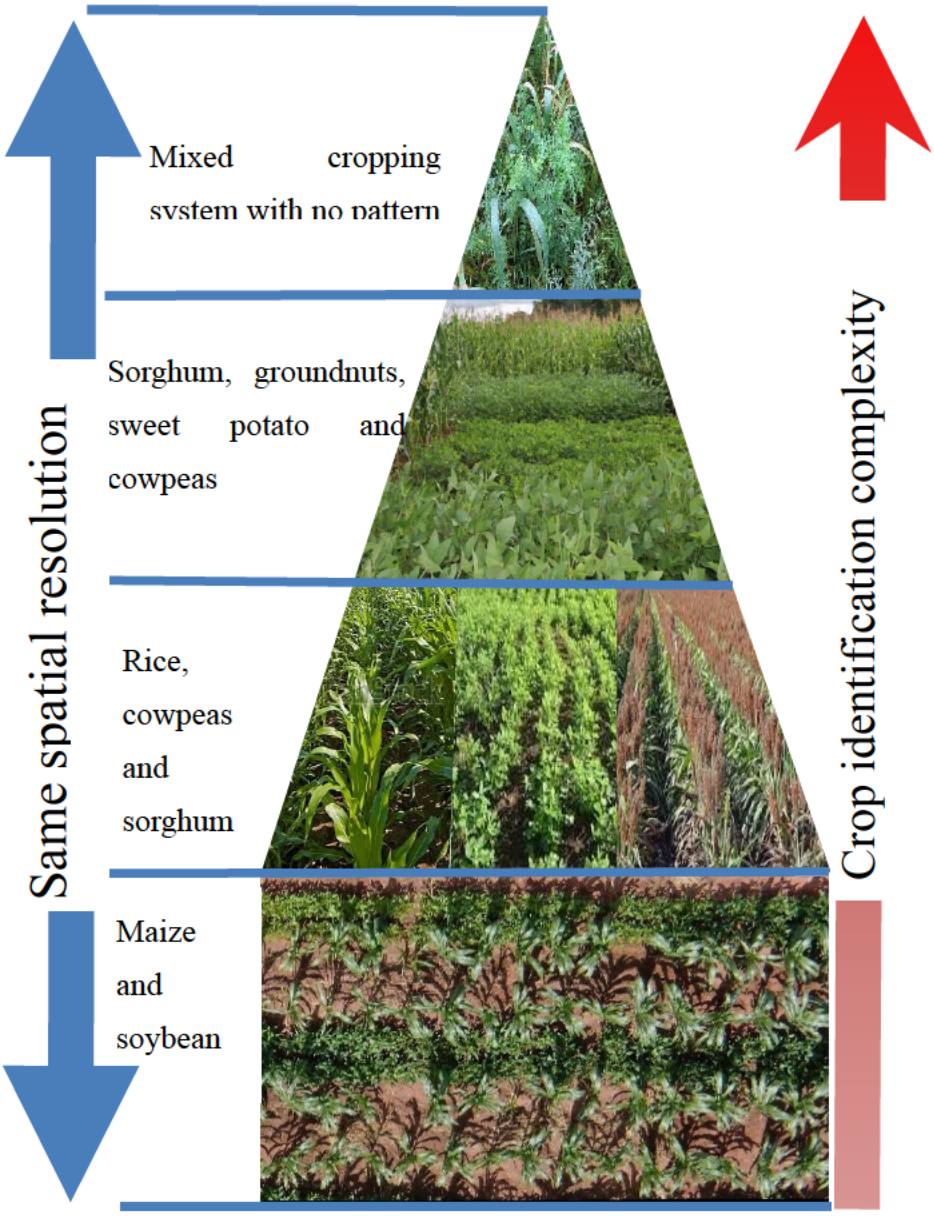


**Figure 1-1: Crop identification complexity at the same spatial resolution. From bottom to top, crop mixtures shift from uniform monocultures that are presumed easier to classify, moving to irregular mixed cropping systems that are harder to classify due to increased spectral overlap and canopy variability.**

This system can also contribute to the restoration of soil fertility, as the byproducts and waste material from one crop can facilitate the growth of another. In many smallholder farming systems, various crops may be integrated into mixed cropping practices, influenced by factors such as their economic or nutritional importance and local environmental conditions. Common cereal crops such as maize, sorghum, rice, millet, and wheat are normally mixed together in a single field with leguminous crops such as soybean, groundnuts, roundnuts, and cowpeas. Of particular interest in an African context is the soybean, which is increasingly recognised as a crucial crop for future food security, offering a diversification strategy away from maize monoculture and traditional cash crops like cotton and tobacco (Scoones et al., 2018). Soybean hold a significant socio-economic importance in numerous developing countries, serving as a source of cash income, crude oil, soybean meal for stock feed, and refined cooking oil, while also enhancing the yields of intercropped species and demonstrating competitiveness in global markets (Henrique et al., 2015; Maasdorp & Titterton, 1997; Chisango, 2018). To optimise resource use and enhance production, smallholder farmers frequently interplant soybean with other crops, such as maize, leveraging the legume's capacity to increase soil nitrogen through microbial processing of crop residues. This combination of crops has been shown to produce higher overall grain yields compared to sole cropping (Makate et al., 2016; Ndakidemi, 2006; Ngongoni et al., 2007). Farmers employ various spatial configurations for mixed cropping settings, including planting soybean between rows of maize or dedicating specific field sections to maize and others to soybean monoculture. Diverse crop combinations, such as maize, groundnuts, roundnuts, sorghum, pumpkin, and soybean, may also be planted in varying proportions within the same field, with some farmers adopting row planting while others prefer less structured patterns (Kuri et al., 2014; Maasdorp & Titterton, 1997; Richard et al., 2017; Zhou et al., 2018).

### 1.3 Remote sensing application in agriculture

Effective crop monitoring and management within these complex mixed cropping systems are paramount to ensuring high yields and promoting sustainable farming practices. However, traditional methods for crop mapping and monitoring relying on manual field scouting and visual inspections are often labour-intensive, time-consuming, and prone to human error (Alves et al., 2020; Chandler et al., 2003). These traditional methods are inherently inefficient, often requiring specialised expertise and access to laboratory-based post-processing equipment, thereby limiting their practicality for widespread or timely application in under-resourced environments. A promising approach to address these challenges lies in the transformation of agricultural systems through the integration of geospatial technologies. Remote sensing, being a major element of these geospatial technologies, offers a practical and economical means for mapping and monitoring crops at different scales. This approach provides non-destructive techniques for assessing vegetation conditions and valuable insights into plant health, crop stress, and yield estimation. However, the effective utilisation of remote sensing for crop mapping and monitoring in the diverse agricultural landscapes of Africa presents significant challenges. Consequently, there is a critical need to prioritise the development of reliable agricultural production mapping and monitoring systems tailored to these heterogeneous agro-ecological environments.

Currently, there is an increasing demand for reliable, accurate, and comprehensive agricultural technologies for crop mapping and monitoring. These technologies are valuable input for agricultural management and have found many applications in agriculture, namely, crop acreage (Dadhwal et al., 2002; Löw, 2013; Shoaib, 2023) and yield (Aparicio et al., 2000; Campbell & Fearns, 2018; Ferencz et al., 2010; Rahman, 2014), in a spatially explicit and temporally regular process. Despite remote sensing's crucial role in agricultural monitoring, global trends have shown that traditional crop monitoring methods using satellite imagery and ground surveys struggle to address some challenges, such as crop discrimination in heterogeneous agricultural landscapes.

Freely available satellite imagery, such as Sentinel-2 MSI and Landsat series with 10 m and 30m spatial resolution, respectively, provides consistent coverage but lacks the spatial resolution to discriminate crops within smallholder mixed fields, where intra- and inter-row spacing is typically less than 1 m (Beach et al., 2020; Neetu & Ray, 2019). At 10m spatial resolution, a single Sentinel-2 MSI pixel may encompass multiple crop types, bare soil, and weeds, making spectral separation difficult. Conversely, unmanned aerial systems can achieve ground sampling distances of 5 cm or finer, capturing within-row crop structure and enabling more precise classification. (Prins & Van Niekerk, 2020; Wang et al., 2018).

These satellite datasets are normally interrupted by cloud cover, which frequently disrupts temporal consistency (Aguilar et al., 2015; Bell et al., 2020; Islam et al., 2021). On the other hand, ground surveys, though accurate, are labour-intensive, costly, and impractical for large-scale mapping. This leaves smallholder farmers with inadequate tools to identify and map crop types in these heterogeneous agricultural landscapes. However, spatially explicit monitoring of mixed crop fields requires routinely updated information on the identity of constituent crops and their spatial distribution as input. This underlines the need for developing accurate and effective methods to map crop types and determine their spatial extent using emerging geospatial technologies to serve as a decision support tool.

## 1.4 Unmanned aerial systems (UAS) in agriculture

Given that most agricultural activities are conducted by small-scale private smallholder farmers, there is a substantial demand for affordable, low-cost autonomous platforms that can be deployed to enhance agricultural productivity and operational efficiency. Unmanned aerial systems, commonly known as drones, offer a significant advancement in how agricultural activities are monitored and analysed (Malveaux et al., 2014; Stehr, 2015). The drone technology offers a critical intermediary solution between the broad-scale synoptic capabilities of satellite remote sensing, which lack plot-level precision (Noble & Brown, 2009; Peña-Barragán et al., 2008; Smith & Blackshaw, 2017) and the highly detailed, yet spatially limited, insights provided by ground-based surveys (Table 2-1).

Additionally, unlike satellite imagery, which is constrained by fixed revisit cycles and atmospheric interference, UAS provides on-demand, centimetre-scale spatial resolution, enabling detailed monitoring of crop health and in-field variability. Furthermore, equipped with RGB, multispectral, hyperspectral, thermal and LiDAR sensors, UAS platforms can acquire sub-decimetre spatial resolution imagery, which is highly suitable for plot-level data collection. These plot-level measurements enable the detection and monitoring of crop variability, plant health status, and field conditions at an unprecedented granularity.

Various studies have indicated that relying on satellite imagery for crop discrimination is often constrained by significant delays in data acquisition and availability (Adão et al., 2017), limiting the timeliness of critical agricultural decision-making. Unlike satellite remote sensing, which is also constrained by orbital cycles, weather conditions, and resolution limitations, UAS have been deployed as needed to capture timely datasets for crop mapping and monitoring, including scouting (Ehmke, 2013), spraying (Castaldi et al., 2017; Ehmke, 2013; Meivel et al., 2016; Zhao et al., 2022), and most importantly, health assessment (Mahajan & Raj, 2016), yield estimation (Maimaitijiang et al., 2020), weed (Beeharry & Bassoo, 2020; Lambert et al., 2018; Peña et al., 2013) and disease detection (Amarasingam et al., 2022; Kitpo & Inoue, 2018).

Numerous studies have demonstrated the value of UAS-derived data for improving operational efficiencies, optimising input application, and enhancing overall farm profitability in such contexts. This capacity for rapid, localised deployment is further enhanced by the relatively low cost and accessibility of UAS platforms compared to traditional manned aerial surveys, positioning them as a viable technology for crop mapping and monitoring across phenological stages. Overall, UAS platforms have substantially reduced the costs associated with in-field surveys and manual observational experiments, making them suitable for crop discrimination in a heterogeneous agricultural environment.

### 1.5 Adaptation of UASs for effective crop discrimination in smallholder farms

Smallholder farmers contribute significantly to global food production, yet they remain disproportionately underserved in terms of access to modern agricultural technologies and scientific knowledge (Shoko et al., 2015). Furthermore, in various developing regions, agricultural productivity remains insufficient and inadequate to provide food to their population, primarily due to a lack of reliable crop statistics, particularly in heterogeneous agro-ecological landscapes. To improve the availability of these crop statistics, there is a need for proper management of the infield variations of crops. As such, accurate, reliable, and up-to-date information on infield variation or specific crops in a mixed cropping field is critical for effective resource allocation, yield forecasting, and sustainable agricultural development. Due to the majority of smallholder farmers being poor (Sibanda & Murwira, 2012; Rudel et al., 2016)There is an urgent need to find and adapt precise and cost-effective modern technologies, such as operational UAS systems, that are capable of generating reliable information in complex, mixed cropping environments (Lu & Weng, 2007).

Although remote sensing has been used extensively in developed countries dominated by monoculture (Baret et al., 1987; Marino & Alvino, 2018; Feng et al., 2014; Danner, 2017; Asner, 1998; Melesse et al., 2019; Tian et al., 2011), its application in SSA is constrained by several factors, including small and ill-defined crop boundaries, different cropping systems, spatial heterogeneity of agro-ecological landscapes, and the spectral similarity of co-located crops. These constraints are further compounded by the coarse spatial resolution of widely accessible satellite platforms, such as Sentinel and Landsat. These traditional remote sensing technologies are poorly suited for discriminating crops in fields with high spatial and spectral heterogeneity. As a result, research in crop discrimination needs to focus on low-cost technologies that can be employed to counter the above challenges and reduce spatial uncertainty in crop statistics.

Further complications arise due to environmental variability (Noble & Brown, 2009), spectral similarities (Vaiphasa et al., 2007; Hatfield et al., 2008; Beyer et al., 2015), overlapping phenological stages, and the unregulated number and spatial configuration of crops within a field (Bégué et al., 2018). As illustrated in Figure 1-1, the number of crops in a mixture may vary depending on the growing period of the constituent crops, and there is no limit set on the number of crops that can be grown, leading to convoluted spectral responses that reduce classification accuracy. The application of UASs as a means to identify specific crops in a mixed cropping system requires high accuracy and reliability by the data analysed quantitatively (Arafat et al., 2013; Richard et al., 2017).

Though different methods at a regional scale avail vital information about crop statistics, a number of them are not suitable when trying to understand complex mixed cropping patterns that are usually found under smallholder environments. For use in smallholder environments, there is an extra need to work with data that is affordable, but the spatial resolution is usually coarser and has a problem of mixed pixels. For example, using satellite data from Sentinel and Landsat that have a spatial resolution of 10 to 60 meters with broad spectral bands might not provide desirable crop discrimination accuracy in a mixed cropping field. This occurs due to the inconsistency of pixel sizes of satellite images and patches of mixed crops, due to a considerable limitation of the spatial resolution. As a result, one pixel may have several crops, resulting in mixed pixels, which could affect the accuracy of crop discrimination. Although Sentinel and Landsat series can provide historical data and multispectral imagery, mixed crops in fragmented agro-ecological landscapes are difficult to distinguish from satellite sensors because their spatial resolutions are still not enough for a mixed crop analysis (Yang et al., 2019).

In addition to contributors to the mixed pixel problem, heterogeneity of agro-ecological landscapes, the total number of crops in a field, the cropping pattern, and the field size have an impact when selecting the spatial resolution for discrimination of crops. As can be seen from Fig. 1-1, an increase in the number of mixed crops also implies an increase in the crop identification complexity, and this has an effect on the spectral response within a pixel. As the number of crops increases, the pixel size remains the same, hence creating a mixture of spectral responses, resulting in a mixed pixel problem. In other instances, high spatial resolution sensors are used to provide adequate spatial information of fragmented agro-ecological landscapes, but the problem of different growing stages, the total number of crops in a mixture, and distance between different species of crops is difficult to follow due to high costs and lack of equipment that can be used to handle such data. In such cases, it is crucial to understand the extent of high-resolution sensors that are suitable for the identification of specific crops in a mixed field.

In contrast to satellite imagery, UASs can be adjusted to suit ground and local weather conditions to counter cloud cover challenges and can collect ad hoc data (Yang et al., 2019). Also, the use of UASs in conjunction with cutting-edge machine learning algorithms allows for modest, accurate, and versatile surveillance tools in smart farming (Sandino, Pegg, et al., 2018). Furthermore, UASs have high spatial resolution that ranges from sub-meter to centimetre level, depending on the flight altitude (Yang et al., 2019; Floreano & Wood, 2015; Lausch et al., 2018). UASs equipped with different sensors to collect RGB, thermal, hyperspectral, multispectral, and light detection and ranging (LiDAR) data have been used successfully. Barbedo (2019) used UASs for stress detection and quantification on crops for the management of water, diseases, nutrition deficiencies, and pests, while Chianucci et al. (2016) employed UASs to estimate canopy cover in beech forest using a 16 MP Canon Power Shot/ELPH 110 RGB camera. Matese and Di Gennaro (2018) employed three different sensors (Canon EOS M 10 RGB camera, Tetracam ADC Snap multispectral camera, and a thermal camera FLIR TAU II 320) mounted on a UAS platform to characterise vine vigour, water stress, and missing plants, while others focused on biomass and height in crop plants (Sandino, Pegg, et al., 2018). Hence, UASs offer novel opportunities to discriminate mixed crops with more spatially accurate information.

Although these systems have been used successfully, especially in fields that cover extensive areas with low spatial frequency, there is a need to nurture and improve the knowledge about the discrimination of crops in heterogeneous agro-ecological landscapes using UASs' high spatial resolution data from the affordable RGB sensors. In this study, there were four major obstacles that hindered the accurate estimation of a specific crop area in mixed fields:

- Firstly, we did not know the effect or impact of the total number of crops in a given field on the classification accuracy,
- Secondly, very little is known about the magnitude of mixed crop complexity that can be discriminated using remotely sensed data from UASs,
- Thirdly, there is a lack of knowledge in the quantification of crops in a heterogeneous agro-ecological landscape using remotely sensed data from UASs, and
- Finally, limited research exists that has been carried out to determine what influences the possible discrimination of crops using state-of-the-art machine learning algorithms.

Given the gaps mentioned above, the purpose of this study was to investigate the usefulness of the RGB sensor and to develop techniques that can precisely and accurately identify crop types in heterogeneous agro-ecological landscapes dominated by mixed crops. As such, there was a need to (i) determine the impact of crop diversity on classification accuracy, (ii) examine the limits of UAS in resolving complex crop mixtures, and (iii) determine optimal quantification methods for crops in heterogeneous landscapes.

## 1.6 Objectives of the study

The aim of this study was to develop techniques that attempt to improve mapping and spectral discrimination of maize and soybean in heterogeneous agroecological landscapes. The specific objectives of the study were as follows:

i. To systematically review the current state, challenges and opportunities in the application of unmanned aerial systems for crop discrimination, with a particular focus on smallholder farms and heterogeneous agro-ecological systems.
ii. To investigate the spectral response characteristics of maize and soybean across distinct phenological stages using hyperspectral data, and to determine the stage(s) at which spectral separability is maximised for effective crop discrimination.
iii. To develop and validate machine learning algorithmic approaches for accurately distinguishing crop types in mixed cropping systems using UAS-derived imagery.
iv. To quantify the influence of crop diversity and row spacing on classification accuracy using UAS-based imagery in fragmented agricultural landscapes.
v. To evaluate the efficacy of integrating object-based image analysis with machine learning algorithms in enhancing the classification accuracy of UAS imagery for crop discrimination.

## 1.7 Research Questions

In light of the knowledge gaps highlighted above, this thesis identifies the areas that form the basis for research needs and motivation to address the following key issues with explicit research questions:

i. What is the current state of research on applying UAS in crop discrimination, particularly in smallholder and heterogeneous agro-ecological systems?
ii. How do the spectral responses of maize and soybean differ across various phenological stages, and at which stages do these differences become most significant for effective crop discrimination?

iii. Which algorithmic approaches can be developed to accurately distinguish crop spectral responses in a mixed cropping field using UAS-based imagery?

iv. What are the optimal parameters in terms of crop diversity and row spacing that enable accurate crop discrimination using UAS-derived imagery in fragmented agricultural landscapes?

v. How does the combination of object-based image analysis and machine learning algorithms improve the classification accuracy of UAS imagery for crop discrimination?

## 1.8 Study Area

The study area for this research is located at Panmure Research Station under Shamva District. The district is situated in the Mashonaland Central Province of Zimbabwe, approximately 90 kilometres northeast of the capital city, Harare. The research station is located between 31.623614° and 31.624355°, and between -17.268046° and -17.268073° (Figure 1-2). Shamva District is occupied by both lowland and mountainous regions in the Mazowe valley. The choice of this particular site is because the landscape is characterised by fragmented landscapes that represent different spatial patterns of agricultural production systems in the northern parts of Zimbabwe. The district features both agricultural and mining activities, with heterogeneous field configurations typical of northern Zimbabwe.

In general, the district is one of the warmest in Zimbabwe, with average temperatures typically varying between 12°C to 31°C and rarely falling below 10°C or rising above 34°C (© *WeatherSpark.com*). Unlike most parts of the province, the average rainy season is normally from October to April, which lasts for approximately 6.5 months with a mean annual precipitation of 850mm. These climatic conditions are favourable for most crops, including maize, wheat, rice, cowpeas, soybean and groundnuts. The crops are usually sown between October and January, with the harvests between April and July. Most of the farmers in this region normally practice mixed cropping systems with varying growing periods.

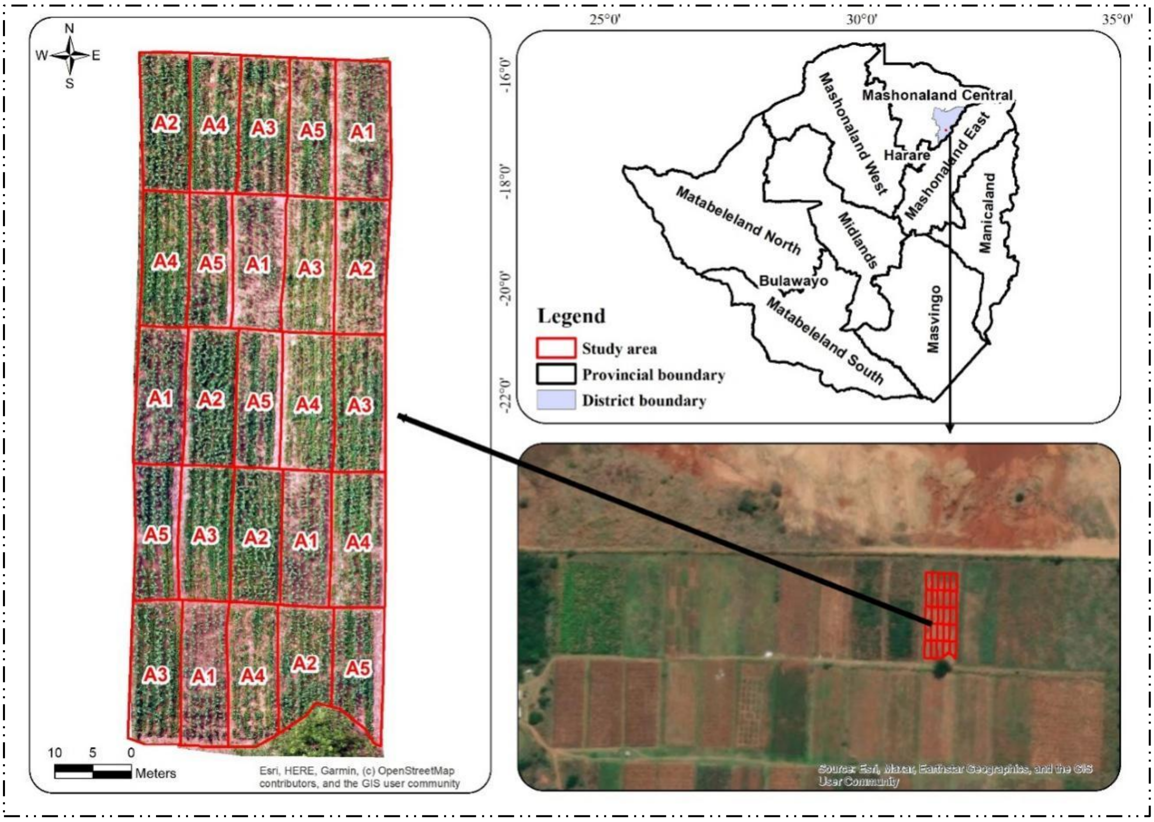


**Figure 1-2: Location of the study area at Panmure Research Station in Shamva District, Zimbabwe**

## 1.9 Outline of Thesis

To achieve the main objectives of this study, the thesis is organised as a collection of 5 papers. Of these 5 papers, two papers have already been published, two are in review, and one is in the preparation phase. In total, this thesis comprises seven Chapters. The first chapter is the general introduction, followed by five chapters that form stand-alone papers, while the last chapter contains a synthesis of the research work. Each Chapter comprises an individual “Introduction”, “Materials and Methods”, “Results” and “Discussion” section. The stand-alone chapters have their own style, according to the corresponding journal. Although attempts were made to conform to a general style in the thesis, there may be some overlapping and repetition in some of the sections. Although the published papers, as well as manuscripts, include other authors, my contribution was greatest and appropriate to being the first author in all cases.

**Chapter One**: Provides the synoptic view of the research background and general statement of the problem, ideas, motives, and justification for the study. It also outlines the objectives and structure of the thesis.

**Chapter Two**: It details a state-of-the-art systematic review of progress on the application of unmanned aerial systems for crop discrimination in smallholder farming systems, focusing on trends, technical challenges and opportunities. The review chapter highlights the challenges faced by technical researchers and smallholder farmers when selecting optimal unmanned aerial systems for crop discrimination in highly fragmented and heterogeneous agricultural landscapes. The factors include drone and sensor characteristics, features, feature extractors, classifiers, feature selection methods and operations procedures. The research gaps and challenges in the application of unmanned aerial systems for crop discrimination in smallholder farming systems are introduced.

**Chapter Three**: The chapter focused on identifying optimal spectral bands and regions for distinguishing between maize and soybean using hyperspectral data. It assessed the discriminating power of hyperspectral data by statistically comparing the mean reflectance of maize and soybean across the 350-1100 nm spectral range, determining wavelengths and spectral regions with significant differences ($p < 0.001$ and $p < 0.005$), and evaluating which band combinations and spectral regions yielded the lowest misclassification rates for crop discrimination. This analysis also sought to pinpoint the specific growth stage(s) where the spectral signatures of these two crops exhibit the greatest degree of separability, thus identifying the optimal time(s) for effective crop discrimination at the leaf level.

**Chapter Four:** This chapter aimed to develop and validate whether a random forest classifier (RF) can accurately distinguish crop types in mixed cropping systems using UAS-derived imagery at the canopy level. In this chapter, the work presented in Chapter 3 is to determine the optimal field parameters, specifically the number of crop species and crop row widths, that facilitate accurate crop discrimination using UAS data and the RF algorithm in fragmented agricultural landscapes.

**Chapter Five:** In this chapter, a novel method for shadow identification and removal was developed using spectral and geometric properties, which significantly enhanced the accuracy of crop discrimination by eliminating the impact of shadows on imagery. A Hue-Intensity-Green-Blue (HIGB) difference technique was proposed to address the shadow effect problem, normally when using RGB data.

**Chapter Six:** This chapter focused on developing a hybrid classification framework integrating region-based segmentation and pixel-based machine learning to tackle the spectral and structural complexity of heterogeneous agro-ecological landscapes. This method used Simple Linear Iterative Clustering (SLIC) superpixels to group spectrally similar pixels into meaningful and targeted regions, followed by the extraction of texture and structural features from these segments. These multi-faceted features were then used to train two machine learning classifiers: Random Forest and Extreme Gradient Boosting.

Finally, **Chapter Seven** provides a comprehensive synthesis of the key findings derived from the study. It presents a critical discussion of the results in relation to the overarching research objectives, highlighting the capabilities and implications of UAS-based crop mapping within smallholder agricultural systems. Additionally, it outlines prospective research directions and methodological advancements necessary to enhance the application of UAS technologies for agricultural monitoring and crop discrimination in heterogeneous agro-ecological landscapes.

# CHAPTER 2 : LITERATURE REVIEW

This chapter is based on:

**Mafuratidze, P.,** Mutanga, O., and Masocha, M. (2024). Application of unmanned aerial systems for crop discrimination in smallholder farming systems: a systematic review of trends, technical challenges and opportunities. *Transactions of the Royal Society of South Africa*, 1–22. https://doi.org/10.1080/0035919X.2024.2409629

**ABSTRACT**

Unmanned aerial systems (UASs) are progressively being employed in an array of agricultural activities, as they come equipped with a controllable platform necessary for near-real-time data acquisition. The UASs are composed of aerial vehicles with mounted small-sized and lightweight sensors. Because of these impressive advancements in geospatial technologies, the collection of important data to achieve various agricultural applications, such as crop discrimination/classification, is increasingly being done using UAS-based remote sensing technologies. While they prove to be cost-effective, autonomous, and flexible in agricultural applications, a key bottleneck in such research was the lack of relevant information relating to UAS types and sensor characteristics, as well as data processing and analytical methods that are applicable for crop discrimination. The review presents the technical characteristics of UAS and sensors and discusses various classification approaches in different cropping systems. Overall, the potential application of UASs for crop mapping and monitoring on heterogeneous smallholder farms is progressing slowly because of technical challenges, operational costs, differing cropping systems, complex classification algorithms, environmental factors, and restrictive policies and regulations, especially in developing countries. Subsequently, research should prioritise developing simple algorithms that can accurately extract crop statistics from high-spatial resolution RGB imagery collected by UAS platforms. This will enable effective mapping and monitoring of crops grown in mixed cropping systems.

Keywords: crop discrimination, mixed cropping systems, smallholder farms, unmanned aerial systems, heterogeneous landscapes

## 2.1 Introduction

Crop discrimination in mixed cropping systems has complex and far-reaching problems in agriculture. They often face challenges in estimating essential statistical information about constituent crops in a mixed-crop approach. As such, remotely sensed data has been accepted as a cost-effective alternative for extracting vital agricultural information. Popular applications of this technology include crop mapping and monitoring, assessment of crop damage, and mapping in-field variation (Candiago et al., 2015; Soria-Ruiz and Fernandez-Ordonez, 2017).

The physical basis for remote sensing is that all vegetation, including crops, contains the same essential components, such as chlorophyll, that influence spectral reflectance (Gracia-Romero et al., 2017a; Hegarty-Craver et al., 2020; Nhamo et al., 2018; van der Merwe et al., 2020). Nevertheless, the spectral curves of various plants exhibit subtle but detectable differences related to variations in leaf pigments, cell structure, and water content (Curran, 1989; Berni et al., 2009; Feng et al., 2022). Under field conditions, the confounding effects of soil reflectance and background noise limit the capability of remote sensing to retrieve desired agricultural statistics from imagery.

Various remote sensing platforms have been employed to acquire the desired information on agriculture; however, each platform has its drawbacks. For example, satellite data needs to be validated via information from other sources, such as ground-based measurements, to be meaningful (Mancini et al., 2019). Also, clouds mainly affect satellite data in the growing season; as such, the usability of the images is limited (Matese et al., 2015). Furthermore, the fixed-time acquisition of satellite data may negatively affect the reliability of the information when monitoring specific phenological stages for target crops. Most importantly, satellites are costly to build, launch into space, operate, and maintain; therefore, it is not effective when targeting small crop fields (Matese et al., 2015; Arafat et al., 2013; Psirofonia et al., 2017).

The critical question arising from the preceding discussion is to what extent recent trends in remote sensing, particularly the increased use of manned aircraft for earth observation, address the above challenges. Table 2-1 shows a comparison of the spatial, spectral, temporal, and flight deployment attributes among various remote sensing systems utilised in crop discrimination. Manned aircraft have inherent advantages, such as increased payload capacity, fine spatial resolution, flexibility, endurance, and the acquisition of images in relatively extensive areas in a short period. This makes them useful in agriculture for the foreseeable future. However, they are costly to operate, coupled with slow information delivery and high operational complexities (Zhang & Kovacs, 2012). Manned aircraft and satellites have low to medium spatial resolution ranging between 0.5 and 60 m (Jensen, 2005; Liaghat & Balasundram, 2010). Such low spatial resolution limits the use of manned craft for identifying crops on smallholder farms. Furthermore, low spatial resolution blurs the image and makes it hard to get detailed information for each crop (Ferencz et al., 2010; Peña-Barragán et al., 2008; Wulder et al., 2009). As such, alternative approaches are required to acquire finer details in line with precision agricultural requirements.

**Table 2-1: A comparison of different types of remote sensing platforms**

| Parameters | Satellites with freely available data | Manned aircraft | UAS | Ground-based |
|---|---|---|---|---|
| Spatial resolution (m) | Low | Medium | High | Very high* |
| Spectral resolution (Number of bands) | <14 | >3 | 4 – 200* | >200 |
| Temporal resolution (days) | Low | High | Very high* | Highest |
| Flight height (km) | >350 | < 30* | < 3 | - |
| Extent ($km^2$) | >1000* | 10 – 100 | 0.1 – 10 | < 0.5 |
| Flexibility (timing) | Very low | Medium | Very high | Highest* |
| Difficulty in the data processing | Medium* | High | Very high | High |
| Viability for minor extents | Negative | Negative | Positive* | Positive |
| Ground coverage | Huge | Intermediate* | Slight | Slightest |

*** Best option for crop discrimination**

Around 2011, the UAS became affordable and easy to operate, which explains why they became an acceptable alternative for satellites and manned aircraft (Frankelius et al., 2019; Radoglou-grammatikis et al., 2020). The improvements in unmanned aerial vehicles' flight times, carrying capacity (payloads), ability to withstand higher wind speeds, and measurement accuracy also contributed towards making UAS a suitable replacement for mapping and monitoring crops at a microscale. Although various UAS suffer from low spectral resolution, they are bridging the current disparity between traditional methods and field monitoring. There is an increasing demand for such UAS systems that acquire images at low altitudes, thereby producing images with high spatial resolution at a relatively low operational cost in near real-time (Hunt Jr & Daughtry, 2018).

Given the challenges above, there is a need to investigate the use of UAS-based remotely sensed data on smallholder farms, mainly focusing on the trends of sensor and camera types, as well as crop discrimination/classification methods. As such, the aim of this paper is to conduct a review of the application of UAS-based remotely sensed data in smallholder farms, focusing particularly on applications directed at extracting specific crop information in mixed cropping systems. This study aims to address the subsequent research questions:

i. Which types of UAS technologies are used in heterogeneous smallholder farming environmental settings, and what suite of characteristics, including the type of unmanned aerial vehicles and sensors, make such technologies relevant?
ii. What is the effectiveness of UAS adoption in crop mapping and monitoring in smallholder farming environments?
iii. What are the existing vital challenges and opportunities for UAS in crop mapping and monitoring?

To address these questions, a comprehensive analysis of the available published literature was carried out. Section 2 reports 1) the techniques used to search for and locate relevant previous studies focusing on databases, and 2) the criteria used to exclude other studies deemed inapplicable. The subsequent sections present current information that includes types, system characteristics, platforms, and payloads of UAS. This article ends by evaluating and interpreting the key results, discussing the current restrictions of UAS, and proposing guidance for future research. The review did not address the history of UAS, since it has been covered extensively in various studies (Radoglou-grammatikis et al., 2020; Tsouros et al., 2019). Instead, our emphasis was on UAS technologies and their application in crop discrimination, particularly on smallholder farms.

## 2.2 Research methodology

This review paper is based on a systematic mapping study (van Tulder et al., 2003) to offer a systematic assessment of the application of UAS in crop mapping and monitoring. As such, we worked on reviewing previous studies systematically to identify the types of UAS technology, the challenges and opportunities, the type of application that is currently being done, and the limitations of the use of UAS in smallholder farms. Using a systematic review approach was preferred since it provided a more extensive inventory of the literature.

### *2.2.1 Literature Search*

To obtain relevant literature, we adopted the Preferred Reporting Items for Systematic Review and Meta-Analysis Protocols (PRISMA 2020)(Page et al., 2021) procedures, as shown in Figure 2-1. An extensive search of various sources of literature was conducted to minimise unbiased samples from both specialist peer-reviewed published and unpublished papers (Onyango et al., 2021; van Tulder et al., 2003) between 2010 (because UAS studies were very few earlier, and this period aligns with the most recent and comprehensive data availability) and April 2023. Search terms or related keyword phrases and controlled vocabulary (Jaén-Carrillo et al., 2020) that complement our topic were derived from the research's primary objective and consultation with experts in the subject area. The carefully selected relevant keywords that constitute parameters of the objective of the study were; i) subject ('drones', 'unmanned aerial vehicles', 'UAV', 'unmanned aerial system', 'UAS'), ii) adjective ('farming', 'small-scale', 'smallholder', 'agriculture', 'crop', 'mixed cropping', 'weed' and 'inter cropping'), and iii) verb ('identification', 'discrimination', 'detection', 'health', 'stress', 'yield', 'hectarage'/'acreage').

Boolean operators 'OR' and 'AND' were employed to reduce false positives (Bramer et al., 2018; Salvador-Oliván et al., 2019). The Boolean operator 'OR' was used between 'drones', 'unmanned aerial vehicles', 'UAV', 'unmanned aerial systems', and 'UAS' since they are used interchangeably in the literature. This was also the same for 'farming', 'agriculture', 'crop', and 'plant'. Keywords such as identification', 'discrimination', 'health', 'stress', 'yield', and 'hectarage'/'acreage' were selected to obtain an overview of crop management strategies using UAS. Most importantly, the authors used interchangeable keywords to obtain the relevant literature for this study. The systematic search targeted the most popular online databases, including Web of Science, Scopus, Google Scholar, and PubMed. The final investigation was done on April 28th, 2023. The search criteria were framed as follows;

> *TITLE-ABS-KEY (((drone* OR "unmanned aerial vehicle" OR UAV* OR "unmanned aircraft system*" OR UAS* OR "remotely piloted aircraft*") AND (classification OR detection OR segmentation OR discrimination) AND (agricultural OR agriculture OR farming OR farmer*))) AND (LIMIT-TO (LANGUAGE, "English")).*

**Table 2-2: Selection criteria for inclusion and exclusion**

| Criteria | Content |
|---|---|
| Inclusion Criteria | papers are written in English |
| | The article was accessible. |
| | must have at least 5 citations for studies conducted in developing countries |
| | only peer-reviewed workshops or conferences, journal papers, or technical reports |
| | Primary research paper |
| Exclusion criteria | not about actual UAS applications for crop discrimination/classification |
| | the paper was not reported in peer-reviewed workshops or conferences or journals or technical reports |
| | abstract, not available |
| | must have at least 10 citations for studies conducted in developed countries and 5 citations in developing countries |

### *2.2.2 Eligibility criteria*

Applying the search string to the selected databases, Web of Science, Scopus, Google Scholar, and PubMed, 2059 records were identified. The results from database searches were imported into Rayyan QCRI (Ouzzani et al., 2016), a free web and mobile application that enables screening and extracting data from many studies for systematic review and meta-analysis using a priori criteria. With the help of the Rayyan QCRI tool (https://www.rayyan.ai/), the authors utilised the tool to remove using inclusion/exclusion criteria, as shown in Table 2-2. Furthermore, the tool was employed to reduce unrelated papers using the exclusion criterion, which requires only reports that focus on UAS applications for crop discrimination in agriculture. A comprehensive analysis was conducted on a total of 83 carefully selected studies to address the research questions, as shown in Figure 2-1. Most of the papers for the analysis were journal articles, with 82%, while conference proceedings accounted for 18% of the total papers.

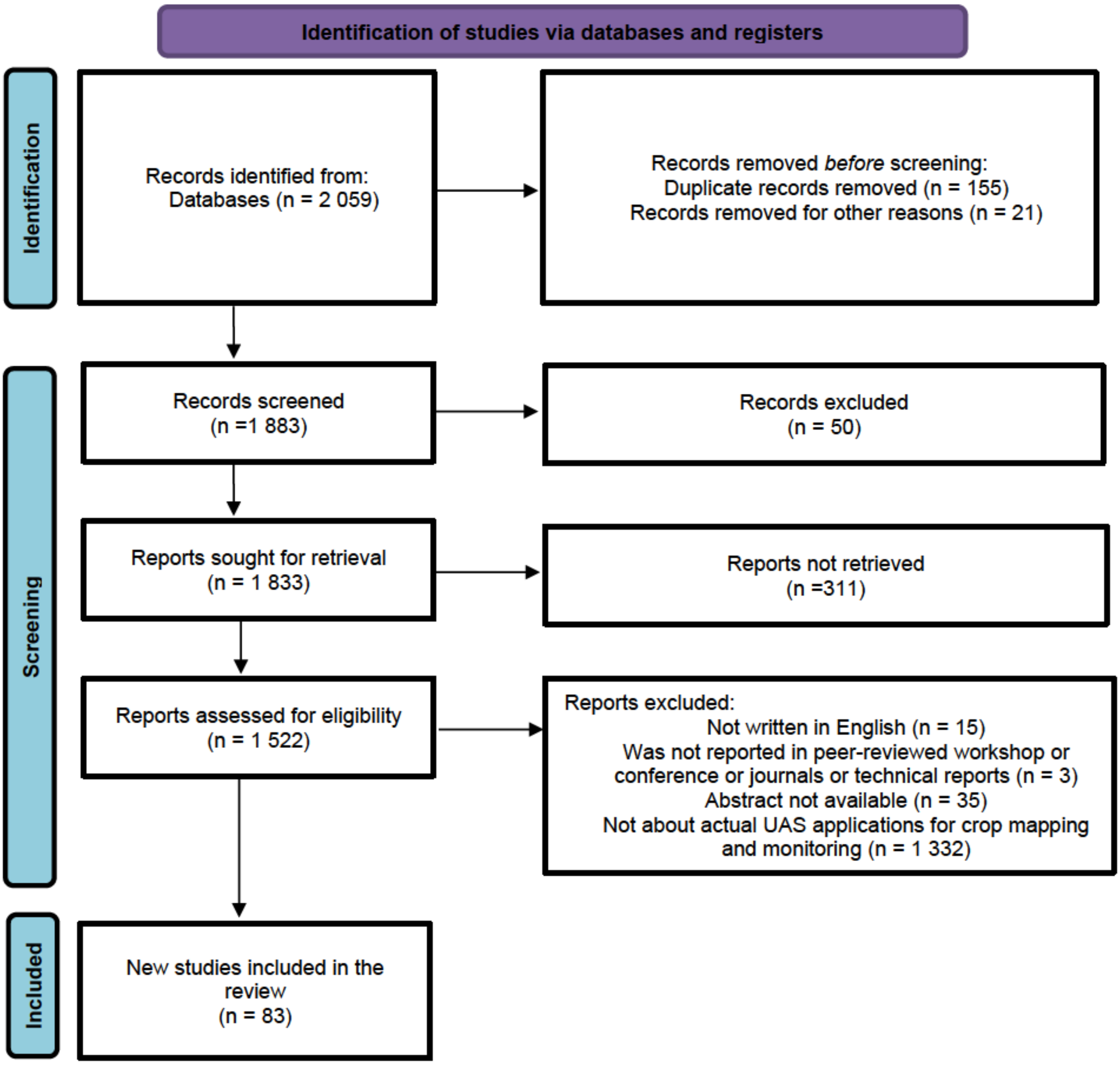


**Figure 2-1: PRISMA flowchart resulting from screening.**

## 2.3 Progress in Using UAS Technologies in Crop Discrimination/Classification

### *2.3.1 Published articles, trends, and keywords analytical outcomes*

UAS systems offer a non-destructive option for obtaining automatic measurements of biophysical and biochemical properties of crops. Characterisation of crops, primarily through analysing spectral responses, has arguably been the most critical application of UAS in agricultural production. The quality of the image or reflectance measured determines whether this application has been a success or a failure. This information acquired by the UAS systems can be used for decision making to mitigate problems encountered. Up to now, UAS systems have become an effective way to produce ground information swiftly and have been successfully employed in crop discrimination. Figure 2-2 shows that there has been an exponential increase in the number of publications in the crop mapping and monitoring field in the last decade. However, the figure depicts a slight decrease in 2019, probably because of the lockdown caused by the outbreak of COVID-19. However, the period between 2020 and 2022 indicates that the publication of articles nearly doubled in contrast to the previous era, except for 2018.

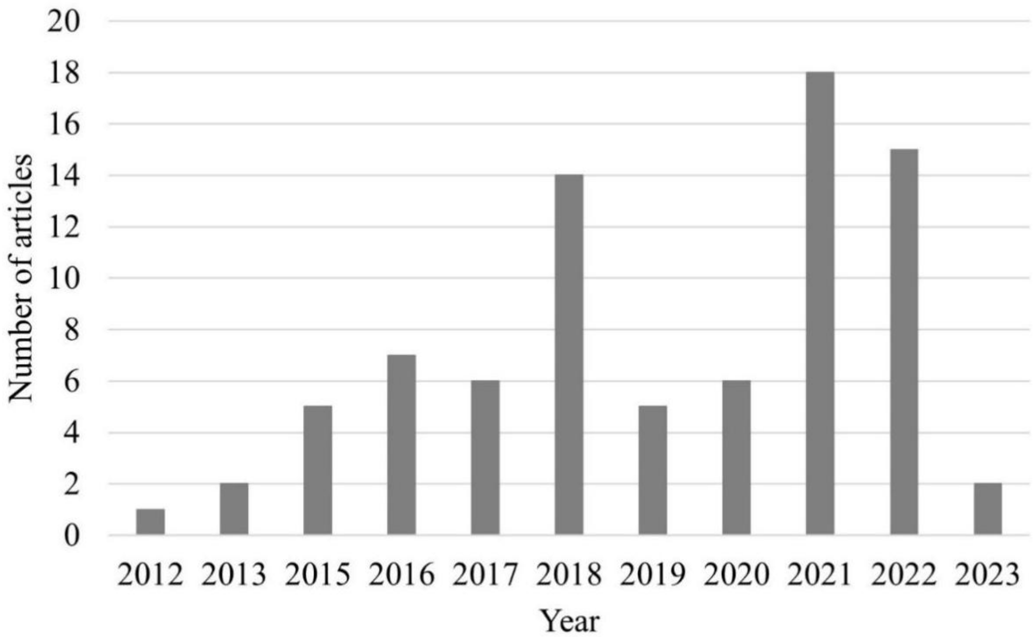


**Figure 2-2: Frequency of published articles on the application of UAS in crop mapping and monitoring.**

To understand the relationship among the selected articles, the articles were subjected to qualitative and quantitative analysis using VOSviewer software version 1.6.20 (https://www.vosviewer.com). The maps created based on bibliographic and text data were carried out to visualise the keyword co-occurrence as well as to analyse the content and connectedness using titles, abstracts and keywords data from the extracted literature (Van Eck & Waltman, 2010).

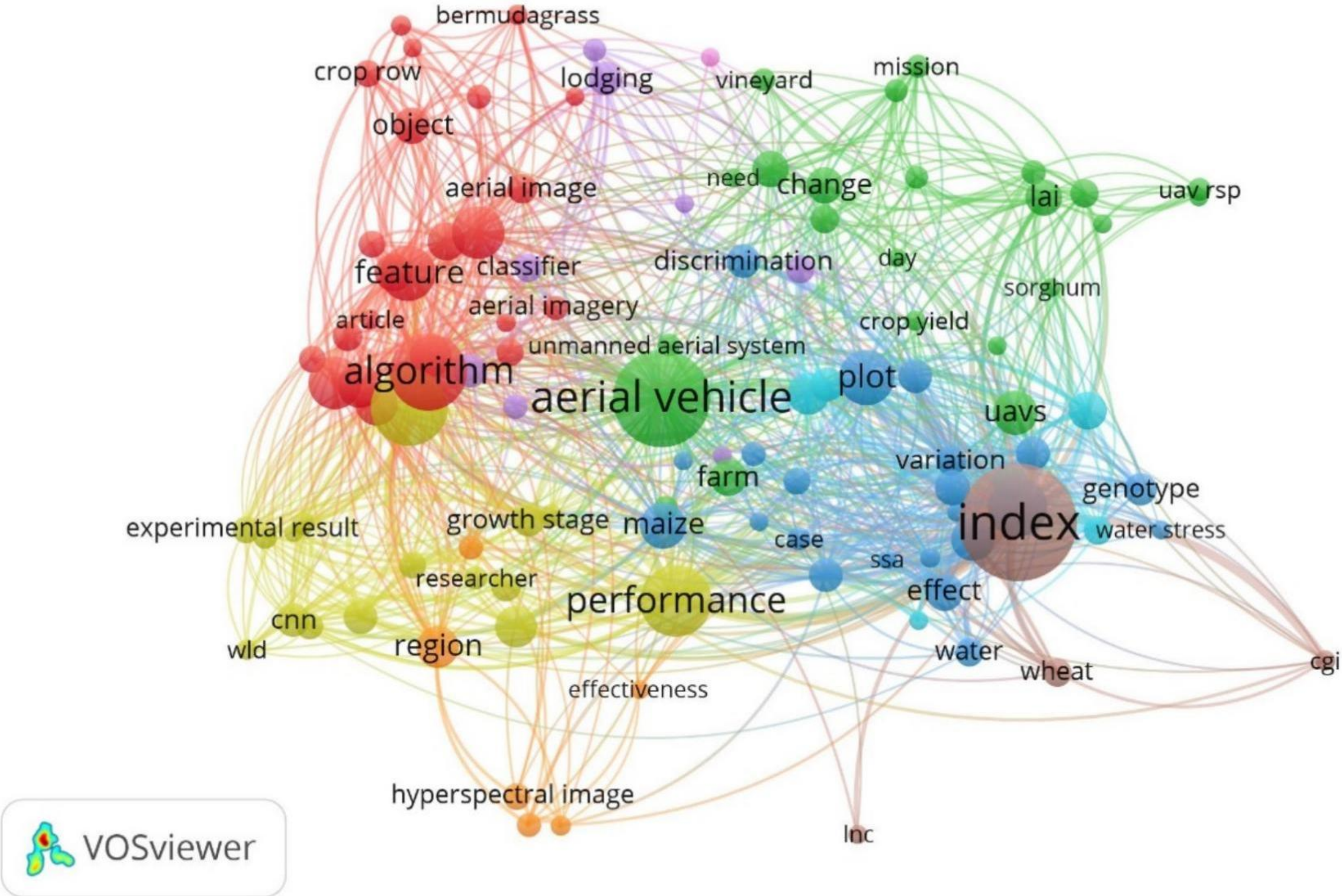


**Figure 2-3: The current perception of crop discrimination of mixed crops in smallholder farms from VOSviewer.**

Using titles, abstracts and keywords in the VOSviewer software to evaluate the current perceptions in crop discrimination under mixed cropping systems, five clusters were produced, as shown in Figure 2-3. The first cluster, which is the red, is characterised by terms such as "crop row", "object", "feature", "aerial imagery", "classifier" and "algorithm". This cluster highlights stages that are critical in crop discrimination, which affect overall accuracy. The second cluster is the green, which consists of "need", "change", "crop yield", "UAV", "sorghum" and "lai" (leaf area index). These linkages demonstrate the need for and effectiveness of unmanned aerial systems in crop discrimination, focusing on changes in spectral responses of important crops. Thirdly, the blue cluster had "maize", "wheat", "variation", "water stress", "effects", "index", "Sub-Saharan Africa" (SSA) and "plot" as its key terms. The information obtained from this cluster shows that there are certain aspects that must be considered or have an effect in terms of crop variation. Each crop species has different biochemical and biophysical characteristics that must be observed. This cluster has also shown that mixed cropping systems are mostly practised in Sub-Saharan Africa. The fourth cluster in orange included key terms such as "region", "effectiveness" and "hyperspectral images", which shows the effectiveness of hyperspectral remote sensing in small regions with high frequency. Finally, the yellow cluster is characterised by key terms such as "experimental result", "growth stage", "performance", and "CNN". These terms relate to the accuracy assessment of algorithms for crop discrimination at various growth stages in an experimental setup.

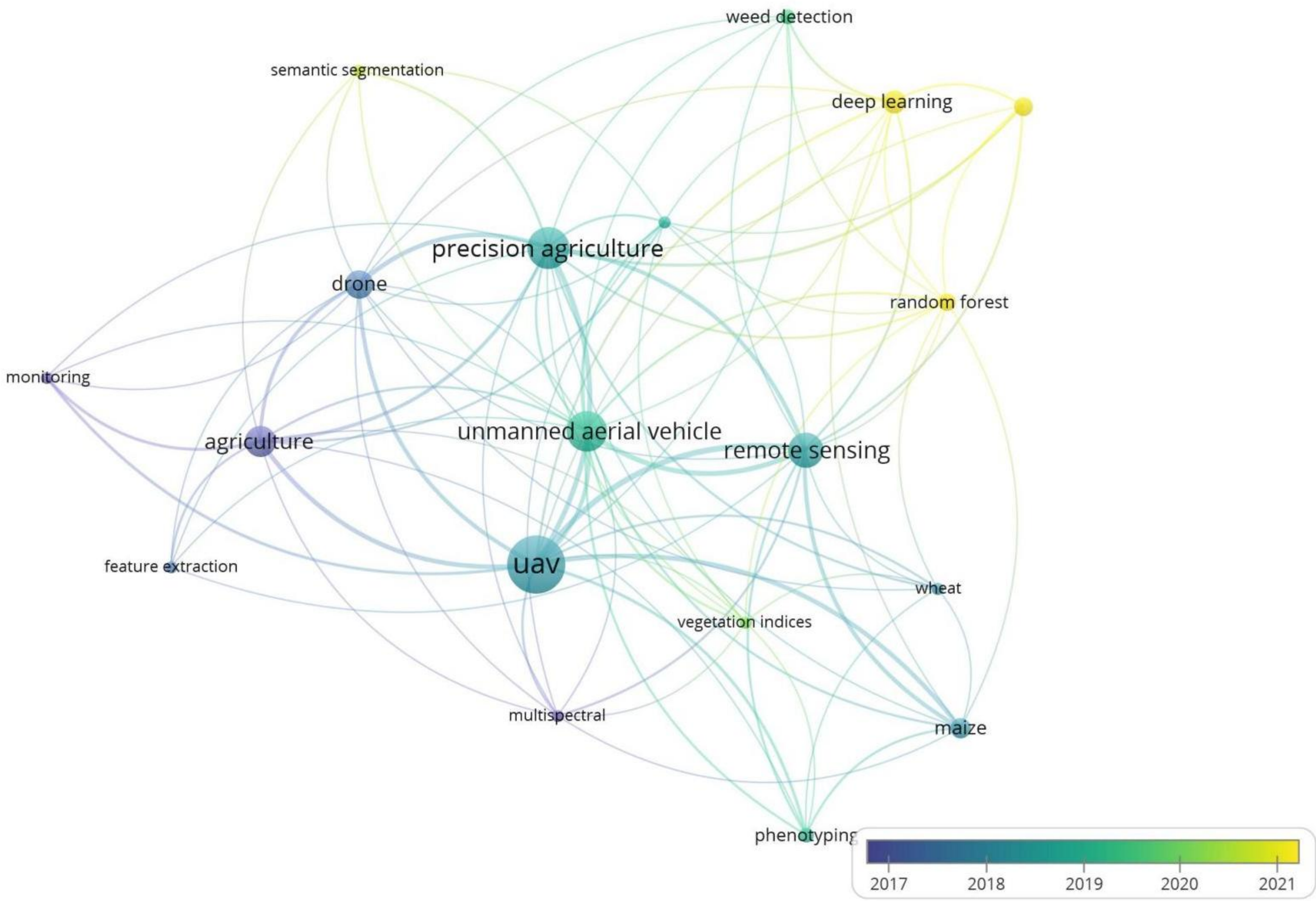


**Figure 2-4: Co-occurrence network of the keywords that appeared at least five times within the final from VOSviewer.**

Figure 2-4 demonstrates that words such as "UAV", "precision agriculture", remote sensing", "agriculture", "maize", "machine learning", "random forest" are among the top ten keywords that were selected with a frequency of ≥5 from 382 keywords. In conclusion, the results from VOSviewer software clusters highlighted key stages for crop discrimination with the presence of keywords from "crop row", "planting methods", "sensors", "crop growth stages", "crop species", "data acquisition", "feature extraction" and "classifiers". It is important to note that, between 2017 and 2021, there is a noticeable change in terms of keywords. The blue cluster between 2017 and 2019 shows that most studies were mainly focusing on crop 'monitoring' using 'feature extracted' from multispectral' sensors. From 2019 to 2021, they shifted to using 'vegetation indices' for 'phenotyping' of 'maize' and 'wheat'. To improve crop discrimination, it is worth noting that between 2021 and 2023, studies were now utilising classification techniques such as 'semantic segmentation', 'random forest', as well as 'deep learning' algorithms.

### *2.3.2 Spatial distribution of published articles*

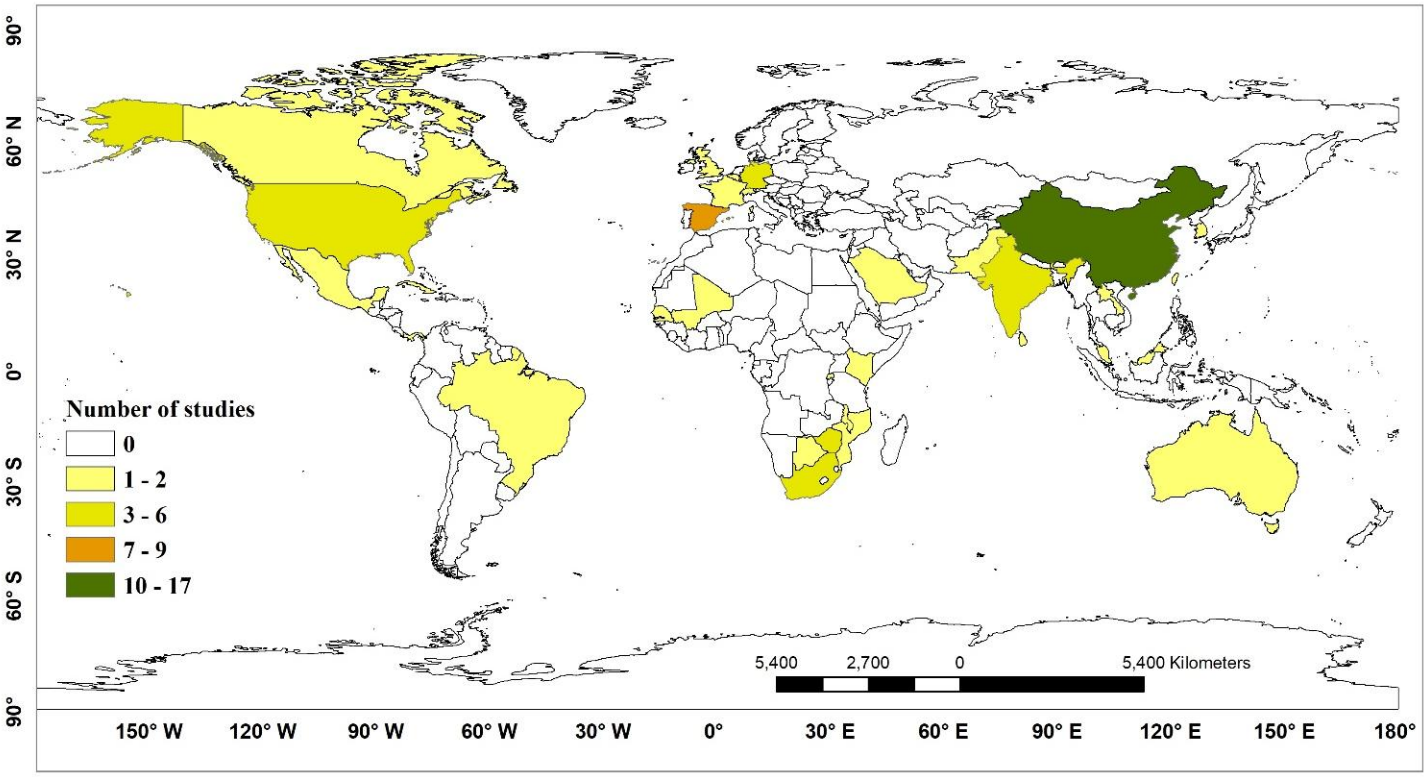


**Figure 2-5 : Worldwide distribution of UAS-based remote sensing studies on crop discrimination at country level (from 2012 to 2023).**

Several studies have been carried out worldwide (Figure 2-5) in applying UAS in agriculture using a wide variety of cameras and sensors, and the results are promising. At a national level, various studies were carried out in thirty-six different countries across the globe. In particular, China had the highest number of published articles, with 21%, followed by Spain (10%). Whereas the United States of America and Zimbabwe had 6%, South Africa (4%), Tanzania and India (3%), Italy, Ghana, Pakistan, Brazil, Spain, Taiwan and the United Kingdom (2%) and the rest had a few studies on crop discrimination. At the continental level, the literature showed that the application of UAS systems had been predominantly in Asia (mainly China and Pakistan) with 35% of the studies, 27% in Africa, 23% in Europe, 10% in North America, 4% in South America and 1% in Australia. Of the 27% of studies conducted in Africa, only three studies explicitly focused on crop discrimination within smallholder farming systems.

Based on the reviewed articles, maize is the dominant crop and was researched by 28% of the total articles. This was followed by rice (8%), wheat (6%), unnamed crops (5%), sorghum (5%), sugarcane (4%), as well as cabbage, olive and pear with 3%. While the rest crops were researched by 1% as shown in Figure 2-6. Overall, cereal crops (maize, wheat, rice and sorghum) have the number of articles since they received substantial attention from the literature. Since most studies were conducted in developed countries, crops such legumes with less attention in terms of cash generation received less to no attention. Furthermore, the findings indicated that 90% of the cropping systems were monocultures, which are limited to developed countries. As a result, the findings show that there are limited to no studies focusing on other cropping systems such as intercropping, mixed cropping, etc.

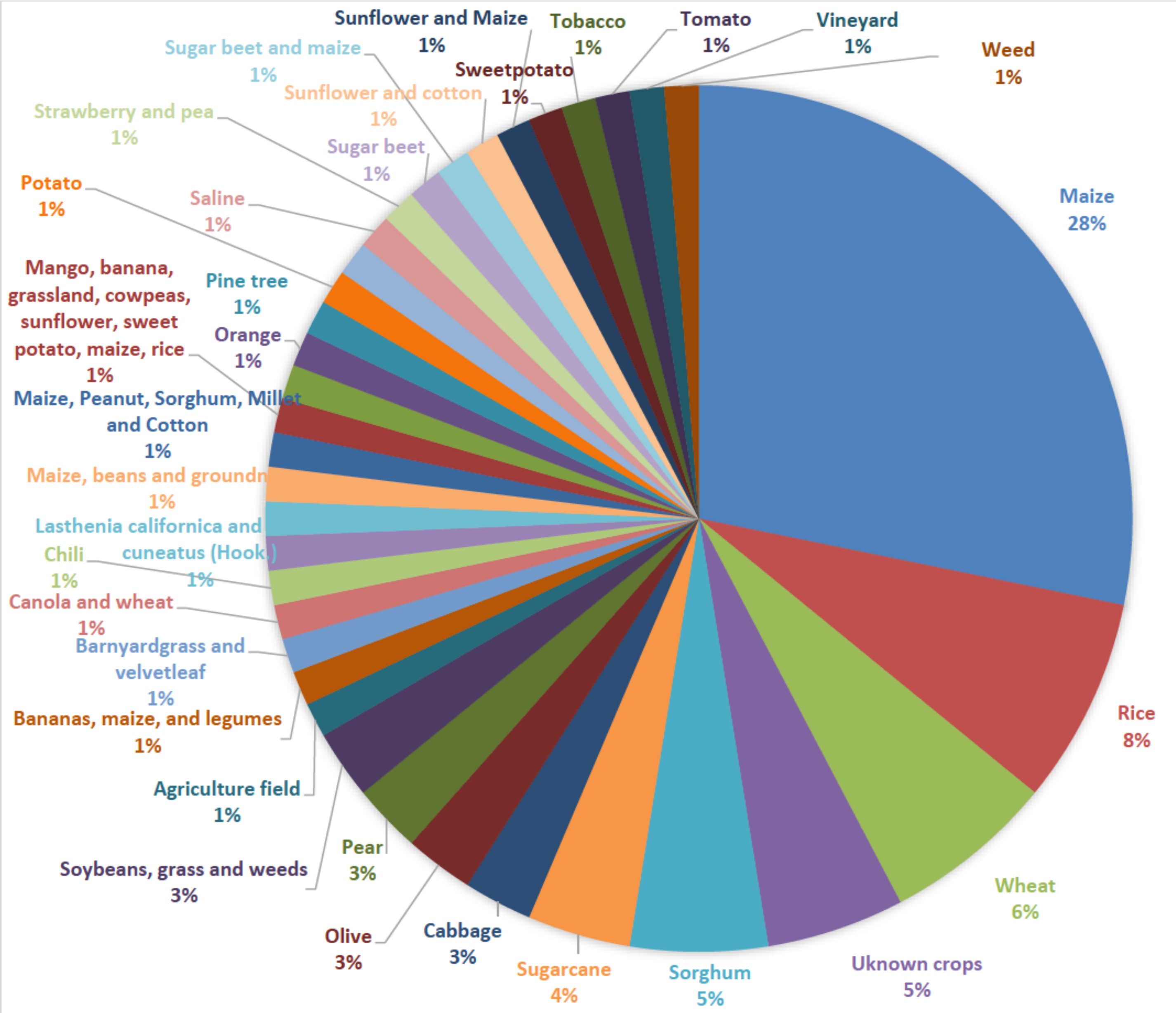


**Figure 2-6: Frequency of articles on crop discrimination.**

### *2.3.3 UAS type and technical characteristics*

The typical UASs deployed for crop mapping and monitoring vary widely in their design (sizes and shapes), depending on their operating platform, mission, and budget. The reviewed articles observed that flight times of various UAS types differ depending on weather conditions, payload, weight, battery capacity, engine fuel, and aerodynamics (Cruzan et al., 2016; de Oca et al., 2018; Hassan et al., 2022; Lambert et al., 2018; Prins & Van Niekerk, 2020; Watts et al., 2012; Zheng et al., 2016). As such, flight endurance varies from a few minutes to several hours.

In that regard, there are numerous UAS types. However, the most common primary types of UAS platforms are rotary-wings and fixed-wings (Figure 2-7), which have prevailed for recent crop mapping and monitoring applications. However, there are also hybrid systems, such as the hybrid VTOL, which is both fixed-wing and multirotor but has rotary and fixed-wing characteristics. These systems are not covered in this review, since they are far less frequent in most studies.

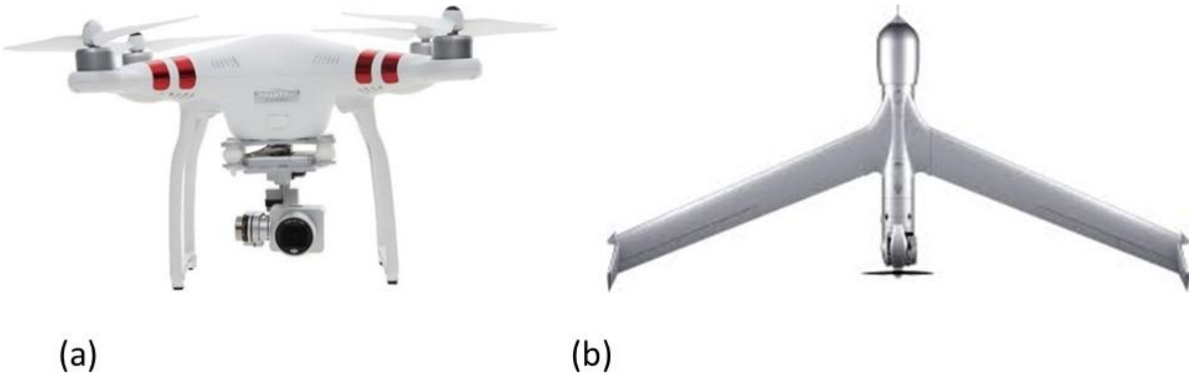


**Figure 2-7: Side-by-side illustration of the wing designs of (a) rotary wings and (b) fixed wings UAS systems. The image (a) is courtesy of dji.com, and (b) is courtesy of newatlas.com.**

The mostly employed UAS types are the rotary-wings, followed by fixed-wings. To show the superiority of rotary-wing aircraft, reviewed articles have shown that 76% of the researchers employed rotary-wing UAS to carry out their mission, while 12% used fixed-wing aircraft, and 12% did not indicate the type of UAS used. Nevertheless, all of this comes at the expense of a smaller payload, rapid flight time, higher energy consumption, and frail wind resistance for rotary-wing aircraft. Furthermore, the results show that the widely used fixed-wing UAS platform is Sensefly eBee since it was employed in over 70% of the fixed-wing platform category. These fixed-wing vehicles use fixed and static wings that give thrust and aerodynamics using forward airspeed to generate lift in conjunction (Abdullahi et al., 2015), which allows them to maximise flight duration. Additionally, fixed-wing vehicles fly at higher speeds and altitudes, sometimes causing potential image blur, thereby making it difficult to obtain accurate information from these systems. Additionally, as stated by Astaoui et al. (2021), their major drawback is that fixed-wing UAS systems require a terrain with sufficient take-off and landing areas, and minimal obstacles are necessary.

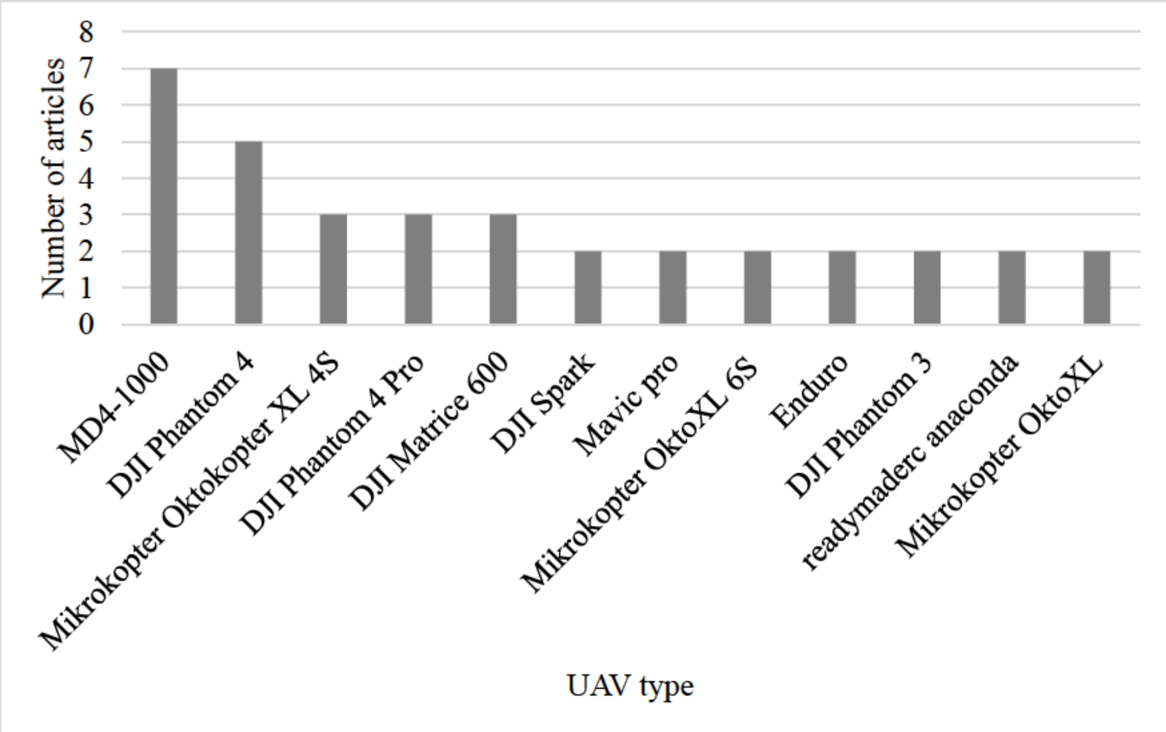


**Figure 2-8: Commonly used UAS types for crop mapping and monitoring.**

As shown in Figure 2-8, MD4-1000 and DJI rotary-wing aircraft are the most commonly used platforms by researchers. Rotary-wing aircraft, which resemble helicopters, are multi-rotor models typically propelled by four, six, or eight rotors, providing excellent manoeuvrability and responsive operation (Watts et al., 2012; Yinka-Banjo & Ajayi, 2020). Their vertical take-off and landing capability allows deployment in small areas, a feature particularly advantageous for smallholder farms where field sizes are constrained. Although fixed-wing platforms offer longer endurance and broader area coverage at higher altitudes, their reduced manoeuvrability and requirement for open take-off and landing spaces make them less suitable for small, fragmented plots (Brito et al., 2019; Psirofonia et al., 2017). The trade-offs between platform types are therefore critical: while rotary-wing aircraft excel in operational flexibility, ease of handling, and rapid data collection over small fields, they are limited by lower endurance and payload capacity. Conversely, fixed-wing systems provide extended flight duration and larger coverage but are constrained by spatial and operational requirements. For smallholder agricultural applications, the advantages of rotary-wing platforms are manoeuvrability, flexibility, and suitability for constrained spaces, outweighing their limitations, making them the preferred choice for smallholder applications (Mesas-Carrascosa et al., 2015; Yinka-Banjo & Ajayi, 2020). Overall, each UAS platform has distinct advantages and disadvantages, as summarised in Table 2-3.

**Table 2-3: Strengths and weaknesses of UAS platforms.**

| UAS system | Pros | Cons | Suitability for agricultural research: (Scale and efficiency) | Suitability for agricultural applications (Scale and efficiency) |
|---|---|---|---|---|
| Rotary wings | 1. High hovering capabilities<br>2. Excellent flight stability<br>3. Ease of operation<br>4. Vertical take-off and landing require little open space ·<br>5. Low cost<br>6. Convenient maintenance<br>7. Interchangeable payloads<br>8. Useful for field trials | 1. Less endurance<br>2. Productivity is often limited by battery life<br>3. These systems are limited to capturing only a singular type of image (RGB, NIR, or thermal) during each flight session | **High**<br>(Pugh et al., 2018; Kulbacki et al., 2018;Stombaugh et al., 2017; Shi et al., 2016) | Low<br>(Watts et al., 2012; Meivel et al., 2016) |
| Fixed wings | 1. Top flight endurance<br>2. Large area coverage per fully charged battery<br>3. Multiple sensors can be mounted<br>4. Large payload capacity<br>5. Fast flight speed<br>6. Useful for large area scanning | 1. They can only move forward<br>2. No hover capability<br>3. Requires open space for take-off and landing<br>4. Limited hovering capacity<br>5. More complex to operate | Low<br>(Delavarpour et al., 2021; van der Merwe et al., 2020; Albani et al., 2017) | **High**<br>(Watts et al., 2012; Tripicchio et al., 2015; Reinecke et al., 2017) |

### *2.3.4 Spectral domains for sensors used for crop discrimination and classification*

In remote sensing studies, various spectral domains of sensors used in crop discrimination play a crucial role in capturing and recording the unique spectral signatures of various crops, aiding in their identification (Peter et al., 2020; Prins & Van Niekerk, 2020). Sensors record electromagnetic radiation from the ultraviolet wavelength to the thermal infrared spectrum portion of the electromagnetic spectrum (Mesas-Carrascosa et al., 2015; Mwinuka et al., 2022; Ndlovu et al., 2021a; Ristorto et al., 2015; van der Merwe et al., 2020; Yang et al., 2017). However, the useful spectral domains in remote sensing range from 440nm in the visible region to 2,500 nm in the shortwave infrared region, and between 7,500 and 13,000nm in the thermal infrared region (Table 2-4).

**Table 2-4: Vegetation spectral domains.**

| Spectral region | Spectral range [nm] | Vegetation traits measured | Reference |
|---|---|---|---|
| Visible | Blue (440 – 510)<br>Green (520 – 590)<br>Red (630 – 680) | chlorophyll a and b, carotenoid, nitrogen | (Brewer et al., 2022; Buchaillot et al., 2019; Chew et al., 2020a; Chivasa et al., 2021; Gano et al., 2021a; Gracia-Romero et al., 2018b, 2020; Mwinuka et al., 2021; Ndlovu et al., 2021a; Vélez et al., 2021; Wahab et al., 2018a) |
| Red edge | 690 – 730 | Canopy cover, plant height, dry matter, nitrogen uptake, equivalent water thickness, fuel moisture content, and specific leaf area. | (Adewopo et al., 2020; Astaoui et al., 2021; Ndlovu et al., 2021a; Mwinuka et al., 2021) |
| Near-Infrared | 760 – 850 | Leaf structural properties (e.g. Biomass, leaf area index, plant density), water stress | (Wahab et al., 2018a; Gracia-Romero et al., 2020; Astaoui et al., 2021; Gano et al., 2021a) |
| Mid-infrared | 1300-2500 | Water stress | (Brewer et al., 2022; Das et al., 2021; A. Feng et al., 2019; Ramírez et al., 2021a; Shafian et al., 2018) |
| Thermal infrared | 7500 – 13000 | Plant water stress | (Mwinuka et al., 2021; Ndlovu et al., 2021; Ramírez et al., 2021b) |

As such, various types of optical sensors, including a digital camera, multispectral, and hyperspectral (and an ultra-spectral camera that is not commonly used), can use any one of the spectral domains. Interestingly, from the reviewed papers, it is observed that a number of researchers preferred the combination of different sensors that include RGB + Multispectral, RGB + Hyperspectral, Modified RGB, Multispectral + LiDAR, and Multispectral + Thermal to improve species discrimination, as shown in Figure 2-9.

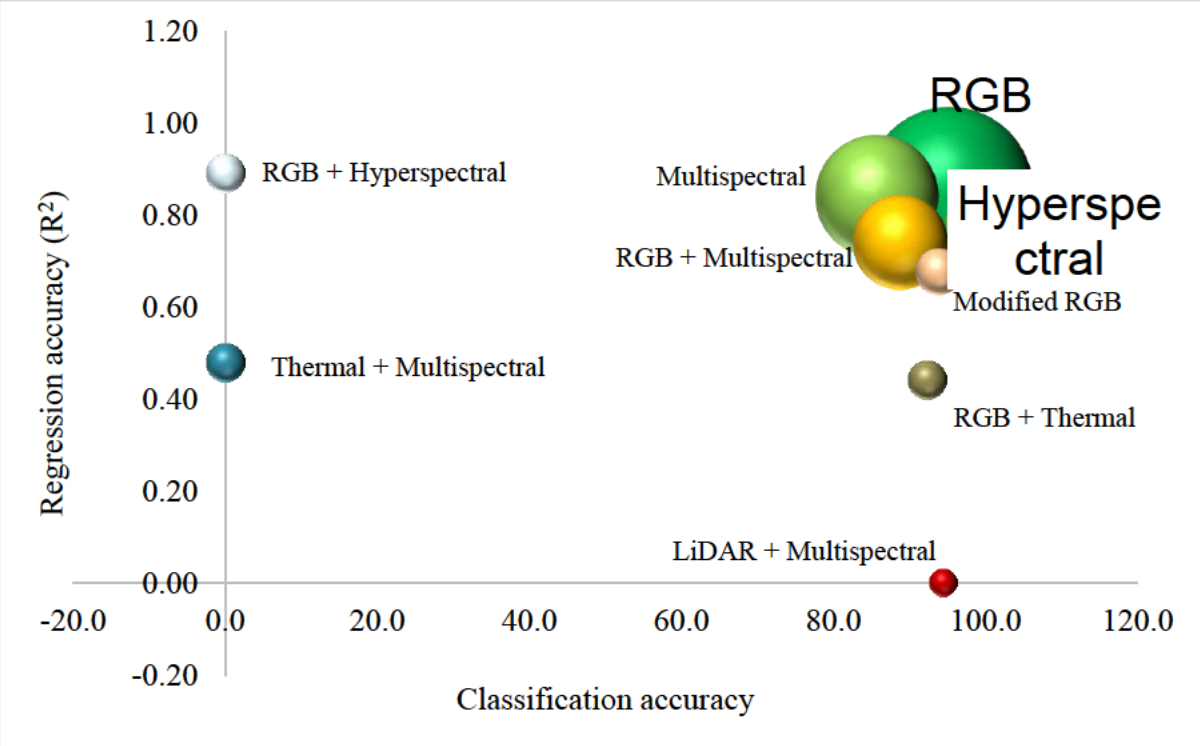


**Figure 2-9: Sensors used for crop classification.**

Of particular interest, in terms of the sensors for crop discrimination, the results of this review showed that RGB sensors yielded the highest number of published articles with 39%, followed by multispectral (26%), RGB + Multispectral (17%), Hyperspectral (5%) and Modified RGB (4%). LiDAR + Multispectral had the least number of publications, followed by RGB + Multispectral, RGB + Hyperspectral and Multispectral + Thermal. In brief, the most commonly employed UAS-mounted sensors in crop discrimination are described as follows:

i. **Digital or RGB (red, green, blue) camera:** Results obtained in this study have shown that RGB sensors are typically the most frequently (39% of the reviewed articles) utilised in crop mapping and monitoring application studies since they are affordable, lightweight, offer high spatial resolution, are easy to operate, have simple data processing, and are easily found in the market (Michez et al., 2018). These are primarily passive sensors that can operate under sunny and cloudy conditions, but not extreme weather conditions. They operate similarly to human vision by capturing only the visible region, approximately within the 400–700 nm band of the electromagnetic spectrum. RGB sensors can rapidly acquire grey-scale or colour images to estimate crop characteristics, such as the severity rating of plants, height, plant centre, plant/weed detection, and leaf colour (Liu et al., 2021; Chen et al., 2017; Lambert et al., 2018; Hall et al., 2018). Most current UAS systems are incorporated with an RGB sensor, permitting near-real-time data acquisition controlled by the operator. RGB sensors are helpful in environments with a low frequency of features of interest, but will not be sufficient to correctly analyse important agro-parameters because of the fewer spectral bands in the visible wavelength (Murugan et al., 2017; Murrieta-Rico et al., 2016; Shi et al., 2016). Additional channels with higher sensitivity to plant biochemicals are required to address this limitation of RGB sensors. Channels such as near-infrared, which reach beyond visible light, are now preferred.

ii. **Multispectral and hyperspectral sensors:** These are also the most deployed sensors (~20% of the reviewed articles) in crop mapping and monitoring studies. Spectral resolution and type of detector are the standard ways used to differentiate a multispectral sensor from a hyperspectral sensor. Multispectral sensors were the first to be invented, and they use red, green, blue, and near-infrared wavebands, usually ranging from 400nm to 1000nm of the electromagnetic spectrum (de Oca et al., 2018). These sensors are employed to obtain spectral characteristics of distinct features and have been deployed in agriculture to monitor plant health status, crop growth, estimate nutrient and water content, as well as other physiological traits (Psirofonia et al., 2017; Kumar et al., 2020; Na et al., 2017). For vegetation, the abrupt change in reflectance between the far end of the red band and the near-infrared band, often referred to as the red edge region (700nm to 850nm), has been used to calculate different spectral indices sensitive to various feature properties. Spectral responses are like fingerprints for plants. They are mathematical formulas that combine reflectance values from specific wavelengths. For example, the combination of the red and near-infrared parts of the spectrum exposes vegetation vigour. Furthermore, it was observed that spectral indices are highly correlated with green-leaf biomass (Mutanga et al., 2003) because of their high chlorophyll absorption in the visible region of the spectrum.

Multispectral cameras are flexible and efficient; however, they are insufficient for specific quality attributes of crops because of multispectral sensors' low spectral resolution and spectral range (de Oca et al., 2018; Raeva et al., 2019; Hassan-Esfahani et al., 2014; Kulbacki et al., 2018; Comba et al., 2015). The specific quality attributes of crops include chemical properties such as pigments, nitrogen, chlorophyll, water, protein, xanthophylls, and carotenoids, which play a role in generating unique spectral signatures for different crops (Berni et al., 2009; Psirofonia et al., 2017). It is worth noting that biochemical properties are responsive to particular narrow bands of wavelengths across several segments of the electromagnetic spectrum (van der Merwe et al., 2020; Gago et al., 2015; Yong et al., 2016).

The drawback of spectral indices with limited bands led to an increased demand for hyperspectral sensors with wavelengths ranging from 350 to 2500nm. This highlights the need for advanced remote sensing technologies, particularly those deployable on UASs, to capture detailed spectral information with an optimal number of channels. As such, hyperspectral sensors capture data in a much more detailed way by measuring light at many very narrow and closely spaced wavelengths (10nm to 20nm wide), creating a kind of continuous spectrum. This increase in data complexity allows for a more precise analysis of materials and their properties. (Ruiz-Altisent et al., 2010; Cao et al., 2020). In the past few years, hyperspectral sensors have been trending in crop mapping and monitoring, especially in acquiring diverse plant trait estimates such as nutrient content, water content, leaf area index, dry matter, plant stress, and other biological and physical characteristics of crops (Zheng et al., 2016; Chivasa et al., 2019; Feng et al., 2022; Shu et al., 2021). This has resulted in a high spectral and spatial resolution that can accurately detect in-field crop variations (Tian et al., 2022; Xia et al., 2022). Nonetheless, the current challenges of mounting hyperspectral sensor payloads include being expensive, coupled with high data dimensionality, vast volumes of data output, low spatial resolution, and high-power requirements.

iii. **Modified Sensors**: To improve spectral responses in features, some studies, such as by Hall et al. (2018), van der Merwe et al. (2020), and Wahab et al. (2018a), modified the normally blocked NIR channel. According to a study by Hall et al. (2018), they modified a normal red, blue, and green camera with the inclusion of NIR spectra for better classification results of maize in smallholder farming systems. To achieve higher classification performance, Hall et al. blocked the red band using a red filter, while the NIR-blocking filter was removed to record data using this same channel. Expectedly, the classification accuracy was increased by an average of 10% after the substitution of NIR into the red channel. Likewise, Wahab et al. (2018b) in Ghana employed the same method of replacing the red band with a specialised filter that allows the camera to capture near-infrared (NIR) wavelengths, beyond the range of human vision, on a GoPro Hero4 Silver 12-megapixel camera.

iv. **Multi-sensor data fusion** (RGB + Multispectral, RGB + Hyperspectral and Multispectral + Thermal): One effective approach to enhance crop discrimination capabilities is the integration of different sensors with unique characteristics, such as RGB and multispectral data. A noteworthy finding was that most studies employing multi-sensor data fusion focused on directly analysing the combined data to identify biochemical differences within plants. It can be concluded that the synergy between two different sensors enhances the ability to discriminate features. For example, the fusion of RGB and multispectral datasets allows for a more subtle analysis. A study by Lottes et al. (2017a) In Germany and Switzerland, the effect of using RGB and NIR from Zenmuse X3, which has an RGB sensor, and JAI AD-130 GE, a multispectral sensor, was evaluated for classifying sugar beets and weed species. Also, Xia et al. (2022), who proposed improving weed identification accuracy by combining the high spatial information captured by the DJI Phantom 4 RTK UAV, which is an RGB sensor, with the detailed spectral information provided by the DJI Phantom 4 Multispectral camera. Furthermore, Feng et al. (2022), who compared the capability of the Sony DSC–QX100 RGB camera against a hyperspectral Firefly imaging spectrometer known as UHD185 for monitoring winter-wheat growth. A combination of multispectral and thermal data was proposed by Ramírez et al. (2021b) in Mozambique, to identify sweet potato genetic constitutions with high throughput and resilience under water stress.

v. **Thermal sensor**: These sensors are mainly employed in agriculture to provide temperature measurements of crop and soil surfaces from the energy that has been emitted from the surface in different regions of the electromagnetic spectrum. Instead of relying on external light sources like passive sensors, thermal and infrared cameras use special sensors. They use infrared detectors and lenses to capture heat radiation emitted by objects, typically in the wavelength range of 7,500nm to 13,500 nm, which is invisible to optical sensors (Raeva et al., 2019; Ramírez et al., 2021b; Stutsel et al., 2021). UAS mounted with infrared thermal imagers are currently being deployed to acquire the crop canopy temperature in a non-destructive manner. Thermographic and infrared cameras are employed to receive infrared radiation energy, which is correlated with plant water and can monitor crop growth or determine crops under stress conditions (Hassan-Esfahani et al., 2014; Berni et al., 2009). The infrared emission signature of the canopy is indirectly linked to biotic and abiotic stress, which alters rates of photosynthesis and transpiration, thereby disturbing the canopy temperature that produces a heat signature. However, these sensors have a low spatial resolution and low frame rate capture related to optical sensors, but they have a high radiometric resolution of typically up to 16 bits (Buchaillot et al., 2019; Variyar et al., 2019). Additionally, they are also sensitive to various weather conditions, and environmental conditions can be affected by their surroundings, and may fail to detect slight temperature differences.

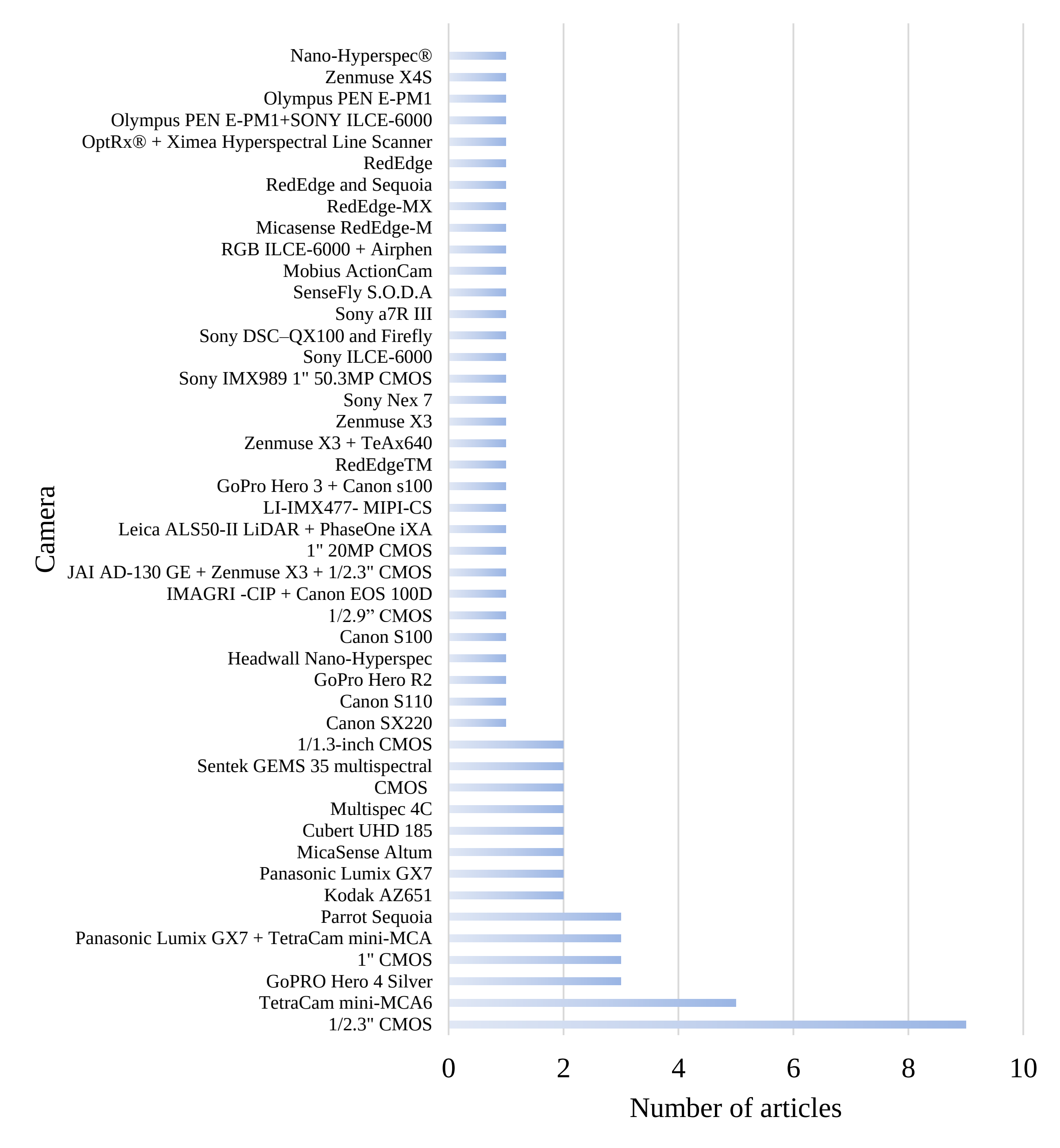


**Figure 2-10: Frequency of studies that utilised a specific sensor system within reviewed studies.**

In summary, findings suggest that multispectral and RGB sensors are the most frequently deployed for mapping and monitoring crop traits. RGB sensors operate in the visible wavelength (approximately 400–780 nm) and acquire high spatial resolution images, and they are relatively inexpensive compared to other sensors. Explicitly, 1/2.3" CMOS was the most widely used sensor with more than five studies, followed by multispectral sensors including TetraCam mini-MCA6 (6 studies), GoPro Hero 4 Silver, Panasonic Lumix GX7 + TetraCam mini-MCA, Parrot Sequoia, and 1" CMOS RGB sensors (3 studies; Figure 2-10). However, RGB images are insufficient for detecting specific vegetation parameters because many biochemical properties are sensitive to narrow wavelength ranges, and RGB sensors lack bands beyond the visible spectrum. Multispectral sensors, while covering selected channels (50–100 nm wide), may suffer from limited spectral resolution, band overlap, and reduced sensitivity to subtle differences in plant biochemistry, which can constrain accurate crop discrimination. Hyperspectral sensors, although providing very fine spectral detail, present high data dimensionality, large storage and processing requirements, potential spectral saturation, and lower spatial resolution, which can limit operational feasibility. These sensors are also very expensive, and as such, they are rarely used in smallholder environments. Thermal sensors, used to measure crop and soil surface temperatures, are sensitive to environmental conditions, have lower spatial resolution and frame rates, and may fail to detect small temperature differences, restricting their utility in some crop monitoring applications. Similarly, modified sensors and multi-sensor fusion approaches, while improving detection capability, require careful calibration and integration, and may introduce complexity, higher costs, and data management challenges. Hence, sensor-specific limitations must be considered when selecting UAS-mounted sensors for accurate and reliable crop trait assessment. Several vegetation indices use the red and near-infrared channels because they strongly correlate with chlorophyll content.

### 2.4 Crop Discrimination and Classification Techniques

UAS-based image acquisition is a fundamental step in crop discrimination, serving as the foundation for extracting valuable insights into crop differences. Because of UASs' ability to capture imagery at the field level with high temporal and spatial resolution, they allow for frequent and detailed monitoring of crops throughout the growing season. This allows the discrimination of distinct plants at different growth stages. (Chen et al., 2017; Chivasa et al., 2020; de Oca et al., 2018; Hall et al., 2018; Handique et al., 2017; Ishengoma et al., 2021a; Liu et al., 2021; Pan et al., 2022; Rajapaksa et al., 2018; Wang et al., 2021; Xia et al., 2022). The choice of UAS type, sensor type, platforms, acquisition parameters, and level of information required significantly influences the quality and applicability of the acquired imagery (Chianucci et al., 2016; Delavarpour et al., 2021; Han et al., 2018; Psirofonia et al., 2017). From the reviewed articles, it is noted that crop discrimination and classification using high spatial resolution RGB images play a pivotal role in improving agricultural activities, allowing farmers and researchers to obtain accurate in-field crop statistics and detect anomalies at an affordable price. This section explores key techniques involved in crop discrimination, mainly focusing on image preprocessing techniques, feature extraction models, classifier models, post-classification processing, and the evaluation of performance through validation metrics.

### *2.4.1 Feature extraction models*

i. ***Spectral indices:*** Numerous reviewed studies employed different spectral indices (SI) for feature extraction. The commonly used SIs are shown in Table 2-5. It can be observed that NDVI and GNDVI are the most frequently used spectral indices in the reviewed articles. This was followed by SAVI, ExG, ExB, VARI and GVRI. These SI are spectral transformations that use numeric combining of various spectral wavelengths. They are calculated to enhance the contribution of vegetation's biochemical and physical traits (leaf area index, canopy biomass, water content, nitrogen content, absorbed radiation, chlorophyll content, etc.), environmental effects, as well as to highlight vegetation's vigour. Spectral indices are calculated directly without any bias or assumptions regarding surrounding conditions. These equations influence the way light interacts with objects at different energy levels (wavelengths) of light to reveal the properties of the material (Tsouros et al., 2019).

**Table 2-5: Most used spectral indices.**

| **Index** | **Computation** | **Used by** |
|---|---|---|
| Normalised Red Intensity | $r = \frac{Red}{Red+Green+Blue}$ | (H. Feng et al., 2022; Kawamura et al., 2021a; Pérez-Ortiz et al., 2016; Schirrmann et al., 2016) |
| Normalised Green Intensity | $g = \frac{Green}{Red+Green+Blue}$ | (H. Feng et al., 2022; Kawamura et al., 2021a; Pérez-Ortiz et al., 2016; Schirrmann et al., 2016; Shu et al., 2021) |
| Normalised Difference Vegetation Index | NDVI = $\frac{Red-NIR}{Red+NIR}$ | (Chivasa et al., 2020; Gano et al., 2021b; Gracia-Romero et al., 2017b, 2020; Handique et al., 2017; Lelong et al., 2008; Mahajan and Raj, 2016; Mesas-Carrascosa et al., 2015; Mwinuka et al., 2022; Nhamo et al., 2018; Peña Barragán et al., 2012; Peña et al., 2013b; Potgieter et al., 2017; Ramírez et al., 2021b; Schut et al., 2018; Shi et al., 2016; Xia et al., 2022; Zheng et al., 2016) |

| Index | Computation | Used by |
|---|---|---|
| Green Normalised Difference Vegetation Index | GNDVI = $\frac{NIR-Green}{Green+NIR}$ | (Chivasa et al., 2020; Gano et al., 2021b; Handique et al., 2017; Lelong et al., 2008; Mwinuka et al., 2022; Peter et al., 2020; Shafian et al., 2018; Wahab et al., 2018b; Watts et al., 2012; Xia et al., 2022) |
| Normalised Green–Red Difference Index | NGRDI = $\frac{Green - Red}{Green + Red}$ | (Buchaillot et al., 2019; Jiménez-Brenes et al., 2019; Mahajan and Raj, 2016; Ndlovu et al., 2021b) |
| Normalised Difference Red-Edge Index | NDRE = $\frac{NIR-Rededge}{NIR+Rededge}$ | (Handique et al., 2017; Mwinuka et al., 2022; Ndlovu et al., 2021a; Potgieter et al., 2017; Xia et al., 2022) |
| Soil-Adjusted Vegetation Index | SAVI = $\frac{1.5(NIR-Red)}{NIR+R+0.5}$ | (Gracia-Romero et al., 2017b, 2018a; Lelong et al., 2008; Mwinuka et al., 2022; Peter et al., 2020; Z. Wang et al., 2022; Yong et al., 2016) |
| Enhanced Vegetation Index | EVI = $\frac{2.5*(NIR-Red)}{(1+NIR+6*Red-7.5*Blue)}$ | (Gracia-Romero et al., 2017b; Mwinuka et al., 2022; Shafian et al., 2018) |
| Excess Green Minus Excess Red Index | ExGR = ExG− 1.4$r - g$ | (Jiménez-Brenes et al., 2019; Kawamura et al., 2021a; Z. Wang et al., 2022) |
| Excess Red Index | ExR = 1.4 * $\frac{Red-Green}{Red+Green+Blue}$ | (Feng et al., 2022; Jiménez-Brenes et al., 2019; Kawamura et al., 2021a) |
| Excess Green Index | ExG = 2$g - r - b$ | (Jiménez-Brenes et al., 2019; Kawamura et al., 2021a; Pérez-Ortiz et al., 2016; Schirrmann et al., 2016; Shu et al., 2021; Z. Wang et al., 2022) |
| Excess Blue Vegetation Index | ExB = 1.4$b - g$ | (Feng et al., 2022; Kawamura et al., 2021a; Pérez-Ortiz et al., 2016; Schirrmann et al., 2016; Shu et al., 2021) |
| Visible Atmospherically Resistant Index | VARI = $\frac{Green-Red}{Red+Green-Blue}$ | (Feng et al., 2022; Jiménez-Brenes et al., 2019; Van De Vijver et al., 2022; Z. Wang et al., 2022; Watts et al., 2012; Xia et al., 2022) |

| Index | Computation | Used by |
|---|---|---|
| Optimised Soil-Adjusted Vegetation Index | OSAVI = $\frac{NIR-Red}{NIR+Red+0.16}$ | (Feng et al., 2022; Gracia-Romero et al., 2017b, 2018a; Jiménez-Brenes et al., 2019; Mwinuka et al., 2022) |
| Colour Index of Vegetation Extraction | CIVE = $0.441r - 0.811g + 0.385b + 18.78745$ | (Jiménez-Brenes et al., 2019; Kawamura et al., 2021a; Z. Wang et al., 2022) |
| Green Ratio Vegetation Index | GRVI = $\frac{g-r}{g+r}$ | (Feng et al., 2022; Kawamura et al., 2021a; Mahajan and Raj, 2016; Stutsel et al., 2021; Wang et al., 2021) |

**ii.** ***Invariant Colour models:*** From the reviewed articles, it can be noted that colour features are described in terms of hue, saturation, and brightness properties, which are derived from several RGB transformation techniques. These techniques include HSI (Hue Saturation Intensity), RGB (Red, Green, Bue), HSV (Hue Saturation Value), Normalised Red Intensity ($r$), Normalised Green Intensity ($g$), Normalised Blue Intensity ($b$), HCV (Hue Chroma Value), HSL (Hue Saturation Luminance), YIQ (NTSC colour TV standard with luma in-phase and quadrature components), $C_1$ $C_2$ $C_3$, CIE Lab, and $YC_bC_r$ (SECAM colour TV standard with luminance and two chrominance components) (Adeline et al., 2013; Deb, 2014; Mahlein, 2016; M-Desa et al., 2022; Oukil et al., 2021). Colour models serve as fundamental tools in remote sensing and precision agriculture, providing a structured framework for the representation, interpretation, and analysis of data collected by sensors. According to Tsai (2006), colour tone is a very influential factor in the visual interpretation of images. It can simplify the process and become the most important aspect when identifying and extracting features. The exploitation of chromaticity in high spatial resolution UAS images is found in two mainstreams, namely those working with RGB combinations and those making use of invariant images.

In precision agriculture, the most familiar and widely used invariant colour models for presentation are the RGB, HIS, and CIE Lab. Application of these invariant colour models for crop discrimination, where subtle colour variations play a crucial role in accurate colour quantification for specific features, was used successfully. Buchaillot et al. (2019) employed invariant colour models such as hue and NDLab for maize breeding and yield assessment and showed that their method outperformed those using only agronomic parameters and field sensors. This was followed by Gracia-Romero et al. (2020), who used HSI, RGB CIELab*, and CIELuv* colour models, and their results showed that these invariant colour models had slightly higher correlations with grain yield and leaf nitrogen content compared to leaf-based measurements. Furthermore, Kawamura et al. (2021a) evaluated the performance of the different combinations of three colour models (RGB, HSV and CIE-L*a*b), a canopy height model, spatial texture, and four vegetation indices, including ExG, ExR, GRVI, and CIVE to discriminate crops and weeds in upland rice fields. The combination of HSV and texture showed the highest accuracy of 0.915 compared to other combinations.

**iii.** ***Texture features:*** Unfortunately, 4% of the studies employed texture analysis, as indicated by the findings in this study. Texture features encapsulate the spatial arrangement of pixel intensities in an image, which is a superficial manifestation of the human visual system of natural objects. Textural features provide critical spatial information about the inherent patterns and structures of an image. In image analysis, texture serves as a powerful discriminator, facilitating the distinction between surfaces with varying visual characteristics. For example, various texture descriptors such as grey-level co-occurrence matrix, local binary patterns, Gabor filters, Haralick texture features, and texture energy measures have been extensively used to extract discriminative texture features for differentiating between crops and detecting anomalies. Rajapaksa et al. (2018) employed textural features from the grey-level co-occurrence matrix, local binary patterns, and Gabor filter into a support vector machine for the classification of crop lodging in Canada. From their study, the grey level co-occurrence matrix had the best performance, with an overall accuracy of 96% for canola and 92.6% for wheat. This was followed by Wang et al. (2021), who compared the classification accuracies of spectral features, textural features, and canopy structure data to determine the degree of lodging in maize with high precision. In their study, they observed that a combination of the original image, digital surface model, and texture features produced the highest overall accuracy using the object-oriented classification method combined with random forest classification, with an accuracy of 86.96% and a kappa coefficient of 0.79.

In general, the results indicate that feature selection strongly impacts classification performance. Spectral indices such as NDVI, GNDVI, SAVI, ExG, ExB, and VARI are well-suited for mixed cropping systems due to their sensitivity to chlorophyll content, canopy structure, and leaf area index, enabling discrimination of overlapping canopies; however, they are limited by their inability to capture subtle biochemical differences beyond the measured bands and may be affected by soil background or illumination variations. Colour features derived from invariant models (RGB, HSI, CIELab) capture subtle pigmentation differences critical for spatially proximate crops, but they are sensitive to lighting conditions and may fail to differentiate crops with similar hues. Texture features provide complementary spatial information by characterising canopy heterogeneity, yet their effectiveness is constrained in small, highly heterogeneous fields where spatial patterns are inconsistent. Overall, integrating spectral, colour, and texture features with machine learning or deep learning classifiers enhances crop discrimination accuracy in heterogeneous smallholder systems, but each feature class has inherent limitations that must be considered when designing classification workflows.

### *2.4.2 Classifier models*

i. ***Traditional methods**:* Unfortunately, only 4% of the reviewed articles utilised traditional methods. In the realm of image classification, traditional algorithms have been influential in categorising and interpreting visual data, although with their advantages and disadvantages. These traditional methods were preferred in the past because they were characterised by their simplicity, computational efficiency, and reliance on predefined rules, making them valuable tools in crop classification/discrimination (Llano et al., 2018; Louargant et al., 2018). These traditional methods are mainly classified into two classes: supervised and unsupervised classification algorithms. Unsupervised classification algorithms include principal component analysis, iterative self-organising data analysis techniques, Gaussian mixture models, and k-means (Ortenzi et al., 2021), which involve iterative procedures to autonomously group pixels or objects based on inherent patterns or clusters within the image dataset without specific guidance. Furthermore, unsupervised classification algorithms do not require much effort to apply, and they are widely available in image processing. Lastly, the user does not require labelled training data for prediction; instead, the algorithms focus on identifying patterns, clusters, and relationships within the image dataset. While supervised classification algorithms, including maximum likelihood classifiers (Prins & Van Niekerk, 2020), minimum distance classifiers, parallelepiped classifiers, and nearest neighbour classifiers, are characterised by their forthright procedures, interpretability, and reliance on statistical measures to assign or predict pixels to predefined classes.

**ii.** ***Machine learning**:* Based on the reviewed articles, machine learning is the most widely used classifier, as shown by the 30% in Table 2-6 below. Machine learning classifiers have been used as powerful tools for agricultural applications, such as crop discrimination, crop monitoring, and yield estimation. They leverage computational algorithms to analyse and classify remotely sensed data. Various algorithms that fall under machine learning are grouped into; i) supervised learning, such as linear regression, logistic regression, decision trees, random forests, support vector machines, k-nearest neighbours and Naïve Bayes, and ii) unsupervised learning, which includes k-means clustering, hierarchical clustering, principal component analysis, singular value, decomposition, and Gaussian mixture models.

Of the 30% of machine learning algorithms employed, 60% mainly used the random forest algorithm, which proved to be the popular algorithm (Chivasa et al., 2020; de Castro, Torres-Sánchez, et al., 2018a; Z. Fan et al., 2018; Feng et al., 2022; Kawamura et al., 2021a; Lambert et al., 2018; Lottes et al., 2017a; Ndlovu et al., 2021b; Ong et al., 2023; Prins & Van Niekerk, 2020; Shu et al., 2021; Wang et al., 2021; Yong et al., 2016; Zhu et al., 2022), as shown in Figure 4. This was followed by a support vector machine used by Fan et al., (2018); Hall et al. (2018); Khan et al., (2021); Nardari et al. (2018); Ndlovu et al. (2021a); Pérez-Ortiz et al. (2016); Rajapaksa et al. (2018); Tian et al. (2022) and Xia et al. (2022). Whilst k-means by Cruzan et al. (2016), principal component analysis by Schirrmann et al. (2016), and unknown unsupervised classifiers employed by Bolo et al. (2019); Llano et al. (2018) and Louargant et al. (2018) were the popular unsupervised classifiers.

***iii.*** ***Deep learning**:* Findings of the review paper have shown that deep learning, a subclass of machine learning, is the fastest-growing trend in crop discrimination and classification, as shown in Table 2-6. From that same table, it is interesting to observe that DL algorithms were employed in ~60% between 2020 and 2023, as compared to

~30% of ML algorithms. Overall, ML were employed in 30% and DL in 20% of the total articles, respectively. This is due to the fact that DL-based approaches can recognise complex patterns from different remotely sensed data (Pan et al., 2022). Unlike machine learning algorithm, which require variables as input feature extractors fed into a learning algorithm to perform classification (Hassan et al., 2022), deep learning performs the tasks automatically and simultaneously by feeding the network with unclassified data to extract spatial and spectral features (Khan et al., 2021; Lottes et al., 2017a; Wang et al., 2021; Zhang et al., 2023). Additionally, the increase in input datasets or training data in the network of deep learning algorithms results in infinite precision and higher accuracy, thereby extracting valuable features (Chew et al., 2020b; Liu et al., 2021; Sa et al., 2018; Xia et al., 2022).

Of particular interest in deep learning architectures are the artificial neural networks, mainly represented by convolutional neural networks (CNNs) are being extensively studied in crop discrimination and classification. These architectures have become even more popular than the popular random forest classifier since 2020, as shown in Figure 4. They can extract spatial and spectral features automatically and simultaneously using either classical or customised architectures. ConvNet (Abdullahi et al., 2015), ResNet (Guo et al., 2021; Stewart et al., 2019; Ukaegbu et al., 2021; Van De Vijver et al., 2022), U-net, Segnet and Deeplab V3+(Jo et al., 2021) are the classical CNN architectures used for image classification. While customised architectures include ImageNet (Chew et al., 2020a), EfficientnetB4, VGG16, ResNet50, and DenseNet121 (Tan et al., 2022), VGG16, VGG19, InceptionV3 and MobileNetV2 (Ishengoma et al., 2021b).

**Table 2-6: Approaches employed by reviewed papers.**

| Approach | Year | | | | | | | | | | | |
|---|---|---|---|---|---|---|---|---|---|---|---|---|
| | **2012** | **2013** | **2014** | **2015** | **2016** | **2017** | **2018** | **2019** | **2020** | **2021** | **2022** | **Total** |
| **ANOVA** | | | | | | | 1 | | 1 | 1 | | 3 |
| **DL** | | | | | | 1 | | 1 | 1 | 7 | 9 | 19 |
| **ML** | | | | 1 | 3 | 2 | 7 | 2 | 3 | 4 | 3 | 25 |
| **ML + DL** | | | | | | | 1 | | 1 | 1 | 2 | 5 |
| **ML + OBIA** | | | | | | | | | | 1 | | 1 |
| **ML + Regression models** | | | | | | | | | | 1 | | 1 |
| **OBIA** | 1 | 2 | | | | | | | 3 | 1 | | 7 |
| **Regression models** | | | | | | | 2 | | | | | 2 |
| **Traditional** | | | | | 2 | | | 2 | 1 | | 1 | 6 |
| **Vegetation indices** | | | | 1 | 1 | 2 | 2 | 1 | 1 | 1 | 2 | 11 |
| **Vegetation indices + Elevation** | | | | | 1 | 1 | | | | 1 | | 3 |
| **Total** | 1 | 2 | 0 | 2 | 7 | 6 | 13 | 6 | 11 | 18 | 17 | 83 |

Where ANOVA = analysis of variance, DL = deep learning, ML = machine learning and OBIA = object-based image analysis

## 2.5 Overall Observations, Limitations and Future Insights

The success of UAS technologies being implemented in agricultural activities, characterised by various studies and subject areas covered, is remarkable. These studies have shown the considerable potential of UAS applications in agriculture. The reviewed literature asserts that UAS systems for crop management can provide reliable, accurate, precise, and real-time data about specific crops for timely responses at the desired spatial and temporal scales. As such, accurate mapping and monitoring of crops are of interest to policymakers, farmers and agronomists in most countries to improve agricultural production. However, based on the reviewed articles focusing on the use of UAS systems in crop discrimination, there are several challenges and opportunities to be dealt with (Table 2-7).

### *2.5.1 General observations*

#### 2.5.1.1 UAS and sensor selection and characteristics

The reviewed articles showed that rotary-wing UAS were the most widely used platforms to acquire remotely sensed images. Most research papers that were reviewed showed that several experimental sites were not large enough for fixed-wing UASs to be used, since they regularly require take-off and landing space. However, rotary-wing UASs, which are characterised by vertical take-off and landing, are more suitable for utilisation in small experimental sites. Furthermore, probably because rotary-wing UASs are less expensive as compared to fixed-wing ones, most reviewed papers employed DJI drones, as shown in Figure 8.

The findings of this article observed that rotary-wing UASs equipped with multispectral sensors and RGB cameras were the most frequently used for crop classification when compared to different sensors, such as hyperspectral sensors and thermal infrared sensors. Moreover, it was noted that a combination of micro, mini, or small UAS systems and RGB cameras is used in most developing countries, can deliver high spatial resolutions, and tends to be much more affordable. While multispectral and hyperspectral sensors provide an enticing combination of high spatial detail and rich spectral information, revealing intricate reflectance patterns, their cost is significantly higher compared to RGB cameras. Therefore, selecting the optimal sensor hinges on a critical trade-off: the potential for enhanced accuracy versus the expense associated with more advanced technology.

#### 2.5.1.2 Data analysis

It was observed that crop discrimination studies predominantly employ computational approaches, which can be categorised into traditional statistical methods, machine learning algorithms, and deep learning frameworks. Traditional statistical methods, such as maximum likelihood or minimum distance classifiers, are valued for their simplicity and interpretability but are limited in capturing complex patterns in heterogeneous cropping systems. Machine learning algorithms, including random forests, support vector machines, and k-nearest neighbours, are widely used in smallholder environments where dataset sizes are moderate, offering robust performance with manageable data requirements. Deep learning approaches, particularly convolutional neural networks, provide powerful automatic feature extraction capabilities and high accuracy but require large annotated datasets, which are often unavailable in smallholder contexts. Feature extraction techniques underpinning these classifiers include spectral indices, invariant colour models, and textural features, each contributing differently to crop discrimination depending on the spatial and spectral characteristics of the study area.

### *2.5.2 Current limitations of UAS application in crop discrimination*

#### 2.5.2.1 UAS specifications

The choice of a UAS for any task is mainly affected by its sensitivity to weather conditions, payload, weight, battery capacity, and aerodynamics (Dvořák et al., 2015; Watts et al., 2012). Firstly, in terms of payload capability, some lightweight UAS systems may have limited capability to carry several sensors per flight mission (de Castro, Torres-Sánchez, et al., 2018b; Ishengoma et al., 2021a; van der Merwe et al., 2020; Zheng et al., 2016). Secondly, in terms of area coverage, most UAS systems have a short battery life, especially rotary-wing systems, resulting in a rapid flight endurance time, ranging from 15 to 30 minutes, hindering progress when mapping large areas since batteries must be changed and recharged regularly. In short, rotary-wing aircraft systems are not suitable for large-scale agricultural operations as compared to fixed-wing UAS systems. Finally, due to the use of lightweight UASs mounted with restricted payloads (sensors), spectral resolution is greatly affected, thereby limiting their usefulness in picking important plant attributes that can improve crop discrimination.

#### 2.5.2.2 Cropping systems and lack of input resources

Based on the referred literature, it can be deduced that 90% of farmers practice a monoculture cropping system, which is predominantly in developed countries. It is also noted that the application of UASs is designed for relatively medium- to large-scale farmers who normally practice monoculture cropping systems. Yet most of the farmers being left out are smallholder farmers in most developing countries who cannot adequately invest in such technologies because of a lack of resources. Unfortunately, mixed cropping systems are inherent to smallholder farming environments. Mapping and monitoring crop growth under such heterogeneous landscapes requires accurate, precise, and timely information that significantly improves productivity. Quality agricultural information and knowledge are greater instrumental values for smallholder farmers for them to be successful and improve food security. Farmers will use agricultural information and knowledge for decision-making, such as crops to plant, crops to mix, when to intervene when crops are stressed, yield estimation, preparation for harvesting, etc. However, government institutions offer blanket solutions to the smallholder farmers without recognising heterogeneity in these agro-ecological landscapes. Also, dissemination of critical quality agricultural information to the intended user (smallholder farmers) is lacking, mainly because farmers are more worried about critical issues such as inputs and other important activities. As such, there is a need to adopt affordable technologies, subsidised access to technology, introduce partnerships and collaborations between and among farmers and other stakeholders, as well as promote policies that support the equitable distribution of agricultural technologies. Furthermore, agricultural extension officers need to be trained on some of the critical skills, such as image interpretation and methods to use for disseminating processed information to smallholder farmers.

#### 2.5.2.3 Cost

UAS technology is an essential tool in the agriculture sector; however, purchasing a super UAS system with a good balance of endurance, stability, durability, and the optional ability to fly autonomously is costly for many farmers in developing countries. In addition, the use of UAS systems requires experts and skilled personnel who can operate the systems and exploit the data acquired, which is costly to many poor smallholder farmers. This is one reason UAS technology is primarily dominant on commercial farms, thereby prohibiting the adoption of such systems in smallholder farming environments.

#### 2.5.2.4 Ethics and privacy

Article 12 of the U.N. Declaration of Human Rights states that "*no one shall be subjected to arbitrary interference with his privacy, family, home or correspondence, nor to attacks upon his honour and reputation*"(UN, 1948). As such, the intention of the users of UASs for mapping and monitoring crops may have the potential for ethics and privacy infringements when using them on smallholder farms. Crop mapping and monitoring involve the collection and examination of large amounts of geospatial data. It's crucial to address how researchers collect, store, and use this data. This includes protecting sensitive information about land ownership, farming methods, and proprietary agricultural data. What's more, ethical issues extend to the potential effects on small farmers and local communities. These groups may feel the impact of insights from crop mapping technologies. It must be imperative to get permission from the Civil Aviation Authority and property owners to use drones in such an area. It's also essential to obtain informed consent from landowners and increase public awareness.

#### 2.5.2.5 Environmental factors

It is important to observe that most agricultural activities in smallholder environments heavily rely on rain. Subsequently, the acquisition of UAS data for crop mapping and monitoring is vulnerable to disturbance by various weather events, including hailstorms, strong winds, heavy cloud cover, and precipitation. These significant challenges to data collection can affect the quality of the data, thereby potentially affecting the precision and accuracy of the classified features. The effects of temporal variability, especially on images acquired under various weather conditions, may exhibit distinct spectral signatures, such that those taken under cloud cover may have a shadow effect.

#### 2.5.2.6 Data processing challenges

Because of the heterogeneous environment on smallholder farms, the prerequisite for photogrammetry processing, which is image overlap, must be sufficiently selected. Images with high quality have more forward and side overlap, which reduces unwanted errors. Furthermore, because of the exponential development of UAS platforms and sensors, the volumes of image datasets are rapidly increasing, thereby demanding computers with high performance in terms of image processing. It is also difficult to comprehend how smallholder farmers might obtain these high-tech computers with large storage facilities. The selection of an appropriate algorithm for crop discrimination is crucial since it is mainly affected by the availability of suitable datasets. Some classifier algorithms, such as DL, require large datasets to reduce underfitting or overfitting. Unfortunately, large datasets increase computational demands.

#### 2.5.2.7 Policy and regulatory issues

Most developing countries are still working on regulations and policies that can be used as guides by UAS users (McCarthy et al., 2023; Mokoena et al., 2023). Based on the reviewed literature, it can be observed that there is a low usage of UAS systems in most developing countries, especially in Africa, as shown in Figure 2-11. Therefore, there is a need to craft some related legislation and national/regional rules that will be used to regulate the users and application of the UAS in different countries. For example, in Africa, there is a lack of integrated regulations across the continent to ensure security and safety for people or wildlife. This is one of the critical challenges of using the UAS in most developing countries. This could be attributed partly to the stringent drone usage policies and regulations (https://www.droneregulations.info, https://drone-laws.com/drone-laws-in-african-countries/). Only 43% of the African countries issued or updated comprehensive regulatory guidelines or policies on the utilisation of UASs for recreational, civilian, and commercial purposes within their airspace. At the same time, 37% of African countries, such as Namibia, Mali, Ethiopia, and Somalia, which, as shown in Figure 11, do not have comprehensive regulations and policies in place to support UAS operations. Furthermore, 13% of the countries are still developing the regulations or are pending, while 7% of the countries, such as Burkina Faso, Chad, and Togo, are adopting International Civil Aviation Organisation (ICAO) laws (Figure 2-11).

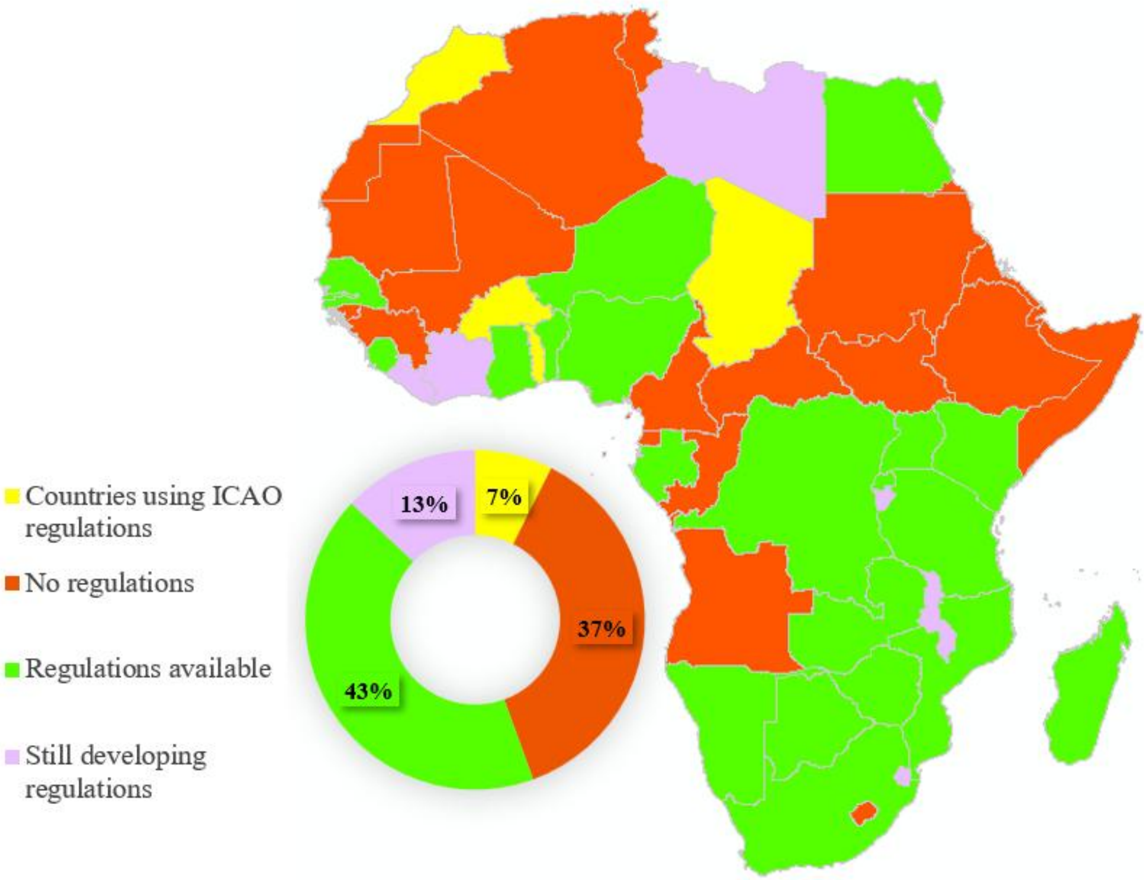


**Figure 2-11: Summary of UAS regulations in Africa (https://www.droneregulations.info, https://drone-laws.com/drone-laws-in-african-countries/ as of April 2023).**

### 2.5.2.8 Technical challenges

The deployment of UAS systems in agricultural activities is hampered by challenges that range from the lack of technical experts who can fly UASs and process data to the limited size of payloads. Furthermore, another critical challenge, for example, in the African context, is licensed UAS operators. Although various countries have enacted regulations that are legally binding and allow civilians to use drones for recreation and commercial purposes, it is expensive to enrol in drone pilot training in a civilian domain, thereby restricting the number of UAS users to only a few (Haula & Agbozo, 2020; McCarthy et al., 2023; Mokoena et al., 2023). As such, most of the population is disadvantaged because they cannot afford drone pilot training.

**Table 2-7: Summarised challenges and opportunities of UAS systems.**

| **Category** | **Challenge** | **Opportunities** |
|---|---|---|
| Technical challenges | ◆ Technical experts<br>◆ Limited size of the payload<br>◆ Short battery lifetime<br>◆ Lack of adequate knowledge | ◆ Improvement in community farming<br>◆ Advances in electronics micro-miniaturisation that will make UAS systems affordable<br>◆ Introduction of solar-powered UAS systems and lightweight battery technology |
| Policy and regulations issues | ◆ Lack of regulations and policies | ◆ Craft-related legislation and national/regional rules<br>◆ Ownership of farm data between farmers and service providers must be clearly defined.<br>◆ Ensure data security |
| Cost | ◆ High cost of UAS systems | ◆ Reduction in the labour force<br>◆ Balance of trade-off between the deployment of UAS versus the potential profits |
| Ethics and privacy | ◆ Invasion of privacy<br>◆ Universal public acceptance of UAS systems | ◆ Certifications or licenses that permit users to fly UAS systems<br>◆ |
| Cropping systems and lack of resources | ◆ Heterogeneous agro-ecological landscapes<br>◆ Lack of research in smallholder environments<br>◆ Lack of resources<br>◆ Awareness issues and lack of information | ◆ The incorporation of UAS systems will significantly improve productivity by increasing exactness in inputs rates and crop management practices.<br>◆ Because of limited space between crop constituencies, balancing the trade-off between spectral and spatial resolution is needed.<br>◆ Competitive advantage through the use of UAS system for the gathering of essential crop traits that are useful for decision making<br>◆ Putting resources together for centralised operations<br>◆ Increase awareness through capacity building, workshops, training and education |
| Environmental factors | ◆ Adverse weather conditions<br>◆ Shadows<br>◆ Seasonal variation | ◆ Improve UASs capabilities<br>◆ Develop algorithms for shadow detection and removal<br>◆ Careful consideration and planning<br>◆ Consider image acquisition at each crop growth stage |
| Data processing challenges | ◆ UASs and sensor type<br>◆ Feature extraction method<br>◆ Classifier model | ◆ Choose an appropriate UAS and sensor<br>◆ Choose appropriate models for feature extraction and a classifier |

### *2.5.3 Implication of the findings and opportunities for the application of UASs in smallholder farming landscapes*

Some key issues need to be addressed for UAS systems to be used in many developing countries, especially in marginalised and heterogeneous smallholder farming environments. Most of the reviewed articles noted that the deployment of these advanced technologies for mapping and monitoring fields was predominantly in monoculture systems. Under such an environment, UAS have been proven to be effective and robust for image classification, as demonstrated in this article. Considering the background of developing nations, agriculture is primarily characterised by smallholder farms that usually practice mixed cropping for different reasons. In such environments, there are still challenges to address and knowledge gaps to fill.

- Most researchers employed complex machine learning and deep learning algorithms; however, these algorithms obscure interpretability and hinder widespread adoption because of their difficulty. Intrinsically, there is a need to develop techniques and algorithms that can be employed to extract useful information from mixed cropping systems for decision-making.
- Similarly, several developing countries must develop favourable regulatory and policy requirements that allow researchers and other interested parties to operate UAS systems timeously.
- It is expected that with the continuous development of UAS systems, costs will be reduced due to competition, and many farmers will afford these systems for crop mapping and monitoring.
- Researchers should intensely focus on integrating freely available satellite data and UAS technologies to enable continuous crop mapping and monitoring even under adverse weather conditions. These technologies are typically utilised equally and separately; however, their differing capabilities (characteristics) may be useful to provide complementary data for crop mapping and monitoring. Hence, additional research is imperative to advance methodologies aimed at harnessing the strong synergies yet to be fully realised.
- Furthermore, research and development are required in the application of UAS systems in small-holder farming environments. More contributions and participation from government institutions, research centres, civil aviation, and equipment providers are critical for upscaling these advanced technologies from experiments to practical use in the fields.

In conclusion, it can be noted that accurate mapping and monitoring of crops in these intensive and highly dense agro-ecological landscapes is greatly affected by

1. Total number of crops in a tiny field (sometimes with no specific dominant crop),
2. Different planting dates cause cropping calendar overlaps,
3. Variations in crop mixtures, row spacing and crop density
4. Availability of ancillary data
5. Type and characteristic of the sensor used and
6. Soil quality, climatic and environmental factors.

## 2.6 Conclusion

In this study, we reviewed the applications of UAS in crop mapping and monitoring between 2012 and 2023. Numerous areas related to the use of UASs in crop mapping and monitoring were covered. As such, the paper attempted to provide a comprehensive survey of the unmanned aerial system types, sensor types, characteristics, and their application in different cropping systems. Based on the reviewed articles, it is noted that the successful application of UASs in agricultural activities is mostly based on sensor characteristics such as spectral range, weight, size, and cost. Despite all these efforts, there are still gaps and opportunities for crop discrimination in mixed cropping systems. The paper also presented various methods used for feature extraction and classification as part of the data analysis. It is critical to note that sensor selection and suitable algorithms to identify constituent crops in mixed cropping systems are greatly affected by spectral and spatial resolution. Thus, the selection or development of a suitable crop discrimination algorithm in heterogeneous landscapes is one of the current topics of discussion. Since most farmers in developing countries cannot afford state-of-the-art broadband multispectral and hyperspectral sensors, there is a need to test the applicability of new technologies, such as deep learning tools, to improve species separability using the affordable high spatial RGB images.

## 2.7 Summary

*This chapter examined the prevailing trends, technical challenges, and emerging opportunities associated with the application of unmanned aerial systems for crop discrimination. The discussion focused on the spatial distribution of published studies, the diversity of UAS platforms and their technical specifications, as well as the spectral domains and sensor types employed for crop classification. Additionally, it addressed data processing challenges associated with high-resolution imagery, particularly the requirement for sufficient image* *overlap to ensure accurate photogrammetric outputs. The findings revealed that the majority of research was conducted in Asia (primarily in China and Pakistan), followed by Africa, Europe, North America, South America, and Australia. Considerable variation in UAS design and flight endurance was noted, largely dictated by mission objectives and budget constraints. Rotary-wing UAS were found to be the preferred platform for crop mapping in smallholder farming systems due to their manoeuvrability. RGB sensors remained the most widely used owing to their affordability and accessibility, although there is growing adoption of multispectral and hyperspectral sensors for advanced crop analysis. Maize was identified as the most frequently studied crop, followed by rice and wheat, with approximately 90% of studies conducted in monoculture systems, highlighting a significant research gap in mixed cropping systems. Consequently, the subsequent chapters will explore the applicability of both hyperspectral and RGB sensors for identifying constituent crops in mixed cropping settings at different spatial scales, including the leaf and canopy levels.*

# CHAPTER 3 : SPECTRAL SEPARABILITY OF MIXED CROP AT FIELD LEVEL

This chapter is based on:

**Mafuratidze, P., Mutanga, O, Masocha, M. (in review).** Spectral separability of maize and soybean using hyperspectral data, *Computers and Electronics in Agriculture*. (Manuscript number: COMPAG-D-25-02423)

## ABSTRACT

Accurate discrimination of crops in mixed-cropping systems is critical for precision agriculture, yet achieving that remains challenging due to spectral similarities between species. This study evaluates the spectral separability of maize (*Zea mays*) and soybean (*Glycine max*) across five phenological stages using hyperspectral data (400–1100 nm) in mixed-cropping systems. The study integrated statistical analysis, distance, divergence, and machine learning methods to optimise band selection and timing. Field spectral measurements were analysed using ANOVA, Jeffries-Matusita (JM) distance, Transform Divergence (TD), Kullback-Leibler Divergence (KLD), and Partial Least Squares-Discriminant Analysis (PLS-DA). Peak separability between maize and soybean occurred during reproductive stages (DAP 85–110), with maximum JM values of 1.12 and 1.13 obtained in the red region (600–700 nm). These values reflect heightened divergence due to chlorophyll dynamics (red) and structural canopy differences (NIR). Minimal separability (JM < 0.2) was observed at early vegetative stages (DAP 15–36) due to spectral overlap. PLS-DA achieved near-perfect classification accuracy with an F1-score of 100% at mid-grain filling (DAP 85), leveraging red-edge (680–750 nm) and NIR (700–1100 nm) bands, while early stages (DAP 36) showed reduced accuracy with an F1-score of 82%. The study underscores the importance of phenological timing, identifying flowering to senescence as optimal windows for remote sensing surveys. These findings advance precision agriculture by prioritising spectral regions and growth stages of crop discrimination, with implications for scaling ground-based insights to airborne and satellite platforms.

**Keywords:** hyperspectral remote sensing, crop discrimination, phenological stages, spectral separability, precision agriculture, maize-soybean mixed cropping.

## 3.1 Introduction

Advancements in precision agriculture that involve detecting, identifying and monitoring specific crop types in mixed cropping systems are essential for resource allocation, herbicide application, acreage and yield estimation. Modern agriculture, widely known as precision agriculture, is characterised by site-specific management and has become increasingly popular even in smallholder farming environments. The commercial availability of numerous sensing, monitoring, and geospatial technologies makes these advancements appear safe, efficient, and economical (Manohar Kumar et al., 2024). Remote sensing is one of the most important elements in the precision agriculture industry and has been used to extract specific information about the biophysical and biochemical properties of plants. (Salas and Henebry, 2012). Hyperspectral data with numerous narrow and contiguous bands play a crucial role in advancing precision agriculture techniques by enhancing spectral separability between crops across different phenological stages.

Understanding the spectral characteristics of crops in mixed cropping settings can significantly improve crop monitoring, yield prediction, and resource management in agricultural practices. Since most vegetation species appear to have similar spectral reflectance responses, hyperspectral data with an electromagnetic spectrum ranging between 400 and 2500nm has been proven to indicate significant differences in some spectral regions (Cochrane, 2000; Qin et al., 2023; Schmidt and Skidmore, 2003; Sykas et al., 2013; Vaiphasa et al., 2007). The availability of spectral regions, including visible, red-edge, near-infrared and shortwave spectra, is crucial for identifying optimal wavebands and timing to discriminate between specific crop types.

Previous studies highlighted the potential of integrating machine learning algorithms and hyperspectral data in differentiating crop types across various phenological stages (Chivasa et al., 2019; Liu et al., 2022; Mafuratidze et al., 2020; Sencaki et al., 2019). However, further research is required to enhance the discrimination of key crops such as maize (*Zea mays*) and soybean (*Glycine max*), which are among the most widely cultivated crops globally and are often grown in mixed cropping settings. Despite their taxonomic differences, maize and soybean can exhibit quantitatively similar spectral signatures due to intraspecific variation (Huang et al., 2025). While distinct plant species generally have unique spectral characteristics, these signatures fluctuate based on factors such as growth stage, environmental stress, cropping systems, and ageing. However, discrimination of crop species within the same genus and in mixed cropping systems remains a challenge and frequently results in misclassification.

The classical approach for band and spectral region selection utilises wavelengths in the visible (VIS) (400–700 nm), red edge (680 – 780nm, near-infrared (NIR) (780–900 nm), shortwave infrared (SWIR-I) (900 – 1400nm), and shortwave infrared (SWIR-II) (1400 – 2500nm) to estimate spectral reflection of crops. Biochemical constituents (cellulose, lignin, hemicellulose, chlorophyll-*a* and -*b*, carotenoids, and anthocyanins) (Brewer et al., 2022; Gitelson et al., 2003), water and moisture content (Ndlovu et al., 2021b; Xia et al., 2022), nitrogen and crude protein content (Buchaillot et al., 2019; Crews and Peoples, 2004; Fu et al., 2020; Goñi et al., 2021), mineral and micronutrient content (phosphorus, potassium, magnesium, iron, calcium, sulphur, zinc, manganese) (Bhardwaj et al., 2022; Hassan et al., 2021), biophysical components (leaf cell structure and leaf dry matter content) (Ferencz et al., 2010; Imagery et al., 2018; Piiroinen, 2014) primarily influences the spectral response of crops. Therefore, these differences in leaf properties between maize and soybean should affect leaf reflectance measurements in the VIS, NIR and SWIR regions.

Numerous studies have confirmed the utility of hyperspectral data in accurately distinguishing between different crop types in various cropping systems. In South Africa, Abdel-Rahman and Ahmed (2008) reviewed hyperspectral imaging and spectroscopy to identify sugarcane varieties. The work of Ghiyamat et al. (2013) attempted to discriminate tree species with different ages and between six different tree species, including broadleaves, old Corsican pine, mature Corsican pine, young Corsican pine, old scots pine, and young scots pine with the same age using hyperspectral imagery over Thetford Forest in East Anglia. Aneece and Thenkabail (2018) in the United States explored the use of linear discriminant analysis (LDA) and support vector machines (SVM) to classify and separate five crops (corn, soybean, winter wheat, rice, and cotton) and their growth stages using hyperspectral data. They achieved overall accuracies ranging from 75% to 95% in classifying crop types across various growth stages. However, in this study, they did not explicitly define a single optimal growth stage suitable for crop discrimination. Still, they highlighted that the consolidation of growth stages led to improved classification accuracies.

Chivasa et al. (2019) focused on distinguishing maize varieties across five phenological stages by selecting suitable spectral bands at each growth stage using an Apogee spectrometer. It is important to note that numerous bands selected as optimal bands for variety discrimination were mainly in the VIS (400, 455, 545, 625, and 680 nm) and NIR region (705, 720, 765, 840, and 895 nm). Partial least squares-discriminant analysis (PLS-DA) results indicated crop discrimination was most suitable at flowering and the onset of senescence. Singh et al. (2022) utilised data obtained from ASD FieldSpec®4 and AVIRIS NG to discriminate various crops, including wheat, maize, tobacco, sorghum, linseed, castor, pigeon pea, fennel and chickpea in the Anand district of Gujarat, India. To discriminate these crops, they employed different supervised classifiers such as spectral angle mapper, spectral information divergence, support vector machine, minimum distance classifier, binary encoding, convolution neural network, adaboost, discriminant and RusBoost. From that same work, they concluded that convolutional neural networks yielded the best results with an overall accuracy of 89%. Recently, Tan et al. (2025) attempted to select bands for crop identification in Salinas Valley and Indiana, USA. This study selected various crops for discrimination, including maize, vineyard, broccoli, celery, fallow land, soybean, grapes, oats, wheat, grass, and lettuce. Their study showed that maize exhibited the lowest classification performance, indicating challenges in distinguishing it from other crops due to spectral similarities. These studies demonstrate that strategically selecting optimal spectral bands and regions allows researchers to capitalise on the distinct spectral signatures of different crops, enabling effective differentiation between plant types and improving crop classification systems' precision.

While machine learning algorithms have improved crop classification (Chivasa et al., 2019; Liu et al., 2022), discriminating taxonomically distinct crops in mixed systems remains challenging. For instance, Tan et al. (2025) reported low classification accuracy for maize due to spectral overlap with other crops. These limitations underscore the need to identify the growth stage-specific spectral signatures and refine band selection strategies. Despite these advances, limited studies are focusing explicitly on the spectral separability of maize and soybean across multiple phenological stages in mixed cropping systems. This study aims to address this gap by investigating whether subtle spectral differences between these crops can be detected and quantified using hyperspectral data. Accordingly, the specific objectives of this research are to (i) evaluate spectral separability between maize and soybean, (ii) determine effective spectral bands and regions that maximise class separability, (iii) identify the optimal phenological stage for accurate crop discrimination, and (iv) assess the performance of statistical, distance-based, and machine learning algorithm in quantifying crop separability across phenological stages.

## 3.2 Materials and Methods

### *3.2.1 Study area*

The study was located at Panmure Research Station of the Department of Research Specialist and Services under the Ministry of Lands, Agriculture, Fisheries, Water, and Rural Development, Shamva District, Zimbabwe. The experimental site covered 0.34 ha with 25 plots constituting various crop mixtures of maize and soybean. Researchers experimented using a factorial randomised complete block design with five replications. Each plot measured 17 m × 5 m (0.0085 ha). In the monoculture maize plots, the spacing of the crops was 60 cm between rows and 90 cm between rows. The mixed-crop configuration used 60 cm spacing for the maize rows and 25 cm in-row spacing for the soybean rows, with 45 cm between rows. The experiment relied on rainfall for the plots, and all crop species were planted between January 14$^{th}$ and 15$^{th}$, 2021.

### *3.2.2 Data collection*

Data collection began two weeks after planting, and it continued until the later stages of maize phenology using the days after planting (DAP) method, as shown in Table 3-1. Spectral reflectance data for maize and soybean were collected under controlled laboratory conditions to minimise environmental variability. Leaves were sampled from field-grown plants at five critical phenological stages: early vegetative (DAP 15), mid-vegetative (DAP 36), flowering/tasselling (DAP 48), mid-grain filling (DAP 85), and senescence onset (DAP 110) across diverse maize-soybean intercropping configurations. Immediately after field sampling, representative leaves were transported to a darkroom to ensure stable measurement conditions. To preserve leaf freshness and minimise physiological degradation, all spectral measurements were conducted within 24 hours of sample collection, ensuring minimal chlorophyll degradation (Gitelson et al., 2003). A handheld StellarNet spectrometer (model: BLK-CXR-SR, StellarNet Inc., USA) was used to acquire the maize and soybean spectral reflectance data. Measurements of hyperspectral leaf reflectance were acquired by pointing the fibre optic cable with a 30° field of view at a distance of 0.1 m above the leaf in the darkroom. StellarNet spectrometer could record low noise spectral reflectance data from UV-VIS-NIR wavelength range, covering 220 to 1100 nm wavelength region at 0.5 nm spectral interval. A calibrated white plate (StellarNet plate), a 50mm diameter white, was used on the leaf every 10 to 15 measurements to offset any change in atmospheric conditions and provide light irradiance.

**Table 3-1: Plant phenological stages used in this study.**

| **Growth Phase** | **Days After Planting (DAP),** | **Key Spectral Characteristics** | **Reference** |
|---|---|---|---|
| Early Vegetative | 15 | Low NIR, increasing chlorophyll absorption in blue and red | (Varela et al., 2018) |
| Mid-Vegetative | 36 | High NIR reflectance, increasing canopy cover | (Y.-P. Wang et al., 2022) |
| Flowering/Tasselling | 48 | Substantial red-edge shift, peak chlorophyll content | (Kharat and Musande, 2015) |
| Mid-Grain Filling | 85 | Decisive red-edge shift, peak chlorophyll content | (Chivasa et al., 2020) |
| Onset of Senescence | 110 | Stable high NIR, increasing SWIR for water stress detection | (M. Feng et al., 2014) |

### *3.2.3 Data preprocessing*

Since there were five data acquisitions, a total of 400 spectral measurements were collected across all plots, with 50 spectra per crop plot. We repeated the processing steps for each dataset using Python version 3.11.5 in Spyder version 5.5.6, an Integrated Development Environment (IDE). We pre-processed the data to ensure that the spectral data was clean, formatted, properly structured and optimised for further analysis. The only techniques used for preprocessing were

(i) the application of the Savitzky-Golay filter to reduce high-frequency noise while preserving spectral features important for crop discrimination; (ii) standardisation (feature scaling) to normalise reflectance values across all spectral bands, ensuring comparability and improving classifier performance; and (iii) spectral resampling into different spectral zones: blue (400 – 500nm), red (600 – 700nm), green (500 – 600nm), near-infrared (NIR) (700 – 900nm) and shortwave infrared (SWIR-I) (900 – 1100nm). These spectral regions are essential for the utilisation of their sensitivity to pigments, chlorophyll, carotenoids, biomass, lignin-cellulose content, and leaf cell structure for crop discrimination.

### *3.2.4 Spectral separability analysis*

#### 3.2.4.1 Statistical analysis

To clarify the procedure for band selection and the underlying statistical assumptions, spectral bands were considered significant for crop discrimination if the post-hoc Tukey Honestly Significant Difference (HSD) test indicated p-values below 0.05 or 0.01, corresponding to 95% and 99% confidence levels, respectively. Prior to conducting the one-way ANOVA, key assumptions were verified: (i) normality of residuals using the Shapiro-Wilk test, (ii) homogeneity of variances across groups using Levene's test, and (iii) independence of observations based on the experimental design. ANOVA was then performed to detect statistically significant differences among the mean reflectance values for maize and soybean at each phenological stage. Where significance was detected, Tukey HSD tests and the studentised range distribution were applied to identify specific pairs of wavelengths or spectral regions that differed significantly, thereby informing the selection of optimal narrow bands and spectral zones for crop discrimination. This detailed approach ensures that only spectrally meaningful bands, with verified statistical validity, were considered in subsequent analyses.

#### 3.2.4.2 Distance-based separability metrics

To reduce spectral dimensionality and assess how well the selected wavelengths and spectral regions separate the maize and soybean, we employed distance-based separability metrics. These distance-based separability metrics are used to quantify the dissimilarity between spectral signatures of maize and soybean, which is crucial for evaluating the performance of each wavelength and spectral region. Additional methods employed to assess significant differences between maize and soybean included Jeffries Matusita (JM) distance to identify spectral bands, Transform Divergence (TD) to highlight phenological stages with significant mean reflectance differences and Kullback-Leibler Divergence (KLD) to detect asymmetric divergence patterns (Table 3-2). Researchers have widely applied these distance-based separability metrics in various remote sensing studies, including vegetation density mapping in heterogeneous river floodplains (Verrelst et al., 2012), band selection for optimal feature extraction (Vaiphasa et al., 2007), spectral separability analysis for species discrimination in tropical environments (Ferreira et al., 2013), and the estimation the degree of spectral overlap between leaves and flowers (Campbell & Fearns, 2018).

The JM distance to measure the separability between the spectral reflectance distributions of maize and soybean was employed. This JM distance is derived from the Bhattacharyya Distance and is bounded between zero (no separability) and two (maximum separability). According to Kailath (1967), the JM distance is calculated as follows;

$$\mathrm{JM} = \sqrt{2\,(1 - e^{-B})} \tag{1}$$

where B is the Bhattacharyya Distance using the following formula:

$$\mathrm{B} = \frac{1}{8}(\mu_1 - \mu_2)^T \left(\frac{C_1+C_2}{2}\right)^{-1} (\mu_1 - \mu_2) + \frac{1}{2}\ln\left(\frac{\left|\frac{C_1+C_2}{2}\right|}{\sqrt{|C_1||C_2|}}\right) \tag{2}$$

where $\mu_1$ and $\mu_2$ are mean vectors, and $C_1$ and $C_2$ are the covariance matrices of the two classes. For Transform Divergence (TD)(Sencaki et al., 2019), which quantifies spectral divergence between crop types, the formula is as follows.

$$\mathrm{TD} = \frac{1}{2}Tr((C_1 + C_2)(c_2^{-1}\text{-}c_1^{-1})) + \frac{1}{2}Tr(((c_2^{-1} + c_1^{-1})\,(\mu_1 - \mu_2)(\mu_1 - \mu_2)^T \tag{3}$$

Where TD is the Transform Divergence separability value, and Tr denotes the trace of a matrix For Kullback-Leibler divergence (KLD) that assesses information gain between spectral signatures, the formula is as follows;

$$\mathrm{KLD}\,(w_1||w_2) = \frac{1}{2}\left(Tr(c_2^{-1}C_1) + (\mu_2 - \mu_1)^T c_2^{-1}(\mu_2 - \mu_1) - \ln\left(\frac{|C_1|}{|C_2|}\right) - d\right) \tag{4}$$

Where $w_1$ and $w_2$ are maize and soybean, and d is the dimensionality of the data

**Table 3-2: Summary of distance-based separability metrics.**

| Metric | Range | Sensitivity | Computation | Use Case | Reference |
|---|---|---|---|---|---|
| JM | 0–2 | Covariance + Mean | Moderate (matrix inverse) | Robust class separability assessment | (Sencaki et al., 2019) |
| TD | 0–2 but values >2000 are often capped | Mean differences | Simple | Quick separability screening | (Sencaki et al., 2019) |
| KLD | 0–∞ | Asymmetric divergence | Complex | Directional dissimilarity analysis | (Georgiou & Lindquist, 2003) |

Tukey HSD, JM, KLD, and TD values for paired data groups across the natural wavelength regions blue, green, red, NIR, and SWIR were analysed and compared for each phenological stage. This comparison facilitated the identification of the spectral bands, spectral regions, and phenological stages that exhibited the highest separability values. To conclude the analysis, spectral separability between maize and soybean was quantified by classifying the two species using partial least squares discriminant analysis (PLS-DA). This approach has demonstrated consistent superiority over traditional feature selection methods and has been widely validated as an effective tool for discriminating plant species based on spectral signatures.

## 3.3 Results

### *3.3.1 Spectral responses for maize and soybean from phenological stages.*

Figure 3-1 presents the mean and standard deviation of vegetation spectral reflectance patterns for maize and soya across different phenological stages, from early vegetative (DAP15), mid-vegetative (DAP36), flowering/tasselling (DAP48), mid-grain filling (DAP85), to the onset of senescence (DAP110). The reflectance patterns showed the same trends for different growth stages; however, during early and mid-vegetative stages, the reflectance of maize and soybean gradually increased from the blue region to the near-infrared region with almost similar spectral responses. During these early growth stages, both maize and soybean crops exhibited relatively low reflectance across the entire spectrum. Furthermore, maize shows slightly higher reflectance than soybean, particularly in the green region (around 550 nm) and near-infrared region (700-1100 nm). The flowering/tasselling indicates that the reflectance pattern for both crops continued to increase, suggesting further growth and development, especially from the visible region to the near-infrared region. However, a noticeable change began to emerge at approximately 700 nm for both maize and soybean crops. At this stage, both crops began to show characteristics of healthy vegetation through a sharp increase in reflectance between the red and near-infrared regions. During mid-grain filling and the onset of senescence, the red edge was very pronounced on both crops, indicating vigorous growth. However, soybeans have a slightly higher reflectance in the near-infrared region than maize due to differences in leaf structure and canopy architecture. At the onset of the senescence stage, spectral responses in the near-infrared region remained relatively high, but the red edge was less pronounced compared to the mid-grain filling stage. This decrease indicates senescence or the beginning of crop maturity, where the chlorophyll content decreases. Overall, there were noticeable similarities in the spectral reflectance patterns of maize and soybean.

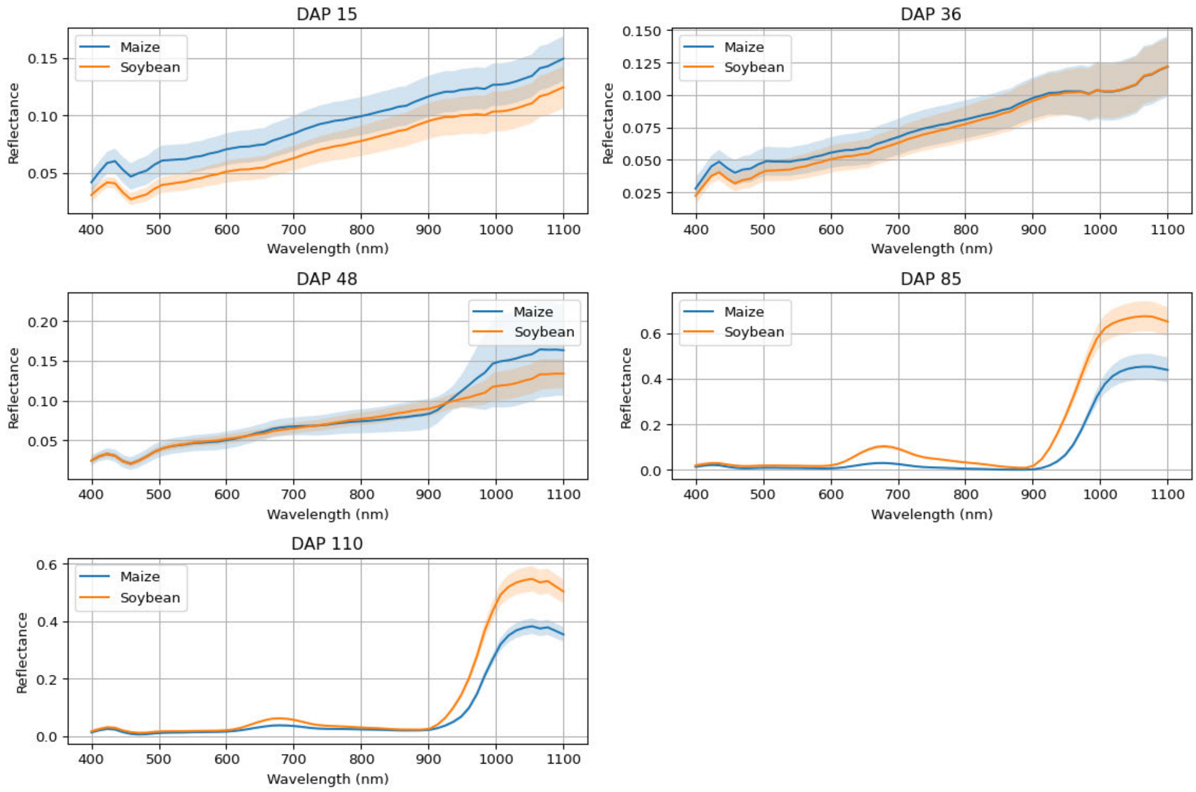


**Figure 3-1: Spectral responses of maize and soybean with days after planting. The solid lines represent the mean reflectance values, while the shaded regions denote the 5th and 95th percentile bounds of reflectance across all samples.**

### *3.3.2 ANOVA statistical analysis for band selection.*

The statistical analysis using ANOVA, as shown in Figure 3-2, indicated that there was a significant difference in reflectance between maize and soybean when a 99% ($p < 0.01$) and 95% ($p < 0.05$) confidence level was used across the growth stages. However, the 95% confidence level using red bands indicated that there is no statistically significant difference in the spectral reflectance between maize and soybean, with $p>0.05$. This was also noticeable in the blue band with a $p>0.05$.

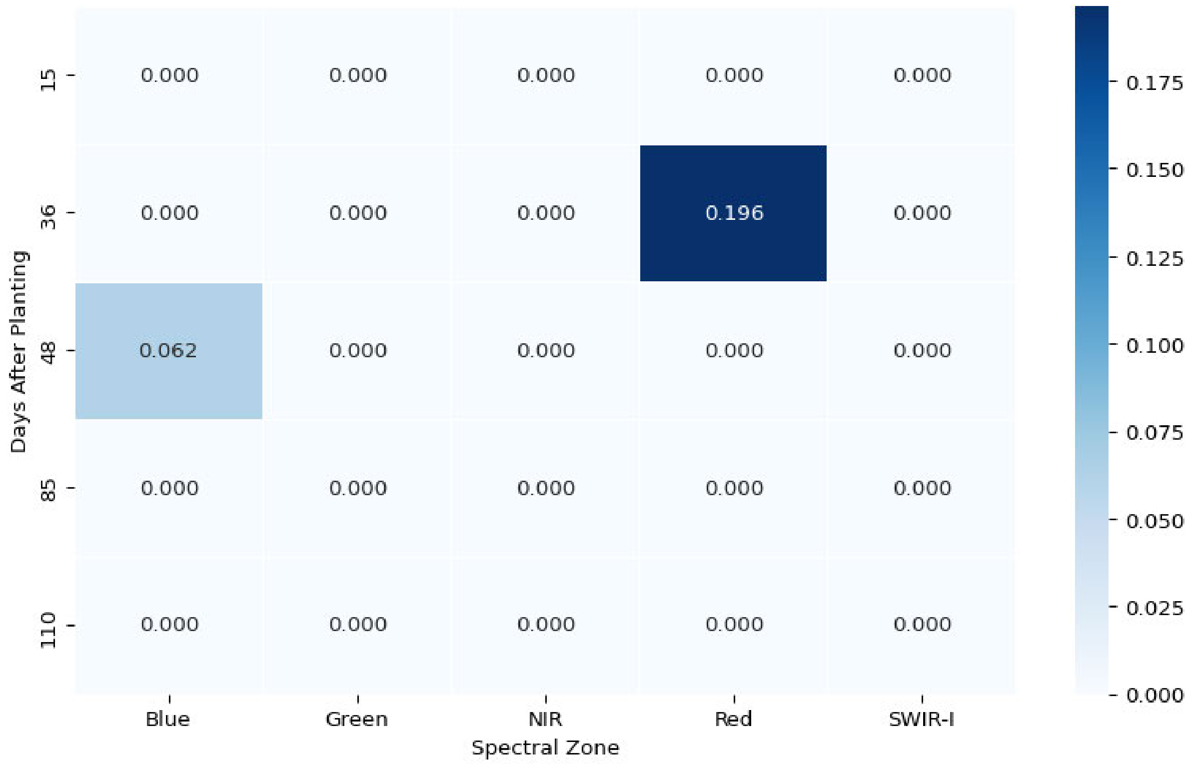


**Figure 3-2: ANOVA results for days after planting across spectral regions.**

However, as shown in Figure 3-3, the various growth stages indicate that there was a significant difference in reflectance between maize and soybean, from early vegetative to the onset of senescence. For DAP15 and DAP36, the F-value was relatively high in the blue region (around 400-500 nm). However, it gradually decreases from 450 to 1100 nm, indicating minor differences between maize and soybean reflectance at these stages. However, there was high variability for DAP48, DAP85 and DAP110, indicating spectral overlap. The results suggest that the F-values for DAP48 peaks in the red between 550 and 610 nm and near-infrared regions between 625 and 711 nm, signifying that the most significant differences in reflectance between maize and soybean are occurring in these spectral regions. These high F-values were also present between 850 and 910 nm, and they sharply increased from 950 to 1100 nm. DAP85 results show the highest F-values in the red edge region (640 to 711nm). Finally, the F-values pattern for DAP110 was similar to DAP48, which shows peaks in the red and near-infrared regions but with lower overall values. This suggests that, while differences are still present, they are less pronounced than at DAP48 and DAP85.

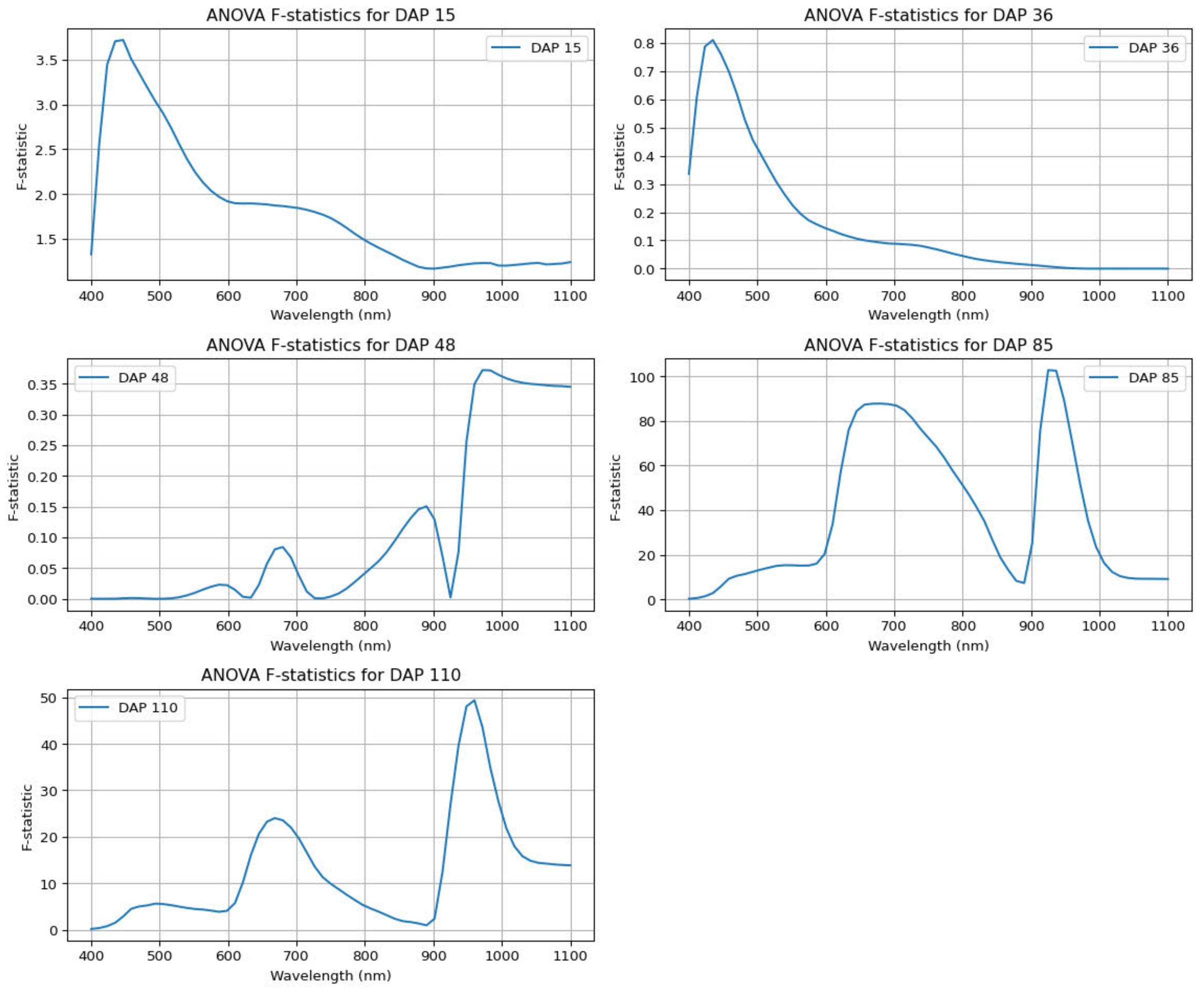


**Figure 3-3: F-statistics for reflectance differences between maize and soybean across growth stages.**

### *3.3.3 Distance and divergence analysis for determining spectral zone importance*

Figure 3-4 indicates three distinct spectral separability outcomes, namely low measure of separability, medium measure of separability, and high measure of separability calculated from DAP15 to DAP110. In the early growing season, which includes early vegetative, mid-vegetative, and flowering/tasselling (DAP 15, 36 and 48), there were primarily low JM distance values of less than 0.2 across all spectral bands. This result highlights that the spectral reflectance values of maize and soybean are very similar, making it difficult to discriminate between them at that stage. This typically occurs because crops may not have developed distinct spectral signatures. However, environmental conditions and surrounding backgrounds, such as soil characteristics and shadows, effectively affect spectral responses at this growth stage. At DAP85, there was a significant increase in JM distance values from 0.13 for the blue band to 1.12 for the red band. These results suggest a strong spectral separability between the crops, indicating that maize and soya have developed unique spectral signatures, most likely due to differences in chlorophyll content, canopy structure, or water absorption properties. However, the highest JM Distance value of the range between 0.32 and 1.13 was obtained in the SWIR-1 and red band at DAP85 and DAP110, respectively, indicating that these spectral regions are the most effective for crop discrimination at this stage. Differences in water absorption or structure are more important at this stage than the biomass-related differences that characterise this far-infrared region.

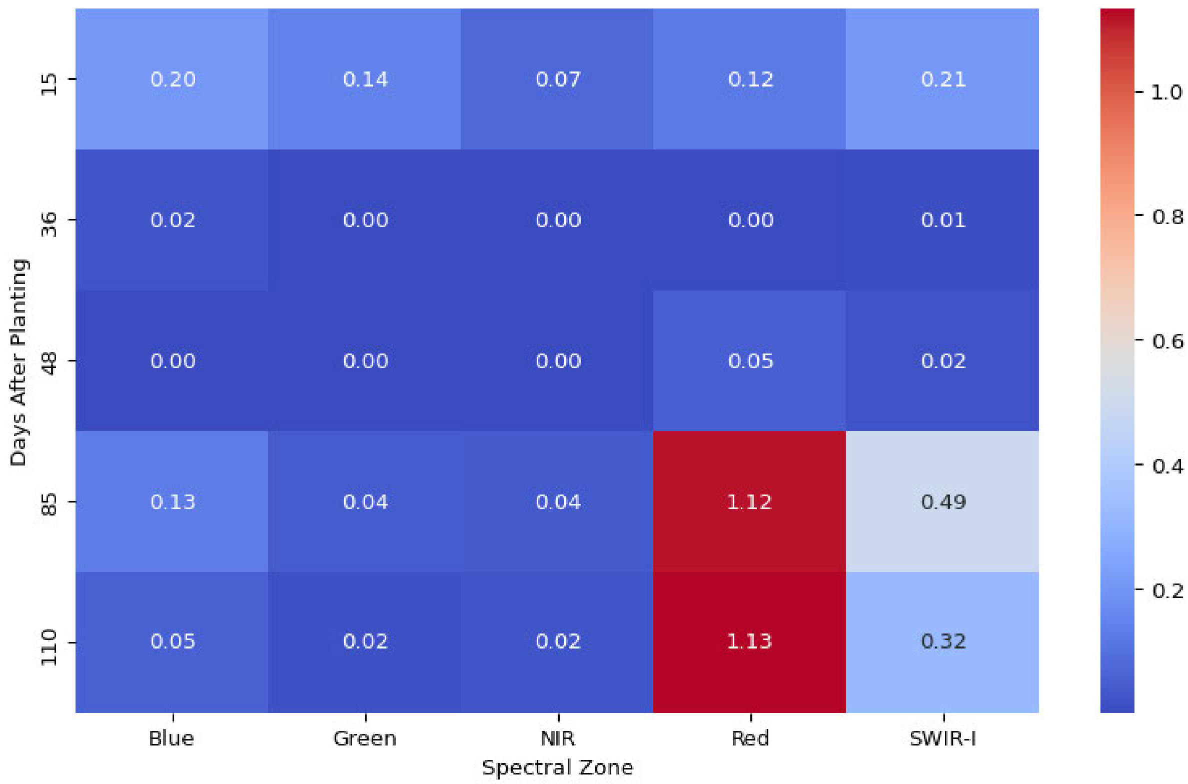


**Figure 3-4: Spectral separability between maize and soybean across spectral zones and phenological stages.**

### *3.3.4 Analysis of the statistical divergence*

Overall, the KLD and TD divergence trends are consistent across the phenological stages using different spectral regions, as shown in Figure 3-5. From DAP15 to DAP48, they show relatively low values across all spectral zones. These results indicate that the spectral responses of maize and soybean are similar during these early growth stages, making them difficult to distinguish. An interesting part is that, for KLD and TD values at DAP85, they show an abrupt increase, particularly in the red and SWIR-I spectral regions, as compared to others, indicating high chances of separability and dissimilarity between spectral responses of maize and soybean. Finally, the KLD and TD gradually decreased, particularly for all other spectral regions except for the KLD values of blue and NIR bands, suggesting that maize and soybean are still relatively distinguishable at this later growth stage. It is important to note that both measures show similar patterns of divergence across different DAPs and spectral regions, suggesting that they provide comparable information about the spectral separability of maize and soybean.

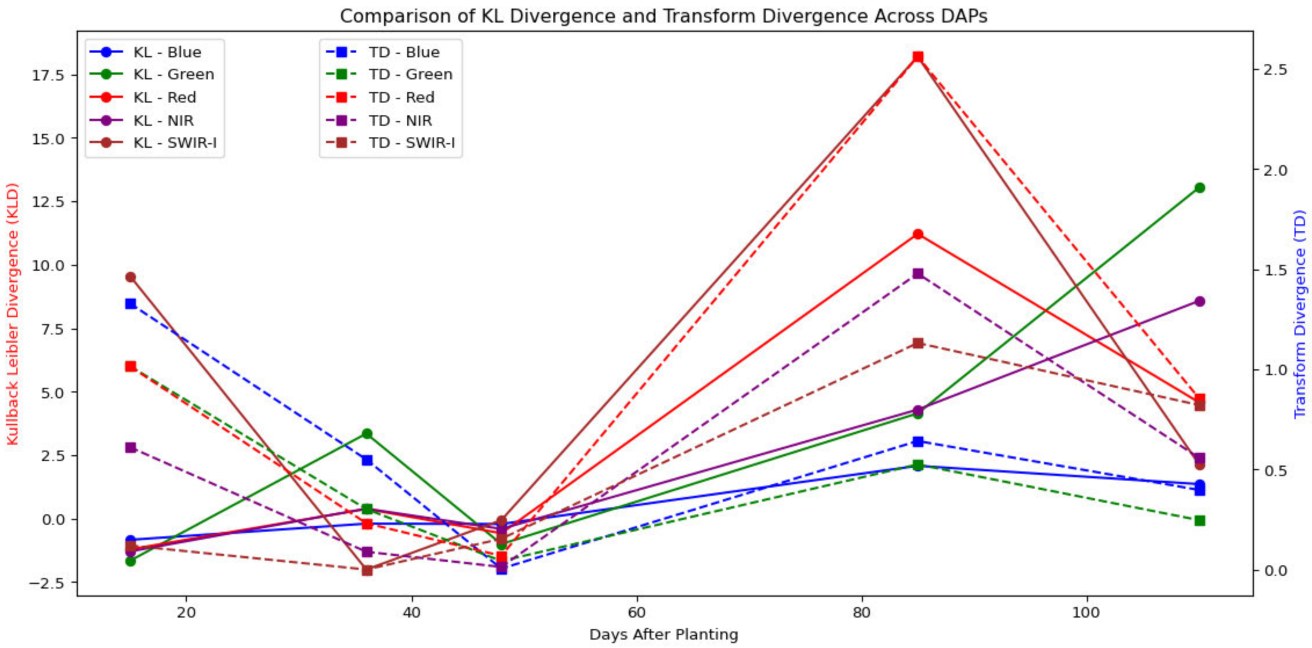


**Figure 3-5: Comparison of Kullback-Leibler Divergence (KLD) and Transform Divergence (TD) across different spectral regions and days after planting.**

### *3.3.5 Machine learning-based feature selection.*

Figure 3-6 and Table 3-3 show the PLS-DA selected bands for crop discrimination between maize and soybean, ranging from DAP15 to DAP110. In Figure 3-6, each line indicates the selected wavelengths identified by the PLS-DA algorithm as most important for discriminating between maize and soybean at that specific DAP. The figures show that the chosen bands for discriminating between maize and soybean vary across different DAPs, highlighting the importance of considering the growth stage when selecting spectral bands for crop classification. Both figures show that most bands chosen for DAP15 and DAP36 are primarily in the blue (400–450 nm) and SWIR (1000–1100 nm) regions, likely capturing differences in initial pigment composition and water content. Although these bands provide some information, their importance is lower than NIR and SWIR-I for crop discrimination. At reproductive stages DAP48 and DAP85, red-edge (680–750 nm) and near-infrared (NIR: 700–1100 nm) bands dominated, aligning with heightened chlorophyll activity and canopy structural complexity. These regions are sensitive to crops' structural and biochemical properties, which change significantly during the growing season, allowing for better crop discrimination. By senescence (DAP110), green (550–600 nm), red (600–650 nm) and persistent NIR bands provided separability, driven by pigment degradation and residual structural contrasts. Overall, the selected optimal bands for crop discrimination varied significantly across different phenological stages, highlighting the importance of considering the growth stage. The red and NIR regions consistently show important bands for discriminating between maize and soybean, particularly at later growth stages (DAP85 and DAP110).

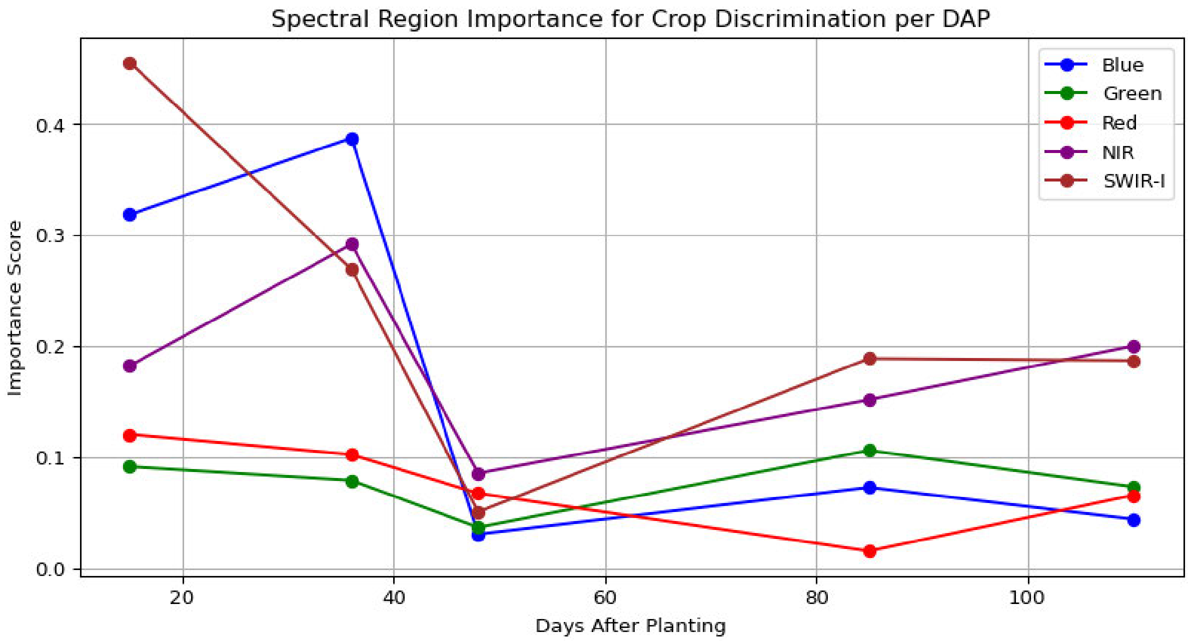


**Figure 3-6: Spectral regions' importance for crop discrimination across different days after planting.**

**Table 3-3: Selected top 10 optimal wavelengths.**

| Rank | DAP15 | DAP36 | DAP48 | DAP85 | DAP110 |
|---|---|---|---|---|---|
| 1 | 1100 | 435 | 696 | 517 | 731 |
| 2 | 1011 | 400 | 699 | 493 | 727 |
| 3 | 1057 | 431 | 602 | 497 | 723 |
| 4 | 1061 | 427 | 703 | 513 | 719 |
| 5 | 423 | 423 | 707 | 583 | 579 |
| 6 | 419 | 404 | 598 | 501 | 587 |
| 7 | 404 | 419 | 711 | 505 | 559 |
| 8 | 416 | 416 | 594 | 509 | 715 |
| 9 | 412 | 408 | 591 | 579 | 583 |
| 10 | 408 | 412 | 587 | 575 | 563 |

## 3.4. Discussion

The key findings of this study provide critical insights into the spectral discrimination of maize and soybean across key phenological stages. These results indicate a dynamic interplay between crop growth progression and spectral reflectance patterns. These results underscore the importance of phenology-driven spectral band selection for accurate crop discrimination, with implications for remote sensing applications in precision agriculture and crop monitoring.

### *3.4.1 Crop spectral reflectance patterns and phenological dynamics*

The analysis of the mean vegetation spectra revealed distinct trends in reflectance patterns across the growing season, mirroring the physiological changes associated with plant development in both crops. Figure 3-2 indicates that the observed seasonal mean vegetation spectra align well with established principles of vegetation optics. The low reflectance in the visible region (400–700 nm) during early growth stages is attributable to chlorophyll absorption. In contrast, the gradual rise in near-infrared (NIR) reflectance reflects increasing leaf area and canopy complexity. Overall, our results indicate that the discrimination of crops is highly effective at early and late growth stages but struggles during mid-season (DAP36). This result partially harmonises with the findings of Chivasa et al. (2019), who reported an absence of significant spectral difference at early and mid-vegetative stages (DAP15 and 36) due to soil background and shadow interference. In the present study, although such interference was also evident, higher crop discrimination was nonetheless achieved at the early stages. Typically, at this growth stage, both crops exhibit a relatively low reflectance across the entire spectrum. These similarities in spectral reflectance can be attributed to the comparable physiological states of the two crops during this early development.

The flowering/tasselling stage (DAP48) and mid-grain filling (DAP85) marked a transition where maize and soybean exhibited a noticeable red edge characteristic. Maize shows a slightly higher reflectance than soybean, particularly in the green region (around 550 nm) and in the red edge region (650-900 nm). Our findings have confirmed that the red and NIR regions are important in discriminating maize and soybean at later growth stages. DAP (48, 85 and 110) shows that Near-Perfect to perfect discrimination results with accuracy ranging from 0.995 to 1, as shown in Table 3-4. This trend is consistent with previous studies by Salas and Henebry (2012), who employed a chlorophyll red-edge index with bands ranging between 690 and 800 nm and observed that the maize and soybean spectra correspond to peak chlorophyll content and photosynthetic activity. Salas and Henebry (2012) and Chivasa et al. (2019) showed that maize plants have denser canopies and higher chlorophyll content, contributing to stronger light absorption in the visible region and higher reflectance in the near-infrared region.

**Table 3-4: Accuracy assessment results of PLS-DA across phenological stages.**

| DAP | Accuracy | Precision | Recall | F1-score | Kappa |
|---|---|---|---|---|---|
| 15 | 0.952 | 0.945 | 0.961 | 0.953 | 0.905 |
| 36 | 0.824 | 0.827 | 0.820 | 0.823 | 0.648 |
| 48 | 0.995 | 0.993 | 0.996 | 0.996 | 0.994 |
| 85 | 1.000 | 1.000 | 1.000 | 1.000 | 0.999 |
| 110 | 0.997 | 0.998 | 0.997 | 0.997 | 0.995 |

The spectral differences of maize and soybean were more pronounced at longer wavelengths compared to other regions, which is consistent with prior studies by Manjunath et al. (2011) linking red-edge shifts to vegetative vigour, making them useful for crop discrimination. The decline in red-edge prominence during senescence (DAP110) mirrors chlorophyll degradation, a hallmark of crop maturation. A decline in chlorophyll content leads to a reduction in the sharpness of the red edge, which is a common indicator of plant ageing and the onset of physiological maturity. Notably, soybean's higher NIR reflectance compared to maize at later stages likely stems from structural differences; soybean's denser, multi-layered canopy may enhance NIR scattering, whereas maize's upright architecture could reduce multiple scattering effects. The findings are similar to those of Li et al. (2024), who noted that the red-edge regions, followed by the green and NIR bands, exhibited the highest separability of stressed pine trees. Despite these subtle differences in growth stages, the overall similarity in spectral reflectance patterns between maize and soybean highlights the challenges in distinguishing these crops based solely on untransformed spectral data, particularly at early growth stages.

### *3.4.2. Statistical significance of spectral differences between maize and soybean.*

As presented in Figure 3, the ANOVA results revealed that there were no significant differences in the reflectance spectra between maize and soybean at a 99% confidence level. However, at a 95% confidence level, a statistically significant difference was observed in the shortwave infrared (SWIR) region, particularly for bands corresponding to water absorption features. The 95% confidence level identified the SWIR, blue, and green bands as discriminatory. This suggests that differences in crop water content or canopy structure become more apparent in the SWIR region, which is sensitive to water and other biophysical properties. The p-values observed in the blue and green areas further indicate that, although reflectance patterns in these regions are somewhat similar across the two crops, subtle differences can still be detected, particularly during the flowering and mid-grain filling stages. This suggests that broad-stroke spectral comparisons mask stage-specific differences.

The F-value peaks in red (550–610 nm) and NIR (625–711 nm) regions during DAP48 and DAP85 (Figure 3-3) highlight these regions as critical for differentiation during reproductive stages. The high F-values observed at these stages suggest that these spectral regions are most informative for discriminating between maize and soybean, aligning with the physiological changes associated with the reproductive and maturity stages. These findings align with distance and divergence analyses (JM, KL, TD), where heightened separability in the red region at DAP85 and 110 with JM values of 1.12 and 1.13, respectively, which underscores the role of water content and structural disparities in late-season discrimination (Morell-Monzó et al., 2023). These results emphasise that phenological timing is pivotal because other stages showed challenges in distinguishing due to overlapping spectral signatures and the influence of environmental factors: classifiers relying on static band sets may underperform compared to models adaptive to growth stages. The consistent identification of the red, near-infrared and SWIR bands (Morell-Monzó et al., 2023; Zhang et al., 2025) is crucial for discrimination, particularly at the flowering/tasselling stage and mid-grain filling, aligns with the physiological changes observed and the statistical significance identified through ANOVA and divergence analyses (Figure 3-7). The results of this study are consistent with those of Sencaki et al. (2019), who noted that flowering and establishment produced the best ability to discriminate between crops, as their JM and TD values were very high.

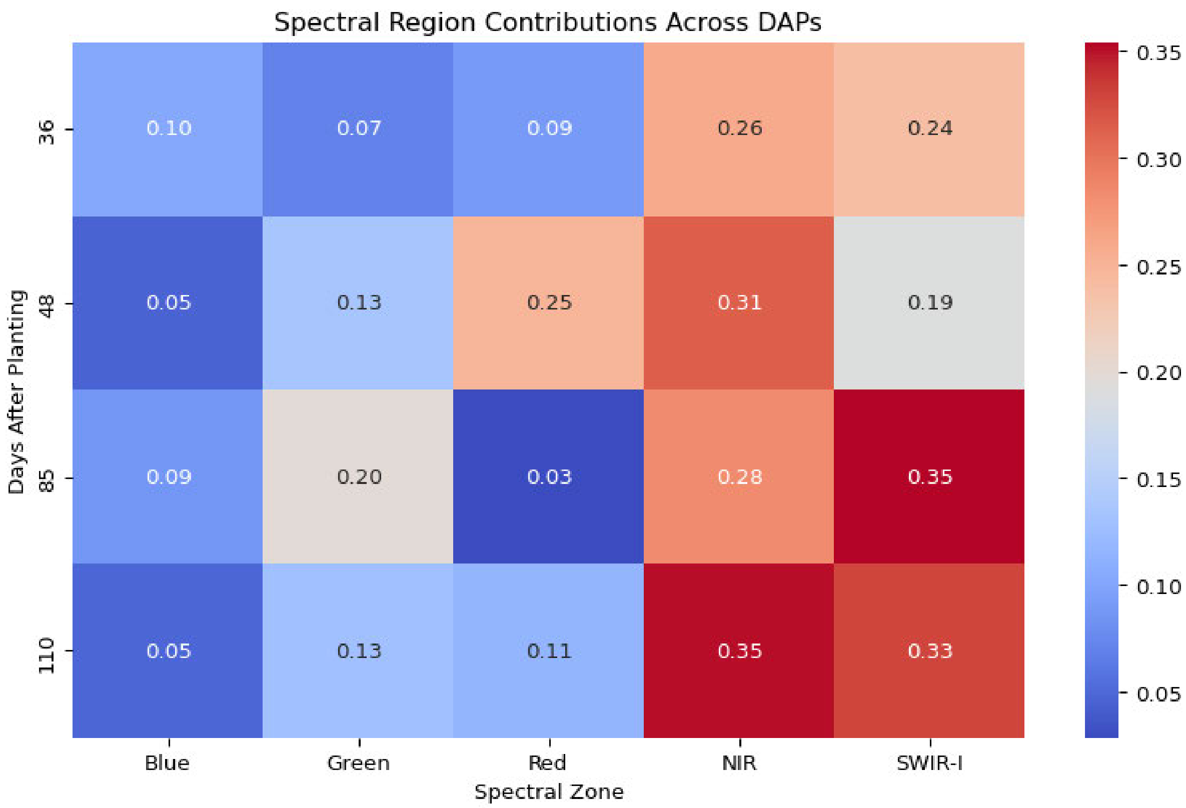


**Figure 3-7: Heatmap showing the contribution of different spectral regions across various days after planting.**

The heightened spectral separability observed during the reproductive stages suggests that remote sensing surveys for crop discrimination in mixed-cropping systems are most effective when timed with these phenological stages. This insight has direct implications for optimising the timing of aerial surveys in precision agriculture practices. However, although this study advances the understanding of crop spectral dynamics, certain limitations warrant consideration. Crop discrimination using spectral features is challenging, especially during the phenological stages. The analysis focused on only maize and soybean crop species in a single growing season; validation across diverse genotypes and environments is needed to generalise these findings. Environmental factors, such as soil and surrounding background, nutrient availability, and shadows, were not explicitly modelled but may influence spectral responses.

## 3.5. Conclusion and future work

This study identified important bands and spectral regions to be used for the discrimination of maize and soybean crops. Our results demonstrate that while conventional statistical methods such as ANOVA, divergence metrics, and distance-based analysis can differentiate maize and soybean at specific phenological stages, their discriminative power is highly stage-dependent. By integrating these analyses with hyperspectral data collected in a mixed cropping context, this study provides novel insights into optimal wavebands and phenological timing for crop discrimination under field conditions. Overall, our analysis further demonstrated the dynamic nature of the spectral separability between maize and soybean across different phenological stages. While early growth stages present challenges owing to overlapping spectral signatures, later stages, particularly at the flowering/tasselling stage and mid-grain filling, offer enhanced separability, primarily in the red and near-infrared regions. The integration of statistical and machine learning techniques provides a comprehensive framework for identifying the optimal spectral bands for crop discrimination, contributing to improved remote sensing applications in agriculture. Therefore, we conclude that the integration of statistical, divergence, and machine learning approaches consistently identifies red, NIR, and SWIR bands as critical during the flowering/tasselling stage and mid-grain filling stages.

The findings of this study underscore the potential of scaling ground-based spectral measurements to airborne and satellite remote sensing platforms for large-area crop discrimination. Imaging sensors could enhance the spatial and temporal resolution of crop classification maps by focusing on phenology-specific spectral zones, particularly the red-edge, NIR, and SWIR regions, during reproductive and senescence stages. However, to operationalise this transition, future research must address critical challenges, including the integration of state-of-the-art sensors in unmanned aerial systems with high spatial resolution. Such platforms could bridge the gap between localised leaf-level measurements and landscape-scale observations while minimising atmospheric and soil background interference. Furthermore, combining spectral data with environmental covariates such as soil moisture, temperature, and topography through multi-sensor fusion frameworks may disentangle confounding factors that obscure crop-specific signals, particularly during early growth stages. While our study demonstrates the utility of integrating spectral separability metrics (Jeffries-Matusita distance, Transformed Divergence and Kullback-Leibler Divergence) with PLS-DA for phenology-driven discrimination between maize and soybean, classification challenges persist during early growth stages, primarily due to spectral overlap and environmental variability. Future research should explore advanced machine learning models, such as random forest, support vector machines and extreme gradient boosting, which are well-suited to capturing non-linear relationships in high-dimensional hyperspectral data. Additionally, hybrid frameworks that adaptively weigh key spectral regions, such as the red-edge and NIR band alongside relevant environmental covariates (e.g., soil moisture, canopy temperature), may enhance classification robustness. The generalisability of our findings, limited to a single growing season in Zimbabwe's mixed-cropping systems, requires validation across diverse agro-ecological zones.

### 3.6. Summary

*This chapter thoroughly examined the applicability of hyperspectral data to determine the spectral separability of maize and soybean across different growth stages in Zimbabwe using UAS-based RGB imagery. The integration of statistical analysis, distance, divergence, and machine learning methods was employed to optimise band selection and timing. ANOVA statistical analysis results indicated significant reflectance differences between maize and soybean. The chapter indicated that low values for JM distance, KLD, and TD were observed during the early growth stages, indicating a high degree of spectral similarity between maize and soybean, limiting effective discrimination. However, abrupt increases in all divergence metrics during the mid-grain filling stage suggested the development of distinct spectral signatures, thereby enhancing separability between the crops. Moreover, the consistent patterns observed across JM distance, KLD, and TD measures throughout the phenological stages indicate that these metrics provide comparable and reliable information regarding the temporal dynamics of crop separability. These results indicated that the discriminative power of maize and soybean is normally effective between 48 to 110 days after planting. Thus, in the following Chapter 4, an approach is proposed to identify crops in a mixed cropping setting at the canopy level using a UAS system mounted with an affordable RGB sensor.*

# CHAPTER 4 : TESTING THE APPLICABILITY OF MACHINE LEARNING MODELS FOR CROP DISCRIMINATION

This chapter is based on:

**Mafuratidze, P.**, Mutanga, O., Masocha, M. and Chivasa, W. Discriminating Maize and Soybean in Mixed Cropping Systems Using Unmanned Aerial Systems Dataset and Random Forest. A book chapter (*Springer Nature*)

## ABSTRACT

The effectiveness of unmanned aerial systems (UASs) in monitoring crops and capturing detailed aerial images, which are essential for estimating crop areas, has been demonstrated. This study evaluated the utility of spectral, textural, and morphological transformations obtained from UAS-based sensor images in distinguishing between maize and soybean in a mixed-cropping environment. The researchers conducted a study on a plot of land measuring 0.324 ha, dividing it into 25 plots with varying mixtures. During the tasselling stage of maize, we used a DJI Matrice 300 drone to capture digital RGB images 48 days after planting. To determine the best features for crop identification, we extracted different types of features (spectral, textural, and morphological) from each plot. For supervised classification using the Random Forest algorithm, we used 26 variables derived from high-spatial-resolution images. Our analysis determined the most significant features of crop classification. The findings of this study revealed that morphological features achieved the highest accuracy of 0.93 and an F1-score of 92, followed by a combination of textural and morphological features, with spectral features being the least effective. These results emphasise the importance of morphological analysis for classifying crops in mixed-cropping systems.

Keywords: morphological operations, texture analysis, heterogeneous environment, mixed crops, high spatial resolution

## 4.1 Introduction

Spectral differentiation of crops in mixed cropping systems (MCS), commonly in smallholder farming environments, is a challenging problem in remote sensing. The MCS is characterised by two or more crop species growing together on the same piece of land (Honrado et al., 2017; Rudel et al., 2016). Although MCS has numerous advantages, such as enhanced soil fertility, reduced occurrence of pests and diseases, and heightened productivity, it also presents obstacles for distinguishing between crops, which involves identifying and mapping various crop types within a field. Obtaining meaningful spatially distributed information on individual crops in an MCS using remotely sensed data can be problematic (Dwivedi et al., 2020; Handique et al., 2020; Löw, 2013). The existence of mixed crops generates difficulties in the discrimination process because different crop types can have similar spectral signatures. Therefore, detecting the distinctions or boundaries between these mixed crops is not straightforward (Christiansen et al., 2017; Khanna et al., 2015; Malveaux et al., 2014; Prins and Van Niekerk, 2020; Ronchetti et al., 2020).

Traditionally, detecting the distinctions between crop species heavily relied on morphological characteristics, manual field surveys and expert knowledge, where trained personnel visually inspect and record crop types (Haider, 2011; Kumar et al., 2022). Regrettably, traditional approaches are subject to human error and can be influenced by factors such as observer bias (Dhau et al., 2018; Jadhav, 2023; Jagadish., 2023; Sishodia et al., 2020; Yadav et al., 2022). Although these methods can be accurate, they are time-consuming, labour-intensive, and often impractical for complex heterogeneous fields, particularly in regions with mixed cropping systems (Champagne, 2019; Pieterse, 2016; Psirofonia et al., 2017; Raja Sekar et al., 2018). Recently, airborne data and satellite imagery with sub-meter resolution and numerous spectral bands useful for crop discrimination have been used extensively, obtaining reasonable results (Hall et al., 2018; McCabe et al., 2016; Yang et al., 2019). Unfortunately, these datasets are difficult and costly to obtain for crop discrimination in mixed agricultural environments.

Consequently, unmanned aerial systems (UAS) have revolutionised the discrimination of crops in MCS in agriculture. As such, this study addresses the challenge of detecting distinctions or boundaries between mixed crops by exploring the potential of unmanned aerial systems (UAS) to classify crop types. This information can empower farmers with valuable insights into optimising their practices and enhancing their agricultural productivity. The UAS offers high-spatial-resolution aerial RGB imagery that can be used to discriminate between different crops. Because of the paucity of sufficient spectral data from UASs, can researchers develop algorithms that can equally discriminate crops in MCS using available high-spatial-resolution RGB images? Currently, acquiring high-spatial-resolution images is relatively straightforward and allows for real-time or near-real-time capture and processing owing to their simplified data (Cheng et al., 2016; Lottes et al., 2017). In addition, high-resolution RGB images result in cost savings because they require less data storage, making them more convenient and manageable, particularly in scenarios with limited computational capabilities (Hamuda et al., 2017; Pulido et al., 2017).

Various approaches have been presented and applied for crop discrimination over a wide range of geographic locations and scales (Kaushik et al., 2025; Manohar Kumar et al., 2024; Mlawa, 2023; Singh et al., 2022). In many cases, researchers have opted to utilise only spectral characteristics (Handique et al., 2017; de Sá et al., 2018) and obtain reasonable results. Nevertheless, crop discrimination is normally performed during the early stages of the growing season, when crops are in their seedling and vegetative growth stages, and up to the tasselling stage (Champagne, 2019; Hunt Jr et al., 2013). However, during the early crop growth stages, mixed crops usually show similar spectral signatures because chlorophyll, which is the most abundant light-interacting molecule at this stage, tends to reflect and absorb light in similar ways across different crop species. Eventually, crop discrimination using remotely sensed data becomes difficult. Furthermore, traditional pixel-based approaches usually yield poor results when applied to UAS images owing to the increased number of detectable features in ultrahigh spatial resolution data.

Several attempts have been made to address pixel-based crop discrimination problems using various methods (Aneece & Thenkabail, 2018; de Castro et al., 2018; Manohar Kumar et al., 2024). Recent studies have demonstrated that approaches that focus on spatial contextual information (texture), as well as shape and structure (morphological operations), are robust (Louargant et al., 2018). Li et al. (2019) identified that the visible index is resistant to atmospheric conditions based on three visible bands, and the texture indices normalised by mean textures from red and green bands were deemed most effective for retrieving the leaf area index. Recently, Kawamura et al. (2021) introduced a segmentation approach that combined hue-saturation-brightness with the canopy height model, texture, and colour indices to differentiate crops and weeds within upland rice fields in the central region of Vientiane, Laos. Various classification methods have been used, ranging from pixel- to object-based, leveraging high-spatial-resolution RGB pictures. Recently, the development of machine learning algorithms such as random forest (RF), support vector machines (SVM), decision trees (DT), artificial neural networks (ANN), and classification and regression trees (CART) has emerged and displayed the ability to achieve high accuracy in classification. Although most of these classifiers have been used for crop discrimination, the RF classifier is the most widely used. Random forest is a popular non-parametric machine learning algorithm that is a highly versatile ensemble that combines multiple decision trees to create a more accurate model, and is robust, especially when dealing with small sample sizes (Breiman, 2001). Each decision tree in the forest was trained by finding a balance between bias and variance on a random subset of the data. Combine the bootstrap aggregation method with randomisation when selecting data nodes to construct a decision tree, reducing overfitting and enhancing the model's generalisation performance (Beard et al., 2007). Lambert et al. (2018) used a RF classifier to map grass weed in wheat crops, obtaining an overall accuracy of 87%. To demonstrate its superiority, Prins and Van Niekerk (2020) applied a RF classifier by combining and classifying LiDAR data, Sentinel-2 imagery, and aerial imagery to discriminate between five crop types in intensively cultivated areas. The researchers obtained an overall accuracy of 94.4%.

However, the existing research lacks a comprehensive understanding of the discrimination performance achieved by combining spectral, textural, and morphological information from high-spatial-resolution RGB images in a small image area with a few samples. Additionally, determining the effect of crop mixtures in MCS on the effectiveness of high-spatial-resolution RGB images for detecting and discriminating mixed crops remains understudied. In this regard, the main objective of this study was to assess the effectiveness of UAS-derived high-resolution RGB images in accurately classifying crops in a mixed-cropping system. Specifically, the study investigated potential improvements in crop classification accuracy through the inclusion of spectral and geostatistical features. The specific objectives of the study were to: (1) evaluate and compare the accuracy of models utilising spectral, textural, and morphological features separately, as well as a combination of all three, (2) identify the contribution of each feature group (spectral, textural, and morphological) to the overall classification accuracy, and (3) implement a random forest variable selection approach to identify the most valuable features for crop classification, addressing the subjectivity and possible inconsistencies in feature selection.

## 4.2 Materials and Methods

### *4.2.1 Study area*

Remote sensing images were acquired on the 12th of March 2022 at an experimental station located at Panmure Research Station in Shamva District (between 31.623614° and 31.624355°, and between -17.268046° and -17.268073°), as shown in Figure 4-1. The Civil Aviation Authority of Zimbabwe approved these flights using a written agreement between the research station and the researcher. Images were taken 48 days after planting during the last vegetative stage of maize (tassel emergence) (Makanza et al., 2018), which is suitable for yield estimation (Kenduiywo et al., 2020).

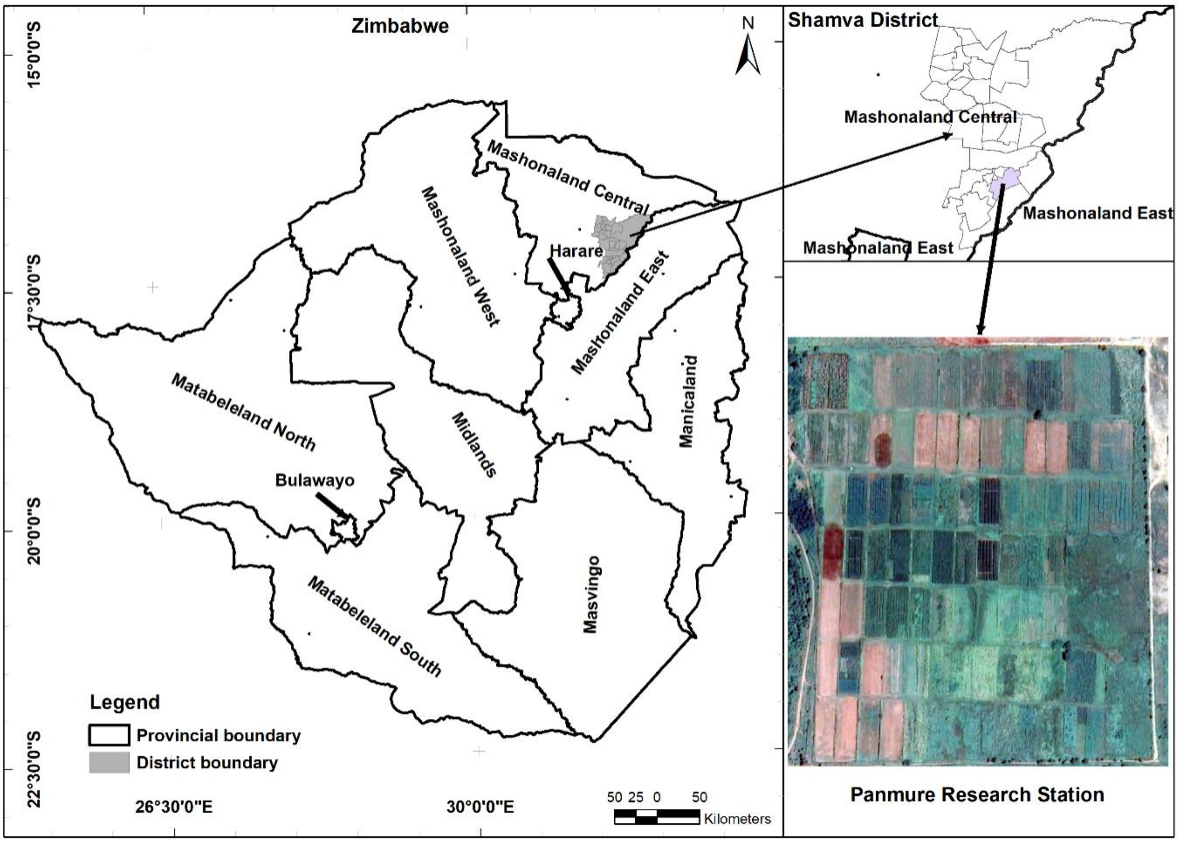


**Figure 4-1: Experimental site and sample images at the Panmure Research Station in the Shamva District of Zimbabwe.**

Agricultural production is one of the main economic activities in most of the study area. The district is largely fertile and falls under the agro-ecological region II. It also receives relatively well-distributed and reliable rainfall annually, ranging between 750 mm and 1000 mm and a mean annual temperature of approximately 24.6ºC (https://weatherandclimate.com). The study site was selected because it has a subtropical climate and is highly suitable for intensive crop production. Farmers in this study area usually practice mixed cropping systems, mainly between cereals and legumes, such as maize, cowpeas, groundnuts, tobacco, and soybeans for subsistence. Sporadic patches of fertile clay and sandy loam characterised the soils.

### *4.2.2 Experimental design and treatments*

All the field experiments were conducted in a block covering 0.324 ha with 25 plots, as shown in Figure 4-2. The experiment was arranged in a factorial-based randomised complete block design with five replicates (each plot was 17 m × 5 m, or 0.0085 ha). In the single maize plot, the crops were spatially arranged with an in-row distance of 60 cm and a between-row distance of 90 cm. For the mixed-crop configuration, the row spacing was 60 cm for maize and 25 cm for soybean in the respective in-row distances, with a between-row distance of 45 cm. This spatial arrangement is illustrated in Figure 4-3, and the proportions of the mixed cropping area occupied by each crop are presented in Table 4-1. Different sections had 1m between them, and the same distance was maintained between plots and replicates. Each section had five plots that were planted with a different crop mixture/treatment, except for plot A1, which contained maize only. In this study, we mixed crops per plot according to their importance, as follows: maize (SC659) and soybean (Serenade). Both crops were planted on the 14$^{th}$ and 15$^{th}$ of January 2022, and standard agronomic practices were applied for cereals (maize (M)) and legumes (soybean (SB)) in Zimbabwe (https://www.zimagrihub.org.zw/maize-growers-guide, accessed 15 December 2021).

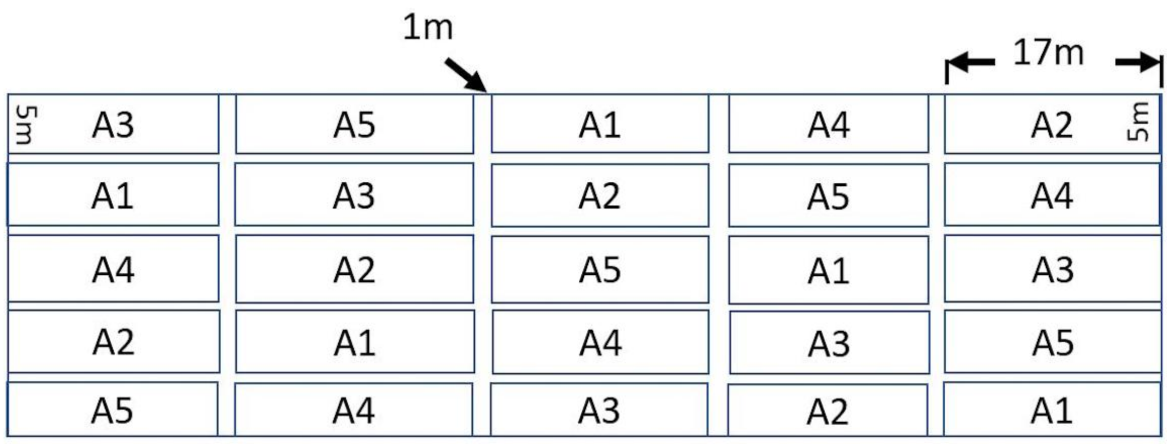


**Figure 4-2: Plots for maize and soybean trials showing the experimental design and replication.**

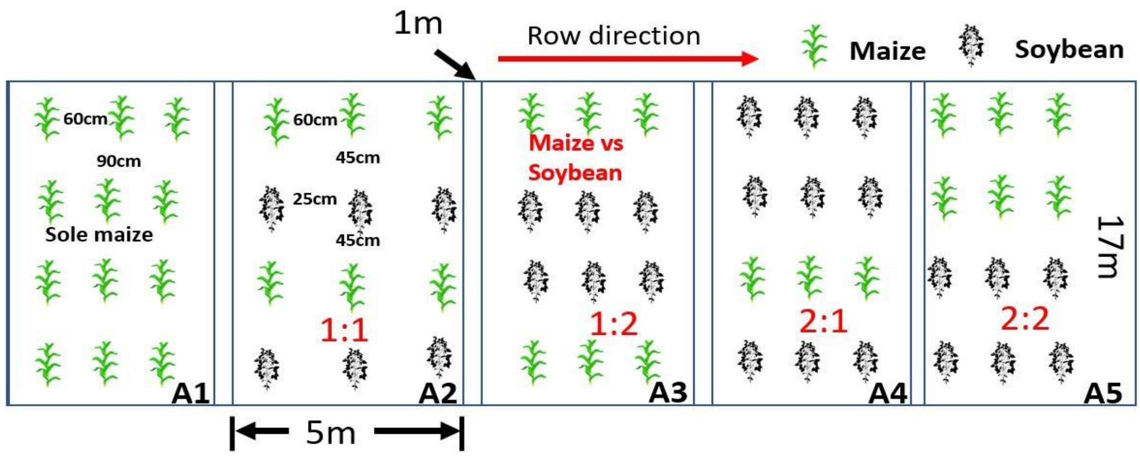


**Figure 4-3: Mixed crop ratios and space intervals.**

**Table 4-1: Experimental treatment with various ratios.**

| Treatment number | Treatment | Ratio | Plot size ($m^2$) |
|---|---|---|---|
| **Plot A**1 | Sole maize | M | 85 |
| **Plot A**2 | One row of maize to one row of soybean | 1M:1SB | 85 |
| **Plot A**3 | One row of maize to two rows of soybean | 1M:2SB | 85 |
| **Plot A**4 | Two rows of soybeans to one row of maize | 2M:1SB | 85 |
| **Plot A**5 | Two rows of maize to two rows of soybean | 2M:2SB | 85 |

### *4.2.3 UAS flights and remotely sensed images*

The images were acquired using DJI MATRICE 300 (M300) (Shenzhen Dajiang 149 Innovation Technology Co., Ltd., China), which is a four-rotor. Zenmuse is an RGB camera with a focal length of 25 mm and an exposure time of 1 / 500 s. The RGB aerial image dataset was captured using a Zenmuse (ZH20T) camera with an image resolution of 5184 × 3888 pixels and a sensing height of 90m. The ground sampling distance for the camera was approximately 1.93 cm, and the estimated field of view was approximately 52.45 degrees. Although cloud cover is normally 50% on average during the rainy season, in this study, we waited for five days after rainfall to ensure the consistency and objectivity of the data (Ge et al., 2019) and obtain a reasonable sample size. Images were captured between 10:30 a.m. and 1:30 p.m. local time to minimise the effects of low-angle illumination and shadows, which are more pronounced in early morning or late afternoon. This time window corresponds to when the sun is relatively high in the sky, ensuring uniform lighting conditions, reducing shadow interference, and improving spectral reflectance consistency across the field, which is critical for accurate crop discrimination. These images were processed using the Pix4Dmapper photogrammetry software package (Cheseaux-Lausanne, Pix4D SA, Lausanne, Switzerland) to merge the aerial imagery into an ortho mosaic. The acquired images were resized to 256 × 256 pixels for the machine learning classifiers.

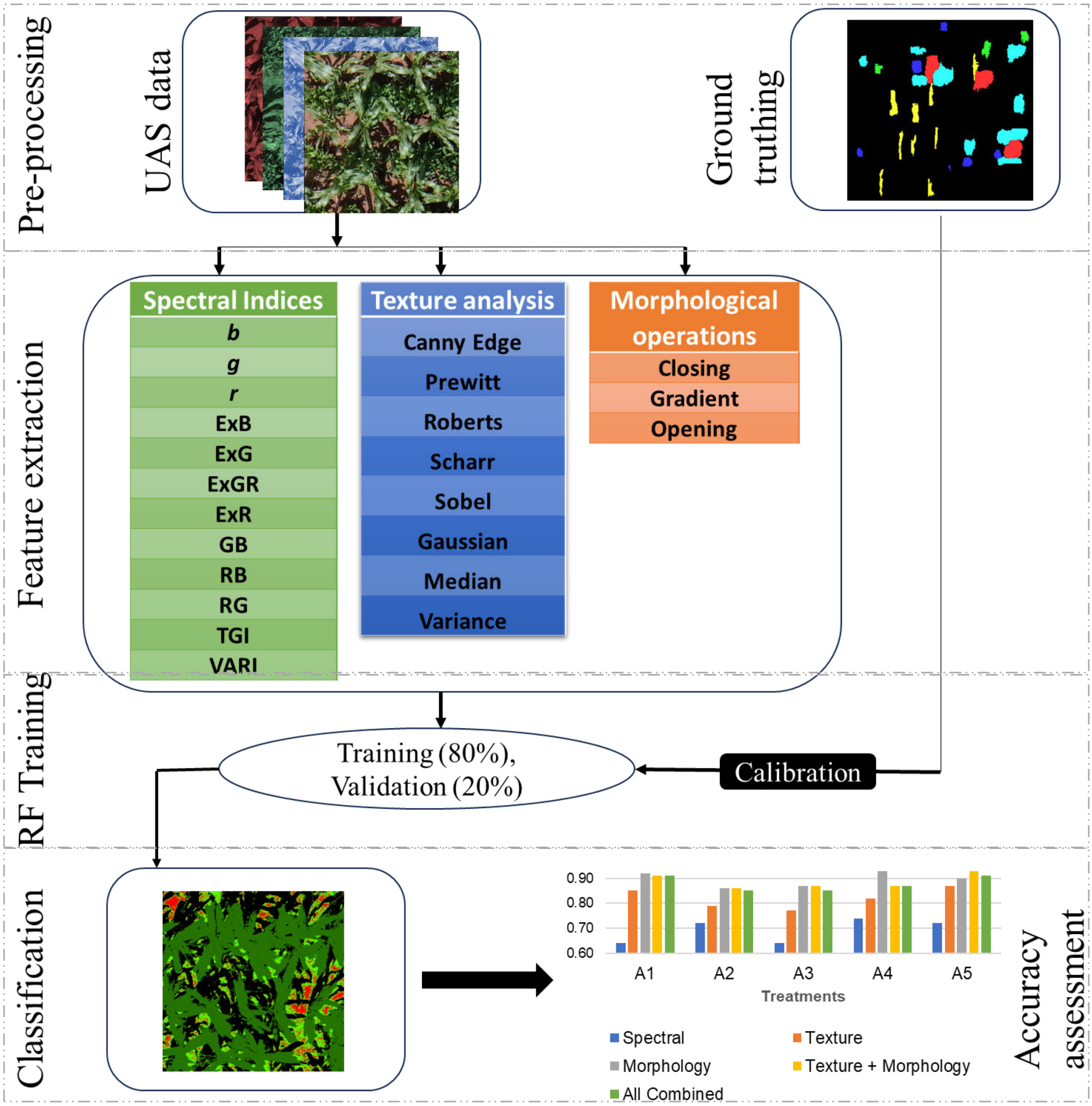


**Figure 4-4: Flowchart of the method.**

## 4.3 Data Analysis

### *4.3.1 Preprocessing and feature extraction*

In terms of crop classification in a mixed cropping system using UAS-derived RGB images, there are two major challenges: the high degree of spectral responses from mixed crops and the lack of spectral information. Using pixel-based image classification methods that do not consider the spatial relationship between a pixel and its neighbours can lead to difficulties in extracting class information from the images. Initially, all images were converted to grayscale and separated into r, g, and b channels (Table 4-2) on all 25 plots. Pixel-level features were extracted and structured into a tabular format using pandas, ensuring compatibility with subsequent machine learning models. As such, the proposed classification approach in this study combines spectral, morphological, and texture information to address these shortcomings and to attain reliable and accurate outcomes (Figure 4-4). The use of multiple feature extractors is effective in improving overall classification accuracy (Fan et al., 2022; Umamaheswari and Jain, 2020). In this study, different feature extraction techniques, such as spectral data, morphological operations, and texture analysis, were employed as the input variables. The processing and analysis of these datasets were programmed using the scikit-learn package in a standalone Scientific Python Development Environment version 5.5.0 with Python 3.11, in a Windows 11 64-bit operating system powered by Intel(R) Core (TM) i5-3210M CPU @ 2.50GHz with 8 GB RAM.

#### 4.3.1.1 Spectral analysis

Spectral indices are widely acknowledged as highly effective features for remote sensing applications focused on vegetation analysis (Balasubramanian, 2017; Fuentes-Peailillo et al., 2019; Gitelson et al., 2002; Hunt Jr et al., 2013; Y. Liu et al., 2021). These indices are powerful tools for analysing vegetation-related phenomena, and are conventionally used and derived from operations with the red, green, and blue chromatic layers of the image (Nyman, 2008). The spectral indices were calculated from the RGB images, as shown in Table 4-2. As such, 12 spectral features in conjunction with the original RGB image were selected as input variables and evaluated in this study.

**Table 4-2: Spectral indices used in this study.**

| Spectral Index | Name | Formula | Reference |
|---|---|---|---|
| b | Blue band | $\frac{B}{B+G+R}$ | (Woebbecke et al., 1995) |
| g | Green band | $\frac{G}{B+G+R}$ | (Woebbecke et al., 1995) |
| r | Red band | $\frac{R}{B+G+R}$ | (Woebbecke et al., 1995) |
| ExB | Excess Blue Vegetation Index | $1.4\text{b} - g$ | |
| ExG | Excess Green Vegetation Index | $2\text{g} - r - b$ | (Nijland et al., 2016) |
| ExGR | Excess Green minus Excess Red Vegetation Index | ExG–ExR | (Meyer and Neto, 2008) |
| ExR | Excess Red Vegetation Index | $1.4r - g$ | |
| GB | Green divide by Blue | $\frac{g}{b}$ | - |
| RB | Red divide by Blue | $\frac{r}{b}$ | - |
| RG | Red divide by Green | $\frac{r}{g}$ | - |
| TGI | Triangular Greenness Index | $g – 0.39 \times r – 0.61 \times b$ | (Hunt Jr et al., 2013) |
| VARI | Visible Atmospherically Resistant Index | $\frac{\text{g} - \text{r}}{\text{g} + \text{r} - \text{b}}$ | (Gitelson et al., 2002) |

Where R, G and B are RGB-values between 0 and 255 and normalised into *r* (red), *g* (green), and *b* (blue) bands

#### 4.3.1.2 Morphological operations

Morphological operations involve the extraction of relevant features using nonlinear mathematical operations that manipulate the shape and structure of objects in an image (Serra, 1986; Raja Sekar et al., 2018). These operations are classified as binary morphological operations and consist of dilation, erosion, triggering and closing, hit-and-miss transformation, and morphological filtering. This process involves adding and removing pixels at the periphery of objects (Banon et al., 2007; Nogueira et al., 2021). Morphological operations are widely used in image processing and are considered state-of-the-art techniques for various applications. In this study, we focused on using a combination of dilation and erosion as follows: 1) opening, which is simply an erosion operation followed by dilation; 2) closing, which is also a reverse of dilation operation followed by erosion; and 3) gradient, which focuses on the difference between the dilated and eroded images to produce a new image that highlights the boundaries and edges of objects in the original image.

#### 4.3.1.3 Texture analysis

Unlike spectral indices, which suffer from the effects of spectral similarities, texture can be considered a distinguishing characteristic of specific land use or cover classes. This is because different classes exhibit unique patterns and structures (Haralick et al., 1973) that can be analysed through texture analysis to extract meaningful information within the predefined kernel (Kupidura, 2019). The texture of an image is determined by the arrangement of the grey levels within the image. This means that it can be conducted at varying scales, wherein micro-textures are observed at a localised level, whereas macro-textures are observed over a wider region. The analysis of micro-textures involves the examination of value distribution within a small neighbourhood, whereas macro-texture analysis involves the evaluation of value distribution across a larger area.

By examining texture at different scales, it is possible to gain a more detailed understanding of the patterns and structures within an image. A considerable amount of literature has been published on the extraction of texture features. Many researchers have proposed techniques for extracting texture features from RGB images (Cucho-Padin et al., 2020; Ghatol and Dhok, 2008; Kawamura et al., 2021b; S. Li et al., 2019; Nardari et al., 2018; Pulido et al., 2017; Varela et al., 2018; Zhao et al., 2019). Although Haralick et al. (1973) identified 28 textural features; 14 texture features were highly correlated with each other. This suggests that including all these texture features would result in duplicate spatial contextual information that does not contribute to classification. Therefore, in this study, we only used a combination of statistical and edge detector-based methods, as shown in Table 4-3.

**Table 4-3: Texture features combining statistical and edge detector-based methods.**

| Statistical methods | Edge detector-based methods |
|---|---|
| Gaussian (Sigma = 3 and 7) | Canny Edge |
| Median (Sigma = 3) | Prewitt |
| Variance (Sigma = 3) | Roberts |
| | Scharr |
| | Sobel |

Edge detection-based methods, such as first-order derivative (Roberts, Sobel, Prewitt, and Scharr) and second-order derivative (Canny edge), are appropriate for assessing the structure and properties of objects in high-spatial-resolution RGB images (Flusser et al., 2007; Gonzalez and Woods, 2019; Miceli et al., 2018). Digital analysis of such images involves understanding abrupt changes in brightness, colour, shape, and texture (Illana Rico et al., 2022; Shu et al., 2021). The importance of these local changes or discontinuities in image intensity is that they can be applied to determine the depth, size, and orientation, as well as the boundaries between different regions of an image.

### *4.3.2 Random forest*

The main reason for choosing RF in this study is that it is much easier to implement and more forgiving about overfitting and outliers than the other algorithms. Random forest is a non-parametric and powerful algorithm that can handle large datasets with high dimensionality (Muharam et al., 2021). Therefore, 26 different input variables were selected for this study. Finally, to achieve pixel-level classification, the random forest classification tool in the scikit-learn package is used to implement the model.

#### 4.3.2.1 RF Fine-Tuning Hyperparameters, Training Set Selection and Classification

To ensure optimal performance of the model, a Random Forest classifier needs a training dataset from all the selected types of features, namely, spectral, textural, and morphological features. These datasets were used as features to discriminate between maize, soybeans, bare soil, shadows, and weeds using the RF algorithm. Data were subjected to random sampling. 80% was allocated for training the model, and the remaining 20% was used to assess its accuracy through validation. The specific hyperparameters to run the RF algorithm were tuned as follows: *n_estimators* = 100, *max_depth* = 25, and *random_state* = 42.

#### 4.3.2.1 Variable Importance

The variable importance in the random forest refers to the measure of the impact of each input feature on the model's performance. This is an important aspect of the algorithm as it helps to identify the most influential features in the dataset, which can be used to improve the interpretability of the model and provide insights into the underlying relationships between the features and the target variable. Random forest uses various methods to calculate the importance of a variable, such as the mean decrease in impurity and the importance of permutation. These methods can identify both the individual and joint contributions of features to the model's predictions and help select the most relevant features for further analysis or feature engineering.

The importance of variables in random forests is also highlighted in situations where numerous input features are available, and it is essential to prioritise the features to be included in the model. By identifying the most important features, it is possible to reduce the dimensionality of the dataset, potentially improve the model's performance, and simplify the interpretation of the model's output.

#### 4.3.2.2 Model validation

Random forest is a powerful machine learning algorithm that can accurately model complex data. However, to ensure that the model is reliable and generalises well using new data, it is important to use appropriate model validation techniques. In the last phase of categorising crops, significant elements such as confusion matrix, overall accuracy, precision, recall, F1 score, and area under the receiver operating characteristic curve (ROC) were employed to assess effectiveness. The F1 score represents a gauge of the accuracy of test data, constituting a weighted mean of precision and recall. The equations for the selected metrics are as follows:

$$\text{Overall accuracy} = \frac{True\ positive}{N}$$

$$\text{Precision} = \frac{True\ positive}{True\ positive + False\ positive}$$

$$\text{Recall} = \frac{True\ positive}{True\ positive + False\ negative}$$

$$\text{F1 score} = 2 \text{ x } \frac{Precision * Recall}{Precision + Recall}$$

where,

true positive is a correct positive prediction

true negative is a correct negative prediction

false positive is an incorrect positive prediction

a false negative is an incorrect negative prediction

## 4.4 Results

### *4.4.1 Spatial distribution of maize, soybean and other*

Spatial distribution analysis of the main land cover types, including maize, soybean, bare soil, shadows, and weeds, revealed interesting findings. The classification model performed better in treatment A5 (two maize vs. two soybeans) than in the mixed ratios in all plots studied. This contradicted the initial hypothesis, which expected better performance in the sole maize treatment (A1) compared to the mixed crops because of the complexity of classifying mixed crops with varied spectral responses.

Additionally, the classification model achieved a prime area under the curve (AUC) value of one for bare soil, indicating excellent classification accuracy owing to the distinct colour difference between soil and green vegetation. Table 4-4 provides an overview of the random forest model performance for different treatments. Treatments A4 and A5 demonstrated the highest classification accuracy of 0.93, precision of 0.93, recall of 0.93, and F1-score of 0.92 when utilising morphology and a combination of texture and morphology. Surprisingly, the sole maize treatment (A1) exhibited a lower accuracy than A4 and A5. Analysis of recall and precision for each category revealed that most errors occurred in the classification of soybeans and shadows.

Figure 4-5 illustrates the quantitative assessment of treatments using the AUC for different crop ratios, further supporting the superior performance of A5 (two maize vs. two soybeans). Conversely, Figure 4-6 (a-e) depicts the performance curves for treatments A1 to A5, demonstrating the variations in classification accuracy across different land cover types. In summary, spatial distribution analysis revealed that treatment A5 had the highest classification accuracy among the tested ratios. This unexpected result challenges the assumption that maize fields are easier to classify than mixed crops. In addition, the classification model exhibited excellent performance in accurately identifying bare soil. However, errors in the classification of soybeans and shadows were more prevalent.

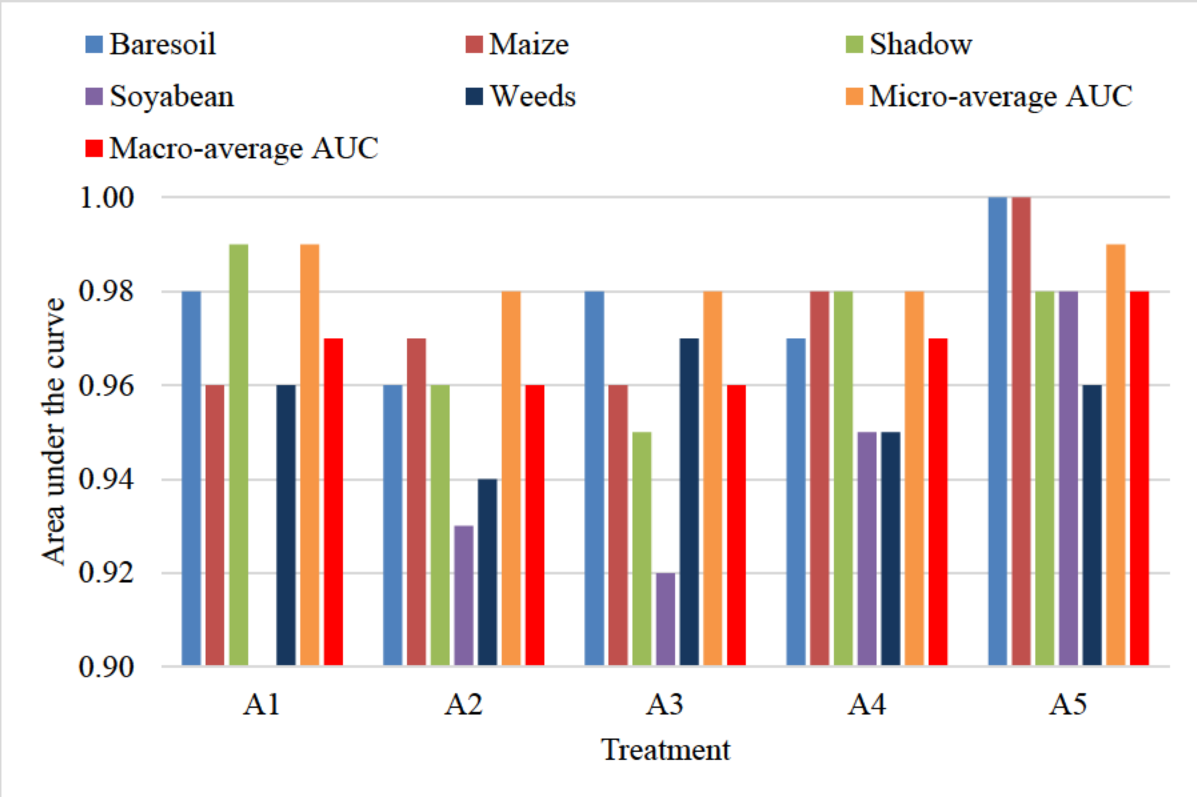


**Figure 4-5: Quantitative assessment of treatments using the area under the curve on different crop ratios.**

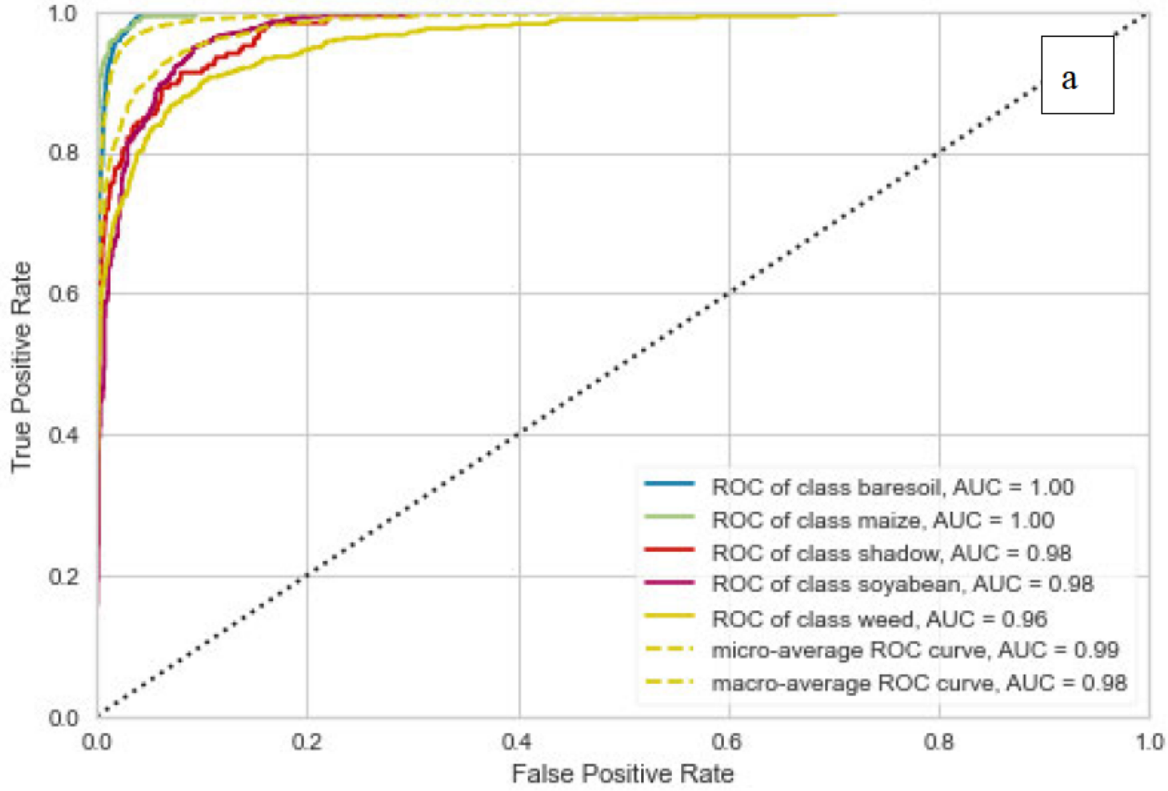
a
True Positive Rate
False Positive Rate
ROC of class baresoil, AUC = 1.00
ROC of class maize, AUC = 1.00
ROC of class shadow, AUC = 0.98
ROC of class soyabean, AUC = 0.98
ROC of class weed, AUC = 0.96
micro-average ROC curve, AUC = 0.99
macro-average ROC curve, AUC = 0.98

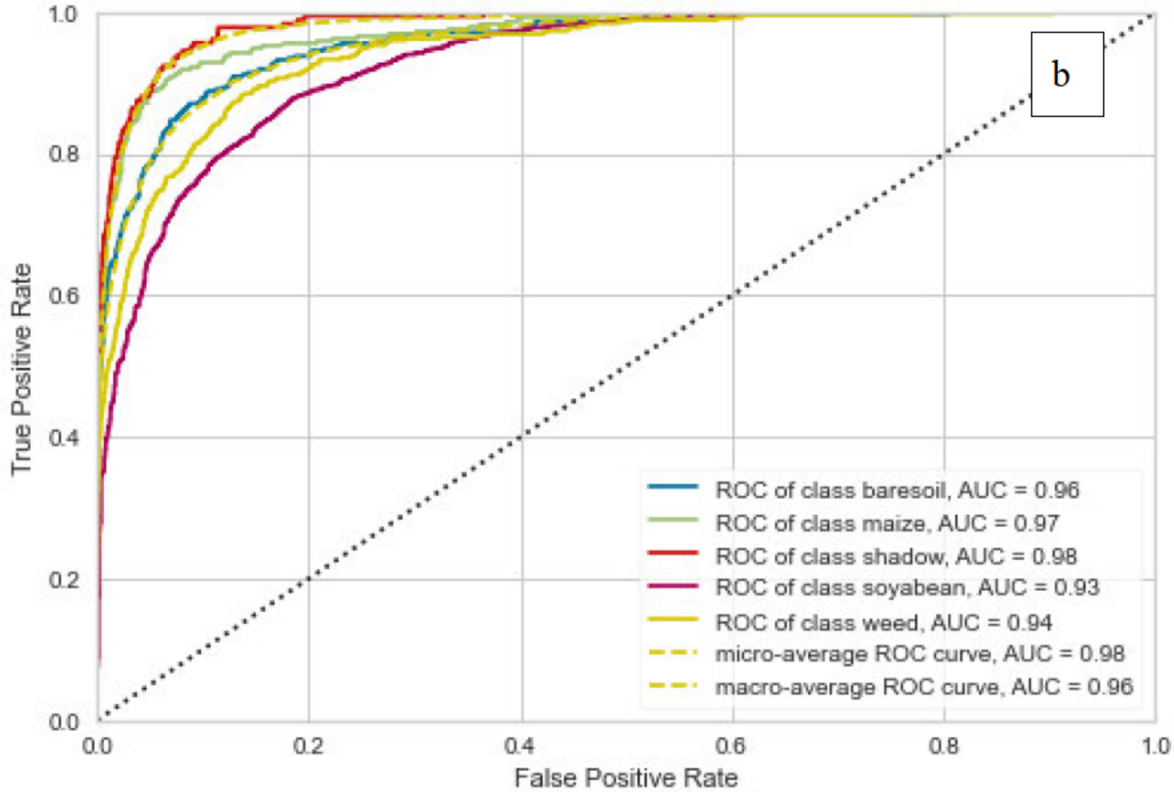
b
True Positive Rate
False Positive Rate
ROC of class baresoil, AUC = 0.96
ROC of class maize, AUC = 0.97
ROC of class shadow, AUC = 0.98
ROC of class soyabean, AUC = 0.93
ROC of class weed, AUC = 0.94
micro-average ROC curve, AUC = 0.98
macro-average ROC curve, AUC = 0.96

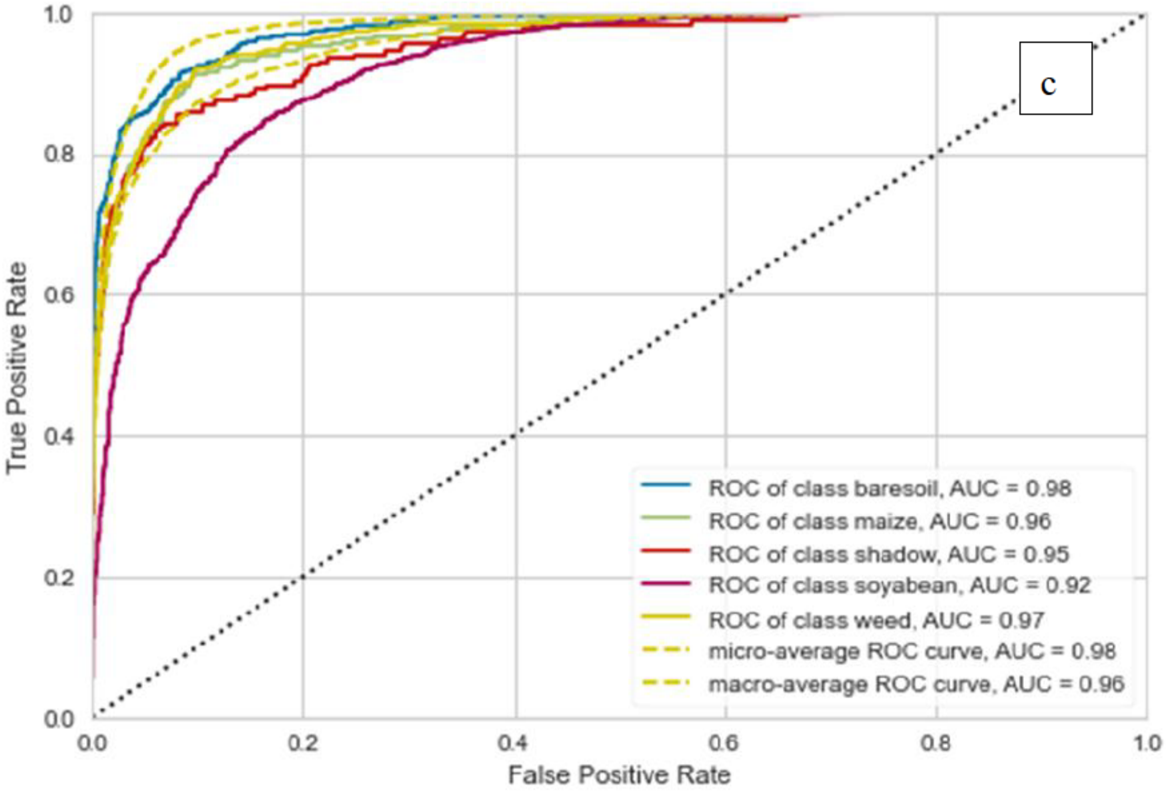
c
1.0
0.8
0.6
0.4
0.2
0.0
True Positive Rate
0.0
0.2
0.4
0.6
0.8
1.0
False Positive Rate
ROC of class baresoil, AUC = 0.98
ROC of class maize, AUC = 0.96
ROC of class shadow, AUC = 0.95
ROC of class soyabean, AUC = 0.92
ROC of class weed, AUC = 0.97
micro-average ROC curve, AUC = 0.98
macro-average ROC curve, AUC = 0.96

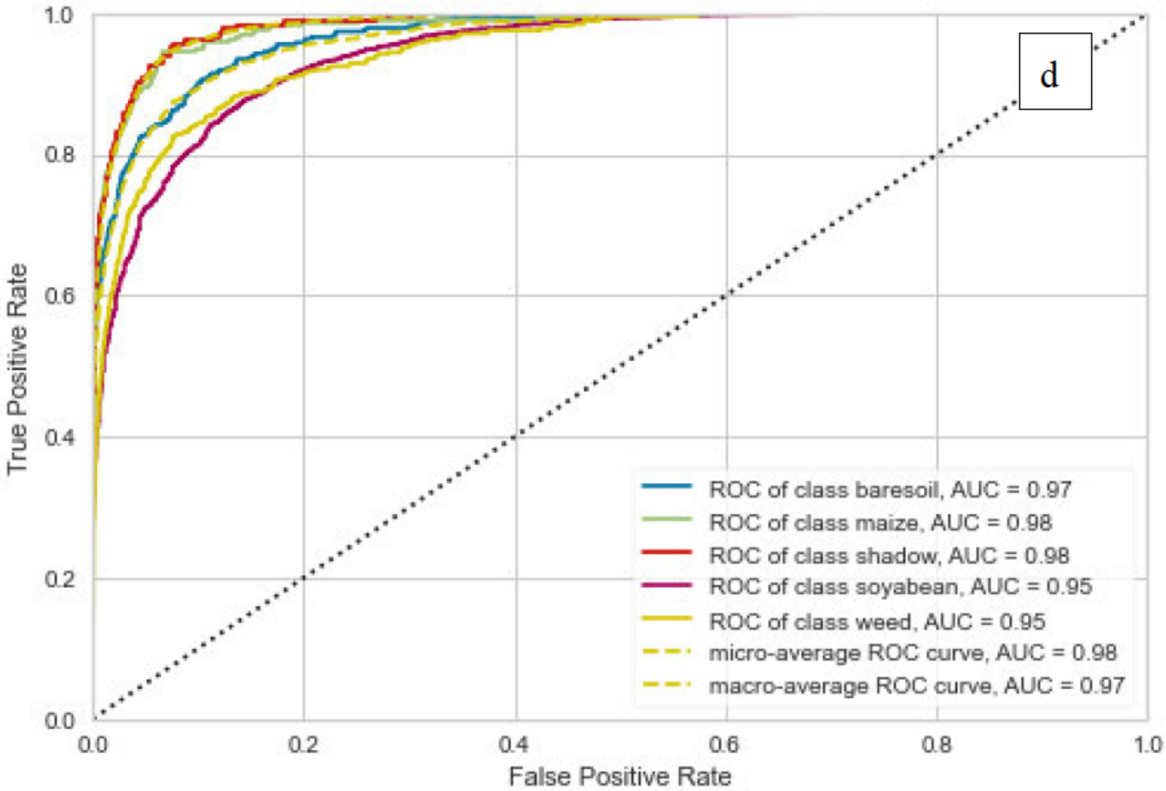
d
1.0
0.8
0.6
0.4
0.2
0.0
True Positive Rate
0.0
0.2
0.4
0.6
0.8
1.0
False Positive Rate
ROC of class baresoil, AUC = 0.97
ROC of class maize, AUC = 0.98
ROC of class shadow, AUC = 0.98
ROC of class soyabean, AUC = 0.95
ROC of class weed, AUC = 0.95
micro-average ROC curve, AUC = 0.98
macro-average ROC curve, AUC = 0.97

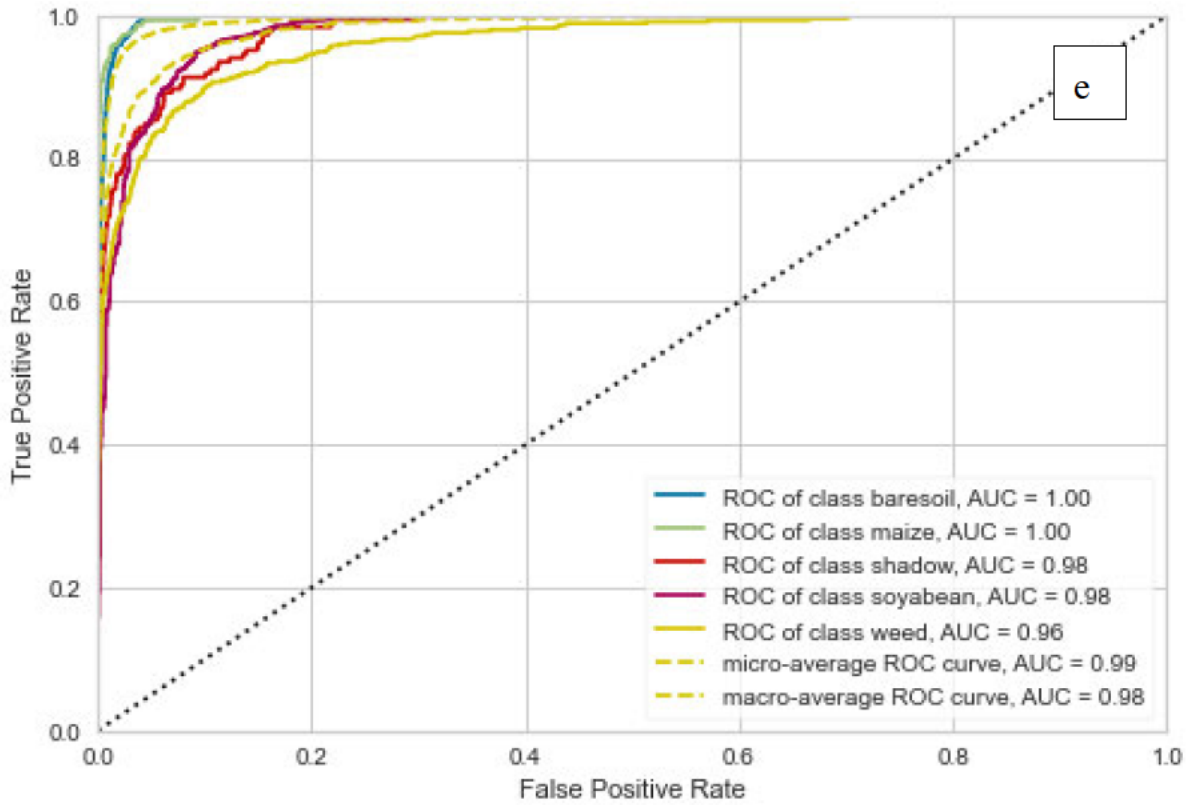


**Figure 4-6: Comparison of the five treatments on crop mixtures based on the AUC. (Treatment descriptions: (a) A1 - Sole maize, (b) A2 - One-row maize vs. one-row soybean, (c) A3: two-row soybean vs. one-row maize, (d) A4: two-row maize vs. one-row soybean, (e) A5.**

**Table 4-4: Classification accuracy for different crops (bold and underlined numbers represent the best results).**

| | Spectral Indices | | | Texture | | | Morphology | | | Texture + Morphology | | | All combined | | |
|---|---|---|---|---|---|---|---|---|---|---|---|---|---|---|---|
| | **Precision** | **Recall** | **F1-Score** | **Precision** | **Recall** | **F1-Score** | **Precision** | **Recall** | **F1-Score** | **Precision** | **Recall** | **F1-Score** | **Precision** | **Recall** | **F1-Score** |
| A1_1 | 0.52 | 0.72 | 0.6 | 0.75 | 0.75 | 0.69 | 0.85 | 0.85 | 0.84 | 0.84 | 0.81 | 0.78 | 0.82 | 0.79 | 0.74 |
| A1_2 | 0.53 | 0.72 | 0.6 | 0.82 | 0.82 | 0.8 | 0.86 | 0.86 | 0.86 | 0.86 | 0.86 | 0.84 | 0.85 | 0.84 | 0.83 |
| A1_3 | 0.62 | 0.71 | 0.63 | 0.85 | 0.86 | 0.84 | **<u>0.92</u>** | **<u>0.92</u>** | **<u>0.92</u>** | 0.91 | 0.91 | 0.9 | 0.91 | 0.91 | 0.9 |
| A1_4 | 0.64 | 0.72 | 0.6 | 0.73 | 0.76 | 0.71 | 0.82 | 0.81 | 0.81 | 0.81 | 0.81 | 0.79 | 0.79 | 0.79 | 0.75 |
| A1_5 | 0.59 | 0.72 | 0.62 | 0.74 | 0.76 | 0.68 | 0.79 | 0.8 | 0.76 | 0.79 | 0.78 | 0.73 | 0.78 | 0.77 | 0.71 |
| A2_1 | 0.65 | 0.75 | 0.66 | 0.76 | 0.77 | 0.7 | 0.86 | 0.85 | 0.83 | 0.84 | 0.81 | 0.76 | 0.83 | 0.79 | 0.72 |
| A2_2 | 0.59 | 0.75 | 0.64 | 0.79 | 0.8 | 0.76 | **<u>0.86</u>** | **<u>0.86</u>** | **<u>0.84</u>** | **<u>0.86</u>** | **<u>0.85</u>** | **<u>0.83</u>** | 0.85 | 0.83 | 0.8 |
| A2_3 | 0.65 | 0.76 | 0.68 | 0.74 | 0.79 | 0.73 | 0.85 | 0.85 | 0.83 | 0.84 | 0.83 | 0.79 | 0.83 | 0.81 | 0.76 |
| A2_4 | 0.61 | 0.75 | 0.65 | 0.79 | 0.77 | 0.7 | 0.84 | 0.84 | 0.81 | 0.83 | 0.8 | 0.75 | 0.82 | 0.79 | 0.72 |
| A2_5 | 0.72 | 0.75 | 0.64 | 0.78 | 0.77 | 0.68 | 0.83 | 0.83 | 0.8 | 0.83 | 0.79 | 0.73 | 0.81 | 0.78 | 0.71 |
| A3_1 | 0.56 | 0.75 | 0.64 | 0.73 | 0.77 | 0.7 | 0.84 | 0.84 | 0.82 | 0.83 | 0.81 | 0.77 | 0.81 | 0.79 | 0.74 |
| A3_2 | 0.6 | 0.75 | 0.65 | 0.75 | 0.77 | 0.7 | 0.85 | 0.85 | 0.83 | 0.84 | 0.82 | 0.78 | 0.81 | 0.8 | 0.74 |
| A3_3 | 0.63 | 0.75 | 0.66 | 0.77 | 0.8 | 0.74 | **<u>0.87</u>** | **<u>0.88</u>** | **<u>0.87</u>** | **<u>0.87</u>** | **<u>0.85</u>** | **<u>0.83</u>** | 0.85 | 0.83 | 0.8 |
| A3_4 | 0.63 | 0.76 | 0.67 | 0.76 | 0.79 | 0.73 | 0.85 | 0.85 | 0.83 | 0.84 | 0.82 | 0.77 | 0.83 | 0.8 | 0.73 |
| A3_5 | 0.64 | 0.75 | 0.65 | 0.77 | 0.78 | 0.71 | 0.86 | 0.87 | 0.85 | 0.85 | 0.83 | 0.8 | 0.83 | 0.81 | 0.76 |
| A4_1 | 0.56 | 0.75 | 0.64 | 0.75 | 0.79 | 0.73 | 0.85 | 0.85 | 0.84 | 0.85 | 0.84 | 0.81 | 0.84 | 0.83 | 0.79 |
| A4_2 | 0.7 | 0.77 | 0.69 | 0.82 | 0.82 | 0.78 | 0.86 | 0.86 | 0.84 | 0.87 | 0.86 | 0.84 | 0.85 | 0.85 | 0.81 |
| A4_3 | 0.7 | 0.78 | 0.69 | 0.82 | 0.81 | 0.76 | 0.85 | 0.85 | 0.83 | 0.86 | 0.84 | 0.81 | 0.85 | 0.83 | 0.79 |
| A4_4 | 0.63 | 0.77 | 0.69 | 0.78 | 0.79 | 0.72 | 0.85 | 0.85 | 0.82 | 0.85 | 0.83 | 0.79 | 0.85 | 0.83 | 0.77 |
| A4_5 | 0.74 | 0.76 | 0.67 | 0.8 | 0.81 | 0.78 | **<u>0.93</u>** | **<u>0.93</u>** | **<u>0.92</u>** | 0.87 | 0.86 | 0.84 | 0.87 | 0.86 | 0.83 |
| A5_1 | 0.6 | 0.75 | 0.65 | 0.77 | 0.79 | 0.73 | 0.83 | 0.83 | 0.8 | 0.84 | 0.83 | 0.79 | 0.82 | 0.81 | 0.75 |
| A5_2 | 0.72 | 0.77 | 0.69 | 0.82 | 0.83 | 0.79 | 0.87 | 0.87 | 0.85 | 0.88 | 0.86 | 0.84 | 0.86 | 0.85 | 0.82 |
| A5_3 | 0.64 | 0.75 | 0.66 | 0.87 | 0.88 | 0.87 | 0.9 | 0.9 | 0.9 | **<u>0.93</u>** | **<u>0.93</u>** | **<u>0.92</u>** | 0.91 | 0.91 | 0.9 |
| A5_4 | 0.63 | 0.75 | 0.65 | 0.79 | 0.81 | 0.77 | 0.86 | 0.87 | 0.85 | 0.87 | 0.87 | 0.85 | 0.85 | 0.84 | 0.82 |
| A5_5 | 0.65 | 0.77 | 0.68 | 0.79 | 0.8 | 0.75 | 0.85 | 0.85 | 0.84 | 0.85 | 0.84 | 0.81 | 0.84 | 0.83 | 0.79 |

### *4.4.2 Model characteristic*

The impact of fine-tuning hyperparameters, specifically the number of trees and their depth, on classification accuracy was investigated. The results indicated that the number of trees had a substantial influence on classification accuracy. Conversely, varying the depth of the trees led to a noteworthy enhancement in classification accuracy. However, the findings revealed that increasing the depth beyond 25 did not yield a proportional increase in the classification accuracy, as depicted in Figure 4-7. As a result, a maximum tree depth of 25 was selected as the optimal value for classification across all treatments.

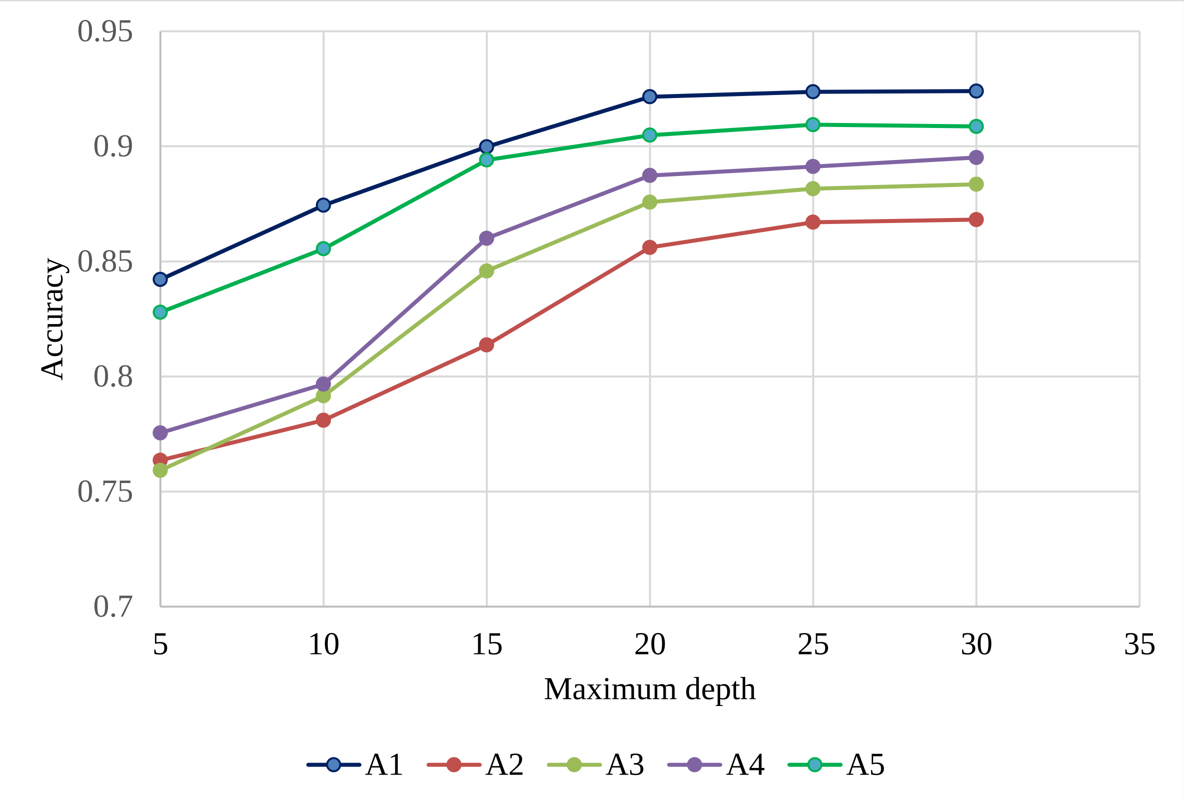


**Figure 4-7: Performance of random forest with increasing maximum depth.**

### *4.4.3 Performance of feature selection in crop classification*

The evaluation of 26 different sets of metrics, based on spectral, morphological, and textural variables within each treatment, revealed varying performance levels. The highest classification accuracy was achieved by utilising the morphological operations feature group across all treatments, resulting in balanced class accuracies ranging from 0.8 to 0.93, as shown in Table 4-5 and Figure 4-8. Among the morphological operations, the Closing and Opening operations, along with the gradient, exhibit comparable results, with the closing operations outperforming other classification schemes.

The second most effective approach was texture analysis, which achieved overall accuracies ranging from 0.75 to 0.86. Within the texture feature group, the Gaussian (Sigma=3 and 7) and median (Sigma=3) variables were identified as the most influential in the classification of mixed crops. In contrast, the spectral datasets alone yielded the lowest classification accuracies, ranging from 0.71 to 0.78. Among the spectral variables, Red, Green, and the original RGB image emerged as the most crucial for crop classification, whereas Blue, ExG, and VARI showed negligible contributions across all treatments. Consequently, spectral indices were observed to be the least significant for crop classification (Figure 4-9).

**Table 4-5: Summary of overall accuracies on the test set for the random forest classifier (bold and underlined numbers are the best results per treatment).**

| Plot | Spectral | Texture | Morphology | Plot | Spectral | Texture | Morphology |
|---|---|---|---|---|---|---|---|
| A1_1 | 0.72 | 0.75 | 0.85 | A2_1 | 0.75 | 0.77 | 0.85 |
| A1_2 | 0.72 | 0.82 | 0.86 | A2_2 | 0.75 | 0.80 | **0.86** |
| A1_3 | 0.71 | 0.86 | **0.92** | A2_3 | 0.76 | 0.79 | 0.85 |
| A1_4 | 0.72 | 0.76 | 0.81 | A2_4 | 0.75 | 0.77 | 0.84 |
| A1_5 | 0.72 | 0.76 | 0.80 | A2_5 | 0.75 | 0.77 | 0.83 |
| A3_1 | 0.75 | 0.77 | 0.84 | A4_1 | 0.75 | 0.79 | 0.85 |
| A3_2 | 0.75 | 0.77 | 0.85 | A4_2 | 0.77 | 0.82 | 0.86 |
| A3_3 | 0.75 | 0.80 | **0.88** | A4_3 | 0.78 | 0.81 | 0.85 |
| A3_4 | 0.76 | 0.79 | 0.85 | A4_4 | 0.77 | 0.79 | 0.85 |
| A3_5 | 0.75 | 0.78 | 0.87 | A4_5 | 0.76 | 0.81 | **0.93** |
| A5_1 | 0.75 | 0.79 | 0.83 | | | | |
| A5_2 | 0.77 | 0.83 | 0.87 | | | | |
| A5_3 | 0.75 | 0.88 | **0.90** | | | | |
| A5_4 | 0.75 | 0.81 | 0.87 | | | | |
| A5_5 | 0.77 | 0.80 | 0.85 | | | | |

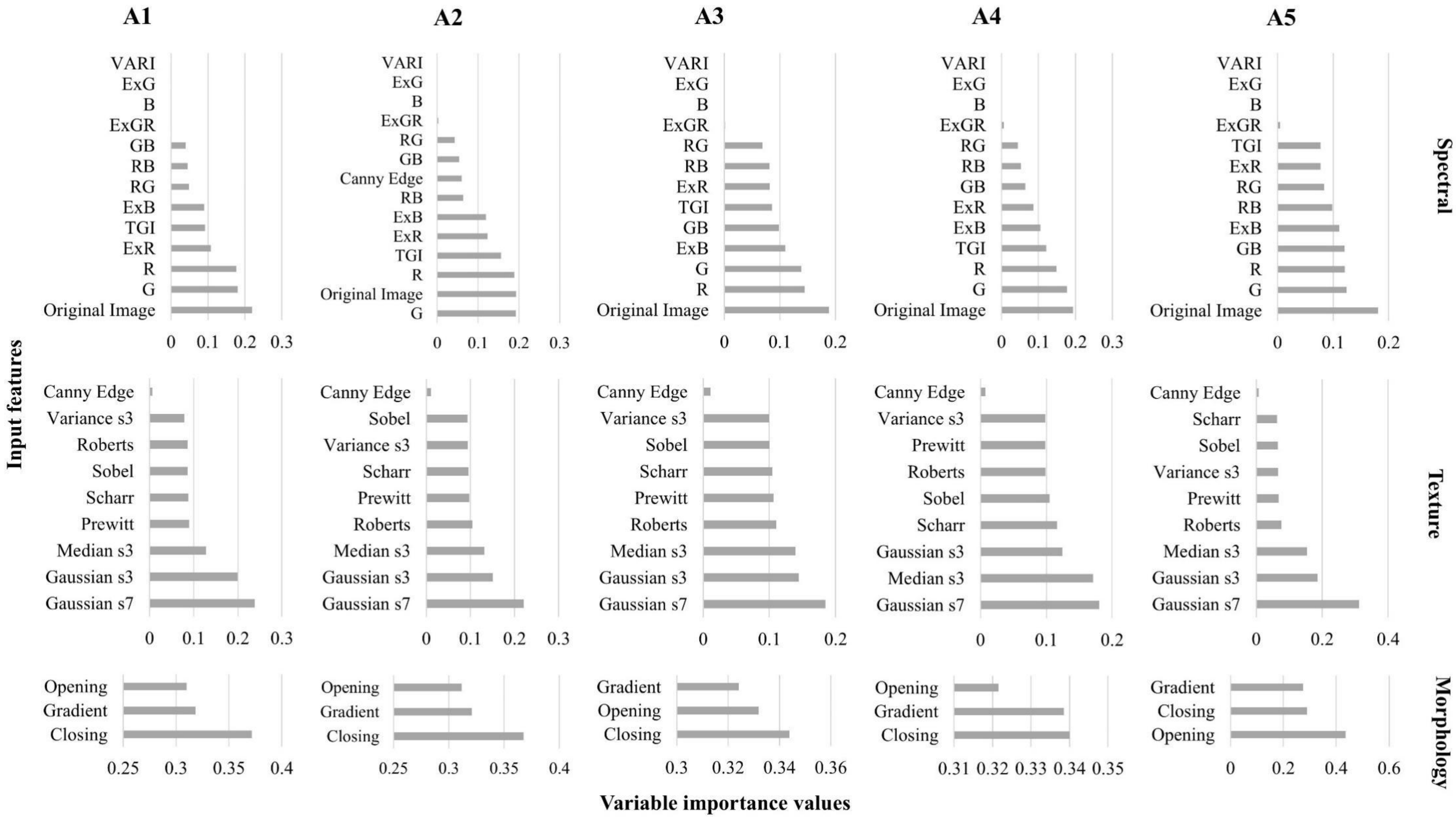


**Figure 4-8: Performance of each variable in different feature groups concerning the contribution of each variable to overall accuracy per treatment.**

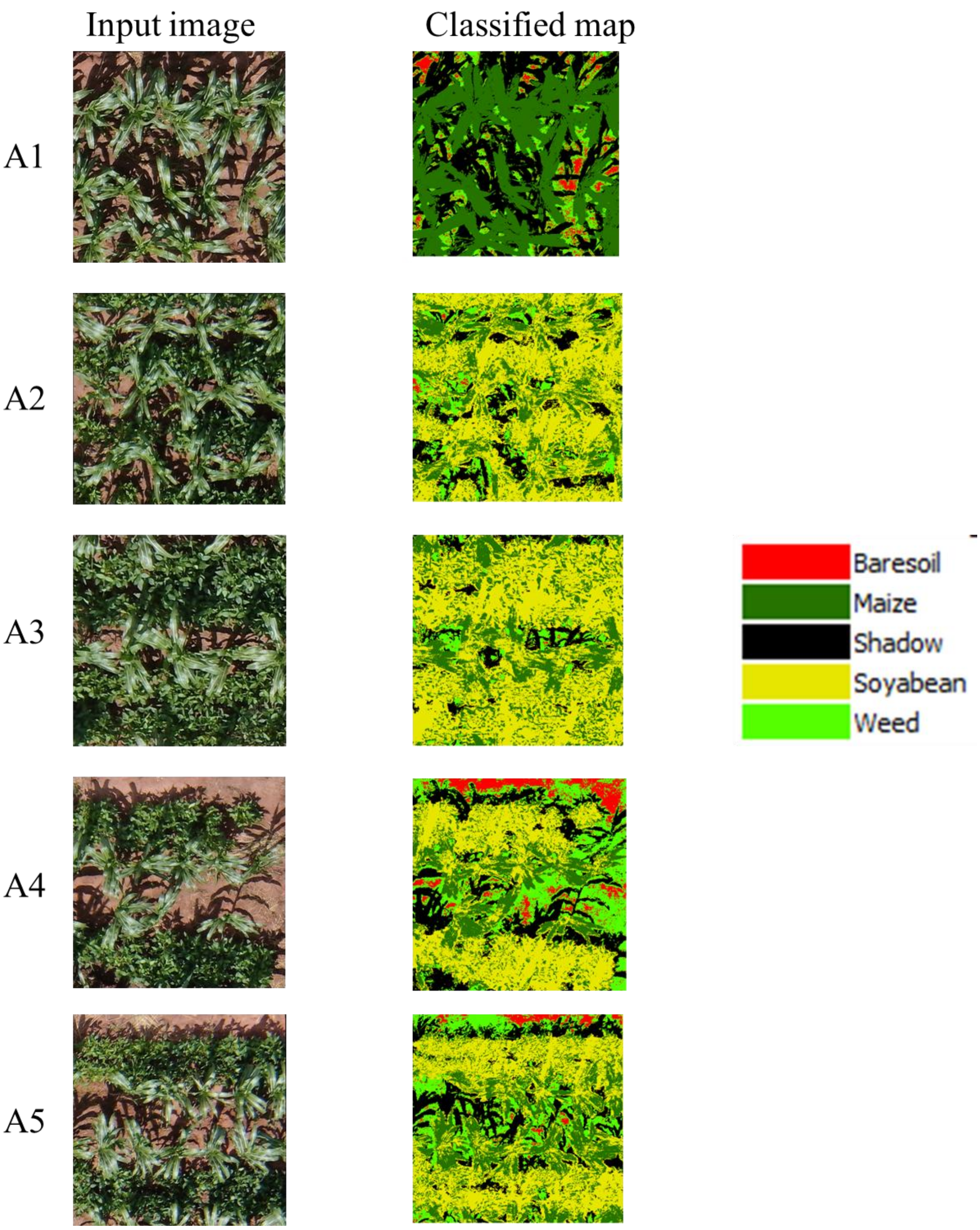


**Figure 4-9: Classified maps for high overall accuracy ratios.**

### *4.4.4 Crop classification with combined variables*

Further analysis was performed by testing a combination of morphological operations and texture-feature groups. These feature groups were selected because they showed a high overall accuracy compared to the spectral group. As shown in Table 4-6, the integration of the morphological operations and texture feature groups significantly improved the overall classification accuracy. Using this approach, it was observed that Gaussian (Sigma = 3 and 7) and closing operations were the most important features for crop classification, with overall accuracy ranging between 0.79 and 0.93. Surprisingly, a relatively lower classification accuracy (0.79) was obtained when classifying maize in monocultures than in mixtures of maize and soybeans.

**Table 4-6: Overall accuracy of combined input features (bold and underlined numbers represent the best results per treatment).**

| Ratio | Text + Morph | All_Combined | Ratio | Text + Morph | All_Combined |
|---|---|---|---|---|---|
| A1_1 | 0.81 | 0.79 | A2_1 | 0.81 | 0.79 |
| A1_2 | 0.86 | 0.84 | A2_2 | <u>**0.85**</u> | 0.84 |
| A1_3 | <u>**0.91**</u> | <u>**0.91**</u> | A2_3 | 0.83 | 0.81 |
| A1_4 | 0.81 | 0.79 | A2_4 | 0.80 | 0.79 |
| A1_5 | 0.78 | 0.77 | A2_5 | 0.79 | 0.78 |
| A3_1 | 0.81 | 0.79 | A4_1 | 0.84 | 0.83 |
| A3_2 | 0.82 | 0.80 | A4_2 | <u>**0.86**</u> | 0.85 |
| A3_3 | <u>**0.85**</u> | 0.83 | A4_3 | 0.84 | 0.83 |
| A3_4 | 0.82 | 0.80 | A4_4 | 0.83 | 0.82 |
| A3_5 | 0.83 | 0.81 | A4_5 | <u>**0.86**</u> | <u>**0.86**</u> |
| A5_1 | 0.83 | 0.81 | | | |
| A5_2 | 0.86 | 0.85 | | | |
| A5_3 | **0.93** | 0.91 | | | |
| A5_4 | 0.87 | 0.84 | | | |
| A5_5 | 0.84 | 0.83 | | | |

Where
Text is texture
Morph is morphology

The combination of morphological, textural, and spectral features reduces the overall performance of the classification model. The All_Combined feature groups had the lowest and highest classification accuracy in the maize treatment (ranging from 0.77 to 0.91). The top ten input features consisted of the texture (Gaussian with sigma 3 and 7, as well as Median with sigma 3) and morphological operations (closing and opening), as shown in Figure 4-10. The spectral features contributed the least to the performance of the classification model.

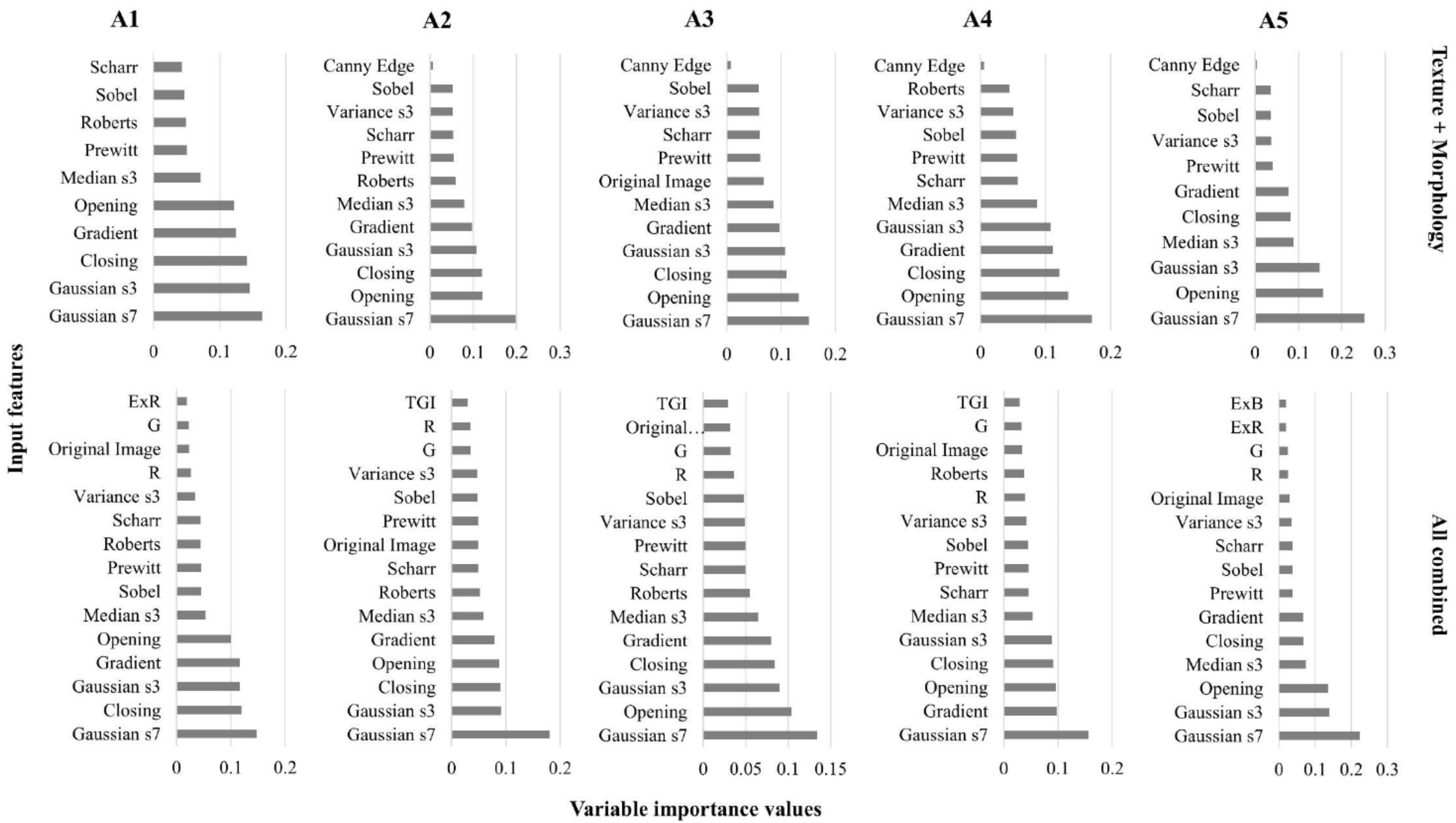


**Figure 4-10: Feature ranking for combined input features concerning the contribution of each variable to overall accuracy per treatment.**

## 4.5 Discussion

In this study, we assessed the discriminative capabilities of fine-scale resolution RGB images obtained from Unmanned Aerial Systems (UASs) in a mixed-cropping experimental setup. The high spatial resolution of these images facilitates the extraction of detailed features, encompassing subtle variations in brightness, colour, texture, shape, and structure. These features proved to be valuable indicators for distinguishing between different crop types and for detecting anomalies. Moreover, the high-resolution datasets enabled improved separation and differentiation of adjacent crops, even in fields characterised by high plant density or complex vegetation structures.

The acquisition of high spatial- and temporal-resolution RGB images yielded geometrically accurate datasets, presenting an unprecedented opportunity to enhance crop discrimination in heterogeneous environments, which has historically posed a challenge (Stutsel et al., 2021). These datasets offer the advantage of timely and cloud-free data acquisition, opening up new possibilities for discriminating mixed crops using spectral, morphological, and textural features within a random forest classification framework (Ball & Wei, 2018; Nair et al., 2019). The results demonstrate high classification accuracy, indicating that the integration of texture and morphological variables within the random forest algorithm improved crop area estimation in these complex cropping environments, characterised by features with intricate spectral properties.

Although high-spatial-resolution RGB images may have limitations in terms of spectral characteristics, the utilisation of shape, colour, and structural features outweighed their deficiencies, rendering these datasets particularly valuable in developing countries with limited financial resources (Mafuratidze et al., 2024; McCarthy et al., 2023; Mugala et al., 2020). The ease of acquisition and cloud-free nature of these datasets further contribute to their practical utility in a range of applications. The performance of the Random Forest classifier was consistent across all mixture treatments, demonstrating robustness in differentiating crops in heterogeneous plots. High overall accuracy, precision, recall, and F1-scores were maintained regardless of the maize-to-soybean ratios, indicating that the ensemble approach effectively leverages spectral, texture, and morphological features. While minor misclassifications occurred between spectrally or structurally similar classes such as soybean, weeds, and shadows, the classifier reliably distinguished the majority of crop areas, highlighting its suitability for mixed-cropping systems.

### *4.5.1 The importance of spectral data, morphology and texture information for crop classifications*

The results of this study indicate that, when considered individually, morphological operations (Opening, Closing, and Gradient) consistently outperformed the spectral and textural approaches in crop differentiation across all treatments using the random forest classification algorithm. Although the setup and environment are different, Tsoeleng et al. (2020) concluded that morphological operations produce higher classification accuracy in heterogeneous environments. Furthermore, the integration of texture and morphological features within a random forest classification scheme improves crop area estimation. The increase in the accuracy metrics considered in this study evidenced this. For instance, the precision, recall, and F1 score increased from 0.52, 0.72 and 0.6 to 0.84, 0.81 and 0.78, respectively, when using a combination of morphological and textural feature group variables (Figure 4-11).

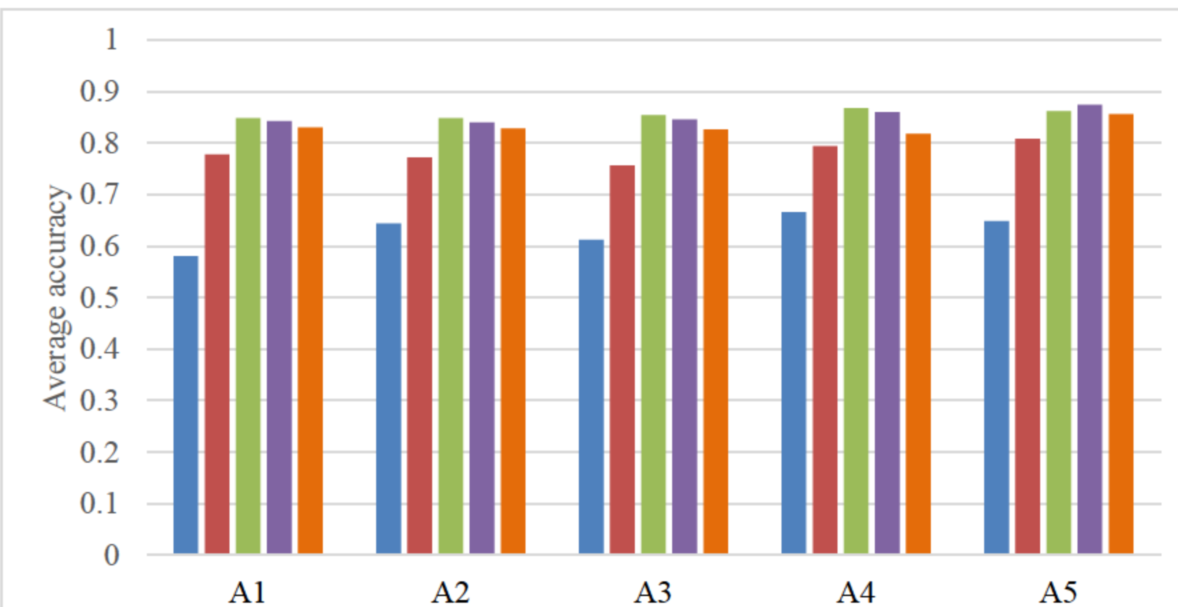


**Figure 4-11: Mean accuracy from the combination of texture and morphological operations group where Text is texture and Morph is morphology.**

Finally, we can deduce that the use of high-spatial-resolution RGB images offers a unique advantage in reducing the impact of cloud cover and highly geometrically accurate image datasets, enabling the accurate discrimination of mixed crops. By utilising these high-spatial-resolution RGB images from UASs, which provide valuable cues for texture analysis, there is an opportunity to improve the accuracy of crop classification by incorporating multiple types of features, particularly morphological and textural features.

### *4.5.2 Evaluation of the separability of crops in a mixed cropping system*

Our study further tested the spectral separability of crops grown under different densities in monocultures and mixtures. Surprisingly, the results indicated that maximum spectral differentiation was obtained when the maize crop was interspersed with soybean at a ratio of 2:1 (A4) or 2:2 (A5). The lowest separability was obtained at the ratio of 1:1 (A2). It is important to note that the initial hypothesis presumed that classifying mixed crops (with varied spectral responses) would be more challenging than classifying a single crop with a uniform spectral signature. However, this study demonstrated comparable or even superior performance in classifying mixed crops. This was also reported by Hall et al. (2018), who obtained an overall accuracy of 98% using a combination of NIR-GB and texture when classifying maize in complex smallholder farming systems. The higher classification accuracies in the mixed cropping systems might be a result of the observations of Senay et al. (2000). In their study, they noted that soybean leaves differ from maize leaves in that they are lighter and reflect more near-infrared energy, thereby offering distinct variations in colour, texture, and structure that are useful for crop discrimination. These results indicate the complexity of crop classification in heterogeneous agricultural landscapes. Nevertheless, the approach adopted here overcomes the complexity of spectrally differentiating crops in mixed cropping systems through the integration of morphological and textural variables within a random forest classification model, suggesting the robustness of the proposed approach.

Interestingly, there was limited spectral separability between the soybean, shadow, and weed classes. The confusion between soybean, shadow, and weeds could be attributed to their similarity in colour, texture, and their similarity in spectral responses, which RGB images cannot adequately distinguish. This suggests that the number of plants in each crop type in the field can affect the accuracy of crop classification. Although the approach adopted in this study demonstrates robustness in A4 and A5, it remains a challenge to distinguish between similar features, such as soybean plants, weeds, and shadows. In this context, it is worth investigating whether models based on segmentation patterns and features can overcome this potential weakness. Deep learning techniques have emerged as a promising solution for addressing these challenges, harnessing the power of neural networks to automatically learn complex relationships, capture intricate patterns, and extract relevant features from data.

Although we found few studies that are directly related to our work, our findings complement other similar studies in the literature. Chew et al. (2020a) used RGB images and deep convolutional neural networks to identify important food crop types in Rwanda. Their study mainly focused on bananas, maize, and legumes and obtained an overall accuracy and F1-score of 0.86. However, they also experience challenges in discriminating legumes from other crops with a precision of 0.57 and an F1-score of 0.49. Classifying certain crops consistently can be challenging. Sa et al. (2018) also found difficulties in distinguishing between crops and weeds because of the similarity in spectral responses. Similarly, Kawamura et al. (2021b) employed a combination of a simple linear iterative clustering algorithm and a random forest classifier to discriminate rice and weeds in Loas. Using colour space images (RGB, HSV, and L*a*b*), CHMs, texture images (spatial variety of the G-band), and vegetation index images (ExG, ExR, GRVI, and CIVE) as input variables to a simple linear iterative clustering algorithm and random forest classifier on RGB images, they obtained an overall accuracy of 0.915, as shown in Table 4-7. Although the combination of HSV and texture managed to discriminate rice from weeds, they found that rice and weeds showed similar green colours and improved accuracy; auxiliary information layers need to be developed.

**Table 4-7: Random Forest classification confusion matrix for crop classification in A5 using the most important feature group.**

| Class | Bare soil | Maize | Shadow | Soybean | Weeds | User Accuracy |
|---|---|---|---|---|---|---|
| **Bare soil** | 355 | 4 | 0 | 5 | 23 | 0.92 |
| **Maize** | 23 | 253 | 0 | 5 | 15 | 0.85 |
| **Shadow** | 1 | 0 | 76 | 106 | 2 | 0.41 |
| **Soybean** | 8 | 1 | 3 | 3936 | 19 | 0.99 |
| **Weeds** | 24 | 2 | 1 | 128 | 297 | 0.66 |
| **Producer accuracy** | 0.86 | 0.97 | 0.95 | 0.94 | 0.83 | |

It is also important to note that, in our study, we employed RGB images for analysis and obtained satisfactory overall classification results, similar to other studies that used multispectral datasets (Chivasa et al., 2020; Hall et al., 2018; JA et al., 2020; Kilwenge et al., 2021; Peña et al., 2013a; Zhao et al., 2019). Various previous studies have used data from existing field setups, but our study used datasets from an experimental setup.

Overall, our findings highlight the significance of utilising fine-scale resolution RGB images acquired from UASs for crop discrimination in mixed-cropping scenarios. The incorporation of texture and morphological features within a random forest classification framework is a promising approach for accurate crop area estimation, especially in heterogeneous environments characterised by complex spectral properties. Furthermore, selecting appropriate training samples and features is crucial for the accurate classification of mixed-cropping systems. This research contributes to the advancement of crop discrimination methodologies, particularly in regions with limited resources, and provides valuable insights for agricultural management and decision-making processes.

## 4.6 Conclusion and Future Directions

The examination of high-spatial-resolution RGB images obtained from UAS for discriminating crops in mixed cropping systems was conducted in this research. The study presented a comprehensive evaluation of the spatial distribution of maize, soybeans, shadow, weed and bare soil within a mixed-cropping experimental setup. The findings underscore the complexity of classifying mixed crops, challenging the initial hypothesis that maize monocultures would be easier to classify due to their homogeneity. Instead, the study found that the two-row maize versus two-row soybean treatment (A5) achieved the highest classification accuracy, precision, recall, and F1-score. This unexpected outcome highlights the intricacies involved in crop classification when dealing with mixed crop ratios.

This study also sheds light on the significance of spectral, morphological, and textural data for crop discrimination. The analysis indicated that morphological characteristics extracted from high-spatial-resolution RGB images consistently outperformed spectral and textural methods for crop discrimination using a random forest classifier. Integrating textural and morphological features achieved the highest classification accuracy. The inclusion of these methods into practical applications could revolutionise crop classification, offering a scalable and accessible solution for smallholder farmers and agricultural stakeholders. Overall, this study contributes to the improvement of crop discrimination techniques by utilising cost-effective high-spatial-resolution RGB images.

### 4.3 Summary

*This chapter evaluated the capabilities of UAS-based RGB imagery for discriminating between maize and soybean across varying crop mix ratios. The study assessed classification performance using different combinations of spectral (12 features), morphological (3 features), and textural (3 features) datasets. Morphological features were found to significantly outperform both spectral and textural features in differentiating features in a mixed cropping field. Moreover, combining morphological and textural features further enhanced classification accuracy, but the results were not significantly different from morphological alone. However, the analysis revealed limited spectral separability between soybean, shadow, and weed classes, highlighting a persistent challenge in RGB-based crop discrimination. Consequently, Chapter 5 builds upon these findings by focusing on the detection and removal of shadow effects to improve the accuracy of crop acreage estimation in mixed cropping systems.*

# CHAPTER 5 : REMOVING SHADOW EFFECTS

This Chapter is based on:

**Mafuratidze, P.,** Mutanga, O., Masocha, M., Dube, T., & Sibanda, M. (2025). Enhancing target crop discrimination: a novel shadow detection technique for RGB datasets in mixed agricultural environments. *Journal of Spatial Science*, 1–16. https://doi.org/10.1080/14498596.2025.2544143

## ABSTRACT

RGB datasets are increasingly used by researchers who cannot afford state-of-the-art multispectral sensors to extract vital agricultural information. However, these datasets tend to be contaminated by shadows. The shadow effect is amplified in the smallholder farming sector, in which farmers often mix two or more crops in the same field. Because smallholder farmers constitute the majority of developing countries, developing robust techniques for shadow detection is crucial for discriminating target crops in such settings. In this study, a new hue-intensity-green-blue (HIGB) difference technique was developed. Its performance was evaluated against the $C_3$ and Normalised Saturation-Value Difference index (NSVDI) models based on five metrics. The metrics were computed based on RGB datasets, in which maize and soybean mixtures were experimentally manipulated. The new technique was developed based on the differences between hue and intensity and the difference between the green and blue channels. The results indicate that the HIGB difference technique consistently outperformed both the $C_3$ and NSVDI models across the five treatments. The HIGB difference technique achieved overall accuracies ranging from 77% to 95% compared to 63% to 84% for NSVDI. The overall accuracy for $C_3$ ranged from 69% to 81%. The results of four other performance metrics revealed a similar pattern. Even for treatments where shadows were either dark or obscured by other plants, the lowest overall accuracy achieved by HIGB was 77% compared to 69% and 63% for NSVDI and $C_3$, respectively. Overall, these results demonstrate the superiority of the new HIGB difference technique for shadow detection.



Keywords: *Glycine max*, cast shadow, crop discrimination, hue intensity, RGB imagery, unmanned aerial systems.

## 5.1 Introduction

In recent years, high spatial-resolution RGB images acquired using unmanned aerial systems (UAS) have been thriving and prevailing in precision agriculture (Andritoiu et al., 2018; H. Feng et al., 2022; Hatfield et al., 2008; Hunt Jr et al., 2013; Ndlovu et al., 2021a). However, when used in mixed cropping systems, the datasets are affected by shadows. This is inevitable, especially in smallholder farms that normally practice mixed cropping systems. A mixed cropping system is a combination of two or more crops in a single field (Sa et al., 2018; Swain et al., 2007; Tikkiwal & Khandelwal, 2012). For example, cereal and legumes are the most popular crop mixtures in most developing countries. Normally, cereal crops are taller than legumes. Therefore, the taller plants will totally or partially occlude direct light and cast shadows on smaller, shorter legumes in mixed cropping systems.

Shadows are classified into two classes: cast shadows, which refer to those shadows cast on the ground by high-rise objects, and self-shadows, which refer to the part of the object that is not illuminated (Huang et al., 2004; Ma et al., 2008; Polidório et al., 2003). In remote sensing, shadows are often regarded as a nuisance, especially in heterogeneous environments (e.g., mixed cropping systems), because you can underestimate or overestimate each constituent crop acreage. Additionally, shadows also change shape and exhibit false colour tones of features. This is normally seen in dark vegetation pixels that may appear like a shaded region if there is low luminance. The presence of cast shadows and self-shadows on images disturb accurate crop discrimination during image analysis, thus severely affecting the quality and the accuracy of the results. Therefore, they cause partial or total loss of accurate and correct statistics in the constituent crop area through misclassification and wrong interpretation of surface information. Furthermore, the identification of targeted features and important vegetation properties (Agarwal et al., 2021) becomes a complex task. Hence, the development of suitable algorithms that can utilise high spatial-resolution RGB images to minimise the shadow effect without losing the integrity of the visual representation is necessary.

The presence of shadows in an image requires the use of algorithms that can detect and remove shadows, which is an unavoidable task during pre-processing. It is a necessary step to remove shadows and restore the actual scenes in remote sensing before feature extraction in the final image classification pipeline (Silva et al., 2018). Several studies have been conducted to investigate shadow detection and removal in remote sensing applications (Alvarado-Robles et al., 2021; Alvarado-Robles et al., 2021; Dharani & Sreenivasulu, 2019; Han et al., 2018; Mostafa & Abdelhafiz, 2017b; Pons & Padró, 2019; Prabhakar & Garg, 2022). It is widely known that colour properties are valid description tools that simplify the identification of visual interpretation tools in remote sensing. Eventually, the retrieval of colour characteristics from high spatial-resolution RGB images requires new methodologies that enhance shadow detection. The initial step for detecting shadows on an image is to identify dark pixels. Previous studies repeatedly categorised shadow detection approaches into two classes: model-based and property-based methods (Ge, 2019; Jiang et al., 2019; M-Desa et al., 2022; Pons & Padró, 2019). However, Adeline et al. (2013) noted that shadow regions are normally detected using several algorithms that include model-based, machine-learning, physics-based, and property-based methods.

In general, the first two methods, model-based and machine-learning, rely on a priori information, while physics-based methods generally use material reflectance (Adeline et al., 2013; Zigh et al., 2016). Furthermore, model-based methods' accuracy is directly limited by the accuracy of 3D geometric models and can be affected by geometrical mismatches during the registration of data types. This method is also invariant to material reflectance. Machine learning methods are specifically unsupervised methods, for example, K-means (Prabhakar & Garg, 2022), have the limitation of the initial choice of the number of classes in the scene, and supervised methods such as the support vector machine (Lorenzi et al., 2012) require reference samples to train the classifier, which may be scarcely available. Physics-based methods require knowledge of accurate metadata to apply atmospheric correction and deal with problems occurring during histogram thresholding. They also require additional information like scene location, sun and viewing angles, and aerosol abundance, which is often lacking (Adler-Golden et al., 2002; Richter & Müller, 2005). Considering all the above-mentioned drawbacks, the accuracy of the shadow identification process is an area that requires further inquiry.

Fortunately, remotely sensed images show that shadow regions are represented by dark pixels, which is a unique characteristic (Gonzalez & Woods, 1992). An image's unique features or properties can be effectively exploited to differentiate it from other features (Tsai, 2006). Unlike the first three algorithms, property-based methods do not require any a priori information. These methods consider shadow properties directly deduced from image characteristics, including both radiometric attributes with spectral features and textural attributes through spatial features. Property-based methods are categorised into four different classes, which include simple histogram thresholding, invariant colour models, classification, and object segmentation. As analysed above, it shows that property-based methods are versatile and adaptable to different data sets without the need for prior knowledge or assumptions and apply to single images.

In the last few years, researchers have proposed various methods for detection and correcting for shadowing in high spatial-resolution RGB images using property-based methods. The early property-based method by Gevers and Smeulders (1997), focused on the application of colour theory in pattern recognition. The method utilised various colour features such as intensity, RGB, normalised colour, hue, and saturation for the development of new colour models. In their study, they found that colour features $l_1l_2l_3$, $C_1C_2C_3$ and RGB are appropriate for multi-coloured objects invariant to shadow. Also, Sarabandi et al. (2004) proposed the use of a non-linear transformation, third dimension C3, to identify shadow boundaries. Tsai (2006) further proposed several invariant colour spaces, including hue, saturation, and intensity (HIS), hue, saturation, and value (HSV), hue, chroma, and value (HCV), luma, in-phase, and quadrature (YIQ), and $YC_bC_r$ models for shadow detection. The researcher compared the effectiveness of these colour features and found that HIS performed better than others in revealing details under shaded regions. In addition, Azevedo et al. (2015) proposed a semi-automatic shadow detection methodology that combined the spectral indices normalised difference vegetation index (NDVI) and normalised saturation-value difference index (NSDVI) based on colour space properties.

According to different literature sources above, various shadow detection algorithms tend to differentiate shadow and non-shadow regions in areas that have features with clear chromaticity and luminance (such as very high chromaticity and very low luminance) gaps. Furthermore, these mainly focused on detecting shadow and non-shadow regions using satellite images (Mostafa & Abdelhafiz, 2017a). However, to the best of our knowledge, there are no shadow detection methods for very high spatial resolution RGB images done in mixed cropping systems. As noted in the literature, mixed crops have high variation and intensity values that cause a loss of information on overall accuracy. For example, dark vegetation pixels are normally misclassified as shaded regions because of low luminance. As a result, it would be desirable to develop a shadow detection algorithm that will minimise the shadow effect based on analysing the spectral features of objects and improving the spatial distribution of neighbouring pixels. The objectives of this study were to: 1) assess the efficacy of image enhancement techniques using high spatial resolution RGB images; 2) enhance class separability; and 3) devise a robust method for shadow detection.

## 5.2 Materials and Methods

### *5.2.1 Steps for developing a new shadow detection technique based on HIS*

Using human interpretation of high-resolution RGB images to identify and find shadows is easy because the shadow itself is one of the fundamental elements of image interpretation. However, in the process of shadow identification for high spatial resolution RGB images, there are complexities which include edge vagueness, colour inconsistency, illumination variation, colour tone variation, and others which seriously affect the quality of classified images (Alvarado-Robles et al., 2021; Silva et al., 2018). Tsai (2006) noted that the luminance and chromaticity properties of shadows on high spatial-resolution RGB images can be used for de-shadowing. Furthermore, it has been observed that shadow areas are characterised by the following features:

- Lower luminance (intensity) because the electromagnetic radiation from the sun is blocked in these regions (Tsai, 2006),
- Higher saturation with short blue-violet wavelength due to the Rayleigh effect of atmospheric scattering (Polidório et al., 2003), and
- Increased hue values, because the intensity change of a shaded area when compared to an unshaded area is proportional to the wavelength values (Huang et al., 2004).

Considering the characteristics of shadows as mentioned above, the proposed approach’s main objective was to improve shadow detection using a variety of variant and invariant indications. Our main goal was to exploit the invariant colour components occurrence for the three primary channels in red, green, and blue in conjunction with colour-transformed hue and intensity to create shadow masks. Firstly, the authors started with pre-processing the input datasets by applying an enhancement technique to minimise the amplification of noise. Secondly, we analysed the effectiveness of the existing colour space and extracted hue, intensity, green, and blue channels for the calculation of the proposed approach. Thirdly, the calculated index was normalised to range between 0 and 255. Fourth, we applied thresholding to obtain a binary mask using Otsu's thresholding method and applied a morphological opening process to the processed image to obtain the binary shadow mask. In this way, we reduced the influence of the small shadows formed by soybeans. To achieve our main goal, the proposed approach for shadow detection had different steps divided into three as follows;

1) Input data and pre-processing,
2) Colour space transformation,
3) Index normalisation, and
4) Post-processing.

The proposed approach is summarised as shown in Figure 5-1.

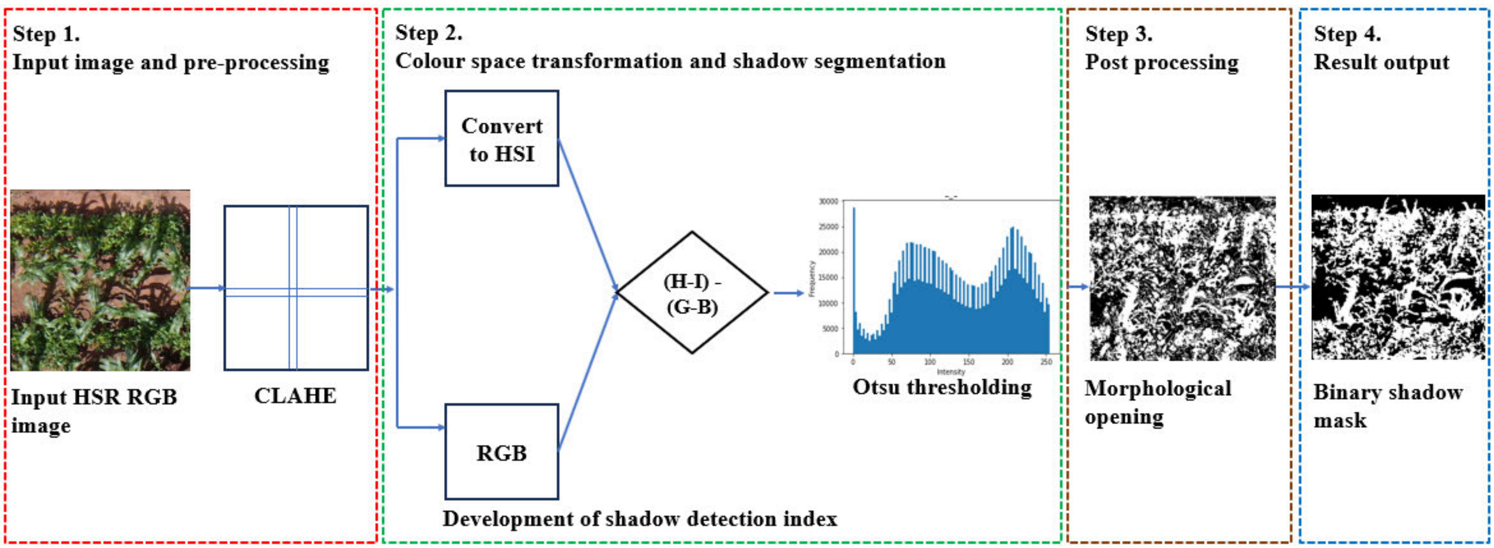


**Figure 5-1: Flowchart of the proposed approach.**

### 5.2.1.1 Input data and preprocessing

*Input data*: The datasets used were obtained from five high spatial-resolution RGB images captured by a DJI Matrice 300 mounted with a Zenmuse (ZH20T) camera. The datasets were captured at an altitude of 90 m above ground level between 10:30 a.m. and 1:30 p.m. local time. The UAS datasets were acquired on the 12$^{th}$ of March 2022, 48 days after planting during maize's last vegetative stage (tassel emergence). At this stage, maize exhibits distinct spectral and structural characteristics, including fully developed leaves and tassels, which improve separability from soybean and background features. Collecting data at 48 DAP maximises the accuracy of crop classification while minimising spectral confusion from soil background or overlapping early growth stages. The five areas of interest (study plots) have different crop mixtures (Figure 5-2a), where A1 (1346 x 1039 pixels) is a sole maize area, A2 (1268 x 1103 pixels) is a mixture of one-row maize and one row of soybean, A3 (1358 x 1063 pixels) is a mixture of one row of maize and two rows soybean, A4 (1258 x 1084 pixels) is two rows of maize and one row of soybean, and A5 (2069 x 1168 pixels) is a mixture of two rows for both maize and soybean. Each treatment was replicated 5 times, and treatments were allocated to plots randomly. Note that the results presented in this work were based on one randomly selected RGB dataset for each treatment.

*Pre-processing*: To maintain the characteristics of local regions while also improving the visual quality of high spatial-resolution RGB images in mixed cropping systems, it is better to employ a local contrast enhancement technique known as contrast-limited adaptive histogram equalisation (CLAHE)(Pizer et al., 1990). The application of this method will avoid the over-enhancement of the homogeneous regions and provide better contrast enhancement in detailed regions. The CLAHE is a spatial domain-based method based on maximising entropy and limiting contrast, which is used to optimise input images (Qassim et al., 2019). Using CLAHE, it divides the input image into several non-overlapping grids of rectangular contextual sub-blocks of equal size. Thus, the initial step in achieving the desired clip limit is capturing every sub-block histogram. These blocks are used as the smallest processing unit, preserving and maintaining homogeneous characteristics. In addition, bilinear interpolation between mapping functions adjacent to blocks is performed to avoid the appearance of block artefacts.

To quantitatively assess image quality and performance on the enhancement algorithms, various metrics such as entropy, mean and root mean square (RMS) contrast were tested. RMS is the most widely used standard model to quantitatively differentiate the detailedness of an image (Velichko et al., 2022). It also predicts human contrast detection thresholds for natural scenes. Larger RMS represents better image contrast and is computed as follows;

$$\text{RMS} = \sqrt{\frac{1}{\sum_{i=1}^{N} W_i} \sum_{i=1}^{N} w_i \frac{(L_i - L)^2}{L^2}} \qquad [1]$$

with

$$L = \frac{1}{\sum_{i=1}^{N} W_i} \sum_{i=1}^{N} w_i\, L_i$$

where N is the total number of pixels in the patch, $W_i$ is the weight of the raised cosine windowing function at the *i^th^* pixel, and $L_i$is the luminance of the $i^{th}$ pixel. Another quantitative evaluation metric is entropy, and it involves the application of statistical metrics to successfully determine the amount of information that an image contains (Qassim et al., 2019). Entropy is calculated as follows;

$$\text{Entropy } (l) = -\sum_{k=0}^{n-1} p_k \log_2 p_k \qquad [2]$$

where *l* is the original image,$p_k$is the probability of occurrence of the value *k* in the image *l*, and $n$ indicates the number of diverse grey levels.

| | RGB images | Histogram of the input image | Ground truth |
|---|---|---|---|
| (A1) Sole maize (1346 x 1039) |  | 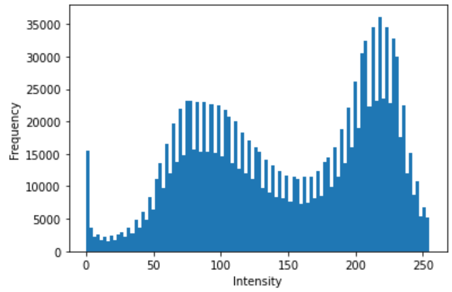 |  |
| (A2) One maize vs one soybean (1268 x 1103) |  | 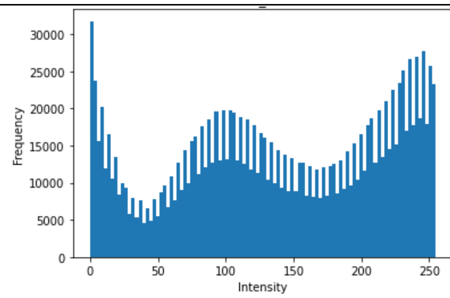 |  |
| (A3) One maize vs two soybean |  | 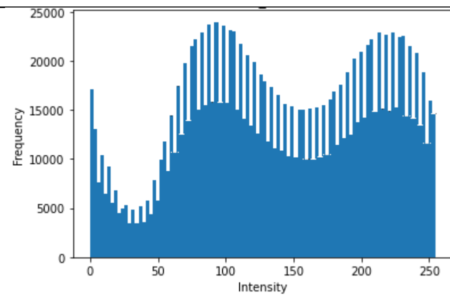 |  |
| (A4) Two maize vs one soybean (1258 x 1084) | 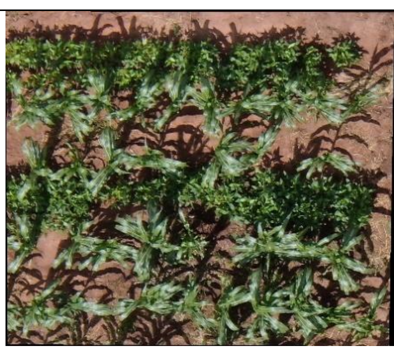 | 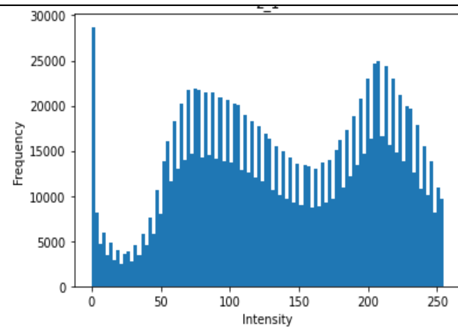 |  |

| | | | |
|---|---|---|---|
| (A5) Two maize vs two soybean (2069 |  | 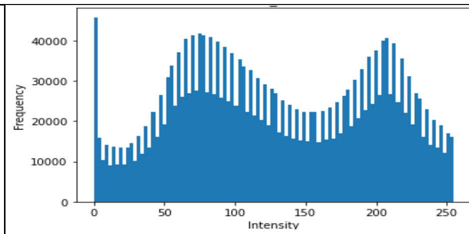 |  |
| | a | b | c |

**Figure 5-2: Input RGB images for the proposed model, (a) Original RGB images, (b) histogram of the input image, and (c) manually annotated ground truth data showing shadow (white) and non-shadow (black) regions.**

#### 5.2.1.2 Selection of spectral properties for Shadow detection (colour space transformation)

The common appearance of shadows on high spatial-resolution RGB images is typically characterised by darker regions than the visual field in which they are situated. Furthermore, their pixel values are generally low in all RGB channels. Nonetheless, the fact that the shadows are simply correlated with the darkness is limited, as any lightless object can produce a shadow, resulting in an inaccurate binary shadow mask. Accordingly, for the proposed approach to work, we used the following steps;

1) Image colour transformation from the RGB model into the photometric invariant HSI colour space, to separate colour from intensity information,
2) Separation and selection of appropriate bands from R, G, B, H, S, and I,
3) Development of a shadow detection index using the combination of HSI and RGB channels to exploit the fact that shadows have larger hue values and are more prevalent and exposed in green and blue channels,
4) Normalisation, and
5) Thresholding.

The use of hue, saturation and intensity colour space is motivated by previous work, for example, Gettinger (2015) and Silva et al. (2018) noted that in shadow detection, single images can be used for detecting shadows and non-shadow regions. They also noted that using RGB pixel values in greyscale did not produce the desired overall accuracy. Furthermore, extracting important shadow regions using single-band information may lead to false categorisation of image pixels. Hence, using other information available in different bands from high spatial-resolution RGB images is useful for increasing the segmentation's overall accuracy as observed by Sarabandi et al. (2004) and Tsai (2006). Generating an illumination-invariant image could provide useful information on the shadow areas. As part of the work presented in this study, a combination of RGB bands and HIS colour space is used to detect shadows based on hue (H), intensity(I), green(G), and blue(B) channels.

The principle of the proposed algorithm is based on the identification of two features, namely shadow and vegetation pixels. Prabhakar and Garg (2022) noted that the original image's pixels in shadow regions have higher values as compared to non-shadow regions when using a hue (larger hue values) to intensity (low luminance) ratio, which heightens the hue attribute of shadows with low intensity. As such, the difference between H and I (H-I) aim to highlight pixels where the intensity is reduced without a significant change in hue, which will highlight potential shadow regions. This colour space provides better separation between chromaticity and intensity and highlights the presence of shadows than the RGB model on its own. Shadow regions are identified by a larger difference between hue and intensity (H-I). Also, RGB bands struggle to highlight the presence of shadows on their own; however, Mostafa and Abdelhafiz (2017a) observed that subtracting blue from green channels results in lower values for shadow pixels, while vegetation pixels have large differences between the two bands. The construction principle of HIGB is based on indicating shadows with higher values due to high differences between hue and intensity (H–I), while there is a small difference between green and blue (G-B) due to the reduced green reflectance. On the contrary, areas with healthy vegetation might have lower HIGB values due to a smaller difference between H and I and potentially a higher difference between green and blue channels.

This study proposed a new technique for shadow detection based on the green and blue bands from the RGB model and hue and intensity from HIS colour space of a high spatial resolution RGB image. Formally, the new technique is:

$$\text{HIGB} = (H - I) - (G - B) \quad [3]$$

where H is the hue component, I is the intensity, and G and B represent the green and blue channels of the image, respectively. The computation proceeds as follows:

i) Hue (H) is derived from the RGB channels using:

$$\text{where } H = \begin{cases} \theta & if\ G \geq B \\ 360° - \theta & if\ G < B \end{cases} \quad [4]$$

with $\theta$ calculated as:

$$\theta = \cos^{-1}\left\{\frac{\frac{1}{2}[(R-G)+(R-B)]}{[(R-G)^2+(R-B)(G-B)]^{1/2}}\right\} \quad [5]$$

and

ii) Intensity (I) derived from:

$$I = \frac{(R+G+B)}{3} \quad [6]$$

iii) Green-Blue Difference (G – B): The equation captures the relative dominance of green over blue, emphasising vegetation reflectance characteristics.

iv) HIGB Index Computation: is computed by combining the hue and intensity components with the green-blue difference as shown in the main formula.

For comparison purposes, the HIGB index result was normalised to the range of values in [0, 1] intervals. Furthermore, the Otsu method proposed by Otsu (1979) is an important model for determining the threshold of binary shadow. It is a threshold determination method, also known as the one which maximises the between-class variance of the two histogram classes and separates the image into two parts, background, and foreground. For the proposed method, a binary shadow mask was obtained using the Otsu method, which extracts the threshold of shadow segmentation automatically.

#### 5.2.1.3 Post-processing

After the thresholding process, the binary shadow mask may be characterised by a “salt and pepper” effect that looks like small gaps due to the misclassification of shadow pixels. Gonzalez and Woods (1992) proposed the use of morphological operations like Opening and Closing to eliminate such small gaps. However, the selection of morphological filters to solve this problem is based on their effectiveness. Hence, for this study, we proposed the use of the morphological Opening operation with a kernel of a 3×3 structuring element to avoid the generation of distorted structures as proposed by Wang et al. (2021).

## 5.3 Image Evaluation

### *5.3.1 Qualitative evaluation of the HIGB difference technique*

To verify the performance and effectiveness of the HIGB difference technique, both qualitative and quantitative measures were used. Specifically, the HIGB difference technique was compared to two widely extensively used shadow detection models, that is, the $C_3$ model from the colour model ($C_1C_2C_3$) constructed by Sarabandi et al. (2004) and the normalised saturation-value difference index (NSVDI) developed by Ma et al. (2008). The important aspect of these models is that they are pixel-based methods and output binary shadow masks. The HIGB, $C_3$ and NSVDI were separately applied to five RGB datasets comprising maize and soybean (*Glycine max*) mixed at varying ratios with patches of bare soil, weeds and shadows. To achieve an unbiased comparison, the ground reference *shadow image* was obtained by manually creating and annotating shadow areas using selection tools in V7 Darwin (https://darwin.v7labs.com).

### *5.3.2 Quantitative evaluation of the HIGB difference technique*

The ground reference shadows, generated through manual interpretations, were employed for accuracy assessment. The error matrix method was used for objective evaluation. As such, evaluation metrics such as user's accuracy (UA), producer’s accuracy, also known as true positive rate (TPR), specificity, also known as true negative rate (TNR), F1_score (FS) and overall accuracy (OA) were computed at pixel level using the following formulas;

$$\text{TPR} = \frac{TP}{TP+FN} \qquad [7]$$

$$\text{UA}= \frac{TP}{TP+FP} \qquad [8]$$

$$OA = \frac{TP + TN}{TP + TN + FP + FN} \qquad [9]$$

$$TNR = \frac{TN}{TN + FP} \qquad [10]$$

$$FS = 2\,\frac{TPR * UA}{TPR + UA} \qquad [11]$$

where: TP, TN, FP, and FN are true positive, true negative, false positive, and false negative, respectively. TP is the number of shadow pixels correctly identified, TN is the number of non-shadow pixels correctly identified, FP is the number of non-shadow pixels incorrectly identified, and FN is the number of shadow pixels incorrectly identified. As a result, the true positive rate shows the probability of the method accurately identifying a pixel as a shadow among the true shadow pixels. On the other hand, specificity provides the probability of the method accurately labelling a pixel as non-shadow among the actual non-shadow pixels. Consequently, higher values for these two measures, as well as the FS score, indicate improved prediction.

## 5.4 Results

### *5.4.1 Image enhancement for shadow detection*

Figure 5-3 presents the results of image enhancement compared against the original images. It can be observed that while the image enhanced using ordinary thresholding appears to resemble the features in the original image, the technique struggled to identify cast and self-shadows across the five treatments. If one zooms in on the image, it is apparent that ordinary thresholding works better in relatively homogeneous sub-areas of the image with less intensity. When image enhancement was performed using CLAHE, this technique was able to identify shadows regardless of the degree of crop mixing. For example, treatments A2, A3 and A5 have high crop density resulting in huge canopy differences. Despite this, CLAHE proved useful for discriminating target features from shadows. An interesting aspect of images enhanced using CLAHE is that they do not look ‘perfect’ when evaluated against the perception of the human eye. The images appear over-enhanced, especially in the homogeneous regions, as reflected in the A1 and A4 treatments. Results in Table

5-1 confirm that CLAHE enhanced all the images for the five treatments, resulting in higher values for both entropy and root mean square (RMS) compared to ordinary thresholding. The RMS values for CLAHE ranged from 1.628 to 1.677, while those for ordinary thresholding ranged from 1.482 to 1.610.

**Table 5-1: Quantitative metrics of Ordinary Threshold and CLAHE algorithms for enhancing RGB images acquired over five crop mixing treatments.**

| | Ordinary Threshold | | | CLAHE | | |
|---|---|---|---|---|---|---|
| **Treatment** | **Entropy** | **RMS** | **Mean** | **Entropy** | **RMS** | **Mean** |
| A1 | 2.31 | 1.521 | 138.99 | 2.54 | 1.645 | 130.3 |
| A2 | 2.34 | 1.579 | 150.29 | 2.55 | 1.646 | 128.5 |
| A3 | 2.42 | 1.610 | 141. 90 | 2.59 | 1.677 | 125.9 |
| A4 | 2.26 | 1.482 | 134.99 | 2.53 | 1.628 | 126.5 |
| A5 | 2.33 | 1.517 | 132.07 | 2.56 | 1.651 | 127.6 |

RMS = root mean square, CLAHE = contrast-limited adaptive histogram equalisation. A1 is a sole maize (control) plot, A2 is one-row maize and one row of soybean grown in the same plot, A3 is a mixture of one row of maize and two rows of soybean, A4 is two rows of maize and one row of soybean, and A5 is a mixture of two rows for both maize and soybean.

| **Treatments** | **Original image** | **Ordinary thresholding image** | **CLARE enhanced image** |
|---|---|---|---|
| Sole maize (A1) |  |  | 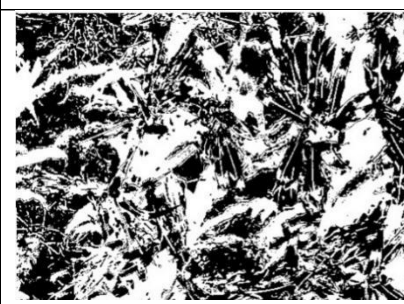 |

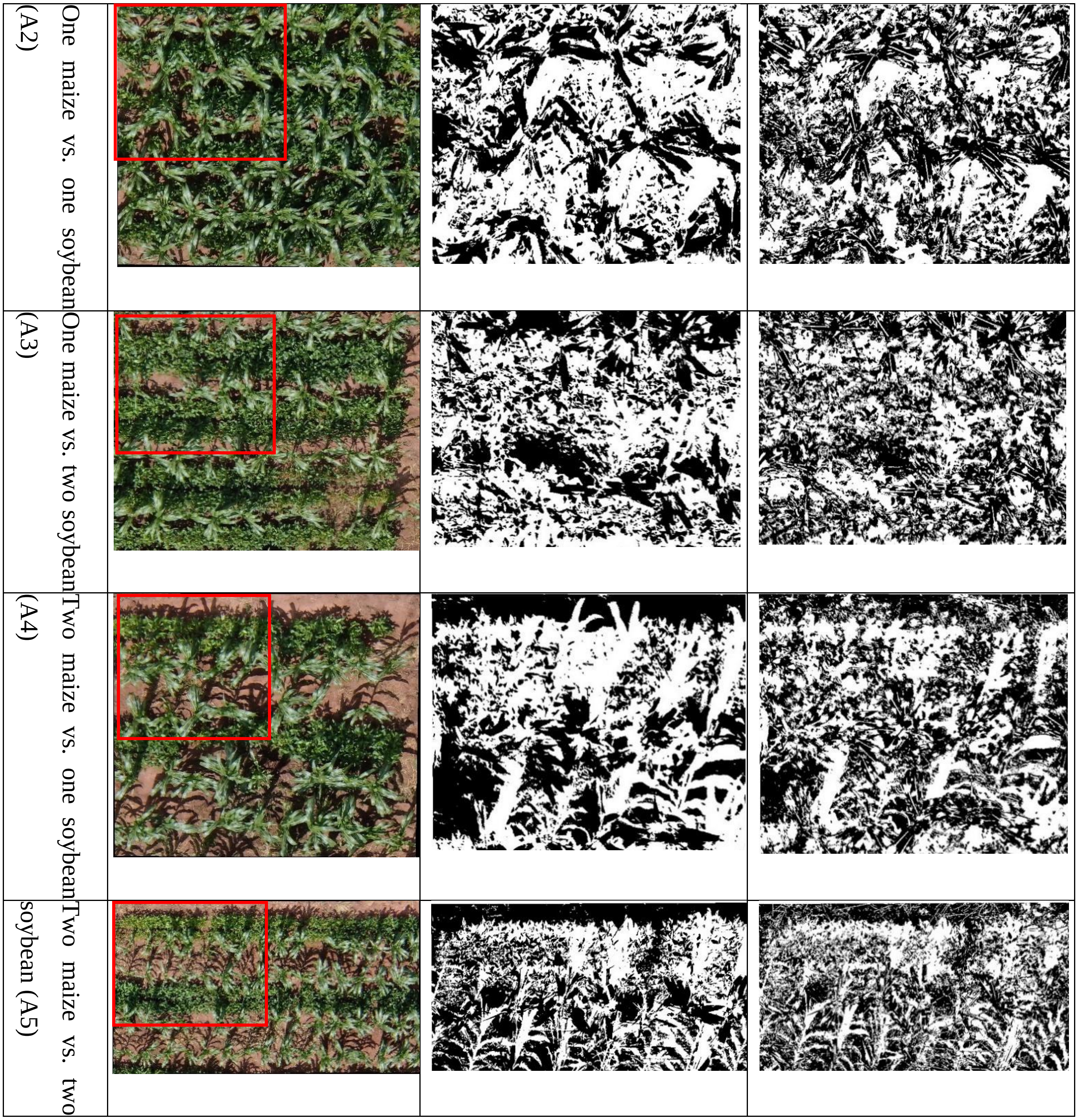


**Figure 5-3: Comparison of ordinary thresholding and CLAHE images showing shadow (white) and non-shadow (black) regions in enhanced RGB images for five plots with maize and soya mixed at different ratios.**

### *5.4.2 Qualitative analysis of shadow detection results of the proposed model*

Figure 5-4 presents shadow detection results of the HIGB difference technique, the $C_3$, and the NSVDI methods applied on the original RGB image for the five crop treatments**.** The detected shadows were compared to a manually created ground reference dataset of shadows. Comparatively, the HIGB difference technique detected shadows better than either of the two methods. This result was consistent across the five crop treatments.

| **Treatments** | **Original image** | **HIGB** | **$C_3$** | **NSVDI** | **Ground Reference** |
|---|---|---|---|---|---|
| Sole maize (A1) |  |  |  |  |  |
| One maize vs. one soybean (A2) |  | 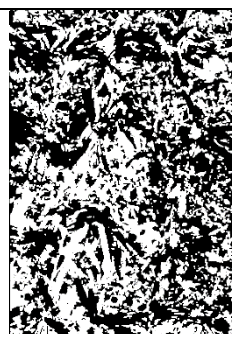 | 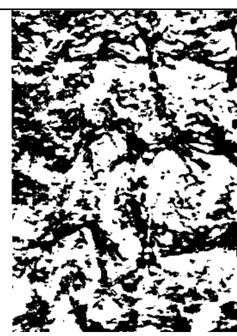 | 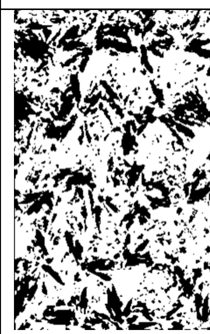 |  |
| One maize vs. two soybean (A3) |  | 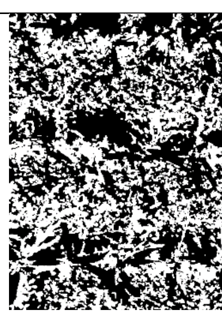 | 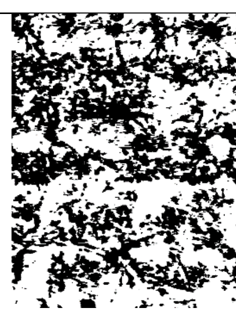 |  |  |

| Treatments | Original image | HIGB | $C_3$ | NSVDI | Ground Reference |
|---|---|---|---|---|---|
| Two maize vs. one soybean (A4) |  | 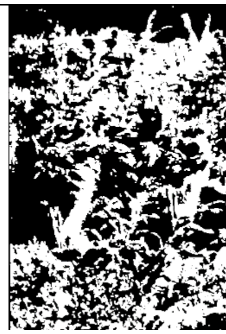 |  | 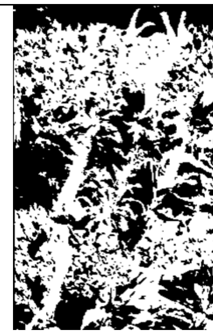 |  |
| Two maize vs. two soybean (A5) |  | 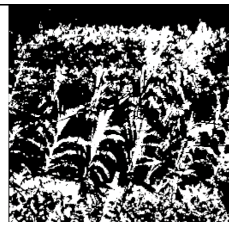 |  |  |  |

**Figure 5-4: The shadow detection results of the new HIGB difference technique, the C3 model, and the NSVDI index when applied to five RGB datasets consisting of maize and soya mixed at different ratios. The original RGB datasets and manually delineated shadows are presented for ease of comparison. Shadows are white and non-shadows are black.**

### *5.4.3 Quantitative analysis of the proposed approach*

The study compared the results of the proposed methodology with those of conventional methodology. Given that our proposed approach utilises data from HSI and colour components, it becomes important to assess quantitatively the extent of their contributions to the achieved results. The accuracy assessment of shadow extraction for each index across different crop mixtures is presented in Table 5-2. The NSVDI index produced reasonable results of 0.83 and 0.84 with treatments A1 and A5, respectively. This was followed by treatments A3 and A4 with an overall accuracy of 0.76 and 0.82, respectively, while at treatment A2, the accuracy decreased to 0.63, mainly due to high crop density causing darkness of vegetation pixels. The $C_3$ model produced high overall accuracy in treatments A1 and A4 of 0.77 and 0.81, respectively. The OA decreased to 0.74 and 0.71 for treatments A3 and A2, respectively, followed by the lowest on A5 with 0.69.

**Table 5-2: Error matrix for the HIGB index, C3 and NSVDI models applied on five RGB datasets acquired by a UAS in mixed settings.**

| | HIGB | | | | | $C_3$ | | | | | NSVDI | | | | |
|---|---|---|---|---|---|---|---|---|---|---|---|---|---|---|---|
| **Crop mixture** | **TPR** | **UA** | **TNR** | **OA** | **FS** | **TPR** | **UA** | **TNR** | **OA** | **FS** | **TPR** | **UA** | **TNR** | **OA** | **FS** |
| Sole maize (A1) | 0.95 | 0.93 | 0.95 | **0.95** | 0.93 | 0.76 | 0.74 | 0.70 | 0.77 | 0.76 | 0.83 | 0.83 | 0.81 | 0.83 | 0.81 |
| One row of maize vs. one row of soybean (A2) | 0.77 | 0.71 | 0.77 | 0.77 | 0.74 | 0.70 | 0.69 | 0.68 | 0.71 | 0.65 | 0.63 | 0.62 | 0.60 | 0.63 | 0.59 |
| One row of maize vs. two rows of soybean (A3) | 0.80 | 0.63 | 0.81 | **0.81** | 0.71 | 0.75 | 0.71 | 0.72 | 0.74 | 0.73 | 0.76 | 0.76 | 0.73 | 0.76 | 0.74 |
| Two rows of maize vs. one row of soybean (A4) | 0.89 | 0.71 | 0.84 | **0.86** | 0.79 | 0.81 | 0.79 | 0.78 | 0.81 | 0.78 | 0.82 | 0.70 | 0.79 | 0.82 | 0.81 |
| Two rows of maize vs. two rows of soybean (A5) | 0.84 | 0.73 | 0.84 | **0.84** | 0.82 | 0.79 | 0.77 | 0.66 | 0.69 | 0.44 | 0.84 | 0.82 | 0.83 | **0.84** | 0.79 |

Where HIGB = hue, intensity, green, and blue difference index, TPR = true positive rate, UA = user's accuracy, TNR = true negative rate, OA = overall accuracy, FS = F1 score, and NSVDI = normalised saturation-value difference index.

A careful examination of the results demonstrates that the proposed HIGB difference technique achieved higher overall accuracies than the two widely used shadow detection methods. Even though some treatments, such as A2, A3, and A4, had a high crop density with more dark vegetation pixels, the HIGB was stable and achieved TPR ranging from 0.71 to 0.79. The results demonstrate the effectiveness of the proposed method, achieving an overall average accuracy of 0.85 across all treatments. These results are particularly promising, especially within the context of the intricate and diverse treatments examined, reflecting the complexity of the heterogeneous environment under consideration, as shown in Table 5-3.

**Table 5-3: Comparison of the average overall accuracy performance of our proposed approach with two state-of-the-art techniques.**

| Technique/method | TPR | UA | TNR | OA | FS |
|---|---|---|---|---|---|
| **HIGB** | 0.850 | 0.742 | 0.842 | 0.846 | 0.798 |
| **NSVDI** | 0.776 | 0.746 | 0.752 | 0.776 | 0.748 |
| **$C_3$** | 0.762 | 0.740 | 0.708 | 0.744 | 0.672 |

Where TPR = true positive rate, UA = user’s accuracy, TNR = true negative rate, OA = overall accuracy, FS = F1 score, and NSVDI = normalised saturation-value difference index.

## 5.5 Discussion

This study successfully developed and tested a new technique for shadow detection on RGB datasets, demonstrating its applicability for discriminating target crops in heterogeneous agricultural settings. Comparison with two other start-of-the-art shadow detection methods revealed that the HIGB difference technique can efficiently and accurately detect shadows in a variety of crop mixtures. For example, in instances where the shadows were dark or obscured by other objects, the HIGB difference technique outperformed both the $C_3$ and the NSVDI methods.

An important aspect of the comparison is that the widely used NSVDI was unable to detect shadows cast by maize plants as well as artificially coloured soybean pixels. This result is shown in Figure 5-5. As a result of this inability, most of the pixels that are non-shadow were mistakenly detected as shadow pixels in treatments A2, A3, and A4 by this method. To our knowledge, this is the first time this result has been reported. The observed limitation likely arises from the nature of the HSI colour space, where an issue arises that when the pixel values of the Red (R), Green (G), and Blue (B) channels are equal, the denominator in the HSI model becomes zero. This situation leads to the generation of invalid values within the HSI space (Kawamura et al., 2021). Equally, the $C_3$ method is susceptible to the impact of high crop density, causing it to mistakenly label dark green pixels within shadowed regions as non-shadow pixels. This leads to inaccurate shadow detection results, affecting the overall effectiveness of the algorithm. This pattern of results in this study is consistent with the previous study by Azevedo et al. (2015), who found that NSVDI had difficulty detecting shadows in vegetation due to similar behaviour in saturation and value components. Mostafa and Abdelhafiz (2017) also supported this and compared $C_3$*, NSVDI, and their proposed shadow detector index. In their study, the NSVDI index showed difficulty separating vegetation and shadow pixels. This observation by Mostafa and Abdelhafiz (2017) agrees with current results. Taken together, the findings imply that in areas with mixed vegetation, the accuracy of the NSVDI index tends to decrease, resulting in these vegetation pixels being misclassified as shadows. This is because the value of NSVDI for vegetation pixels approximates zero, causing instability in the approach based on the darkness degree of these pixels.

A similar shortcoming was observed for the $C_3$ method, that is, it is sensitive to shadow (Arévalo et al., 2008) which can lead to the misclassification of non-shadow pixels as shadows due to their instability in discerning certain colour values. This instability can result in inaccurate shadow detection. They also noted that some of the surface features with high-intensity values can be easily detected as shadows, leading to further misclassification.

| | **Original image** | **HIGB** | **$C_3$** | **NSVDI** |
|---|---|---|---|---|
| Sole maize |  |  | 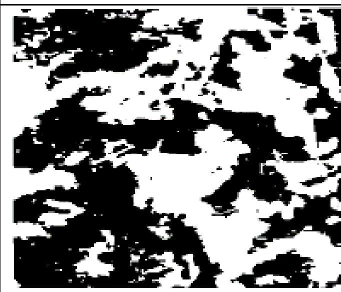 |  |
| One maize vs. one soybean |  |  | 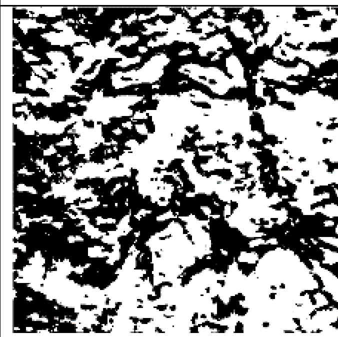 |  |
| One maize vs. two soybean |  | 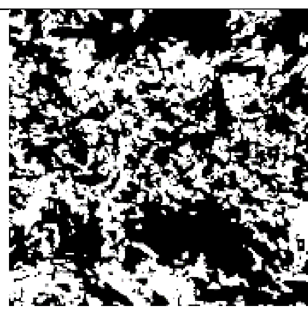 | 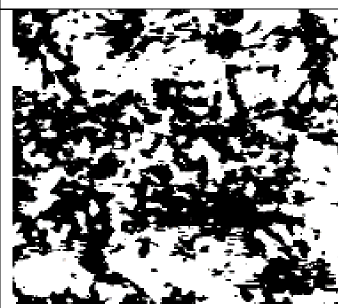 | 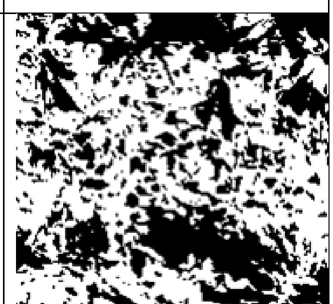 |
| Two maize vs. one soybean |  | 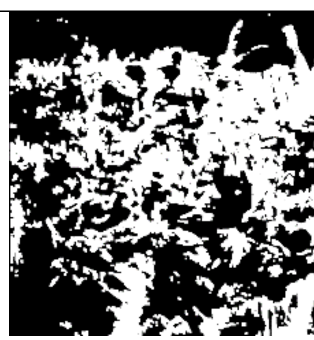 | 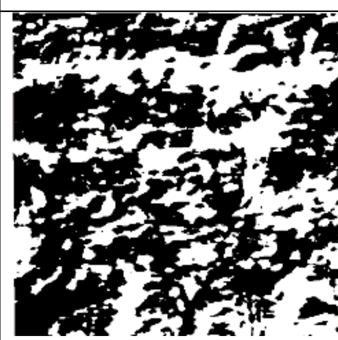 |  |

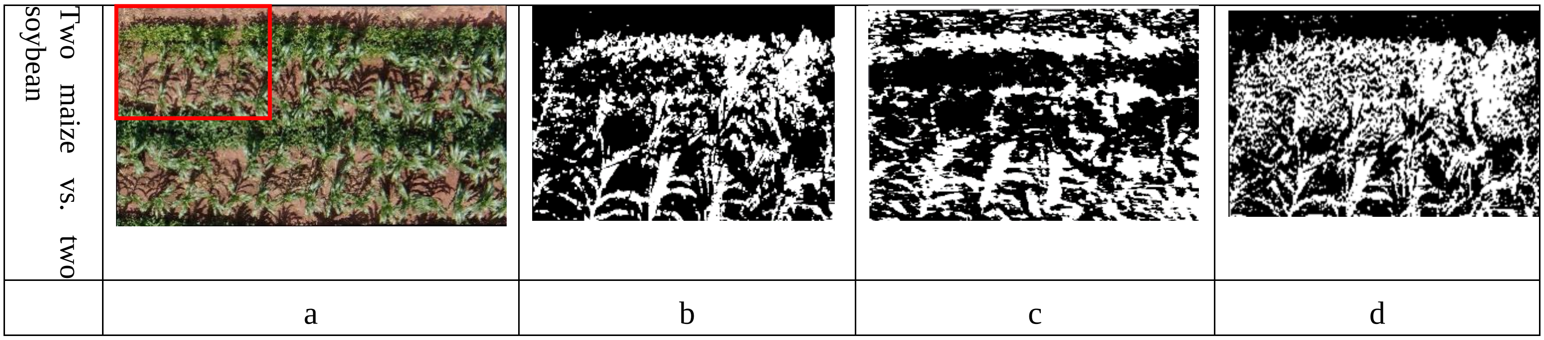


**Figure 5-5: Misclassified shadows in different crop mixtures: (a) the original RGB image, (b) the HIGB index, (c) the C3 model, (d) the NSVDI index showing shadow (white) and non-shadow (black) regions.**

By contrast, the results of the newly developed HIGB difference technique illustrate the respectable reliability of shadow detection across all five treatments, as shown in Figure 5-5. Notably, the proposed method demonstrated stability even in scenarios with high crop density and dark vegetation pixels, where other methods might struggle due to increased darkness caused by other crop shadows (maize shadows on top of soybean plants). The HIGB difference technique maintained a high overall accuracy ranging from 0.77 to 0.95, even in such cases. This underscores its robustness. The effectiveness of the new HIGB difference technique is further indicated by the fact that it achieved an average overall accuracy of 0.85 across all five treatments compared to 0.74 and 0.78 for $C_3$ and NSVDI, respectively.

This achievement is noteworthy given the complex and diverse treatment scenarios, reflecting the model's capacity to handle the challenges posed by heterogeneous environments. This was also supported by Arévalo et al. (2008), who found that the $C_3$ model tends to be quite noisy, leading to misclassification of shadow pixels as non-shadow pixels and inaccuracies in shadow boundaries. It also becomes unstable for low saturation values, causing the misclassification of non-shadow pixels as shadow pixels. Additionally, colours close to blue are often wrongly detected as shadows. Furthermore, while Sarabandi et al. (2004) and Ma et al. (2008) methods have demonstrated satisfactory outcomes in eliminating basic shadows within their specific datasets, they prove to be less suitable for addressing shadow detection challenges in high spatial-resolution RGB images characterised by multiple shadows in complex and heterogeneous environments. The complexities introduced by complex and heterogeneous environments tend to limit the efficacy of these methods in achieving accurate and comprehensive shadow detection.

The complete assessment of the proposed shadow detection approach revealed its robustness, adaptability, and superior performance compared to traditional methods. The experimental nature of this study, in which two crops with different growth habits and canopy characteristics, that is, maize (a cereal with an erect habit) and soybean (a short legume with a spread-out canopy), were grown under a controlled mixing regime, made it possible to test the efficiency of the new model. The proposed approach makes the detection of shadows in complex heterogeneous environments much easier. Furthermore, comparing HIGB against the traditional models has shown that our proposed model achieved the highest accuracy as the degree of crop mixture increases.

Regarding image enhancement before shadow detection, results have shown that image enhancement using the CLAHE algorithm improves complementary information about the image's distribution of pixel values and variations in intensity. As shown in Figure 5-5, high values for both entropy and RMS contrast showed that there is a wide range of pixel values and significant variations in intensity, which demonstrate that CLAHE can expose images with complex patterns and textures. As such, it is observed that treatment A3 (one row of maize vs. two rows of soybean) and A5 (two rows of maize vs. two rows of soybean) have more variation in intensity and have a wide range of pixel values as compared to A4 (two rows of maize vs. one row of soybean) and A1 (one row of maize vs. one row of soybean). The purpose of this investigation is to propose an innovative approach for shadow detection and extraction suitable for a single high spatial RGB image with multiple shadows and complex surfaces in mixed cropping systems.

Despite the success demonstrated by the proposed approach, there are some limitations, such as the fact that the proposed model was only tested on five different crop mixtures with varying land cover. Furthermore, the applicability of the HIGB index in other scenarios can be influenced by weather conditions, illumination conditions, camera pitch angle, sensor characteristics, and crop type, since it relies on raw RGB values. Also, high correlation between RGB channels in maize and soybean crop canopies can limit discrimination power. Thus, future research needs to assess the applicability of this new technique for remotely sensed datasets with higher spectral and radiometric resolutions since the RGB images used are optimised only for high spatial resolution. Furthermore, while the HIGB index demonstrated significant success in crop discrimination, we acknowledge limitations (such as illumination normalisation, sensor integration and fusion, edge computing and model optimisation as well as generalisation on larger datasets) that point toward necessary future research, particularly for automation of shadow and real-time applications.

### 5.6 Conclusion

A new technique for shadow detection based on the HIS was developed and tested in a mixed crop setting at an experimental station in a subtropical climate in Zimbabwe. This new HIGB difference technique was applied to RGB datasets, and its performance was evaluated against two state-of-the-art shadows developed specifically to detect cast and self-shadows on images. The quantitative analysis revealed that the proposed model surpasses the $C_3$ model and NSVDI indices in terms of all evaluation metrics, including overall accuracy, user's accuracy, true positive rate, true negative rate, and F1 score. The proposed model obtained an average OA of 0.85 across all treatments, which is significantly higher than the OAs of 0.77 and 0.83 achieved by the $C_3$ model and the NSVDI indices, respectively. This technique contributes to a suite of methods capable of dealing with the issue of shadows in RGB imagery. This potentially leads to better crop discrimination outcomes compared to existing techniques.

### 5.7 Summary

*This chapter proposed a novel algorithm for shadow detection and removal. The method aims to enhance shadow detection by utilising invariant and variant indicators, specifically by exploiting colour components and transforming hue and intensity channels to generate more accurate shadow masks. Quantitative analysis demonstrated that the proposed HIGB difference technique outperformed the $C_3$ model and NSVDI indices across all evaluation metrics, including overall accuracy, user's accuracy, true positive rate, true negative rate, and F1 score. In contrast, the proposed LIRB method worked in most parts of shadow areas; however, it exhibited limited effectiveness for low spectral resolution images, with persistent fuzziness, particularly in areas of dense shadow pixels, such as those associated with soybean crops, thereby increasing the likelihood of misclassification. To address these limitations, a region-based approach is recommended to mitigate misclassification errors, as it incorporates contextual information from* *neighbouring pixels. The availability of region-based segmentation algorithms, such as SLIC, along with textural and morphological feature extraction techniques, provides a robust foundation for implementing advanced machine learning classifiers, including Random Forest (RF) and Extreme Gradient Boosting (XGBoost). The next chapter will explore integrating region-based segmentation methods with machine learning classifiers to assess the potential benefits of combining multiple diverse datasets for improved crop classification accuracy.*

# CHAPTER 6 : DEVELOPMENT OF A HYBRID APPROACH FOR CROP DISCRIMINATION

This Chapter is based on:

**Mafuratidze, P., Mutanga, O., and Masocha, M. (in review).** Improving Mixed-Crop Classification in Heterogeneous Agricultural Landscapes by Leveraging Multi-Feature Integration, *ISPRS Journal of Photogrammetry and Remote Sensing.* (Manuscript Number: PHOTO-D-25-00616)

## ABSTRACT

Heterogeneous agricultural landscapes pose a challenge for accurate crop discrimination. This problem is common, especially in developing regions where mixed-cropping systems are prevalent. The spectral and structural complexity of mixed-crop systems frequently presents challenges for conventional remote sensing techniques, leading to misclassification of crops with overlapping phenological cycles. To deal with these problems, this study used a novel hybrid approach that integrates region-based segmentation and pixel-based classification. This method integrates simple linear iterative clustering (SLIC) superpixels with texture and structural features, combining multiple characteristics to boost overall classification accuracy. The researchers then employed these features to train Random Forest (RF) and Extreme Gradient Boosting (XGBoost) classifiers. Experimental results demonstrated reasonable detection accuracy, with precision, recall and F1-scores exceeding 0.98 for both RF and XGBoost. In terms of feature contribution, mean intensity and standard deviation features derived from SLIC were found to have the greatest influence, followed by textural and morphological traits. Error rates decreased from 8% with SLIC-derived features alone to 1% when various features were integrated. Results of this study recommend the integration of multi-feature and machine learning classifiers to enable scalable high-resolution crop mapping. These results confirmed the benefits of employing such a robust solution for precision agriculture, especially in resource-constrained agricultural systems and heterogeneous landscapes.



Keywords: SLIC; multi-feature, machine learning classifiers, feature combination, mixed cropping systems

## 6.1 Introduction

Estimating the type of crops and their spatial distribution in heterogeneous agricultural landscapes is critical for precision agriculture, enabling efficient resource management and improved yield estimation for food security. These heterogeneous agricultural landscapes, popularly termed agro-ecological systems, are prevalent in developing regions as a sustainable alternative to monocropping. Recent studies, such as those by Ouko et al. (2024) highlighted that agro-ecology is growing role in addressing food system sustainability, particularly in developing regions, where smallholder farming dominates. However, over 80% of farmers in developing regions rely on rainfed agriculture (Richard et al., 2017), leaving crops vulnerable to climate variability and hindering resilience. To mitigate this, governments and different organisations are increasingly encouraging and adopting climate-smart agriculture approaches, including crop diversification through mixed and intercropping systems (FAO, 2017; Honrado et al., 2017; Mafuratidze et al., 2024; Maurice et al., 2015; Persello et al., 2019; Richard et al., 2017) on smallholder farms. Yet, the success of these strategies depends on accurate, scalable methods to map crop types in fragmented, mixed-crop landscapes, which is a challenge unresolved by existing approaches.

Satellite-based cropland mapping has been extensively utilised for yield estimation globally (Hegarty-Craver et al., 2020; Khan et al., 2021; Löw et al., 2018; Zhang et al., 2021). However, detailed and current information regarding the actual crop type and its spatial distribution in a mixed cropping system remains limited. In practice, information on crop type and spatial distribution is primarily updated manually by farmers and agricultural officers through field surveys and local reporting systems. While these traditional methods are accurate, they are constrained by long data acquisition times and high costs, rendering them less practical for fragmented landscapes. Furthermore, these methods are labour-intensive and time-consuming. Their limited spatial coverage makes them impractical for fragmented landscapes with complex crop mixtures.

In contrast to monocropping, mixed cropping systems involve cultivation of multiple crop species within a single field, resulting in spectral and structural complexity due to similar development cycles and crop phenology, which presents challenges to traditional classification methods (Arafat et al., 2013; Gerstmann et al., 2016; Shao et al., 2021). For instance, crops with overlapping phenological cycles or similar spectral profiles, such as maize and sorghum, are frequently misclassified (Champagne, 2019; Chew et al., 2020a; Forkuor et al., 2014; Peña et al., 2013a). Advances in unmanned aerial systems (UAS) and computational algorithms now enable high-resolution crop mapping, but their potential in heterogeneous landscapes remains under-exploited (Li et al., 2019; Michez et al., 2018; Psirofonia et al., 2017). Crop mapping approaches integrate various classes, taking into account the complex characteristics of the mixed crop system, which pose challenges for accurately identifying crop types and determining their spatial extent.

Several researchers have investigated the use of crop spectral features and have indicated that they could contribute to the improvement in overall classification accuracy (Bosilj et al., 2018; Hebbar et al., 2014; Lottes et al., 2017b). Effective crop discrimination should involve three key steps: (1) reducing spectral confusion by masking non-vegetation pixels and isolating crop-specific signals (Lottes et al., 2017b), (2) identifying discriminative features beyond spectral data, such as textural, structural, and spatial patterns (Louargant et al., 2018; Meer et al., 2014; Stutsel et al., 2021), and (3) selecting optimal classifiers that balance accuracy and computational efficiency (Huang and Jensen, 1997). While spectral features such as NDVI, ExG, SAVI, etc., are foundational, they often fail to distinguish crops with overlapping reflectance profiles. For example, legumes and cereals in intercropped fields may share near-identical spectral profiles but differ in canopy texture or plant geometry. Hall, et al. (2018) and Kawamura et al. (2021b) indicated that it is difficult to identify different crop types using spectral features alone because maize shares similar spectral characteristics with other crops.

Consequently, several researchers have shown that combining spectral features with spatial information and vegetation structure elements can significantly enhance classification accuracy (Ennouri et al., 2021; Li et al., 2019; Louargant et al., 2018; Lu & Weng, 2007b; Piermattei et al., 2018; Xia et al., 2022). High-resolution UAS imagery enables the extraction of textural features to quantify spatial variability in canopy structure, morphological features to characterise crop geometry, and Simple Linear Iterative Clustering (SLIC) superpixels to partition fields into homogeneous regions, reducing spectral noise and aligning with natural crop boundaries (Blaschke, 2010; de Castro, Six, et al., 2018; Hu et al., 2018; Hunt & Daughtry, 2018; Ozdarici-Ok et al., 2015; Zhao et al., 2019). While these features have been explored individually, their synergistic integration remains under-exploited in mixed-crop systems. Hence, optimal feature combinations vary by crop type and landscape configuration, necessitating systematic evaluation (Zhao et al., 2019). Furthermore, even for identical crop types, the ideal features differ based on their spatial distribution.

Classification methodologies are primarily categorised into pixel-wise and region-based approaches (Jin et al., 2019). Pixel-wise analysis provides fine-grained detail but suffers from computational inefficiency and noise in high-resolution imagery (such as variations in lighting or soil background) (Bosilj et al., 2018). In contrast, region-based methods classify segmented objects, leveraging spatial, shape, and contextual features to emulate human interpretation (Andrew et al., 2022; de Castro, Six, et al., 2018; Hebbar et al., 2014; Peña et al., 2013b; Wagner and Oppelt, 2020; Wang et al., 2021). Unfortunately, neither approach alone resolves the challenges of overlapping canopies and partial occlusion in mixed-crop fields.

Numerous studies on species discrimination have aimed to enhance specific stages of this general framework (Aragones et al., 2019; Kaushik et al., 2025; Pieterse, 2016; Sencaki et al., 2019). To address this, Aguilar et al. (2015) incorporated textural features which capture spatial patterns in canopy structure and spectral indices, enabling distinction between crops with similar spectral profiles. Concurrently, morphological features were employed by Bosilj et al. (2018) to characterise crop geometry, particularly in fragmented fields. Studies like Balasubramanian (2017) demonstrated that combining spectral and textural data improved classification accuracy in crop-weed detection, while Kawamura et al. (2021b) emphasised the complementary role of spatial-contextual features. However, few studies have systematically integrated all three feature types, such that spectral, textural, and morphological features within a unified framework. For instance, Kupidura (2019); Lu et al. (2018); and Zhang et al. (2021) optimised spectral-textural combinations but overlooked morphological traits, while Hamuda et al. (2017) focused on spectral-structure synergies without leveraging advanced segmentation techniques.

To address the limitations of existing crop discrimination approaches, this study aimed to achieve three primary objectives: (1) reduce spectral ambiguity in mixed cropping systems through vegetation masking, (2) identify and prioritise optimal features for discriminating maize and soybean, and (3) enhance classification accuracy by integrating pixel-based analysis with region-based segmentation. To meet these objectives, a hybrid approach was employed using UAS-derived RGB imagery, combining the granularity of pixel-level methods with the contextual coherence of object-based segmentation. This methodology is designed to address the unique complexities of heterogeneous agricultural landscapes and provide a scalable solution for precision agriculture in resource-limited environments.

## 6.2 Materials and Methods

### *6.2.1 Methodological framework*

The employed methodology to enhance crop classification accuracy consists of four stages, as shown in Figure 6-1. The initial pre-processing stage emphasises vegetation masking, which is subsequently followed by superpixel segmentation in the next phase. The third stage is textural and morphological feature extraction, and the fourth stage is pixel-based spectral classification. To achieve the aforementioned tasks, we utilised Spyder version 5.5, which is an IDE tailored for scientific computing and machine learning. A significant aspect of utilising Spyder is its intuitive multiplane interface with tools for code editing, debugging, and variable exploration, rendering it suitable for handling large datasets. Spyder seamlessly blends with popular Python libraries, such as OpenCV, NumPy, Pandas, and Matplotlib, enhancing its capability for data processing and visualisation. Scikit-Learn is the primary Python library used for image processing. This library provides a comprehensive suite of classification tools. It includes robust model evaluation techniques, hyperparameter tuning, and preprocessing utilities to facilitate efficient data-driven decision-making. When used within Spyder, Scikit-Learn leverages performance optimisations for improved computational efficiency, making it well-suited for large-scale data analysis and predictive modelling.

#### 6.2.1.1 Vegetation Masking

Vegetation masking constitutes the foundational step in the employed methodology, aimed at isolating crop pixels from non-vegetation background elements, such as soil, shadows, and debris. This process mitigates spectral interference and enhances feature extraction accuracy. The Excess Green Index (ExG), a vegetation-sensitive metric defined as:

$$\mathrm{ExG} = 2g - r - b$$

Where r, g, and b represent normalised red, green, and blue spectral channels, respectively. ExG was developed by Woebbecke et al. (1995) to amplify greenness signals characteristic of photosynthetic activity. To differentiate vegetation from non-vegetation regions, Otsu's thresholding algorithm (Otsu, 1979) was applied systematically to the ExG-derived grey-scale image. This non-parametric method iteratively optimises the threshold value by maximising inter-class variance between vegetation and background pixels, ensuring robust segmentation across heterogeneous scenes.

The resultant binary mask encodes vegetation pixels as 1 (white) and non-vegetation pixels as 0 (black) (Figure 6-2). An inversion was selectively applied during post-processing, rendering vegetated areas as white against a black background. This inversion facilitates intuitive visualisation while preserving analytical integrity. The mask's efficacy was validated through visual inspection, confirming its capacity to suppress spectral noise and focus subsequent analyses on mixed cropping settings.

#### 6.2.1.2 Superpixel Segmentation

To address the complexity of mixed cropping systems, where fields often contain multiple crop types with irregular boundaries, we employed the Simple Linear Iterative Clustering (SLIC) algorithm. SLIC functions by decomposing the image into smaller, adaptive regions called superpixels. These superpixels align with natural crop boundaries, making it easier to analyse and classify different crops within the same field (Kailasam et al., 2021). By grouping pixels into coherent units while preserving edges, SLIC reduces computational complexity and helps efficiently process mixed cropping settings (Stutsel et al., 2021). In this study, the SLIC algorithm was implemented with the following parameter settings: number of segments = 250, maximum iterations = 100, compactness = 10, and start label = 1.

#### 6.2.1.3 Textural and Morphological Feature Extraction

After segmenting the image into superpixels, the subsequent step involves extracting features that capture the unique characteristics of each region. In mixed cropping systems, crops often differ not only in colour but also in texture and shape. To account for this variation, both textural and morphological features were extracted from the superpixels (Table 6-1). These features provide valuable information for distinguishing between crop types and improving classification accuracy.

#### 6.2.1.4 Pixel-Based Spectral Classification

The final critical stage in the employed approach is the section on the optimal classifier. In this study, we opted for a pixel-based spectral classification which employs two widely used ensemble machine learning classifiers (random forest and extreme gradient boosting) to classify maize and soybean using spectral data while integrating superpixel-derived contextual features. These classifiers were selected for their robustness in handling high-dimensional datasets, resistance to overfitting, and capacity to model non-linear relationships in heterogeneous agricultural landscapes (Breiman, 2001).

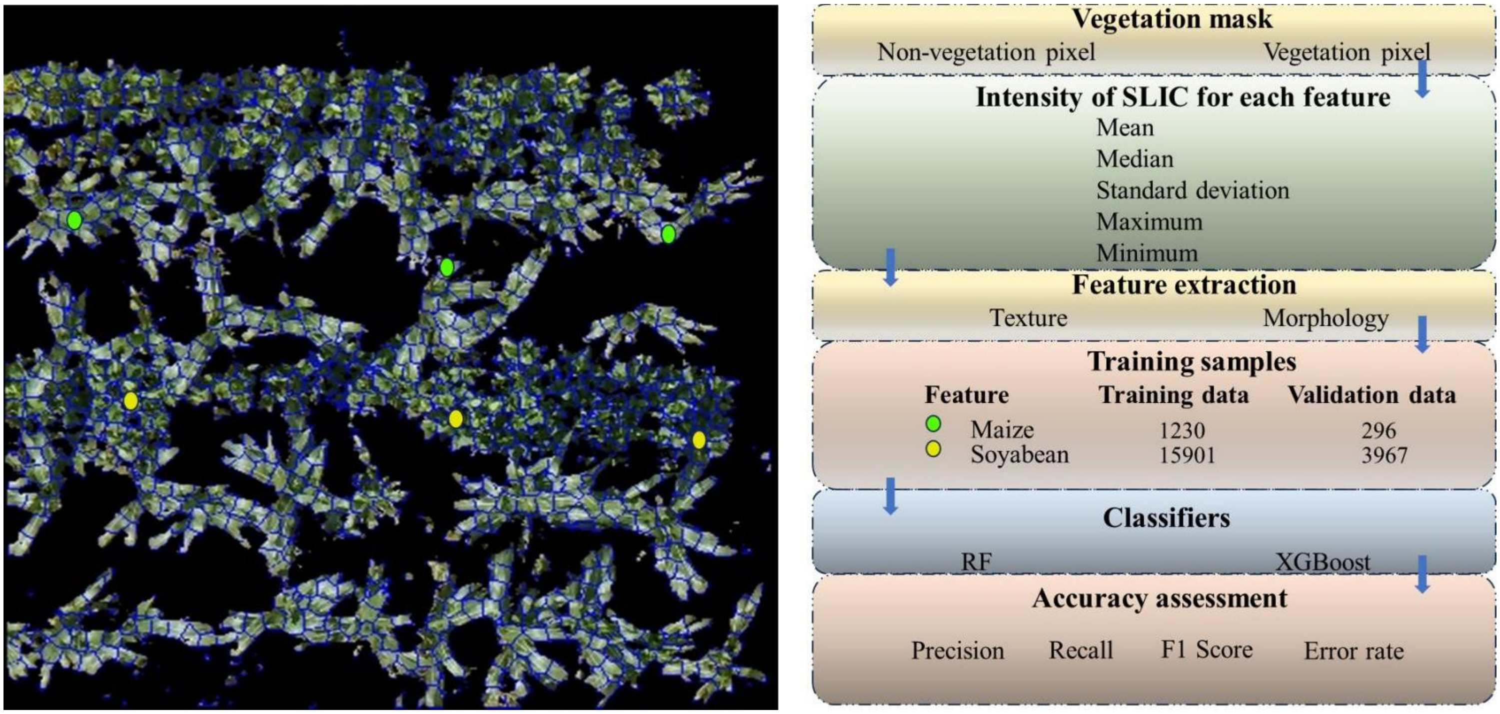


**Figure 6-1: Flow of the input image, feature extraction, and classification process.**

### *6.2.2 Data collection and preprocessing*

#### 6.2.2.1 Dataset

The dataset used in this study was collected from two plots characterised by mixed-cropping systems. The dataset comprises two images, each depicting distinct cropping arrangements: one image features a single row of soybean adjacent to two rows of maize (1 vs. 2) (A3), while the other presents a configuration of two rows of maize alongside two rows of soybean (2 vs. 2) (A5). The data acquisition was conducted using an unmanned aerial system (UAS) equipped with a Zenmuse camera, which captured RGB imagery at a spatial resolution of 2 cm per pixel. The dataset was divided into training and testing subsets, with 80% of the images used for model training and the remaining 20% reserved for validation and performance evaluation. Ground truth data, including crop type labels and spatial distribution maps, were collected through field surveys.

#### 6.2.2.2 Input dataset composition

Accurate identification and discrimination of different crop species require a comprehensive approach that combines multiple image-processing techniques to improve their separability. In this work, we employed feature extraction processes that regularly involve the use of textural features, morphological operations, segmentation-based clustering (Table 6-1) or a combination of these features to enhance the quality of images and extract meaningful crop segments. Each of these variables plays a significant role in image pre-processing, segmentation, and classification.

**Table 6-1: Feature extractors used in this study.**

| Type | Variable | Description |
|---|---|---|
| Texture | Median | A filtering technique used to reduce noise in an image |
| | Gaussian S3 | A filter with a standard deviation (sigma) of 3 |
| | Gaussian S7 | A filter with a standard deviation (sigma) of 7 |
| Morphological operations | Gradient | The difference between the dilation and erosion |
| | Closing | The dilation of an image followed by erosion |
| | Opening | The erosion of an image followed by dilation |
| SLIC clusters | Mean | The average pixel value across all pixels |
| | Median | The median intensity of pixels within a superpixel |
| | Standard deviation | The standard deviation of an object/pixel in band x |
| | Minimum | The smallest pixel value found in the superpixel |
| | Maximum | The largest pixel value found in the superpixel |

## 6.3 Data analysis

### *6.3.1 Image segmentation*

Various techniques have been applied to segment UAS images into homogeneous regions by analysing colour similarity and spatial proximity (Bellón et al., 2017; Jin et al., 2019; X. Liu et al., 2022; Marino & Alvino, 2018; Tian et al., 2022). Simple Linear Iterative Clustering (SLIC) is one of the simplest methods to segment raw images into pixels that represent common characteristics (Sodjinou et al., 2022). The SLIC algorithm operates by clustering pixels in the dimensional space of colour and spatial coordinates (x, y), ensuring that the generated segments adhere to natural object boundaries. The algorithm initialises the cluster centres across the image and iteratively refines them using k-means clustering until convergence (Guo et al., 2021). This results in visually coherent superpixels that preserve important image structures while significantly reducing the computational complexity. In crop classification, SLIC enhances feature extraction by grouping spectrally and texturally similar pixels, improving model accuracy by reducing noise and capturing meaningful spatial patterns.

### *6.3.2 Image classification*

Random forest is a robust ensemble-based machine learning algorithm renowned for its efficacy in classification tasks (Breiman, 2001). This model operates through the construction of multiple decision trees, each trained on a randomly selected subset of the training data using bootstrap aggregation (commonly known as *bagging*). By leveraging parallel processing, RF independently builds these trees, ensuring diversity in the ensemble through feature and sample randomisation. The advantage of using this classifier is that it minimises overfitting and enhances generalisation, as the final prediction is derived from majority voting across all trees (Pandey et al., 2022). The inherent parallelism of the algorithm not only accelerates training but also improves scalability, making it particularly advantageous for large datasets. In agricultural applications, the ability of RF to handle high-dimensional data while maintaining computational efficiency underscores its utility in resource-constrained environments. The RF classifier hyperparameters were set as follows;

maximum number of estimators = 1 000,
maximum depth = 25, and
random state= 42

Extreme Gradient Boosting Classifier is a robust machine learning algorithm for crop classification, leveraging multiple input features to refine predictions iteratively (Chen & Guestrin, 2016; Sandino, Pegg, et al., 2018). Unlike traditional boosting methods, it constructs trees in parallel, efficiently capturing complex feature relationships while minimising overfitting through built-in regularisation. Its superior classification accuracy and ability to highlight key features make it highly effective for crop discrimination. Bellis et al. (2022) and Sandino et al. (2018) noted that with strong scalability and computational efficiency, XGBoost is a well-suited model for processing large datasets. The XGBoost classifier hyperparameters were set as follows;

maximum number of iterations = 500,
maximum depth = 25,
learning rate = 0.3, and
gamma = 0.3

### *6.3.3 Input feature selection and evaluation metrics*

From each superpixel, a suite of features was derived, including SLIC-based clusters, morphological operators, and textural indices. To minimise redundancy, variables exhibiting high multicollinearity ($r > 0.9$) were systematically excluded. Subsequently, feature importance ranking was conducted using RF and XGBoost, enabling the retention of only the most discriminative predictors. This sequential selection strategy ensured that the final feature set effectively integrated both spectral and spatial attributes, enhanced classifier robustness, and mitigated risks of overfitting. Several metrics were considered for evaluating the performance of the classification models. The most commonly used method for evaluating the classification performance is the confusion matrix table. Precision, recall, kappa and F1-score were used to evaluate the classification performance for each category (maize and soybean). The metrics provide deeper insights into the ability of the model to avoid false positives, detect all relevant cases, and balance both aspects. Finally, the feature importance was examined to identify the most influential features used by each model, allowing for comparisons and insights into how the models interpreted the data.

## 6.4 Results

This study evaluated the effectiveness of multi-feature integration, which consists of textural, morphological, and SLIC features, for improving maize and soybean discrimination in a mixed cropping setting. The discrimination of crops was conducted using random forest and XGBoost algorithms, and the outputs were refined with a vegetation mask to exclude non-crop areas. Following this, SLIC-based segmentation was applied to generate small homogeneous regions for analysis. In terms of overall feature contribution, the results indicated that mean intensity and standard deviation features derived from SLIC were found to have the greatest influence, followed by textural and, lastly, morphological traits. In this study, key findings demonstrated reasonable classification accuracy between maize and soybean, with high precision, recall and F1-scores exceeding 0.98 for both RF and XGBoost.

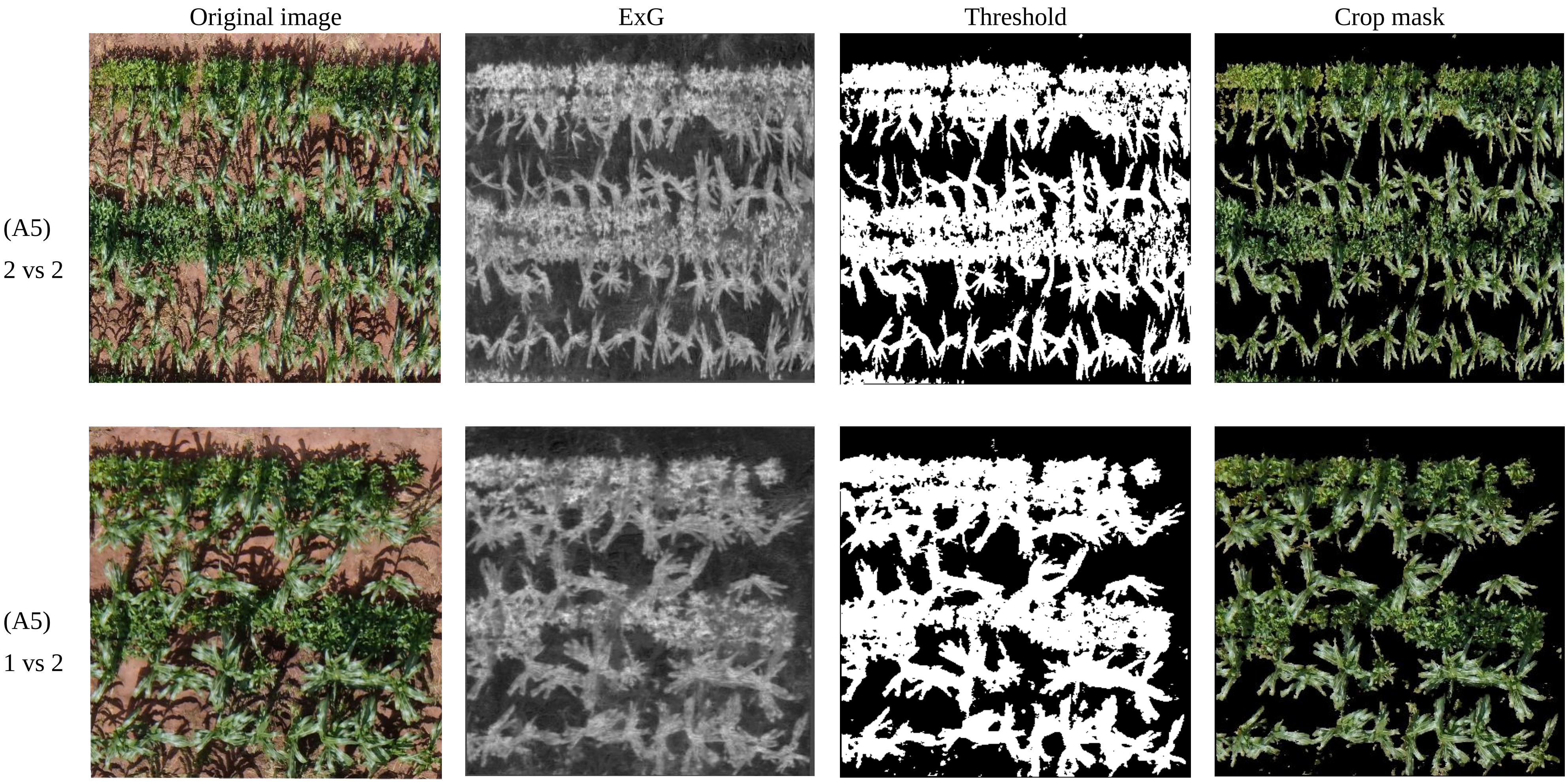


**Figure 6-2: Image processing procedure.**

### *6.4.1 Classification accuracy and model performance*

The findings shown in Table 6-2 present a performance comparison of the RF and XGBoost classifiers for two distinct scenarios: 1 vs. 2 (one row of soybean and two rows of maize) (A3) and 2 vs. 2 (two rows of soybean and two rows of maize) (A5). Both RF and XGBoost exhibited optimal classification performance for maize and soybean discrimination, with extremely low error rates and near-perfect precision, recall, kappa coefficient and F1-scores.

**Table 6-2: Evaluation metrics for RF and XGBoost.**

| | **RF** | | | |
|---|---|---|---|---|
| | **Precision** | **Recall** | **F1-score** | **Kappa** |
| 1 vs 2 | 0.98 | 0.98 | 0.98 | 0.95 |
| 2 vs 2 | 0.99 | 0.99 | 0.99 | 0.98 |
| | **XGBoost** | | | |
| 1 vs 2 | 0.98 | 0.98 | 0.98 | 0.95 |
| 2 vs 2 | 0.99 | 0.99 | 0.99 | 0.97 |

Both machine learning algorithms, RF and XGBoost, achieved an average of precision, recall, and F1-scores of 0.98, 0.98 and 0.99, respectively, indicating highly accurate predictions with minimal errors in both positive and negative classes. This performance was consistent across the A3 and A5 plots, demonstrating the model's effectiveness in distinguishing maize from soybean. Interestingly, both classifiers obtained a very low number of misclassifications with 0.02 and 0.01 error rates, respectively, for A3 and A5. The fundamental difference between the two models was that RF had a marginally higher Kappa value of 0.98 compared to a slight difference for XGBoost with 0.97, suggesting slightly better agreement with ground truth training data.

### *6.4.2 Confusion matrix analysis*

**Table 6-3: Confusion matrix for RF and XGBoost.**

| | **Random forest** | | **XGBoost** | |
|---|---|---|---|---|
| | **One row of soybean vs two rows of maize** | | | |
| | Maize | Soybean | Maize | Soybean |
| Maize | 8438 | 222 | 8411 | 249 |
| Soybean | 164 | 7065 | 189 | 7040 |
| | **Two rows of maize vs two rows of soybean** | | | |
| Maize | 8570 | 90 | 8544 | 116 |
| Soybean | 88 | 7141 | 99 | 7130 |

Table 6-3 summarises the metrics derived from the confusion matrices for the RF and XGBoost classifiers under two mixed cropping settings of A3 and A5. The differences in the mean overall accuracy between these classifiers indicate that their performance was comparable. In more detail, from the A3 plot, maize is slightly more accurately classified compared to soybean, as indicated by the lower number of misclassifications with 164 against 222 when using RF. Similarly, XGBoost on A3 produced comparable results, but with a slightly higher number of misclassifications, with 27 more maize instances and 25 more soybean instances. On A5, the RF model achieved high accuracy with only 178 total misclassifications across both classes, as compared to 215 total misclassifications for XGBoost, which indicated a slightly lower classification accuracy. Overall, RF consistently exhibited slightly fewer misclassifications than XGBoost, thereby showing a stronger ability to discriminate between maize and soybean in these mixed cropping settings.

### *6.4.3 Feature importance analysis*

From Figure 6-3, general trends are revealed in the pattern of each variable utilising XGBoost and RF across the two experimental conditions, represented by plots A3 and A5. In this study, each dataset was analysed using four distinct feature groups: (i) SLIC, (ii) SLIC + Texture, (iii) SLIC + Morphology and (v) All variables. In all these procedures, SLIC consistently emerged as the most influential variable for both A3 and A5. For A3, the four most important features were SLIC, SLIC_Std_Intensity, SLIC_Mean_Intensity, and SLIC_Max_Intensity, while

SLIC_Min_Intensity and SLIC_Median_Intensity showed limited contribution to the classification.

Additional features, including textural and morphological features, contributed moderately to the models' performance. These features are more prominent under A3, particularly for XGBoost, which tends to prioritise them over RF. For instance, in plot A3, RF assigned greater importance to morphological operators, especially Gradient and Closing, whereas XGBoost continued to focus predominantly on Gaussian_s7. Finally, in A5, both classifiers align more closely, with SLIC and its related statistics being the most significant, followed by the moderate importance assigned to Opening and Median_s3.

**Table 6-4: Error rates of each crop mixture for RF and XGBoost.**

| | **SLIC** | | **SLIC + Texture** | | **SLIC + Morphology** | | **All variables** | |
|---|---|---|---|---|---|---|---|---|
| | RF | XGBoost | RF | XGBoost | RF | XGBoost | RF | XGBoost |
| 1 vs 2 | 0.08 | 0.08 | 0.05 | 0.05 | 0.03 | 0.04 | 0.02 | 0.02 |
| 2 vs 2 | 0.06 | 0.06 | 0.02 | 0.03 | 0.02 | 0.02 | 0.01 | 0.01 |

To determine the effectiveness of each feature class, the analysis showed that combining different feature types significantly improves the accuracy of maize and soybean classification. Table 6-4 shows that using only SLIC features results in relatively high error rates between 0.06 and 0.08. However, when texture and morphological features were added, the error rates decreased drastically, with morphology providing the most significant improvement. The best classification results occur when all features, such as SLIC, texture, and morphology, are combined, achieving the lowest error rate of 0.01 for both crop mixtures. This demonstrates that a multi-feature approach is crucial for effectively distinguishing between maize and soybean, leading to improved classification performance.

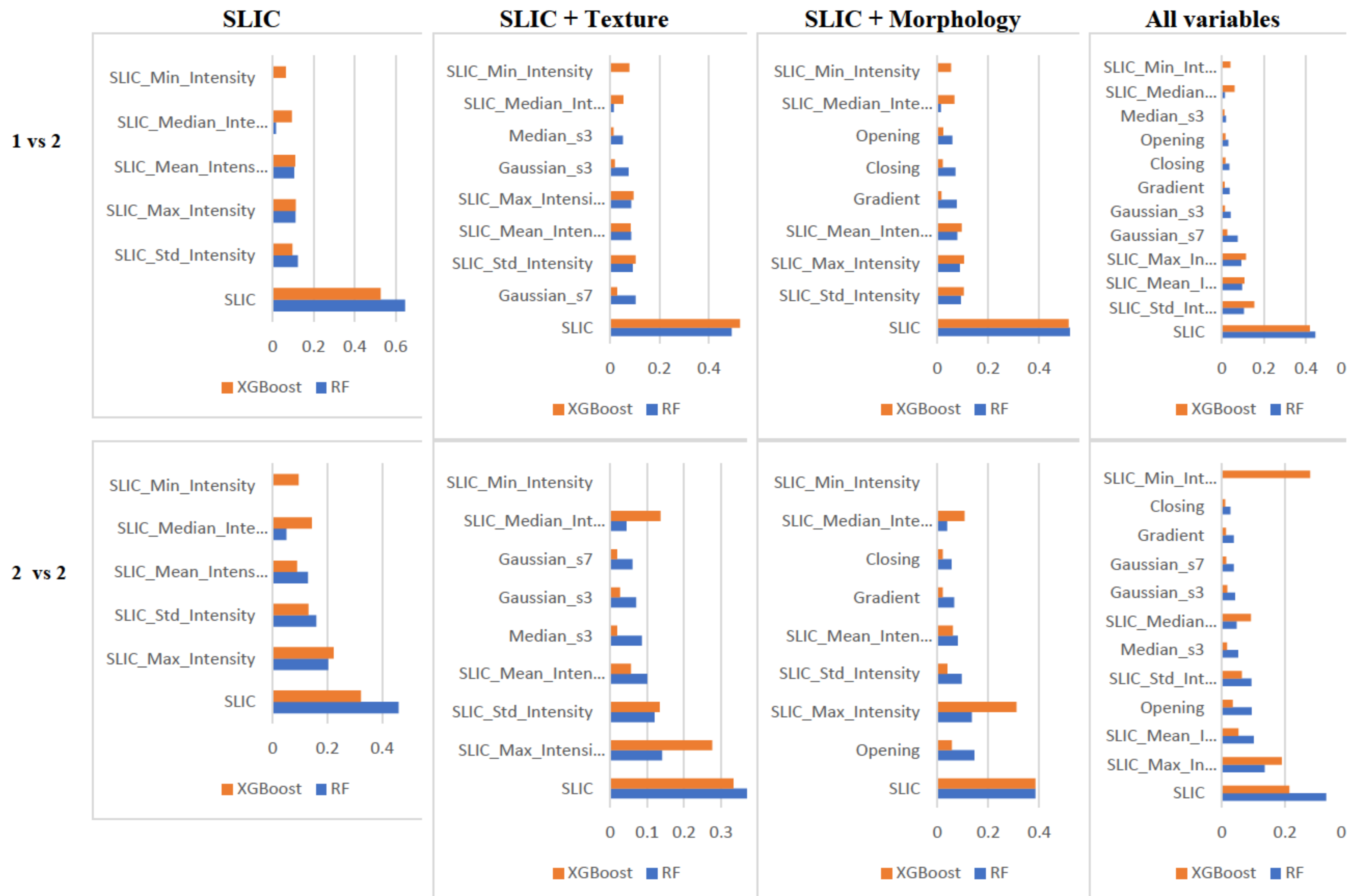


**Figure 6-3: Feature importance for each combination.**

### *6.4.4 Spatial distribution of maize and soybean*

The spatial distribution maps of maize and soybean were derived using the Random Forest and

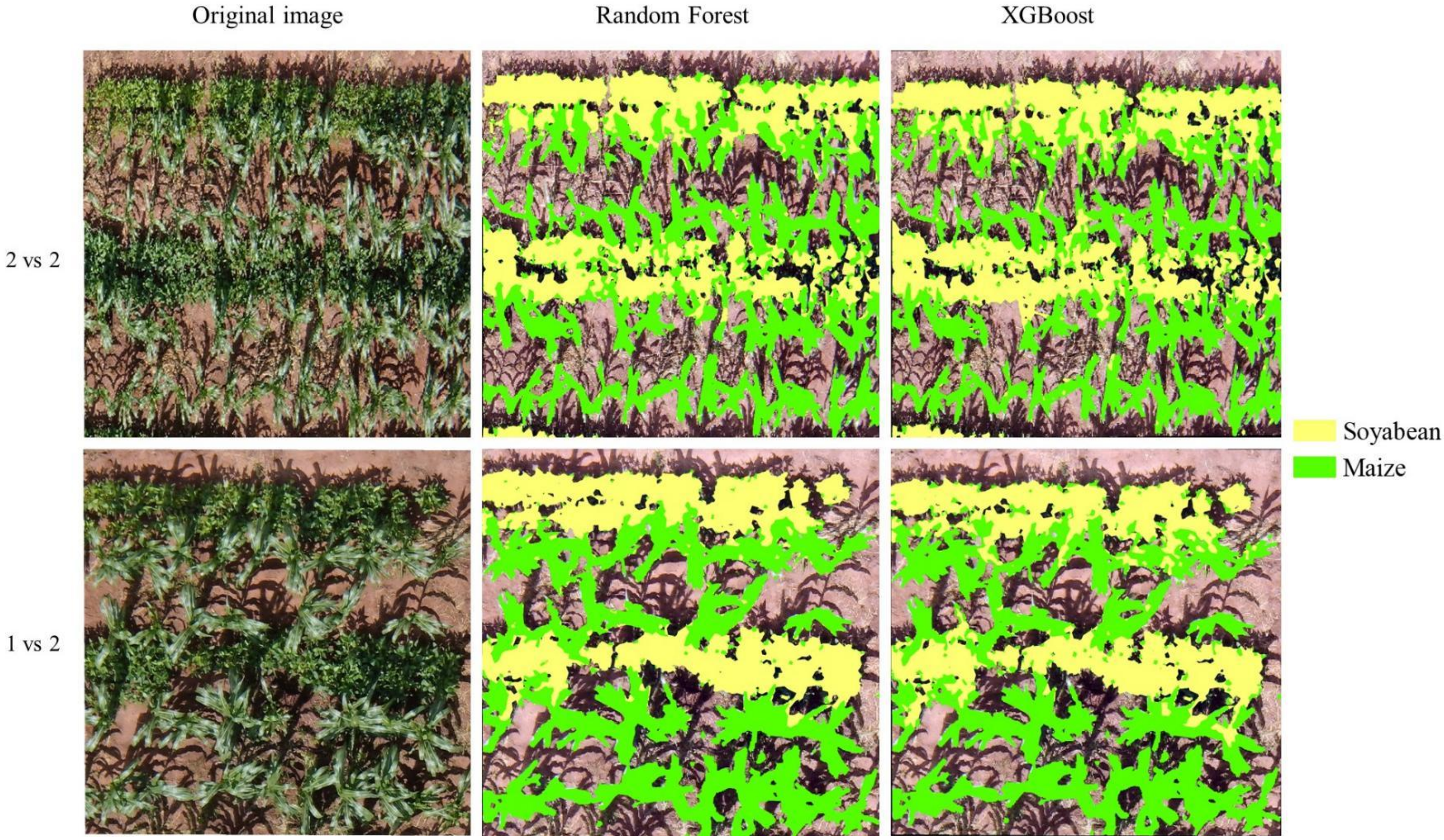


**Figure 6-4: Spatial distribution of maize and soybean.**

XGBoost classifiers, as shown in Figure 6-4. With results displayed for two cropping scenarios: 2 vs. 2 (two rows of maize and two rows of soybean) (A5) and 1 vs. 2 (one row of maize and two rows of soybean) (A3). The results highlight the effectiveness of machine learning classifiers in discriminating between maize and soybean crops in high-resolution imagery. Although both RF and XGBoost achieved reasonable accuracy, XGBoost consistently delivered superior spatial accuracy and robustness against boundary effects and shadows. These findings underscore the importance of selecting advanced classification algorithms for precision agriculture applications, where high-resolution and accurate crop mapping are essential.

### *6.4.5 Model robustness*

Table 6-5 presents a comparison analysis of RF and XGBoost, based on their training times for different crop mixtures. The results indicate that XGBoost consistently requires more training time than RF, with 12.12 seconds vs. 8.16 seconds for A3 and 16.69 seconds vs. 12.61 seconds for the A5. This disparity highlights that RF is 33% faster than XGBoost's for A3 and a 24% for 2 vs. 2 ratios. Although XGBoost can be more accurate for complex predictions, Random Forests are faster and use less computing power. The potential performance gains of XGBoost come with higher computational costs, whereas RF prioritises efficiency, making it preferable for time-sensitive and hardware-limited agricultural applications.

**Table 6-5: Algorithm's training times (seconds) across crop mixtures.**

| | **RF** | **XGBoost** |
|---|---|---|
| Ratio | Training Times (seconds) | |
| 1 vs 2 (A3) | 8.16 | 12.12 |
| 2 vs 2 (A5) | 12.61 | 16.69 |

## 6.5 Discussion

### *6.5.1 Model performance and feature integration*

Both RF and XGBoost achieved exceptional classification accuracy with F1-scores well above 0.98 across A3 and A5 plots, underscoring their suitability for fine-scale crop discrimination. The minimal error rates of less than 0.02 and high Kappa values ranging between 0.95 and 0.98 reflect firm agreement with ground truth, aligning with studies that highlight machine learning's efficacy in precision agriculture (Gao et al., 2018; Kilwenge et al., 2021; Yang et al., 2017). Notably, the integration of SLIC-derived features, texture indices, and morphological operators proved pivotal, reducing error rates from 0.06–0.08 (SLIC alone) to 0.01 (all features combined). These findings align with previous studies that have employed machine learning models for crop classification, such as those by Bellis et al. (2022); Prins (2019) and Hao et al. (2018), where RF and XGBoost achieved high accuracies for distinguishing different crop types. This aligns with the growing emphasis on multi-feature fusion to capture crop-specific spectral, structural, and textural traits (Maia et al., 2021; Maimaitijiang et al., 2020; Psirofonia et al., 2017).

However, unlike these earlier studies, our approach showed that SLIC's dominance in feature importance suggests that superpixel segmentation effectively delineates crop boundaries, whereas textural and morphological features augment discrimination by characterising leaf arrangement and canopy structure. Although most studies rely solely on spectral and textural features, our results indicate that SLIC-derived metrics, for example, mean intensity and standard deviation, were the most influential variables. This contrasts with the findings of Maia et al. (2021), that emphasised spectral indices as the dominant features for crop classification. Our results suggest that structural properties derived from the SLIC improve object-based classification, particularly in mixed cropping systems, where individual plant boundaries are less distinct.

### *6.5.2 Comparative model insights*

While RF and XGB exhibited comparable overall accuracy, RF demonstrated marginally superior performance in balanced ratios (2 vs. 2), with fewer misclassifications (178 vs. 215) and a higher Kappa (0.98 vs. 0.97). This stems from the inherent RF resistance to overfitting via ensemble averaging (Breiman, 2001). Conversely, XGBoost's superior spatial accuracy in boundary highlights its strength in handling complex spatial hierarchies through gradient-boosted tree optimisation (Chen & Guestrin, 2016). However, the computational cost for XGBoost relative to RF is 48.5% for A3 and 32.4% for A5, which is a trade-off between accuracy and resource efficiency. This means that in a field with a higher crop ratio, distinguishing between them becomes more computationally demanding for both RF and XGBoost.

### *6.5.3 Statistical and practical implications*

When comparing the baseline SLIC features with the addition of texture indices, both RF and XGBoost demonstrated a statistically significant improvement. Similarly, incorporating morphological operators significantly improved RF and XGBoost's performance. This aligns with RF and XGBoost's reputation for excelling in high-dimensional spaces (Kondal, 2023). However, when comparing SLIC + Texture and SLIC + Morphology against the use of all variables, neither RF with a p-value of 0.344 and 0.205 nor XGBoost with a p-value of 0.205 and 0.295 respectively showed statistically significant improvements. This suggests that texture and morphology are the most influential variables in enhancing classification accuracy, particularly for XGBoost, whereas additional variables provide diminishing returns on performance improvement. Additionally, maize and soybean exhibit distinct textural and structural patterns, and XGBoost is effectively leveraged for better discrimination.

A key innovation of this study is the systematic evaluation of feature combinations, which provides critical insights into the role of different data layers in enhancing the classification performance:

1. Utilising only SLIC-based features resulted in higher misclassification rates (6–8%), confirming that spectral segmentation alone is insufficient for precise crop differentiation.
2. The inclusion of textural features reduced the error rate to ≤3%, highlighting the importance of structural variation in crop identification.
3. Morphological operators provided additional refinement, leading to the lowest error rate (1%) when combined with the SLIC.

Unlike previous studies that primarily compare, our findings emphasise the complementary role of different feature sets in improving classification performance. This aligns with the results of Kawamura et al. (2021a), that demonstrated that multi-feature integration enhances remote sensing classification. However, our study extends this by demonstrating that morphological operators, which are rarely used in crop mapping, play a critical role in refining object-based segmentation. From a practical perspective, this study validates the utility of UAS-based mapping for mixed-crop systems with models that accurately resolve row-specific planting configurations. Such precision supports yield estimation and resource management in precision agriculture.

### *6.5.4 Limitations and future directions*

While the models demonstrated robust performance within the tested crop ratios, their scalability and applicability across diverse agro-ecologies remain to be fully established. In particular, mixed cropping systems with more than two species, varying planting densities, or contrasting phenological patterns may present additional spectral and textural variability that affect model generalisation. Moreover, environmental factors such as soil type, topography, microclimate, and seasonal variability influences canopy structure and reflectance, potentially reducing the transferability of models trained under specific conditions.

The current reliance on a pre-trained vegetation mask introduces further constraints; inaccuracies in this mask, especially under heterogeneous agro-ecological contexts, could propagate errors through the classification pipeline. To enhance scalability, future work should explore end-to-end deep learning approaches capable of learning hierarchical features directly from imagery, potentially reducing dependency on pre-defined masks. Additionally, systematic validation across multiple agro-ecological zones, encompassing different crop combinations, management practices, and climatic conditions, would provide insights into model robustness and operational viability at larger spatial scales. This would not only improve model generalisation but also support broader adoption for precision agriculture and crop monitoring in heterogeneous landscapes.

## 6.6 Conclusion

This study showed the feasibility of the synergy of SLIC-based segmentation, multi-feature integration (texture, morphological and SLIC), and machine learning classifiers (random forest and extreme gradient boosting) for crop discrimination in a heterogeneous agricultural landscape. While both RF and XGBoost excel with an overall accuracy of more than 0.98, their trade-offs in accuracy, speed, and spatial precision necessitate context-driven model selection. Furthermore, the lack of statistical significance when using all variables compared to texture or morphology alone implies that adding more features beyond these does not necessarily improve performance. This indicates that texture and morphology are the most important factors for crop classification. Furthermore, this has shown that incorporating excessive variables may lead to redundancy rather than meaningful improvements. These insights contribute to scalable, high-resolution crop monitoring frameworks essential for sustainable agricultural management.

## 6.7 Summary

*Chapter Six presented a comprehensive data-driven approach for crop discrimination within smallholder farming systems. By leveraging UAS-based RGB data, the chapter highlights the importance of integrating diverse datasets for accurately distinguishing maize from soybean with high classification accuracies. The following Chapter Seven synthesises the key findings from this study, contextualises their implications and provides recommendations for future research, offering a comprehensive conclusion to this dissertation*

# CHAPTER 7 : SYNTHESIS AND CONCLUSION

## Application of unmanned aerial systems for crop discrimination in smallholder farms: A Synthesis

### 7.1 Introduction

Why do we need remotely sensed data for the accurate detection and identification of crop types in mixed cropping systems? Identification and estimation of the spatial extent of constituent crops in a mixed cropping system is crucial for better agricultural production and for food management. It is also important to note that understanding each crop type and its spatial distribution within the field is vital not only for resource allocation and yield estimation but also for ensuring food security. Emerging UAS technology has the ability to discriminate and spatially quantify the extent of specific crop types in complex configurations and spatial heterogeneity of agro-ecological landscapes.

Previous studies demonstrated that crops with similar development and overlapping phenological cycles exhibit high spectral, structural and spatial variability, making it difficult to accurately delineate crop boundaries using traditional satellite remote sensing. Generally, satellite remotely sensed data lacks the optimal spatial and spectral resolution needed to map small, intercropped plots, which normally cover less than a metre for intra and across rows. Similarly, although ground surveys are accurate in terms of spectral separability, they are labour-intensive, costly, and impractical for large-scale mapping. Various studies mainly focused on discriminating crops grown under a monoculture environment with very minimal challenges in terms of spectral separability. Also, they did not focus on distinguishing crops in heterogeneous agro-ecological landscapes or incorporate phenological data obtained from emerging technologies. As such, this implies that accurately detecting each crop type extent in mixed cropping systems is important to filter out undesirable results. Unlike satellite remote sensing, which is constrained by orbital cycles, weather conditions, and resolution limitations, UASs can be deployed as needed to capture timely datasets for crop discrimination across phenological stages. The UASs have the capacity for rapid and localised deployment, which provides a potential for crop discrimination across phenological stages in a mixed cropping environment at a relatively low cost.

The spectral responses of crops in agro-ecological landscapes are normally affected by surrounding features such as soil background, shadows and atmospheric conditions, limiting the effectiveness of remote sensing techniques. Crop discrimination in such environments requires critical selection of optimal feature extractors and classification algorithms that can process large amounts of data with limited resources. These critical problems have limited the application of remotely sensed imagery to discriminate and quantify constituent crops in mixed cropping systems at different levels. Therefore, this study sought to develop innovative techniques that employ UAS-based imagery for crop discrimination in heterogeneous agro-ecological landscapes to create accurate, specific crop masks. Specifically, the proposed approaches in this thesis focused on the following objectives:

i. To systematically review the current state, challenges and opportunities in the application of unmanned aerial systems for crop discrimination, with a particular focus on smallholder farms and heterogeneous agro-ecological systems.
ii. To investigate the spectral response characteristics of maize and soybean across distinct phenological stages using hyperspectral data, and to determine the stage(s) at which spectral separability is maximised for effective crop discrimination.
iii. To develop and validate machine learning algorithmic approaches for accurately distinguishing crop types in mixed cropping systems using UAS-derived imagery.
iv. To determine the optimal field parameters, specifically the number of crop species and crop row widths, that facilitate accurate crop discrimination using UAS data in fragmented agricultural landscapes.
v. To evaluate the efficacy of integrating object-based image analysis with machine learning algorithms in enhancing the classification accuracy of UAS imagery for crop discrimination.

**Table 7-1: Highlighting the main contributions of this thesis to UAS-based crop discrimination in heterogeneous agro-ecological systems.**

| Chapter | Main Objectives | Key Findings | Innovations / Contributions |
|---|---|---|---|
| Introduction | Introduce research problem, objectives, and rationale | Identified gaps in UAS-based crop discrimination in heterogeneous smallholder systems | Developed research questions targeting mixed cropping systems in agro-ecological landscapes |
| Literature review | Review UAS applications, UAS types and characteristics, feature extractors and classifier methods for crop discrimination | UAS use in agriculture has increased, especially rotary-wing platforms with RGB sensors; challenges remain in heterogeneous and mixed cropping systems; hyperspectral approaches are promising but limited | Synthesised gaps in crop discrimination; highlighted the need for plot-to-field-level scaling |
| Hyperspectral crop discrimination | Evaluate *in-situ* hyperspectral data to discriminate maize and soybean | Narrow-band hyperspectral data effectively distinguished maize and soybean, especially between flowering and senescence; red-edge and NIR bands were most informative | Demonstrated optimal phenological windows and spectral regions for mixed crop discrimination; validated analytical methods (statistical, distance/divergence-based, PLS-DA) |
| UAS RGB-based feature analysis | Evaluate RF classifier with spectral, textural, and morphological features from UAS RGB imagery | Morphological features outperformed spectral and textural features; combining textural + morphological features gave the highest accuracy; shadows caused misclassification | Results showed that hybrid feature extraction enhances crop discrimination at the field scale; highlighted limitations of spectral-only approaches |
| Shadow detection and removal | Develop methods to detect and remove shadow pixels | The HIGB difference technique outperformed C3 and NSVDI for shadow detection; the LIRB removal approach introduced artefacts | Introduced novel HIGB shadow detection; emphasised scene- and context-sensitive shadow handling for improved classification accuracy |
| Segmentation and machine learning integration | Integrate SLIC segmentation with machine learning classifiers (RF, XGBoost) using multi-feature datasets | Achieved up to 99% accuracy in maize-soybean discrimination; texture + morphology outperformed spectral indices; RF and XGBoost trade-offs observed | Demonstrated scalable approach combining superpixel segmentation and hybrid feature engineering; addressed spectral overlap and spatial heterogeneity; validated potential for operational precision agriculture |
| Conclusion and recommendations | Summarise contributions and future directions | Validated the effectiveness of SLIC -XGBoost for mixed cropping; outlined operational relevance | Recommended operational adoption for precision agriculture and testing across diverse agro-ecologies to enhance robustness |

As summarised in Table 7-1, the contributions of this thesis span both theoretical and practical dimensions. Theoretical contributions include methodological advances in UAS-based crop discrimination, including hybrid feature extraction, SLIC segmentation, and machine learning applications in heterogeneous agro-ecological landscapes. Practical contributions, on the other hand, involve operational workflows and actionable tools that can be implemented in smallholder farming systems for crop monitoring, yield estimation, and resource allocation. Table 7-1 provides a concise overview of these chapter-wise innovations and their relevance to both knowledge advancement and real-world application.

## 7.2 Conclusion

The central aim of this thesis was to explore the potential of UAS-based RGB-derived feature datasets for distinguishing between maize and soybean in a mixed cropping system. Despite the inherent limitations associated with RGB datasets, the findings presented in this study have demonstrated their utility in achieving reasonable levels of accuracy in crop discrimination. The overarching conclusion of this research is that the integration of region-based segmentation, a comprehensive multi-feature approach encompassing texture, morphological characteristics, and SLIC-derived features within varied feature sets, coupled with the application of machine learning classifiers (random forest and XGBoost), significantly contributes to the feasibility of accurate crop discrimination within heterogeneous agricultural landscapes.

The synthesis of the key conclusions drawn from this study, directly addressing the research objectives, is as follows:

a) Evidence from literature indicates that the application of UASs in agricultural activities, particularly crop mapping and monitoring, has been extensively documented. A review of published studies reveals that the use of UAS technology in this domain has grown significantly, especially over the past decade. Rotary-wing UAS platforms have emerged as the preferred choice among researchers due to their superior manoeuvrability in spatially constrained environments. These platforms, when equipped with RGB sensors, represent the most commonly utilised combination, reflecting a broader preference for cost-effective, accessible, and adaptable tools, especially in developing regions. Despite these advancements, challenges persist in the domain of crop discrimination, particularly within heterogeneous and complex mixed cropping systems. Current remote sensing platforms, including satellites and conventional ground surveys, often struggle to resolve spectral overlaps between crop types at varying spatial and temporal scales. This limitation constrains the accuracy of crop-type classification in such environments. Additionally, while hyperspectral data analytics offer promising potential for improving crop discrimination, their application remains in infancy with little progress. Existing studies are limited, and methodological refinement is required to fully exploit the high spectral resolution offered by hyperspectral sensors in operational agricultural monitoring.

b) To address the aforementioned challenges, experimental surveys were conducted using *in-situ* hyperspectral measurements to collect spectral signatures of maize and soybean. These measurements utilised narrow-band spectral settings, which possess the capability to capture fine spectral details, thereby enhancing the potential to accurately extract and discriminate between the two crop species. Accordingly, this chapter aimed to evaluate the utility of hyperspectral data in discriminating maize from soybean and to compare the performance of statistical, distance-based, divergence-based, and PLS-DA methods in characterising crop types cultivated under mixed cropping systems. The results presented in this chapter demonstrate the effectiveness of *in-situ* hyperspectral remote sensing data, along with various analytical techniques, in discriminating between maize and soybean cultivated under mixed cropping systems. The study underscores the importance of phenological timing, identifying flowering to senescence as optimal windows for discrimination of maize and soybean. This was achieved by specific wavelengths located within the red-edge and near-infrared regions of the electromagnetic spectrum. This finding underscores the fundamental spectral differences between the two crop types. However, despite the high overall classification accuracies achieved using hyperspectral remotely sensed data, its applicability remains largely constrained to the plot level. The data lacks sufficient spatial coverage for effective large-scale mapping of maize and soybean distributions. Therefore, there is a need to evaluate the same objective using UAS-acquired remotely sensed data collected across different phenological stages, in order to validate the above observations and assess the generalisability of the findings beyond the plot level.

c) The significance of this study was to evaluate the performance of the RF algorithm for discriminating between maize and soybean based on their spectral, textural and morphological differences using UAS-based RGB imagery. This foundational insight validates the applicability of extending spectral analysis from field spectrometry to UAS-based RGB imagery to distinguish crop types in complex agro-ecological environments. Results obtained from this chapter indicated that morphological features consistently outperformed spectral and textural features for crop discrimination using a random forest classifier, while integrating textural and morphological features achieved the highest classification accuracies. The normally preferred features, particularly spectral features, were the least effective for discriminating and mapping mixed crop species. This chapter has shown that employing diverse feature extraction techniques can indeed enhance the spectral discrimination capabilities between maize and soybean within the same agricultural field. However, misclassification among the soybean, shadow, and weed classes was observed, highlighting the challenges of accurately distinguishing crop types within mixed cropping systems. This confusion caused by the presence of shadow pixels has tangible implications for the detection and characterisation of vegetation features, ultimately compromising the reliability of crop acreage estimation.

d) Although the random forest classifier effectively discriminated and mapped the spatial extent of various features using UAS-based RGB imagery, the presence of shadow pixels, particularly those overlapping with soybean, negatively affected overall classification accuracy. Consequently, this chapter focused on shadow detection and removal, processes that are often regarded as critical steps in image preprocessing. The primary objective was to develop and evaluate a novel hue-intensity-green-blue (HIGB) difference technique for accurately detecting shadows within diverse crop mixtures. The results demonstrated that the HIGB difference technique consistently outperformed both the $C_3$ and normalised shadow vegetation difference index (NSVDI) models across all five experimental treatments. Although the HIGB successfully detected shadows, the alternative light intensity ratio-based (LIRB) shadow removal approach failed to meet performance expectations, often introducing blurry artifacts in dense shadow pixels rather than effectively removing shadows. These findings underscore the importance of contextual sensitivity and the differential efficacy of shadow-handling techniques depending on scene composition and image complexity.

e) Previous chapters have shown that crops may share near-identical spectral profiles but differ in canopy texture or plant geometry. As such, this chapter focused on a model that only utilises vegetation pixels for discrimination, thereby eliminating surrounding features such as soil, shadow and weeds. The proposed integration of SLIC-based segmentation with machine learning classifiers, specifically RF and XGBoost, demonstrated exceptional performance in distinguishing maize and soybean crops within heterogeneous agricultural landscapes, achieving an overall classification accuracy of 99%. The highest classification accuracies were obtained through the combination of SLIC-based segmentation with multi-feature datasets, incorporating textural and morphological features, whereas the inclusion of spectral indices reduced accuracy levels. This underscores the significance of spatial coherence and hybrid feature engineering in addressing the spectral and structural complexity inherent in agro-ecological systems. The trade-offs observed between the RF and XGBoost classifiers regarding accuracy, speed, and spatial precision necessitate a context-driven approach to model selection. Notably, the lack of statistically significant improvement when using all variables compared to texture or morphology alone suggests that simply adding more features does not guarantee enhanced classification accuracy. Overall, the synergy of SLIC segmentation and machine learning classifiers effectively addressed spatial heterogeneity and spectral overlap, demonstrating its potential scalability for precision agriculture applications, particularly in resource-constrained regions.

These findings collectively underscore the potential of advanced image processing and machine learning techniques applied to UAS-based RGB imagery for effective crop discrimination in complex agricultural settings. This capability holds significant implications for improved resource management, yield estimation, and ultimately, enhanced food security in regions relying on mixed cropping systems. Importantly, the contributions of this thesis are novel in their explicit focus on smallholder mixed-cropping systems in sub-Saharan Africa, which remain significantly underrepresented in the remote sensing and precision agriculture literature. By tailoring UAS-based crop discrimination methods to heterogeneous, resource-constrained contexts, this study not only advances methodological innovation but also provides regionally relevant solutions for sustainable agricultural intensification. Furthermore, the study demonstrates the complete methodological pipeline, from spectral theory through feature extraction and image processing to operational classification, highlighting both the scientific rigour and practical applicability of the approach.

## 7.3 Policy Relevance and Pathways for Regional Scalability

The findings of this study have clear implications for agricultural policy and operational crop monitoring, demonstrating that low-cost UAS-RGB imagery, processed through automated SLIC segmentation and machine learning, provides a scalable and policy-relevant tool for accurate crop discrimination. This approach offers a practical framework for precision agriculture interventions that can enhance yield estimation and resource allocation in heterogeneous smallholder systems, enabling policymakers to leverage these insights for evidence-based decision-making, particularly where traditional methods are limited. From an extension perspective, the outputs generated can be transformed into advisory products such as field-level crop maps, weed infestation alerts, and seasonal acreage estimates. These can be delivered through agricultural advisory services, mobile platforms, or integration into decision-support systems to guide farmers on input use and management practices. At the policy level, such tools can support national crop assessments, food security monitoring, and the design of targeted subsidy or input-distribution programs.

For regional scalability, this affordable technology stack shows significant potential for adaptation across diverse agro-ecological zones. Successful adoption will depend on calibrating models with local crop varieties and conditions, leveraging robust multi-feature datasets, and addressing key infrastructural needs like UAS accessibility, personnel training, and context-specific adjustments to ensure reliable deployment beyond the study site.

## 7.4 Practical Steps and Implementation Tools

To operationalise the findings of this study, the following steps are recommended:

- **i.** Deploy UASs (rotary-wing for smallholder fields and fixed-wing for larger areas) equipped with RGB sensors, and schedule flights at key crop phenological stages: early vegetative, mid-vegetative, flowering/tasselling, mid-grain filling, and senescence onset**.**
- **ii.** Apply pre-processing procedures, including shadow detection and compensation via the HIGB difference technique, supplemented by appropriate image restoration methods**,**

iii. Conduct image segmentation using SLIC-based superpixels to improve object-level feature extraction, and classify imagery using XGBoost or Random Forest with hybrid feature sets (SLIC clusters, morphological indices, and textural features),

iv. Calibrate the model to local crop varieties, planting densities, and agro-ecological conditions to ensure regional scalability and robustness,

v. Integrate outputs with GIS platforms and farm management systems to produce actionable products for crop monitoring, acreage estimation, yield forecasting, and resource allocation, and

vi. Build capacity by training local personnel and immediate data users in UAS operations, data processing, and interpretation to ensure sustainable adoption.

## 7.5 Challenges and Future Directions

While this study has highlighted the significant potential of UAS-based imagery and advanced feature extraction methods for enhanced crop discrimination in heterogeneous agro-ecological landscapes, several challenges remain, paving the way for future research endeavours.

- Firstly, the inherent limitation of RGB sensors lies in their spectral resolution compared to multispectral and hyperspectral remotely sensed data. This can restrict their ability to differentiate crops with similar reflectance characteristics in the visible spectrum. Future research should explore the integration of data from other parts of the electromagnetic spectrum, such as thermal regions, to ascertain if they can further enhance the results obtained in this study. Combining RGB sensors with affordable alternatives like LiDAR, thermal, multispectral and hyperspectral imaging sensors could provide complementary datasets, including 3D structural information and canopy temperature, thereby enriching spectral and structural insights.

- Secondly, the intrinsic spectral similarities and high spatial heterogeneity prevalent in mixed cropping systems often lead to fragmented or overlapping crop boundaries in imagery. To address this, future research should focus on developing region-specific crop libraries containing spectral signatures of locally relevant crops. Furthermore, the creation of open-access repositories of well-labelled imagery for mixed cropping systems is crucial for improving the transferability and robustness of developed models across different regions and agricultural practices.

- Thirdly, the substantial data variability and noise inherent in heterogeneous agro-ecological landscapes necessitate significant computational resources, often requiring GPU clusters for the effective implementation of hybrid methods. In particular, the generation of superpixels and the extraction of spatially explicit features are computationally intensive processes, especially when applied across large datasets or extensive geographic scales. As the complexity of crop mixtures and the ratio of different crops increase, these demands grow considerably, underscoring the need for more advanced computational infrastructure and optimisation strategies (e.g., parallelisation, cloud-based pipelines) to enable practical scalability.

- Fourthly, future research should prioritise enhancing the separability of crop classes with overlapping spectral and structural characteristics. This can be achieved by incorporating advanced preprocessing techniques and leveraging attention-based deep learning models. For such models to perform effectively under erratic weather conditions, the integration of water-resistant sensors, such as Synthetic Aperture Radar (SAR), is recommended. These sensors can ensure continuous image acquisition across different phenological stages, regardless of cloud cover or precipitation. Furthermore, optimisation of deep learning architectures should focus on the integration of spectral, textural, morphological, and temporal features, while simultaneously mitigating the noise introduced by mixed pixels and the inherent complexity of heterogeneous agricultural systems.

- Furthermore, no field-based ground truth measurements of physiological or biophysical parameters (e.g., leaf area index, biomass) were collected to validate the spectral responses. As such, future work should integrate such field data to enhance the calibration and validation of UAS-based models, thereby improving biophysical interpretability and strengthening the reliability of crop discrimination outcomes.

- Finally, beyond methodological advances, future work should prioritise the development of lightweight, user-friendly tools that can translate UAS-based analytics into actionable insights for end-users. One possible pathway is the design of a mobile-friendly application, web-based application or plugin, capable of integrating classification outputs into simple dashboards accessible to local users. Coupling this with cloud-based processing pipelines such as Google Earth Engine, Amazon Web Services or UAS-specific platforms like Pix4Dcloud and DroneDeploy would minimise computational demands on local devices, making the approach more accessible across diverse agro-ecological and infrastructural contexts.

In conclusion, this research contributes valuable insights into the application of UAS-based RGB imagery for crop discrimination in mixed cropping systems. The identified challenges and proposed future directions highlight the ongoing need for innovation and development in this critical area of precision agriculture, with the ultimate goal of supporting sustainable agricultural practices and ensuring global food security.

## REFERENCES


Abdel-Rahman, E. M., and Ahmed, F. B. (2008). The application of remote sensing techniques to sugarcane (Saccharum spp. hybrid) production: A review of the literature. *International Journal of Remote Sensing*, *29*(13), 3753–3767. https://doi.org/10.1080/01431160701874603

Abdullahi, H. S., Mahieddine, F., and Sheriff, R. E. (2015). Technology impact on agricultural productivity: A review of precision agriculture using unmanned aerial vehicles. *Lecture Notes of the Institute for Computer Sciences, Social-Informatics and Telecommunications Engineering, LNICST*, *154*(November), 388–400. https://doi.org/10.1007/978-3-319-25479-1_29

Adeline, K. R. M., Chen, M., Briottet, X., Pang, S. K., and Paparoditis, N. (2013). Shadow detection in very high spatial resolution aerial images: A comparative study. *ISPRS Journal of Photogrammetry and Remote Sensing*, *80*, 21–38. https://doi.org/10.1016/j.isprsjprs.2013.02.003

Adewopo, J., Peter, H., Mohammed, I., Kamara, A., Craufurd, P., and Vanlauwe, B. (2020). Can a combination of uav-derived vegetation indices with biophysical variables improve yield variability assessment in smallholder farms? *Agronomy*, *10*(12). https://doi.org/10.3390/agronomy10121934

Adler-Golden, S. M., Matthew, M. W., Anderson, G. P., Felde, G. W., and Gardner, J. A. (2002). Algorithm for de-shadowing spectral imagery. *Proc. SPIE, Imaging Spectrometry VIII*, *4816*, 203–210. https://doi.org/10.1117/12.451691

African Union, and New Partnership for Africa's Development (NEPAD). (2018). Drones on the Horizon Transforming Africa's Agriculture. In *High Level Apet Report*.

Agarwal, A., Kumar, S., and Singh, D. (2021). An Adaptive Technique to Detect and Remove Shadow from Drone Data. *Journal of the Indian Society of Remote Sensing, 49* (3), 491–498. https://doi.org/10.1007/s12524-020-01227-z

Aguilar, M. A., Vallario, A., Aguilar, F. J., Lorca, A. G., and Parente, C. (2015). Object-based greenhouse horticultural crop identification from multi-temporal satellite imagery: A case study in Almeria, Spain. *Remote Sensing*, *7*(6), 7378–7401. https://doi.org/10.3390/rs70607378

Alvarado-Robles, G., Osornio-Ríos, R. A., Solís-Muñoz, F. J., and Morales-Hernández, L. A. (2021). An Approach for Shadow Detection in Aerial Images Based on Multi-Channel Statistics. *IEEE Access*, *9*, 34240–34250. https://doi.org/10.1109/ACCESS.2021.3061102

Alvarado-Robles, G., Solís-Muñoz, F. J., Garduño-Ramón, M. A., Osornio-Ríos, R. A., and Morales-Hernández, L. A. (2021). A novel shadow removal method based upon color transfer and color tuning in UAV imaging. *Applied Sciences (Switzerland)*, *11*(23). https://doi.org/10.3390/app112311494

Andrew, J., Eunice, R. J., Popescu, D., Chowdary, M. K., and Hemanth, D. J. (2022). Deep Learning-Based Leaf Disease Detection in Crops Using Images for Agricultural Applications. *Agronomy*. https://doi.org/10.3390/agronomy12102395

Andritoiu, D., Bazavan, L.-C. C., Besnea, F.-L. L., Roibu, H., and Bizdoaca, N.-G. G. (2018). Agriculture autonomous monitoring and decisional mechatronic system. *2018 19th International Carpathian Control Conference (ICCC), November 2019*, 241–246. https://doi.org/10.1109/CarpathianCC.2018.8399635

Aneece, I., and Thenkabail, P. (2018). Accuracies achieved in classifying five leading world crop types and their growth stages using optimal earth observing-1 hyperion hyperspectral narrowbands on Google Earth Engine. *Remote Sensing*, *10*(12), 1–29. https://doi.org/10.3390/rs10122027

Aparicio, N., Villegas, D., Casadesus, J., Araus, J. L., & Royo, C. (2000). Canopy reflectance indices: a new tool for assessing durum wheat LAI and yield. Options Mediterraneennes, 119(40), 117–119

Arafat, S. M., Aboelghar, M. A., and Ahmed, E. F. (2013). Crop Discrimination Using Field Hyper Spectral Remotely Sensed Data. *Advances in Remote Sensing*, *02*(02), 63–70. https://doi.org/10.4236/ars.2013.22009

Arévalo, V., González, J., and Ambrosio, G. (2008). Shadow detection in colour high-resolution satellite images. *International Journal of Remote Sensing*, *29*(7), 1945–1963. https://doi.org/10.1080/01431160701395302

Asner, G. P. (1998). Biophysical and Biochemical Sources of Variability in Canopy Reflectance. *Remote Sensing of Environment*, *253*(October 1997), 234–253.

Astaoui, G., Dadaiss, J. E., Sebari, I., Benmansour, S., and Mohamed, E. (2021). Mapping Wheat Dry Matter and Nitrogen Content Dynamics and Estimation of Wheat Yield Using UAV Multispectral Imagery Machine Learning and a Variety-Based Approach: Case Study of Morocco. *AGRIENGINEERING*, *3*(1), 29–49. https://doi.org/10.3390/agriengineering3010003 WE - Emerging Sources Citation Index (ESCI)

Azevedo, S. C., Silva, E. A., and Pedrosa, M. M. (2015). Shadow detection improvement using spectral indices and morphological operators in Urban Areas in high resolution images.

*International Archives of the Photogrammetry, Remote Sensing and Spatial Information Sciences - ISPRS Archives*, *40*(7W3), 587–592. https://doi.org/10.5194/isprsarchives-XL-7-W3-587-2015

Balasubramanian, K. I. (2017). *Identifying the Most Important Spectral and Textural Features to Map Specific Crops with Very High Resolution Images*. University of Twente.

Banon, G., Barrera, J., and Braga-Neto, U. (Eds.). (2007). Mathematical Morphology and Its Applications to Signal and Image Processing. In *Proceedings of the 8th International Symposium on Mathematical Morphology*. Springer.

Barbedo, J. G. A. (2019). A Review on the Use of Unmanned Aerial Vehicles and Imaging Sensors for Monitoring and Assessing Plant Stresses. *Drones*, *3*(2), 40. https://doi.org/10.3390/drones3020040

Baret, F., Champion, I., Guyot, G., and Podaire, A. (1987). Monitoring wheat canopies with a high spectral resolution radiometer. *Remote Sensing of Environment*, *22*(3), 367–378. https://doi.org/10.1016/0034-4257(87)90089-7

Beach, R., Lapidus, D., Hegarty-Craver, M., O'Neil, M., Rineer, J., & Temple, D. (2020). Crop mapping using Sentinel-1 and Sentinel-2 imagery and UAV-acquired ground truth data. Gates Open Res, 4, 27709

Beard, K. H., Cutler, D. R., Edwards, T. C., Beard, K. H., Cutler, A., Hess, K. T., Gibson, J., and Lawler, J. J. (2007). Random forests for classification in ecology. *Ecology*, *88*(11), 2783–2792. https://doi.org/10.1890/07-0539.1

Beeharry, Y., & Bassoo, V. (2020). Performance of ANN and AlexNet for weed detection using UAV-based images. 2020 3rd *International Conference on Emerging Trends in Electrical, Electronic and Communications Engineering* (ELECOM), 163–167. https://doi.org/10.1109/ELECOM49001.2020.9296994

Bégué, A., Arvor, D., Bellon, B., Betbeder, J., de Abelleyra, D., Ferraz, R. P. D., Lebourgeois, V., Lelong, C., Simões, M., and Verón, S. R. (2018). Remote sensing and cropping practices: A review. *Remote Sensing*, *10*(1), 1–32. https://doi.org/10.3390/rs10010099

Bellis, E. S., Hashem, A. A., Causey, J. L., Runkle, B. R. K., Moreno-García, B., Burns, B. W., Green, V. S., Burcham, T. N., Reba, M. L., and Huang, X. (2022). Detecting Intra-Field Variation in Rice Yield With Unmanned Aerial Vehicle Imagery and Deep Learning. *Frontiers in Plant Science*, *13*(March), 1–13. https://doi.org/10.3389/fpls.2022.716506

Bellón, B., Bégué, A., Seen, D. Lo, de Almeida, C. A., and Simões, M. (2017). A remote sensing approach for regional-scale mapping of agricultural land-use systems based on NDVI time series. *Remote Sensing*, *9*(6), 1–17. https://doi.org/10.3390/rs9060600

Berni, J. A. J., Zarco-Tejada, P. J., Suarez, L., and Fereres, E. (2009). Thermal and Narrowband Multispectral Remote Sensing for Vegetation Monitoring From an Unmanned Aerial Vehicle. *IEEE Transactions on Geoscience and Remote Sensing*, *47*(3), 722–738. https://doi.org/10.1109/TGRS.2008.2010457

Beyer, F., Jarmer, T., and Siegmann, B. (2015). Identification of agricultural crop types in northern israel using multitemporal rapideye data. *Photogrammetrie, Fernerkundung, Geoinformation*, *2015*(1), 21–32. https://doi.org/10.1127/pfg/2015/0249

Bhardwaj, A. K., Chejara, S., Malik, K., Kumar, R., and Yadav, R. K. (2022). Agronomic Biofortification of Food Crops: An Emerging Opportunity for Global Food and Nutritional Security. *Frontiers in Plant Science*. https://doi.org/10.3389/fpls.2022.1055278

Blaschke, T. (2010). Object based image analysis for remote sensing. *ISPRS Journal of Photogrammetry and Remote Sensing*, *65*(1), 2–16. https://doi.org/10.1016/j.isprsjprs.2009.06.004

Bolo, B. G., Mpoeleng, D., and Zlotnikova, I. (2019). Application of Unmanned Aerial Vehicle (UAV) for Small Scale Precision Farming in Botswana. *Earth Observations and Geospatial Science in Service OfSustainable Development Goals*, 91–100. https://doi.org/10.1007/978-3-030-16016-6_9

Bosilj, P., Duckett, T., and Cielniak, G. (2018). Analysis of Morphology-Based Features for Classification of Crop and Weeds in Precision Agriculture. *IEEE Robotics and Automation Letters*, *3*(4), 2950–2956. https://doi.org/10.1109/LRA.2018.2848305

Bramer, W. M., Jonge, G. B. De, Rethlefsen, M. L., Mast, F., and Kleijnen, J. (2018). *Jmla-106-531.Pdf*. *106*(October), 531–541.

Breiman, L. (2001). Breiman2001 - Random forests. *Machine Learning*, *45*, 5–32.

Brewer, K., Clulow, A., Sibanda, M., Gokool, S., Naiken, V., and Mabhaudhi, T. (2022). Predicting the Chlorophyll Content of Maize over Phenotyping as a Proxy for Crop Health in Smallholder Farming Systems. *REMOTE SENSING*, *14*(3). https://doi.org/10.3390/rs14030518 WE - Science Citation Index Expanded (SCI-EXPANDED)

Brito, R. C., Lorencena, M. C., Loureiro, J. F., Favarim, F., and Todt, E. (2019). A Comparative Approach on the use of Unmanned Aerial Vehicles kind of Fixed-Wing and Rotative Wing

Applied to the Precision Agriculture Scenario. *2019 IEEE 43rd Annual Computer Software and Applications Conference (COMPSAC)*, *2*, 522–526.

Buchaillot, M., Gracia-Romero, A., Vergara-Diaz, O., Zaman-Allah, M. A., Tarekegne, A., Cairns, J. E., Prasanna, B. M., Araus, J. L., and Kefauver, S. C. (2019). Evaluating maize genotype performance under low nitrogen conditions using RGB UAV phenotyping techniques. *Sensors, 19*(8), 1815. https://doi.org/10.3390/s19081815

Buchaillot, M. L., Gracia-Romero, A., Vergara-Diaz, O., Zaman-Allah, M. A., Tarekegne, A., Cairns, J. E., Prasanna, B. M., Araus, J. L., and Kefauver, S. C. (2019). Evaluating maize genotype performance under low nitrogen conditions using RGB UAV phenotyping techniques. *Sensors (Switzerland)*, *19*(8). https://doi.org/10.3390/s19081815

Campbell, T., and Fearns, P. (2018). Honey Crop Estimation From Space : Detection of Large Flowering Events in Western Australian Forests. *The International Archives of the Photogrammetry, Remote Sensing and Spatial Information Sciences*, *XLII*, 10–12.

Candiago, S., Remondino, F., De Giglio, M., Dubbini, M., and Gattelli, M. (2015). Evaluating multispectral images and vegetation indices for precision farming applications from UAV images. *Remote Sensing*, *7*(4), 4026–4047.

Castaldi, F., Pelosi, F., Pascucci, S., & Casa, R. (2017). Assessing the potential of images from unmanned aerial vehicles (UAV) to support herbicide patch spraying in maize. *Precision Agriculture*, 18(1), 76–94. https://doi.org/10.1007/s11119-016-9468-3

Champagne, C. (2019). Detecting crop damage using Sentinel-2 imagery in a smallholder agriculture landscape Chipinge and Makoni Districts, Zimbabwe. Université catholique de Louvain.

Chen, T., and Guestrin, C. (2016). XGBoost: A scalable tree boosting system. *Proceedings of the ACM SIGKDD International Conference on Knowledge Discovery and Data Mining*, *13-17-Augu*, 785–794. https://doi.org/10.1145/2939672.2939785

Chen, Y., Ribera, J., Boomsma, C., and Delp, E. (2017). Locating Crop Plant Centers from UAV-Based RGB Imagery. *2017 IEEE International Conference on Computer Vision Workshops (ICCVW)*, 2030–2037.

Chew, R., Rineer, J., Beach, R., O'neil, M., Ujeneza, N., Lapidus, D., Miano, T., Hegarty-Craver, M., Polly, J., and Temple, D. S. (2020a). Deep neural networks and transfer learning for food crop identification in UAV images. *Drones*, *4*(1), 1–14. https://doi.org/10.3390/drones4010007

Chew, R., Rineer, J., Beach, R., O'neil, M., Ujeneza, N., Lapidus, D., Miano, T., Hegarty-Craver, M., Polly, J., and Temple, D. S. (2020b). Deep neural networks and transfer learning for food crop identification in UAV images. *Drones*, *4*(1), 1–14. https://doi.org/10.3390/drones4010007

Chianucci, F., Disperati, L., Guzzi, D., Bianchini, D., Nardino, V., Lastri, C., Rindinella, A., and Corona, P. (2016). Estimation of canopy attributes in beech forests using true colour digital images from a small fixed-wing UAV. *International Journal of Applied Earth Observation and Geoinformation*, *47*, 60–68. https://doi.org/10.1016/j.jag.2015.12.005

Chisango, F. F. T. (2018). Challenges and Prospects of Zimbabwe's Command Farming in Unlocking the Country's Smallholder Agricultural Economy. *International Journal of Agricultural Economics*, *3*(4), 76–82. https://doi.org/10.11648/j.ijae.20180304.13

Chivasa, W., Mutanga, O., and Biradar, C. (2019). Phenology-based discrimination of maize (Zea mays L.) varieties using multitemporal hyperspectral data. *Journal of Applied Remote Sensing*, *13*(01), 1. https://doi.org/10.1117/1.jrs.13.017504

Chivasa, W., Mutanga, O., and Biradar, C. (2020). UAV-based multispectral phenotyping for disease resistance to accelerate crop improvement under changing climate conditions. *Remote Sensing*, *12*(15). https://doi.org/10.3390/RS12152445

Chivasa, W., Mutanga, O., and Burgueno, J. (2021). UAV-based high-throughput phenotyping to increase prediction and selection accuracy in maize varieties under artificial MSV inoculation. *COMPUTERS AND ELECTRONICS IN AGRICULTURE*, *184*. https://doi.org/10.1016/j.compag.2021.106128 WE - Science Citation Index Expanded (SCI-EXPANDED)

Christiansen, M. P., Laursen, M. S., Jørgensen, R. N., Skovsen, S., and Gislum, R. (2017). Designing and testing a UAV mapping system for agricultural field surveying. *Sensors (Switzerland)*, *17*(12), 1–19. https://doi.org/10.3390/s17122703

Cochrane, M. A. (2000). Using vegetation reflectance variability for species level classification of hyperspectral data. *International Journal of Remote Sensing*, *21*(10), 2075–2087. https://doi.org/10.1080/01431160050021303

Comba, L., Gay, P., Primicerio, J., and Ricauda Aimonino, D. (2015). Vineyard detection from unmanned aerial systems images. *Computers and Electronics in Agriculture*, *114*, 78–87. https://doi.org/10.1016/j.compag.2015.03.011

Crews, T. E., and Peoples, M. B. (2004). Legume versus fertilizer sources of nitrogen: Ecological tradeoffs and human needs. *Agriculture, Ecosystems and Environment*, *102*(3), 279–297. https://doi.org/10.1016/j.agee.2003.09.018

Cruzan, M. B., Weinstein, B. G., Grasty, M. R., Kohrn, B. F., Hendrickson, E. C., Arredondo, T. M., and Thompson, P. G. (2016). Small unmanned aerial vehicles (micro-UAVs, drones) in plant ecology. *Applications in Plant Sciences*, *4*(9).

Cucho-Padin, G., Loayza, H., Palacios, S., Balcazar, M., Carbajal, M., and Quiroz, R. (2020). Development of low-cost remote sensing tools and methods for supporting smallholder agriculture. *Applied Geomatics*, *12*(3), 247–263. https://doi.org/10.1007/s12518-019-00292-5

Curran, P. J. (1989). Remote sensing of foliar chemistry. *Remote Sensing of Environment*, *30*(3), 271–278. https://doi.org/10.1016/0034-4257(89)90069-2

Danner, M. (2017). Retrieval of Biophysical Crop Variables from Multi-Angular Canopy Spectroscopy. *Remote Sensing*, *9*(7), 726. https://doi.org/10.3390/rs9070726

Das, S., Christopher, J., Apan, A., Choudhury, M. R., Chapman, S., Menzies, N. W., and Dang, Y. P. (2021). Evaluation of water status of wheat genotypes to aid prediction of yield on sodic soils using UAV-thermal imaging and machine learning. *Agricultural and Forest Meteorology*, *307*. https://doi.org/10.1016/j.agrformet.2021.108477

Dadhwal, V. K., Singh, R. P., Dutta, S., & Parihar, J. S. (2002). Remote sensing based crop inventory: A review of Indian experience. Tropical Ecology, 43(1), 107–122.

de Castro, A. I., Six, J., Plant, R. E., and Peña, J. M. (2018). Mapping crop calendar events and phenology-related metrics at the parcel level by object-based image analysis (OBIA) of MODIS-NDVI time-series: A case study in central California. *Remote Sensing*, *10*(11). https://doi.org/10.3390/rs10111745

de Castro, A. I., Torres-Sánchez, J., Peña, J. M., Jiménez-Brenes, F. M., Csillik, O., and López-Granados, F. (2018a). An automatic random forest-OBIA algorithm for early weed mapping between and within crop rows using UAV imagery. *Remote Sensing*, *10*(2). https://doi.org/10.3390/rs10020285

de Castro, A. I., Torres-Sánchez, J., Peña, J. M., Jiménez-Brenes, F. M., Csillik, O., and López-Granados, F. (2018b). An automatic random forest-OBIA algorithm for early weed mapping between and within crop rows using UAV imagery. *Remote Sensing*, *10*(2), 1–21. https://doi.org/10.3390/rs10020285

de Oca, A. M., Arreola, L., Flores, A., Sanchez, J., and Flores, G. (2018). Low-cost multispectral imaging system for crop monitoring. *2018 International Conference on Unmanned Aircraft Systems (ICUAS)*, 443–451.

de Sá, N. C., Castro, P., Carvalho, S., Marchante, E., López-Núñez, F. A., and Marchante, H. (2018). Mapping the Flowering of an Invasive Plant Using Unmanned Aerial Vehicles: Is There Potential for Biocontrol Monitoring? *Frontiers in Plant Science*, *9*(293), 293. https://doi.org/10.3389/fpls.2018.00293

Deb, K. (2014). Shadow Detection and Removal Based on YCbCr Color Space. *The Smart Computing Review*, *4*(1). https://doi.org/10.6029/smartcr.2014.01.003

Delavarpour, N., Koparan, C., Nowatzki, J., Bajwa, S., and Sun, X. (2021). A Technical Study on UAV Characteristics for Precision Agriculture Applications and Associated Practical Challenges. *Remote Sensing*, *13*(1204), 1–25. https://doi.org/https://doi.org/10.3390/rs13061204

Dharani, M., and Sreenivasulu, G. (2019). Shadow detection using index-based principal component analysis of satellite images. *Proceedings of the 3rd International Conference on Computing Methodologies and Communication, ICCMC 2019*, *September*, 182–187. https://doi.org/10.1109/ICCMC.2019.8819805

Dhau, I., Adam, E., Mutanga, O., Ayisi, K., Abdel-Rahman, E. M., Odindi, J., and Masocha, M. (2018). Testing the capability of spectral resolution of the new multispectral sensors on detecting the severity of grey leaf spot disease in maize crop. *Geocarto International*, *33*(11), 1223–1236. https://doi.org/10.1080/10106049.2017.1343391

Dvořák, P., Müllerová, J., Bartaloš, T., Brůna, J., and Br\uuna, J. (2015). Unmanned aerial vehicles for alien plant species detection and monitoring. *International Archives of the Photogrammetry, Remote Sensing and Spatial Information Sciences*, *40*(1W4), 83–90. https://doi.org/10.5194/isprsarchives-XL-1-W4-83-2015

Dwivedi, A. K., Roy, S., and Singh, D. (2020). An Adaptive Neuro-Fuzzy Approach for Decomposition of Mixed Pixels to Improve Crop Area Estimation Using Satellite Images. *IGARSS 2020 - 2020 IEEE International Geoscience and Remote Sensing Symposium*, 4191–4194. https://doi.org/10.1109/IGARSS39084.2020.9323128

Ehmke, T. (2013). Unmanned aerial systems for field scouting and spraying. *Crops & Soils*, 46(6), 4–9.

Ennouri, K., Smaoui, S., Gharbi, Y., Cheffi, M., Ben Braiek, O., Ennouri, M., and Triki, M. A. (2021). Usage of Artificial Intelligence and Remote Sensing as Efficient Devices to Increase Agricultural System Yields. *Journal of Food Quality*, *2021*. https://doi.org/10.1155/2021/6242288

Fan, J., Zhou, J., Wang, B., de Leon, N., Kaeppler, S. M., Lima, D. C., and Zhang, Z. (2022). Estimation of Maize Yield and Flowering Time Using Multi-Temporal UAV-Based Hyperspectral Data. *Remote Sensing*, *14*(13), 1–16. https://doi.org/10.3390/rs14133052

Fan, Z., Lu, J., Gong, M., Xie, H., and Goodman, E. D. (2018). Automatic Tobacco Plant Detection in UAV Images via Deep Neural Networks. *IEEE Journal of Selected Topics in Applied Earth*

*Observations and Remote Sensing*, *11*(3), 876–887. https://doi.org/10.1109/JSTARS.2018.2793849

FAO. (2002). *Zimbabwe*.

FAO (Food and Agriculture Organization of the UN). (2017). *Methodology for Estimation of Crop Area and Crop Yield under Mixed and Continuous Cropping*. *March*. https://doi.org/10.1080/00102200601049953

Feng, A., Zhang, M., Sudduth, K. A., Vories, E. D., and Zhou, J. (2019). Cotton yield estimation from UAV-based plant height. *Transactions of the ASABE*, *62*(2), 393–404. https://doi.org/10.13031/trans.13067

Feng, H., Tao, H., Zhao, C., Li, Z., and Yang, G. (2022). Comparison of UAV RGB imagery and hyperspectral remote-sensing data for monitoring winter-wheat growth. *Remote Sensing*, *14*(15), 3811. https://doi.org/https://doi.org/10.3390/rs14153811

Feng, M., Xiao, L., Zhang, M., Yang, W., and Ding, G. (2014). *Integrating Remote Sensing and GIS for Prediction of Winter Wheat ( Triticum aestivum ) Protein Contents in*. *9*(1). https://doi.org/10.1371/journal.pone.0080989

Ferencz, C., Bognár, P., Lichtenberger, J., Hamar, D., Tarcsai, G., Timár, G., Molnár, G., Pásztor, S. Z., Steinbach, P., and Székely, B. (2010). *Crop yield estimation by satellite remote sensing*. *1161*. https://doi.org/10.1080/01431160410001698870

Ferreira, M. P., Grondona, A. E. B., Rolim, S. B. A., and Shimabukuro, Y. E. (2013). Analyzing the spectral variability of tropical tree species using hyperspectral feature selection and leaf optical modeling. *Journal of Applied Remote Sensing*, *7*(1), 073502. https://doi.org/10.1117/1.JRS.7.073502

Floreano, D., and Wood, R. J. (2015). Science, technology and the future of small autonomous drones. *Nature*, *521*(7553), 460–466. https://doi.org/10.1038/nature14542

Flusser, J., Sroubek, F., and Zitov, B. (2007). *Image Fusion : Principles , Methods , and Applications*.

Forkuor, G., Conrad, C., Thiel, M., Ullmann, T., and Zoungrana, E. (2014). Integration of optical and synthetic aperture radar imagery for improving crop mapping in northwestern Benin, West Africa. *Remote Sensing*, *6*(7), 6472–6499. https://doi.org/10.3390/rs6076472

Frankelius, P., Norrman, C., and Johansen, K. (2019). Agricultural Innovation and the Role of Institutions : Lessons from the Game of Drones. *Journal of Agricultural and Environmental Ethics*, *32*(5), 681–707. https://doi.org/10.1007/s10806-017-9703-6

Fu, Y., Yang, G., Li, Z., Song, X., Li, Z., Xu, X., Wang, P., and Zhao, C. (2020). Winter wheat nitrogen status estimation using uav-based rgb imagery and gaussian processes regression. *Remote Sensing*, *12*(22), 1–27. https://doi.org/10.3390/rs12223778

Fuentes-Peailillo, F., Ortega-Farias, S., Rivera, M., Bardeen, M., and Moreno, M. (2019). Comparison of vegetation indices acquired from RGB and Multispectral sensors placed on UAV. *IEEE ICA-ACCA 2018 - IEEE International Conference on Automation/23rd Congress of the Chilean Association of Automatic Control: Towards an Industry 4.0 - Proceedings*, *January 2023*. https://doi.org/10.1109/ICA-ACCA.2018.8609861

Gago, J., Douthe, C., Coopman, R. E., Gallego, P. P., Ribas-Carbo, M., Flexas, J., Escalona, J., and Medrano, H. (2015). UAVs challenge to assess water stress for sustainable agriculture. *Agricultural Water Management*, *153*, 9–19.

Gano, B., Dembele, J. S. B. S. B., Ndour, A., Luquet, D., Beurier, G., Diouf, D., and Audebert, A. (2021a). Using UAV Borne, Multi-Spectral Imaging for the Field Phenotyping of Shoot Biomass, Leaf Area Index and Height of West African Sorghum Varieties under Two Contrasted Water Conditions. *Agronomy*, *11*(850). https://doi.org/10.3390/agronomy11050850 WE - Science Citation Index Expanded (SCI-EXPANDED)

Gano, B., Dembele, J. S. B. S. B., Ndour, A., Luquet, D., Beurier, G., Diouf, D., and Audebert, A. (2021b). Using UAV Borne, Multi-Spectral Imaging for the Field Phenotyping of Shoot Biomass, Leaf Area Index and Height of West African Sorghum Varieties under Two Contrasted Water Conditions. *AGRONOMY-BASEL*, *11*(5). https://doi.org/10.3390/agronomy11050850 WE - Science Citation Index Expanded (SCI-EXPANDED)

Gao, J. F., Liao, W. Z., Nuyttens, D., Lootens, P., Vangeyte, J., Pizurica, A., He, Y., and Pieters, J. G. (2018). Fusion of pixel and object-based features for weed mapping using unmanned aerial vehicle imagery. *International Journal of Applied Earth Observation and Geoinformation*, *67*, 43–53. https://doi.org/10.1016/j.jag.2017.12.012

Ge, W. (2019). Shadow Detection Method Based on HMRF with Soft Edges for High-Resolution Remote-Sensing Images. *Journal of Signal and Information Processing*, *10*, 200–210. https://doi.org/10.4236/jsip.2019.104011

Ge, X., Wang, J., Ding, J., Cao, X., Zhang, Z., Liu, J., and Li, X. (2019). *Combining UAV-based hyperspectral imagery and machine learning algorithms for soil moisture content monitoring*. *May*.

Gebregergis, Z. (2016). Cropping Systems of East Africa: A review. *Developing Country Studies*, *6*(4), 30–33.

Georgiou, T. T., and Lindquist, A. (2003). Kullback-Leibler Approximation of Spectral Density Functions. *IEEE Transactions on Information Theory*, *49*(11), 2910–2917. https://doi.org/10.1109/TIT.2003.819324

Gerstmann, H., Möller, M., and Gläßer, C. (2016). Optimization of spectral indices and long-term separability analysis for classification of cereal crops using multi-spectral RapidEye imagery. *International Journal of Applied Earth Observation and Geoinformation*, *52*, 115–125. https://doi.org/10.1016/j.jag.2016.06.001

Gevers, T., and Smeulders, A. W. M. (1997). Color based object recognition. *Lecture Notes in Computer Science (Including Subseries Lecture Notes in Artificial Intelligence and Lecture Notes in Bioinformatics)*, *1310*(December 1997), 319–326. https://doi.org/10.1007/3-540-63507-6_217

Ghatol, N., and Dhok, G. P. (2008). Texture Based Features Approach for Crop Diseases Classification and Diagnosis-a Research. *International Research Journal of Engineering and Technology*, *May*, 7469.

Ghiyamat, A., Shafri, H. Z. M., Mahdiraji, G. A., Shariff, A. R. M., and Mansor, S. (2013). Hyperspectral discrimination of tree species with different classifications using single- and multiple-endmember. *International Journal of Applied Earth Observation and Geoinformation*, *23*(1), 177–191. https://doi.org/10.1016/j.jag.2013.01.004

Gitelson, A. A., Gritz, Y., and Merzlyak, M. N. (2003). Relationships between leaf chlorophyll content and spectral reflectance and algorithms for non-destructive chlorophyll assessment in higher plant leaves. *Journal of Plant Physiology*, *160*(3), 271–282. https://doi.org/10.1078/0176-1617-00887

Gitelson, A. A., Stark, R., Rundquist, D., Gitelson, A. A., Kaufman, Y. J., Stark, R., and Rundquist, D. (2002). *DigitalCommons @ University of Nebraska - Lincoln Novel Algorithms for Remote Estimation of Vegetation Fraction*.

Goñi, O., Łangowski, Ł., Feeney, E., Quille, P., and O’Connell, S. (2021). Reducing Nitrogen Input in Barley Crops While Maintaining Yields Using an Engineered Biostimulant Derived From Ascophyllum Nodosum to Enhance Nitrogen Use Efficiency. *Frontiers in Plant Science*. https://doi.org/10.3389/fpls.2021.664682

Gonzalez, R. C., and Woods, R. E. (1992). *Digital image processing*. Addison-Wesley.

Gonzalez, R. C., and Woods, R. E. (2019). *Digital image processing* (M. Horton, Ed.; 4th Editio). Pearson Education, Inc.

Gracia-Romero, A., Kefauver, S. C., Vergara-Díaz, O., Hamadziripi, E., Zaman-Allah, M. A., Thierfelder, C., Prassana, B. M., Cairns, J. E., and Araus, J. L. (2020). Leaf versus whole-canopy remote sensing methodologies for crop monitoring under conservation agriculture: a case of study with maize in Zimbabwe. *Scientific Reports*, *10*(1), 1–17. https://doi.org/10.1038/s41598-020-73110-3

Gracia-Romero, A., Kefauver, S. C., Vergara-Díaz, O., Zaman-Allah, M. A., Prasanna, B. M., Cairns, J. E., and Araus, J. L. (2017a). Comparative Performance of Ground vs. Aerially Assessed RGB and Multispectral Indices for Early-Growth Evaluation of Maize Performance under Phosphorus Fertilization. *Frontiers in Plant Science*, *8*, 2004. https://doi.org/10.3389/fpls.2017.02004

Gracia-Romero, A., Kefauver, S. C., Vergara-Díaz, O., Zaman-Allah, M. A., Prasanna, B. M., Cairns, J. E., and Araus, J. L. (2017b). Comparative Performance of Ground vs. Aerially Assessed RGB and Multispectral Indices for Early-Growth Evaluation of Maize Performance under Phosphorus Fertilization. *Frontiers in Plant Science*, *8*, 2004. https://doi.org/10.3389/fpls.2017.02004

Gracia-Romero, A., Vergara-Díaz, O., Thierfelder, C., Cairns, J. E. J. E., Kefauver, S. C. S. C., and Araus, J. L. J. L. (2018a). Phenotyping Conservation Agriculture Management Effects on Ground and Aerial Remote Sensing Assessments of Maize Hybrids Performance in Zimbabwe. *Remote Sensing*, *10*(2), 349. https://doi.org/10.3390/rs10020349

Gracia-Romero, A., Vergara-Díaz, O., Thierfelder, C., Cairns, J. E., Kefauver, S. C., and Araus, J. L. (2018b). Phenotyping conservation agriculture management effects on ground and aerial remote sensing assessments of maize hybrids performance in Zimbabwe. *Remote Sensing*, *10*(2). https://doi.org/10.3390/rs10020349

Guo, R., Dai, Q., and Hoiem, D. (2013). Paired regions for shadow detection and removal. *IEEE Transactions on Pattern Analysis and Machine Intelligence*, *35*(12), 2956–2967. https://doi.org/10.1109/TPAMI.2012.214

Guo, Y., Du, C., Zhao, Y., Ting, T. F., and Rothfus, T. A. (2021). Two-level K-nearest neighbors approach for invasive plants detection and classification. *Applied Soft Computing*, *108*, 107523. https://doi.org/10.1016/j.asoc.2021.107523

Haider, N. (2011). Identification of plant species using traditional and molecular-based methods. *Wild Plants: Identification, Uses and Conservation*, 1–62.

Hall, O., Dahlin, S., Marstorp, H., Archila Bustos, M. F., Öborn, I., and Jirström, M. (2018). Classification of Maize in Complex Smallholder Farming Systems Using UAV Imagery. *Drones*, *2*(3), 22.

Hall, O., Dahlin, S., Marstorp, H., Bustos, M. F. A., Öborn, I., and Jirström, M. (2018). Classification of maize in complex smallholder farming systems using UAV imagery. *Drones*, *2*(3), 1–8. https://doi.org/10.3390/drones2030022

Hall, O., Dahlin, S., Marstorp, H., Bustos, M. F. A., Öborn, I., Jirström, M., Archila Bustos, M. F., Öborn, I., and Jirström, M. (2018). Classification of Maize in Complex Smallholder Farming Systems Using UAV Imagery. *Drones*, *2*(3), 22. https://doi.org/10.3390/drones2030022

Hamuda, E., Mc Ginley, B., Glavin, M., and Jones, E. (2017). Automatic crop detection under field conditions using the HSV colour space and morphological operations. *Computers and Electronics in Agriculture*, *133*, 97–107. https://doi.org/10.1016/j.compag.2016.11.021

Han, H., Han, C., Xue, X., Hu, C., and Huang, L. (2018). A Mixed Property-Based Automatic Shadow Detection Approach for VHR Multispectral Remote Sensing Images. *Applied Sciences*, *8*(1883). https://doi.org/10.3390/app8101883

Handique, B. K., Goswami, C., Gupta, C., Pandit, S., Gogoi, S., Jadi, R., Jena, P., Borah, G., Raju, P. L. N., N., P., C., M., F., L., J., J., A., S., H., Z., X., L., B., O., U., S., E., H., … F.S., F. (2020). Hierarchical classification for assessment of horticultural crops in mixed cropping pattern using uav-borne multi-spectral sensor. *Int. Arch. Photogramm., Remote Sens. Spat. Inf. Sci. - ISPRS Arch.*, *43*, 67–74. https://doi.org/10.5194/isprs-archives-XLIII-B3-2020-67-2020

Handique, B. K., Khan, A. Q., Goswami, C., Prashnani, M., Gupta, C., and Raju, P. L. N. (2017). Crop Discrimination Using Multispectral Sensor Onboard Unmanned Aerial Vehicle. *Proceedings of the National Academy of Sciences India Section A - Physical Sciences*, *87*(4), 713–719. https://doi.org/10.1007/s40010-017-0443-9

Hao, P., Wu, M., Niu, Z., Wang, L., and Zhan, Y. (2018). Estimation of different data compositions for early-season crop type classification. *PeerJ*, *6*, e4834. https://doi.org/10.7717/peerj.4834

Haralick, R. M., Dinstein, I., and Shanmugam, K. (1973). Textural Features for Image Classification. *IEEE Transactions on Systems, Man and Cybernetics*, *SMC-3*(6), 610–621. https://doi.org/10.1109/TSMC.1973.4309314

Hassan, S. I., Alam, M. M., Illahi, U., Al Ghamdi, M. A., Almotiri, S. H., and Su'ud, M. M. (2021). A Systematic Review on Monitoring and Advanced Control Strategies in Smart Agriculture. *IEEE Access*, *9*, 32517–32548. https://doi.org/10.1109/ACCESS.2021.3057865

Hassan, S. I., Alam, M. M., Zia, M. Y. I., Rashid, M., Illahi, U., and Su'ud, M. M. (2022). Rice Crop Counting Using Aerial Imagery and GIS for the Assessment of Soil Health to Increase Crop Yield. *Sensors*, *22*(21), 1–19. https://doi.org/10.3390/s22218567

Hassan-Esfahani, L., Torres-Rua, A., Ticlavilca, A. M., Jensen, A., and McKee, M. (2014). Topsoil moisture estimation for precision agriculture using unmmaned aerial vehicle multispectral imagery. *2014 IEEE Geoscience and Remote Sensing Symposium*, 3263–3266.

Hatfield, J. L., Gitelson, A. A., Schepers, J. S., and Walthall, C. L. (2008). Application of spectral remote sensing for agronomic decisions. *Agronomy Journal*, *100*(3 SUPPL.), 1–29. https://doi.org/10.2134/agronj2006.0370c

Haula, K., and Agbozo, E. (2020). A systematic review on unmanned aerial vehicles in Sub-Saharan Africa: A socio-technical perspective. *Technology in Society*, *63*(July 2019), 101357. https://doi.org/10.1016/j.techsoc.2020.101357

Hebbar, R., Ravishankar, H. M., Trivedi, S., Subramoniam, S. R., Raj, U., and Dadhwal, V. K. (2014). Object oriented classification of high resolution data for inventory of horticultural crops. *International Archives of the Photogrammetry, Remote Sensing and Spatial Information Sciences - ISPRS Archives*, *40*(8), 745–749. https://doi.org/10.5194/isprsarchives-XL-8-745-2014

Hegarty-Craver, M., Polly, J., O'Neil, M., Ujeneza, N., Rineer, J., Beach, R. H., Lapidus, D., and Temple, D. S. (2020). Remote crop mapping at scale: Using satellite imagery and UAV-acquired data as ground truth. *Remote Sensing*, *12*(12), 1–15. https://doi.org/10.3390/rs12121984

Henrique, C., Souza, W. De, Mercante, E., Adriani, J., Augusto, R., Lamparelli, C., and Uribe-opazo, M. A. (2015). Mapping and discrimination of soya bean and corn crops using spectro-temporal profiles of vegetation indices. *International Journal of Remote Sensing*, *36*(7), 1809–1824. https://doi.org/10.1080/01431161.2015.1026956

Holloway, J., and Mengersen, K. (2018). Statistical Machine Learning Methods and Remote Sensing for Sustainable Development Goals : A Review. *Remote Sensing*, *10*(1365). https://doi.org/10.3390/rs10091365

Honrado, J. L. E., Solpico, D. B., Favila, C. M., Tongson, E., Tangonan, G. L., and Libatique, N. J. C. (2017). UAV imaging with low-cost multispectral imaging system for precision agriculture applications. *2017 IEEE Global Humanitarian Technology Conference (GHTC)*, 1–7. https://doi.org/10.1109/GHTC.2017.8239328

Hu, M., Zhai, G., Zhao, Y., and Wang, Z. (2018). Uses of selection strategies in both spectral and sample spaces for classifying hard and soft blueberry using near infrared data. *Scientific Reports*, *8*(1), 1–10. https://doi.org/10.1038/s41598-018-25055-x

Huang, J., Weixin, X., and Liang, T. (2004). Detection of and compensation for shadows in colored urban aerial images. *International Journal of Innovative Computing, Information and Control*, *7*, 5631–5644. https://doi.org/10.1109/WCICA.2004.1343090

Huang, J., Xie, W., and Tang, L. (2004). Detection of and compensation for shadows in colored urban aerial images. *Proceedings of the World Congress on Intelligent Control and Automation (WCICA)*, *4*, 3098–3100.

Huang, L., Miao, B., She, B., Zhang, A., Zhao, J., and Ruan, C. (2025). Rapid mapping of soybean planting areas under complex crop structures: A modified GWCCI approach. *Computers and Electronics in Agriculture*, *235*(October 2024), 110326. https://doi.org/10.1016/j.compag.2025.110326

Huang, X., and Jensen, J. R. (1997). A machine-learning approach to automated knowledge-base building for remote sensing image analysis with GIS data. *Photogrammetric Engineering and Remote Sensing*, *63*(10), 1185–1194.

Hunt, E. R., and Daughtry, C. S. T. (2018a). What good are unmanned aircraft systems for agricultural remote sensing and precision agriculture? *International Journal of Remote Sensing*, *39*(15–16), 5345–5376. https://doi.org/10.1080/01431161.2017.1410300

Hunt, E. R., and Daughtry, C. S. T. (2018b). What good are unmanned aircraft systems for agricultural remote sensing and precision agriculture? *International Journal of Remote Sensing*, *39*(15–16), 5345–5376. https://doi.org/10.1080/01431161.2017.1410300

Hunt Jr, E. R., and Daughtry, C. S. T. (2018). What good are unmanned aircraft systems for agricultural remote sensing and precision agriculture ? *International Journal of Remote Sensing*, *39*(15–16), 5345–5376. https://doi.org/10.1080/01431161.2017.1410300

Hunt Jr, E. R., Doraiswamy, P. C., McMurtrey, J. E., Daughtry, C. S. T., and Perry, E. M. (2013). A visible band index for remote sensing leaf chlorophyll content at the canopy scale. *International Journal of Applied Earth Observation and Geoinformation*, *21*, 103–112.

Illana Rico, S., Martínez Gila, D. M., Cano Marchal, P., and Gómez Ortega, J. (2022). Automatic Detection of Olive Tree Canopies for Groves with Thick Plant Cover on the Ground. *Sensors*, *22*(16), 1–25. https://doi.org/10.3390/s22166219

Imagery, H. R., Mareya, H. T., Tagwireyi, P., Ndaimani, H., Gara, T. W., and Gwenzi, D. (2018). *Estimating Tree Crown Area and Aboveground Biomass in Miombo Woodlands From*. 1–8.

Ishengoma, F. S., Rai, I. A., and Said, R. N. (2021a). Identification of maize leaves infected by fall armyworms using UAV-based imagery and convolutional neural networks. *Computers and Electronics in Agriculture*, *184*(March), 106124. https://doi.org/10.1016/j.compag.2021.106124

Ishengoma, F. S., Rai, I. A., and Said, R. N. (2021b). Identification of maize leaves infected by fall armyworms using UAV-based imagery and convolutional neural networks. *Computers and Electronics in Agriculture*, *184*(March), 106124. https://doi.org/10.1016/j.compag.2021.106124

Islam, M. P., Nakano, Y., Lee, U., Tokuda, K., & Kochi, N. (2021). TheLNet270v1 – A Novel Deep-Network Architecture for the Automatic Classification of Thermal Images for Greenhouse Plants. Frontiers in Plant Science. https://doi.org/10.3389/fpls.2021.630425

JA, F.-G., Lootens, P., Borra-Serrano, I., Derycke, V., Haesaert, G., Roldán-Ruiz, I., JL, A., and SC, K. (2020). Automatic wheat ear counting using machine learning based on RGB UAV imagery. *The Plant Journal : For Cell and Molecular Biology*, *103*(4), 1603–1613. https://doi.org/10.1111/tpj.14799

Jadhav, A. (2023). Brain Tumor Detection by Using Fine-Tuned MobileNetV2 Deep Learning Model. *International Journal on Recent and Innovation Trends in Computing and Communication*. https://doi.org/10.17762/ijritcc.v11i5.6587

Jaén-Carrillo, D., Roche-Seruendo, L. E., Cartón-Llorente, A., Ramírez-Campillo, R., and García-Pinillos, F. (2020). Mechanical power in endurance running: A scoping review on sensors for power output estimation during running. *Sensors (Switzerland)*, *20*(22), 1–20. https://doi.org/10.3390/s20226482

Jagadish., K. (2023). Detection and Classification of Cassava Diseases Using Machine Learning. *International Journal for Research in Applied Science and Engineering Technology*. https://doi.org/10.22214/ijraset.2023.57452

Jensen, J. R. (2005). *Introductory digital image processing: A remote sensing perspective 2*.

Jiang, H., Wang, S., Cao, X., Yang, C., Zhang, Z., and Wang, X. (2019). A shadow- eliminated vegetation index (SEVI) for removal of self and cast shadow effects on vegetation in rugged terrains. *International Journal of Digital Earth*, *12*(9), 1013–1029. https://doi.org/10.1080/17538947.2018.1495770

Jiménez-Brenes, F. M., López-Granados, F., Torres-Sánchez, J., Peña, J. M., Ramírez, P., Castillejo-González, I. L., and de Castro, A. I. (2019). Automatic UAV-based detection of Cynodon dactylon for site-specific vineyard management. *PLoS ONE*, *14*(6). https://doi.org/10.1371/journal.pone.0218132

Jin, B., Ye, P., Zhang, X., Song, W., and Li, S. (2019). Object-Oriented Method Combined with Deep Convolutional Neural Networks for Land-Use-Type Classification of Remote Sensing Images. *Journal of the Indian Society of Remote Sensing*, *47*(6), 951–965. https://doi.org/10.1007/s12524-019-00945-3

Jo, Y., Lee, S., Lee, Y., Kahng, H., Park, S., Bae, S., Kim, M., Han, S., and Kim, S. (2021). Semantic segmentation of cabbage in the south korea highlands with images by unmanned aerial vehicles. *Applied Sciences (Switzerland)*, *11*(10). https://doi.org/10.3390/app11104493

Kailasam, S., Achanta, S. D. M., Rao, P. R. K., Vatambeti, R., and Kayam, S. (2021). An IoT-based Agriculture Maintenance Using Pervasive Computing With Machine Learning Technique. *International Journal of Intelligent Computing and Cybernetics*. https://doi.org/10.1108/ijicc-06-2021-0101

Kailath, T. (1967). The Divergence and Bhattacharyya Distance Measures in Signal Selection. *IEEE Transactions on Communication Technology*, *15*(1), 52–60. https://doi.org/10.1109/TCOM.1967.1089532

Kawamura, K., Asai, H., Yasuda, T., Soisouvanh, P., and Phongchanmixay, S. (2021a). Discriminating crops/weeds in an upland rice field from UAV images with the SLIC-RF algorithm. *Plant Production Science*, *24*(2), 198–215. https://doi.org/10.1080/1343943X.2020.1829490

Kawamura, K., Asai, H., Yasuda, T., Soisouvanh, P., and Phongchanmixay, S. (2021b). Discriminating crops/weeds in an upland rice field from UAV images with the SLIC-RF algorithm. *Plant Production Science*, *24*(2), 198–215. https://doi.org/10.1080/1343943X.2020.1829490

Kenduiywo, B. K., Ghosh, A., Hijmans, R., and Ndungu, L. (2020). Maize yield estimation in kenya using modis. *ISPRS Annals of the Photogrammetry, Remote Sensing and Spatial Information Sciences*, *5*(3), 477–482. https://doi.org/10.5194/isprs-Annals-V-3-2020-477-2020

Khan, S., Tufail, M., Khan, M. T., Khan, Z. A., Iqbal, J., and Alam, M. (2021). A novel semi-supervised framework for UAV based crop/weed classification. *PLoS ONE*, *16*(5 May 2021). https://doi.org/10.1371/journal.pone.0251008

Khanna, R., Möller, M., Pfeifer, J., Liebisch, F., Walter, A., and Siegwart, R. (2015). Beyond point clouds - 3D mapping and field parameter measurements using UAVs. *2015 IEEE 20th Conference on Emerging Technologies Factory Automation (ETFA)*, 1–4.

Kharat, S. A., and Musande, V. B. (2015). Cotton Crop Discrimination Using Landsat-8 Data. *International Journal of Computer Science and Information Technologies*, *06*(5), 4381–4384.

Kilwenge, R., Adewopo, J., Sun, Z., and Schut, M. (2021). Uav-based mapping of banana land area for village-level decision-support in rwanda. *Remote Sensing*, *13*(24). https://doi.org/10.3390/rs13244985

Kitpo, N., & Inoue, M. (2018). Early rice disease detection and position mapping system using drone and IoT architecture. *Proceedings - 12th SEATUC Symposium, SEATUC* 2018, March. https://doi.org/10.1109/SEATUC.2018.8788863

Kondal, E. R. (2023). Multi-Scale Hybrid Spectral Network for Feature Learning and Hyperspectral Image Classification. *International Journal on Recent and Innovation Trends in Computing and Communication*. https://doi.org/10.17762/ijritcc.v11i7s.7026

Kuang-Idba, K., Kisyombe, V., and Dobardzic, S. (2016). Climate Adaptation for Rural Livelihoods and Agriculture in Malawi. In *Time to Adapt: Insights from the Global Environment Facility's Experience in Adaptation to Climate Change* (pp. 102–110). https://doi.org/10.1038/srep05423

Kuemmerle, T., Erb, K., Meyfroidt, P., Müller, D., Verburg, P. H., Estel, S., Haberl, H., Hostert, P., Jepsen, M. R., Kastner, T., Levers, C., Lindner, M., Plutzar, C., Verkerk, P. J., van der Zanden, E. H., and Reenberg, A. (2013). Challenges and opportunities in mapping land use intensity globally. *Current Opinion in Environmental Sustainability*, *5*(5), 484–493. https://doi.org/10.1016/j.cosust.2013.06.002

Kulbacki, M., Segen, J., Knieć, W., Klempous, R., Kluwak, K., Nikodem, J., Kulbacka, J., and Serester, A. (2018). Survey of Drones for Agriculture Automation from Planting to Harvest. *2018 IEEE 22nd International Conference on Intelligent Engineering Systems (INES)*, 353–358.

Kumar, A., Taparia, M., Rajalakshmi, P., Desai, U. B., Naik, B., and Guo, W. (2020). UAV Based Remote Sensing for Tassel Detection and Growth Stage Estimation of Maize Crop using F-RCNN. *IGARSS 2020 - 2020 IEEE International Geoscience and Remote Sensing Symposium*, 15–17.

Kumar, S., Swaroop, R., Sheoran, S., Kumar, C., and Kumar, M. (2022). Remote sensing for agriculture and resource management. In *Natural Resources Conservation and Advances for Sustainability*. Elsevier Inc. https://doi.org/10.1016/B978-0-12-822976-7.00012-0

Kupidura, P. (2019). The comparison of different methods of texture analysis for their efficacy for land use classification in satellite imagery. *Remote Sensing*, *11*(10). https://doi.org/10.3390/rs11101233

Lambert, J. P. T., Hicks, H. L., Childs, D. Z., and Freckleton, R. P. (2018). Evaluating the potential of Unmanned Aerial Systems for mapping weeds at field scales: a case study with Alopecurus myosuroides. *Weed Research*, *58*(1), 35–45. https://doi.org/10.1111/wre.12275

Lausch, A., Bastian, O., Klotz, S., Leitão, P. J., Jung, A., Rocchini, D., Schaepman, M. E., Skidmore, A. K., Tischendorf, L., and Knapp, S. (2018). Understanding and assessing vegetation health by in situ species and remote-sensing approaches. *Methods in Ecology and Evolution*, *9*(8), 1799–1809. https://doi.org/10.1111/2041-210X.13025

Lelong, C. C. D., Burger, P., Jubelin, G., Roux, B., Labbé, S., and Baret, F. (2008). Assessment of unmanned aerial vehicles imagery for quantitative monitoring of wheat crop in small plots. *Sensors*, *8*(5), 3557–3585.

Li, N., Huo, L., and Zhang, X. (2024). Using only the red-edge bands is sufficient to detect tree stress: A case study on the early detection of PWD using hyperspectral drone images. *Computers and Electronics in Agriculture*, *217*(January), 108665. https://doi.org/10.1016/j.compag.2024.108665

Li, S., Yuan, F., Ata-ui-karim, S. T., Zheng, H., and Cheng, T. (2019). Combining Color Indices and Textures of UAV-Based Digital Imagery for Rice LAI Estimation. *Remote Sensing*, *11*(1763). https://doi.org/doi:10.3390/rs11151763

Liaghat, S., and Balasundram, S. K. (2010). A review: The role of remote sensing in precision agriculture. *American Journal of Agricultural and Biological Science*, *5*(1), 50–55. https://doi.org/10.3844/ajabssp.2010.50.55

Lin, B. B. (2013). *Resilience in Agriculture through Crop Diversification : Adaptive Management for Environmental Change*. *March 2011*. https://doi.org/10.1525/bio.2011.61.3.4

Liu, C., Li, H., Su, A., Chen, S., and Li, W. (2021). Identification and Grading of Maize Drought on RGB Images of UAV Based on Improved U-Net. *IEEE Geoscience and Remote Sensing Letters*, *18*(2), 198–202. https://doi.org/10.1109/LGRS.2020.2972313

Liu, K.-H., Yang, M., Huang, S. J., and Lin, C. (2022). Plant Species Classification Based on Hyperspectral Imaging via a Lightweight Convolutional Neural Network Model. *Frontiers in Plant Science*. https://doi.org/10.3389/fpls.2022.855660

Liu, X., Yang, F., Wei, H., and Gao, M. (2022). Shadow Removal from UAV Images Based on Color and Texture Equalization Compensation of Local Homogeneous Regions. *Remote Sensing*, *14*(11), 2616. https://doi.org/10.3390/rs14112616

Liu, Y., Hatou, K., Aihara, T., Kurose, S., Akiyama, T., Kohno, Y., Lu, S., and Omasa, K. (2021). *A Robust Vegetation Index Based on Different UAV RGB Images to Estimate SPAD Values of Naked Barley Leaves*. 1–19.

Llano, E. G., Roig, D. O., and Cabrera, Y. C. (2018). Unsupervised Segmentation of Agriculral Crops in UAV RGB Images. *Revista Cubana de Ciencias Informáticas*, *12*(4), 17–28.

Lobell, D. B. (2013). The use of satellite data for crop yield gap analysis. *Field Crops Research*, *143*, 56–64. https://doi.org/10.1016/j.fcr.2012.08.008

Lorenzi, L., Melgani, F., and Mercier, G. (2012). A complete processing chain for shadow detection and reconstruction in VHR images. *IEEE Transactions on Geoscience and Remote Sensing*, *50*(9), 3440–3452. https://doi.org/10.1109/TGRS.2012.2183876

Lorenzi, L., Melgani, F., Mercier, G., and Bazi, Y. (2013). Assessing the reconstructability of shadow areas in VHR images. *IEEE Transactions on Geoscience and Remote Sensing*, *51*(5), 2863–2873. https://doi.org/10.1109/TGRS.2012.2217503

Lottes, P., Khanna, R., Pfeifer, J., Siegwart, R., and Stachniss, C. (2017a). UAV-based crop and weed classification for smart farming. *2017 IEEE International Conference on Robotics and Automation (ICRA)*, 3024–3031.

Lottes, P., Khanna, R., Pfeifer, J., Siegwart, R., and Stachniss, C. (2017b). UAV-based crop and weed classification for smart farming. *Proceedings - IEEE International Conference on Robotics and Automation*, *May*, 3024–3031. https://doi.org/10.1109/ICRA.2017.7989347

Louargant, M., Jones, G., Faroux, R., Paoli, J.-N., Maillot, T., Gée, C., and Villette, S. (2018). Unsupervised classification algorithm for early weed detection in row-crops by combining spatial and spectral information. *Remote Sensing*, *10*(5), 761.

Löw, F. (2013). *Agricultural crop mapping from multi-scale remote sensing data - Concepts and applications in heterogeneous Middle Asian agricultural landscapes*. *November*.

Löw, F., Prishchepov, A. V., Waldner, F., Dubovyk, O., Akramkhanov, A., Biradar, C., and Lamers, J. P. A. (2018). Mapping Cropland abandonment in the Aral Sea Basin with MODIS time series. *Remote Sensing*, *10*(2). https://doi.org/10.3390/rs10020159

Lu, B., He, Y., and Liu, H. H. T. (2018). Mapping vegetation biophysical and biochemical properties using unmanned aerial vehicles-acquired imagery. *International Journal of Remote Sensing*, *39*(15–16), 5265–5287. https://doi.org/10.1080/01431161.2017.1363441

Lu, D., and Weng, Q. (2007a). A survey of image classification methods and techniques for improving classification performance. *International Journal of Remote Sensing*, *28*(5), 823–870. https://doi.org/10.1080/01431160600746456

Lu, D., and Weng, Q. (2007b). A survey of image classification methods and techniques for improving classification performance. *International Journal of Remote Sensing*, *28*(5), 823–870. https://doi.org/10.1080/01431160600746456

Ma, H., Qin, Q., and Shen, X. (2008). Shadow segmentation and compensation in high resolution satellite images. *International Geoscience and Remote Sensing Symposium (IGARSS)*, *2*(1), 1–3. https://doi.org/10.1109/IGARSS.2008.4779175

Maasdorp, B. V., and Titterton, M. (1997). Nutritional improvement of maize silage for dairying: Mixed crop silages from sole and intercropped legumes and a long season variety of maize. 2. Ensilage. *Animal Feed Science and Technology*, *69*(1–3), 263–270. https://doi.org/10.1016/S0377-8401(97)81640-9

Mafuratidze, P., Chibarabada, T. P., Shekede, M. D., and Masocha, M. (2023). A new four-stage approach based on normalized vegetation indices for detecting and mapping sugarcane hail damage using multispectral remotely sensed data. *Geocarto International*, *38*(1). https://doi.org/10.1080/10106049.2023.2245788

Mafuratidze, P., Mutanga, O., and Masocha, M. (2024). Application of unmanned aerial systems for crop discrimination in smallholder farming systems: a systematic review of trends, technical challenges and opportunities. *Transactions of the Royal Society of South Africa*, *October*, 1–22. https://doi.org/10.1080/0035919X.2024.2409629

Mafuratidze, P., Muumbe, T. P., and Gara, T. W. (2020). Dominant wetland vegetation species discrimination and quantification using in situ hyperspectral data. *Transactions of the Royal Society of South Africa*, *75*(3), 229–238. https://doi.org/htttp://

Mahajan, U., and Raj, B. (2016). Drones for normalized difference vegetation index (NDVI), to estimate crop health for precision agriculture: A cheaper alternative for spatial satellite sensors. *International Conference on Innovative Research in Agriculture, Food Science, Forestry, Horticulture, Aquaculture, Animal Sciences, Biodiversity, Ecological Sciences and Climate Change*, *22*.

Mahlein, A.-K. (2016). Plant disease detection by imaging sensors–parallels and specific demands for precision agriculture and plant phenotyping. *Plant Disease*, *100*(2), 241–251.

Maia, D. S., Pham, M., Aptoula, E., Guiotte, F., Maia, D. S., Pham, M., Aptoula, E., Guiotte, F., Classi-, S. L., Maia, D. S., Pham, M., Aptoula, E., and Guiotte, F. (2021). *Classification of remote sensing data with morphological attributes profiles : a decade of advances To cite this version : HAL Id : hal-03199357 Classification of remote sensing data with morphological attributes profiles : a decade of advances*.

Maimaitijiang, M., Sagan, V., Sidike, P., Hartling, S., Esposito, F., and Fritschi, F. B. (2020). Soybean yield prediction from UAV using multimodal data fusion and deep learning. *Remote Sensing of Environment*, *237*, 111599.

Makanza, R., Zaman-Allah, M., Cairns, J. E., Magorokosho, C., Tarekegne, A., Olsen, M., and Prasanna, B. M. (2018). High-throughput phenotyping of canopy cover and senescence in maize field trials using aerial digital canopy imaging. *Remote Sensing*, *10*(2), 330. https://doi.org/10.3390/rs10020330

Makate, C., Wang, R., Makate, M., and Mango, N. (2016). Crop diversification and livelihoods of smallholder farmers in Zimbabwe : adaptive management for environmental change. *SpringerPlus*. https://doi.org/10.1186/s40064-016-2802-4

Malveaux, C., Hall, S., and Price, R. R. (2014). Using drones in agriculture: Unmanned aerial systems for agricultural remote sensing applications. *American Society of Agricultural and Biological Engineers Annual International Meeting 2014, ASABE 2014*, *6*, 4075–4079. https://doi.org/10.13031/aim.20141911016

Mancini, A., Frontoni, E., and Zingaretti, P. (2019). Satellite and UAV data for Precision Agriculture Applications. *2019 International Conference on Unmanned Aircraft Systems (ICUAS)*, 491–497. https://doi.org/10.1109/ICUAS.2019.8797930

Manjunath, K. R., Ray, S. S., and Panigrahy, S. (2011). Discrimination of Spectrally-Close Crops Using Ground-Based Hyperspectral Data. *Journal of the Indian Society of Remote Sensing*, *39*(4), 599–602. https://doi.org/10.1007/s12524-011-0099-x

Manohar Kumar, C. V. S. S., Jha, S. S., Nidamanuri, R. R., and Dadhwal, V. K. (2024). Precision crop mapping: within plant canopy discrimination of crop and soil using multi-sensor hyperspectral imagery. *Scientific Reports*, *14*(1), 24903. https://doi.org/10.1038/s41598-024-75394-1

Marino, S., and Alvino, A. (2018). Detection of homogeneous wheat areas using multi-temporal UAS images and ground truth data analyzed by cluster analysis. *European Journal of Remote Sensing*, *51*(1), 266–275. https://doi.org/10.1080/22797254.2017.1422280

Matese, A., and Di Gennaro, S. F. (2018). Practical applications of a multisensor UAV platform based on multispectral, thermal and RGB high resolution images in precision viticulture. *Agriculture (Switzerland)*, *8*(7). https://doi.org/10.3390/agriculture8070116

Matese, A., Toscano, P., Di Gennaro, S. F., Genesio, L., Vaccari, F. P., Primicerio, J., Belli, C., Zaldei, A., Bianconi, R., and Gioli, B. (2015). Intercomparison of UAV, aircraft and satellite remote sensing platforms for precision viticulture. *Remote Sensing*, *7*(3), 2971–2990. https://doi.org/10.3390/rs70302971

Maurice, D. C., Adamu, Y., and Joseph, M. (2015). Analysis of Cost Efficiency in Food Crop Production Among Small-Scale Farmers in Adamawa State, Nigeria. *Global Journal of Agricultural Sciences*, *14*, 17–25. https://doi.org/10.4314/gjas.v14i1.3

McCabe, M. F., Houborg, R., and Lucieer, A. (2016). High-resolution sensing for precision agriculture: from Earth-observing satellites to unmanned aerial vehicles. *SPIE Remote Sensing*, *9998 99981*. https://doi.org/doi: 10.1117/12.2241289

McCarthy, C., Nyoni, Y., Kachamba, D. J., Banda, L. B., Moyo, B., Chisambi, C., Banfill, J., and Hoshino, B. (2023). Can Drones Help Smallholder Farmers Improve Agriculture Efficiencies and Reduce Food Insecurity in Sub-Saharan Africa? Local Perceptions from Malawi. *Agriculture (Switzerland)*, *13*(5), 1–16. https://doi.org/10.3390/agriculture13051075

M-Desa, S., Zali, S. A., Mohd-Isa, W. N., and Che-Embi, Z. (2022). Color-based shadow detection method in aerial images. *Journal of Physics: Conference Series*, *2312*(1). https://doi.org/10.1088/1742-6596/2312/1/012081

Meer, F. D. Van Der, Werff, H. M. A. Van Der, and Ruitenbeek, F. J. A. Van. (2014). Remote Sensing of Environment Potential of ESA ' s Sentinel-2 for geological applications. *Remote Sensing of Environment*, *148*, 124–133. https://doi.org/10.1016/j.rse.2014.03.022

Meivel, S., Dinakaran, K., Gandhiraj, N., and Srinivasan, M. (2016). Remote sensing for UREA Spraying Agricultural (UAV) system. *2016 3rd International Conference on Advanced Computing and Communication Systems (ICACCS)*, *1*(August), 1–6. https://doi.org/10.1109/ICACCS.2016.7586367

Melesse, A. M., Weng, Q., Thenkabail, P. S., and Senay, G. B. (2019). Remote Sensing Sensors and Applications in Environmental Resources Mapping and Modelling. *Sensors*, *7*(12), 1–32. https://doi.org/10.3390/s7123209

Mesas-Carrascosa, F.-J. J., Torres-Sánchez, J., Clavero-Rumbao, I., García-Ferrer, A., Peña, J.-M. M., Borra-Serrano, I., and López-Granados, F. (2015). Assessing optimal flight parameters for generating accurate multispectral orthomosaicks by UAV to support site-specific crop management. *Remote Sensing*, *7*(10), 12793–12814. https://doi.org/10.3390/rs71012793

Meyer, G. E., and Neto, J. C. (2008). Verification of color vegetation indices for automated ˜ Camargo Neto b. *Computers and Electronics in Agriculture*, *63*, 282–293. https://doi.org/10.1016/j.compag.2008.03.009

Miceli, P. A., Blair, W. D., and Brown, M. M. (2018). Isolating Random and Bias Covariances in Tracks. In *2018 21st International Conference on Information Fusion, FUSION 2018*. https://doi.org/10.23919/ICIF.2018.8455530

Michez, A., Bauwens, S., Brostaux, Y., Hiel, M., Garr, S., Lejeune, P., and Dumont, B. (2018). How Far Can Consumer-Grade UAV RGB Imagery Describe Crop Production ? A 3D and Multitemporal Modeling Approach Applied to Zea mays. *Remote Sensing*, *10*(1798). https://doi.org/10.3390/rs10111798

Mokoena, Q., Daniyan, I. A., Mpofu, K., and Abisuga, O. A. (2023). Investigating the Technological Growth of the Drone Industry in South Africa. *South African Journal of Industrial Engineering*, *34*(2), 106–123. https://doi.org/10.7166/34-2-2817

Morell-Monzó, S., Estornell, J., and Sebastiá-Frasquet, M. T. (2023). Assessing the capabilities of high-resolution spectral, altimetric, and textural descriptors for mapping the status of citrus parcels. *Computers and Electronics in Agriculture*, *204*(746). https://doi.org/10.1016/j.compag.2022.107504

Mostafa, Y., and Abdelhafiz, A. (2017a). Accurate Shadow Detection from High-Resolution Satellite Images. *IEEE Geoscience and Remote Sensing Letters*, *14*(4), 494–498. https://doi.org/10.1109/LGRS.2017.2650996

Mostafa, Y., and Abdelhafiz, A. (2017b). Shadow identification in high resolution satellite images in the presence of water regions. *Photogrammetric Engineering and Remote Sensing*, *83*(2), 87–94. https://doi.org/10.14358/PERS.83.2.87

Moyo, S. (2011). Changing agrarian relations after redistributive land reform in Zimbabwe. *Journal of Peasant Studies*, *38*(5), 939–966. https://doi.org/10.1080/03066150.2011.634971

Muharam, F. M., Nurulhuda, K., Zulkafli, Z., Tarmizi, M. A., Abdullah, A. N. H., Hashim, M. F. C., Zad, S. N. M., Radhwane, D., and Ismail, M. R. (2021). UAV- and Random-Forest-AdaBoost (RFA)-Based Estimation of Rice Plant Traits. *AGRONOMY-BASEL*, *11*(5). https://doi.org/10.3390/agronomy11050915 WE - Science Citation Index Expanded (SCI-EXPANDED)

Murrieta-Rico, F. N., Hernandez-Balbuena, D., Rodriguez-Quiñonez, J. C., Petranovskii, V., Raymond-Herrera, O., Gurko, A. G., Mercorelli, P., Sergiyenko, O., Lindner, L., Valdez-Salas, B., and Tyrsa, V. (2016). Resolution improvement of accelerometers measurement for drones in agricultural applications. *IECON 2016 - 42nd Annual Conference of the IEEE Industrial Electronics Society*, 1037–1042. https://doi.org/10.1109/IECON.2016.7793466

Murugan, D., Garg, A., and Singh, D. (2017). Development of an Adaptive Approach for Precision Agriculture Monitoring with Drone and Satellite Data. *IEEE Journal of Selected Topics in Applied Earth Observations and Remote Sensing*, *10*(12), 5322–5328. https://doi.org/10.1109/JSTARS.2017.2746185

Mutanga, O., Dube, T., and Galal, O. (2017). Remote sensing of crop health for food security in Africa: Potentials and constraints. *Remote Sensing Applications: Society and Environment*, *8*(July), 231–239. https://doi.org/10.1016/j.rsase.2017.10.004

Mwanyumba, P. M., Wahome, R. G., Mwang'ombe, A., Lenihan, E., and Badamana, M. S. (2010). An analysis of factors affecting smallholder mixed farming activities, performance and interactions in wundanyi location, taita district, Kenya. In *Livestock Research for Rural Development* (Vol. 22, Issue 3, p. 50).

Mwinuka, P. R., Mbilinyi, B. P., Mbungu, W. B., Mourice, S. K., Mahoo, H. F., and Schmitter, P. (2021). The feasibility of hand-held thermal and UAV-based multispectral imaging for canopy water status assessment and yield prediction of irrigated African eggplant (Solanum aethopicum L). *Agricultural Water Management*, *245*(xxxx). https://doi.org/10.1016/j.agwat.2020.106584

Mwinuka, P. R., Mourice, S. K., Mbungu, W. B., Mbilinyi, B. P., Tumbo, S. D., and Schmitter, P. (2022). UAV-based multispectral vegetation indices for assessing the interactive effects of water and nitrogen in irrigated horticultural crops production under tropical sub-humid conditions: A case of African eggplant. *Agricultural Water Management*, *266*(January), 107516. https://doi.org/10.1016/j.agwat.2022.107516

Na, S., Park, C., So, K., Park, J., and Lee, K. (2017). Mapping the spatial distribution of barley growth based on unmanned aerial vehicle. *2017 6th International Conference on Agro-Geoinformatics, Agro-Geoinformatics 2017*. https://doi.org/10.1109/Agro-Geoinformatics.2017.8047029

Nardari, G. V, Romero, R. A. F., Guizilini, V. C., Mareco, W. E. C., Milori, D. M. B. P., Villas-Boas, P. R., and Dias Santos, I. A. (2018). Crop Anomaly Identification with Color Filters and Convolutional Neural Networks. *2018 Latin American Robotic Symposium, 2018 Brazilian Symposium on Robotics (SBR) and 2018 Workshop on Robotics in Education (WRE)*, 363–369.

Nardari, G. V., Romero, R. A. F., Mareco, W. E. C., Milori, D. M. B. P., Villas-Boas, P. R., Guizilini, V. C., and Santos, I. A. D. (2018). Crop anomaly identification with color filters and convolutional neural networks. *Proceedings - 15th Latin American Robotics Symposium, 6th Brazilian Robotics Symposium and 9th Workshop on Robotics in Education, LARS/SBR/WRE 2018*, *November*, 333–338. https://doi.org/10.1109/LARS/SBR/WRE.2018.00072

Ndakidemi, P. A. (2006). Manipulating legume/cereal mixtures to optimize the above and below ground interactions in the traditional African cropping systems. *African Journal of Biotechnology*, *5*(25), 2526–2533. https://doi.org/10.1016/j.ijcard.2011.01.032

Ndlovu, H. S., Odindi, J., Sibanda, M., Mutanga, O., Clulow, A., Chimonyo, V. G. P., and Mabhaudhi, T. (2021a). A Comparative Estimation of Maize Leaf Water Content Using Machine Learning Techniques and Unmanned Aerial Vehicle (UAV)-Based Proximal and Remotely Sensed Data. *REMOTE SENSING*, *13*(20). https://doi.org/10.3390/rs13204091 WE - Science Citation Index Expanded (SCI-EXPANDED)

Ndlovu, H. S., Odindi, J., Sibanda, M., Mutanga, O., Clulow, A., Chimonyo, V. G. P., and Mabhaudhi, T. (2021b). A comparative estimation of maize leaf water content using machine learning techniques and unmanned aerial vehicle (Uav)-based proximal and remotely sensed data. *Remote Sensing*, *13*(20). https://doi.org/10.3390/rs13204091

Neetu, & Ray, S. S. (2019). Exploring machine learning classification algorithms for crop classification using sentinel 2 data. International Archives of the Photogrammetry, Remote Sensing and Spatial Information Sciences - ISPRS Archives, 42(3/W6), 573–578. https://doi.org/10.5194/isprs-archives-XLII-3-W6-573-2019

Nhamo, L., van Dijk, R., Magidi, J., Wiberg, D., and Tshikolomo, K. (2018). Improving the accuracy of remotely sensed irrigated areas using post-classification enhancement through UAV capability. *Remote Sensing*, *10*(5), 1–12. https://doi.org/10.3390/rs10050712

Nijland, W., Bolton, D. K., Coops, N. C., and Stenhouse, G. (2016). Remote Sensing of Environment Imaging phenology ; scaling from camera plots to landscapes. *Remote Sensing of Environment*, *177*, 13–20. https://doi.org/10.1016/j.rse.2016.02.018

Noble, S. D., and Brown, R. B. (2009). Plant species discrimination using spectral / spatial descriptive statistics. *1st International Workshop on Computer Image Analysis in Agriculture Held in Potsdam*, 82–92.

Nogueira, K., Chanussot, J., Mura, M. D., and Santos, J. A. D. (2021). An Introduction to Deep Morphological Networks. *IEEE Access*, *9*, 114308–114324. https://doi.org/10.1109/ACCESS.2021.3104405

Nyman, M. (2008). *Image Analysis and Morphological Operations as Tools for Weed and Crop Detection*.

Ong, P., Teo, K. S., and Sia, C. K. (2023). UAV-based weed detection in Chinese cabbage using deep learning. *Smart Agricultural Technology*, *4*(December 2022), 100181. https://doi.org/10.1016/j.atech.2023.100181

Onyango, C. M., Nyaga, J. M., Wetterlind, J., Söderström, M., and Piikki, K. (2021). Precision Agriculture for Resource Use Efficiency in Smallholder Farming Systems in Sub-Saharan Africa: A Systematic Review. *Sustainability*, *13*(3), 1158.

Otsu, N. (1979). A Tlreshold Selection Method from Gray-Level Histograms. *IEEE Transactions on Systems, Man, and Cybernetics*, *SMC-9*(1), 62–69.

Oukil, S., Kasmi, R., Mokrani, K., and Garcia-Zapirain, B. (2021). Automatic Segmentation and Melanoma Detection Based on Color and Texture Features in Dermoscopic Images. *Skin Research and Technology*. https://doi.org/10.1111/srt.13111

Ouko, K. O., Yugi, C. L., Oketch, M. O., Mboya, J. B., Ogola, R. J., Muthoka, M., and Midamba, D. C. (2024). A review of the landscape of agroecology policies towards transforming food systems in Sub-Saharan Africa. *Cogent Social Sciences*, *10*(1), 2363491. https://doi.org/10.1080/23311886.2024.2363491

Ouzzani, M., Hammady, H., Fedorowicz, Z., and Elmagarmid, A. (2016). Rayyan-a web and mobile app for systematic reviews. *Systematic Reviews*, *5*(1), 1–10. https://doi.org/10.1186/s13643-016-0384-4

Ozdarici-Ok, A., Ok, A. O., and Schindler, K. (2015). Mapping of agricultural crops from single high-resolution multispectral images-data-driven smoothing vs. parcel-based smoothing. *Remote Sensing*, *7*(5), 5611–5638. https://doi.org/10.3390/rs70505611

Page, M. J., McKenzie, J. E., Bossuyt, P. M., Boutron, I., Hoffmann, T. C., Mulrow, C. D., Shamseer, L., Tetzlaff, J. M., Akl, E. A., Brennan, S. E., Chou, R., Glanville, J., Grimshaw, J. M., Hróbjartsson, A., Lalu, M. M., Li, T., Loder, E. W., Mayo-Wilson, E., McDonald, S., … Moher, D. (2021). The PRISMA 2020 statement: An updated guideline for reporting systematic reviews. *RESEARCH METHODS AND REPORTING*, 372. https://doi.org/10.1136/bmj.n71

Pan, Y., Zhu, N., Ding, L., Li, X., Goh, H. H., Han, C., and Zhang, M. (2022). Identification and Counting of Sugarcane Seedlings in the Field Using Improved Faster R-CNN. *Remote Sensing*, *14*(22), 0–18. https://doi.org/10.3390/rs14225846

Pandey, V., Anand, K., Kalra, A., Gupta, A., Roy, P. P., and Kim, B. G. (2022). Enhancing object detection in aerial images. *Mathematical Biosciences and Engineering*, *19*(8), 7920–7932. https://doi.org/10.3934/mbe.2022370

Prajapati, H. P., Antani, Y. B., & Singh, M. (2017). Imaging of crop canopies for the remote diagnosis and quantification of field responses. *2017 International Conference on Inventive Systems and Control (ICISC)*, 1–5.

Peña Barragán, J. M., Kelly, M., Castro, A. I. de, and López Granados, F. (2012). Object-based approach for crop row characterization in UAV images for site-specific weed management. *Procedings of the 4th GEOBIA*, 426–430.

Peña, J. M., Torres-Sánchez, J., de Castro, A. I., Kelly, M., and López-Granados, F. (2013a). Weed Mapping in Early-Season Maize Fields Using Object-Based Analysis of Unmanned Aerial Vehicle (UAV) Images. *PLoS ONE*, *8*(10). https://doi.org/10.1371/journal.pone.0077151

Peña, J. M., Torres-Sánchez, J., de Castro, A. I., Kelly, M., and López-Granados, F. (2013b). Weed Mapping in Early-Season Maize Fields Using Object-Based Analysis of Unmanned Aerial Vehicle (UAV) Images. *PLoS ONE*, *8*(10). https://doi.org/10.1371/journal.pone.0077151

Peña-Barragán, J. M., López-Granados, F., García-Torres, L., Jurado-Expósito, M., Sánchez de la Orden, M., and García-Ferrer, A. (2008). Discriminating cropping systems and agro-environmental measures by remote sensing. *Agronomy for Sustainable Development*, *28*(2), 355–362. https://doi.org/10.1051/agro:2007049

Perera, P., and Patel, V. M. (2018). Learning Deep Features for One-Class Classification. *IEEE Transactions on Geoscience and Remote Sensing*, 1–12.

Pérez-Ortiz, M., Peña, J. M., Gutiérrez, P. A., Torres-Sánchez, J., Hervás-Martínez, C., and López-Granados, F. (2016). Selecting patterns and features for between- and within- crop-row weed mapping using UAV-imagery. *Expert Systems with Applications*, *47*(November), 85–94. https://doi.org/10.1016/j.eswa.2015.10.043

Persello, C., Tolpekin, V. A., Bergado, J. R., and de By, R. A. (2019). Delineation of agricultural fields in smallholder farms from satellite images using fully convolutional networks and combinatorial grouping. *Remote Sensing of Environment*, *231*(June). https://doi.org/10.1016/j.rse.2019.111253

Peter, B. G., Messina, J. P., Carroll, J. W., Zhi, J. J., Chimonyo, V., Lin, S. P., and Snapp, S. S. (2020). Multi-Spatial Resolution Satellite and sUAS Imagery for Precision Agriculture on Smallholder Farms in Malawi. *PHOTOGRAMMETRIC ENGINEERING AND REMOTE SENSING*, *86*(2), 107–119. https://doi.org/10.14358/PERS.86.2.107 WE - Science Citation Index Expanded (SCI-EXPANDED)

Piermattei, L., Marty, M., Karel, W., Ressl, C., Hollaus, M., Ginzler, C., and Pfeifer, N. (2018). Impact of the Acquisition Geometry of Very High-Resolution Pléiades Imagery on the Accuracy of Canopy Height Models over Forested Alpine Regions. *Remote Sensing*, *10*(10), 1542. https://doi.org/10.3390/rs10101542

Pieterse, Y. L. (2016). *Use of multispectral and hyperspectral remotely sensed data for vegetation species discrimination*. *4*(10), 344–353.

Piiroinen, R. (2014). *Classification of agricultural crops of the Taita Hills, Kenya using airborne AisaEAGLE imaging spectroscopy data*. *64*.

Polidório, A. M., Flores, F. C., Imai, Nn. N., Tommaselli, A. M. G., and Franco, C. (2003). Automatic shadow segmentation in aerial color images. In C. R. M. de Oliveira M.C.F. (Ed.), *Brazilian Symposium of Computer Graphic and Image Processing* (pp. 270–277). IEEE Computer Society. https://doi.org/10.1109/SIBGRA.2003.1241019

Pons, X., and Padró, J. C. (2019). An empirical approach on shadow reduction of uav imagery in forests. *International Geoscience and Remote Sensing Symposium (IGARSS)*, *2019-July*(July), 2463–2466. https://doi.org/10.1109/IGARSS.2019.8899872

Potgieter, A. B., George-Jaeggli, B., Chapman, S. C., Laws, K., Cadavid, L. A. S., Wixted, J., Watson, J., Eldridge, M., Jordan, D. R., and Hammer, G. L. (2017). Multi-Spectral Imaging from an Unmanned Aerial Vehicle Enables the Assessment of Seasonal Leaf Area Dynamics of Sorghum Breeding Lines. *FRONTIERS IN PLANT SCIENCE*, *8*. https://doi.org/10.3389/fpls.2017.01532 WE - Science Citation Index Expanded (SCI-EXPANDED)

Prabhakar, D., and Garg, P. K. (2022). Automatic Shadow Detection for High-Resolution Remote Sensing Data. *International Archives of the Photogrammetry, Remote Sensing and Spatial Information Sciences - ISPRS Archives*, *48*(4/W5-2022), 143–150. https://doi.org/10.5194/isprs-archives-XLVIII-4-W5-2022-143-2022

Prins, A. J. (2019). *Efficacy of machine learning and Lidar data for crop type mapping*. Stellenbosch University.

Prins, A. J., and Van Niekerk, A. (2020). Crop type mapping using LiDAR, Sentinel-2 and aerial imagery with machine learning algorithms. *Geo-Spatial Information Science*, *24*(2), 215–227. https://doi.org/10.1080/10095020.2020.1782776

Psirofonia, P., Samaritakis, V., Eliopoulos, P., and Potamitis, I. (2017). Use of Unmanned Aerial Vehicles for Agricultural Applications with Emphasis on Crop Protection: Three Novel Case-studies. *International Journal of Agricultural Science and Technology*, *5*(1), 30–39. https://doi.org/10.1109/ISPACS.2016.7824758

Pugh, N. A., Horne, D. W., Murray, S. C., Carvalho, G., Malambo, L., Jung, J., Chang, A., Maeda, M., Popescu, S., Chu, T., Starek, M. J., Brewer, M. J., Richardson, G., and Rooney, W. L. (2018). Temporal Estimates of Crop Growth in Sorghum and Maize Breeding Enabled by

Unmanned Aerial Systems. *The Plant Phenome Journal*, *1*(1), 1–10. https://doi.org/10.2135/tppj2017.08.0006

Pulido, C., Solaque, L., and Velasco, N. (2017). Weed recognition by SVM texture feature classification in outdoor vegetable crop images. *Ingenieria e Investigacion*, *37*(1), 68–74. https://doi.org/10.15446/ing.investig.v37n1.54703

Qassim, H. M., Basheer, N. M., and Farhan, M. N. (2019). Brightness preserving enhancement for dental digital x-ray images based on entropy and histogram analysis. *Journal of Applied Science and Engineering*, *22*(1), 187–194. https://doi.org/10.6180/jase.201903_22(1).0019

Qin, J., Monje, O., Nugent, M. R., Finn, J. R., O'Rourke, A., Wilson, K., Fritsche, R., Baek, I., Chan, D. E., and Kim, M. S. (2023). A Hyperspectral Plant Health Monitoring System for Space Crop Production. *Frontiers in Plant Science*. https://doi.org/10.3389/fpls.2023.1133505

Radoglou-grammatikis, P., Sarigiannidis, P., and Lagkas, T. (2020). A compilation of UAV applications for precision agriculture. *Computer Networks*, *172*(January), 107148. https://doi.org/10.1016/j.comnet.2020.107148

Raeva, P. L., Šedina, J., and Dlesk, A. (2019). Monitoring of crop fields using multispectral and thermal imagery from UAV. *European Journal of Remote Sensing*, *52*(sup1), 192–201. https://doi.org/10.1080/22797254.2018.1527661

Rahman, H. (2014). *Satellite Based Crop Monitoring and Estimation System for Food Security Application in Bangladesh*. 1–16. https://doi.org/10.1002/jsfa.6759

Raja Sekar, L., Ambika, N., Divya, V., and Kowsalya, T. (2018). Fruit Classification System Using Computer Vision : A Review. *International Journal of Trend in Research and Development*, *5*(1), 22–26.

Rajapaksa, S., Eramian, M., Duddu, H., Wang, M., Shirtliffe, S., Ryu, S., Josuttes, A., Zhang, T., Vail, S., Pozniak, C., and Parkin, I. (2018). Classification of Crop Lodging with Gray Level Co-occurrence Matrix. *2018 IEEE Winter Conference on Applications of Computer Vision (WACV)*, 251–258.

Ramírez, D. A., Grüneberg, W., I. Andrade, M., De Boeck, B., Loayza, H., S. Makunde, G., Ninanya, J., Rinza, J., Heck, S., and Campos, H. (2021a). Phenotyping of productivity and resilience in sweetpotato under water stress through UAV-based multispectral and thermal imagery in Mozambique. *Journal of Agronomy and Crop Science*. https://doi.org/10.1111/jac.12565

Ramírez, D. A., Grüneberg, W., I. Andrade, M., De Boeck, B., Loayza, H., S. Makunde, G., Ninanya, J., Rinza, J., Heck, S., and Campos, H. (2021b). Phenotyping of productivity and resilience in sweetpotato under water stress through UAV-based multispectral and thermal imagery in Mozambique. *Journal of Agronomy and Crop Science*. https://doi.org/10.1111/JAC.12565

Reinecke, M., Prinsloo, T., and IEEE. (2017). The influence of drone monitoring on crop health and harvest size. *2017 1ST INTERNATIONAL CONFERENCE ON NEXT GENERATION COMPUTING APPLICATIONS (NEXTCOMP), 1st International Conference on Next Generation Computing Applications (NextComp)*, 5–10.

Rezaei, S., and Liu, X. (2019). Deep Learning for Encrypted Traffic Classification: An Overview. *IEEE Geoscience and Remote Sensing Magazine*, 1–9.

Richard, K., Abdel-Rahman, E. M., Subramanian, S., Nyasani, J. O., Thiel, M., Jozani, H., Borgemeister, C., and Landmann, T. (2017). Maize cropping systems mapping using rapideye observations in agro-ecological landscapes in Kenya. *Sensors (Switzerland)*, *17*(11), 1–16. https://doi.org/10.3390/s17112537

Richter, R., and Müller, A. (2005). De-shadowing of satellite/airborne imagery. *International Journal of Remote Sensing*, *26*(15), 3137–3148. https://doi.org/10.1080/01431160500114664

Ristorto, G., Mazzetto, F., Guglieri, G., and Quagliotti, F. (2015). Monitoring performances and cost estimation of multirotor Unmanned Aerial Systems in precision farming. *2015 International Conference on Unmanned Aircraft Systems (ICUAS)*, 502–509.

Ronchetti, G., Mayer, A., Facchi, A., Ortuani, B., and Sona, G. (2020). Crop row detection through UAV surveys to optimize on-farm irrigation management. *Remote Sensing*, *12*(12). https://doi.org/10.3390/rs12121967

Rudel, T. K., Kwon, O.-J., Paul, B. B., Boval, M., Rao, I. M., Burbano, D., McGroddy, M., Lerner, A. M., White, D., Cuchillo, M., Luna, M., and Peters, M. (2016). Do smallholder, mixed crop-livestock livelihoods encourage sustainable agricultural practices? a Meta-analysis. *MDPI*, *5*(1), 6. https://doi.org/10.3390/land5010006

Ruiz-Altisent, M., Ruiz-Garcia, L., Moreda, G. P., Lu, R., Hernandez-Sanchez, N., Correa, E. C., Diezma, B., Nicolaï, B., and García-Ramos, J. (2010). Sensors for product characterization and quality of specialty crops-A review. *Computers and Electronics in Agriculture*, *74*(2), 176–194. https://doi.org/10.1016/j.compag.2010.07.002

Sa, I., Popović, M., Khanna, R., Chen, Z., Lottes, P., Liebisch, F., Nieto, J., Stachniss, C., Walter, A., and Siegwart, R. (2018). WeedMap: A large-scale semantic weed mapping framework using aerial multispectral imaging and deep neural network for precision farming. *Remote Sensing*, *10*(9), 1423.

Sajith Variyar, V. V., Gopalakrishnan, E. A., Sowmya, V., and Soman, K. P. (2019). A complex network approach for plant growth analysis using images. *Proceedings of the 2019 IEEE International Conference on Communication and Signal Processing, ICCSP 2019*, 249–253. https://doi.org/10.1109/ICCSP.2019.8698021

Salas, E. A. L., and Henebry, G. M. (2012). Separability of maize and soybean in the spectral regions of chlorophyll and carotenoids using the Moment Distance Index. *Israel Journal of Plant Sciences*, *60*(1–2), 65–76. https://doi.org/10.1560/IJPS.60.1-2.65

Salvador-Oliván, J. A., Marco-Cuenca, G., and Arquero-Avilés, R. (2019). Errors in search strategies used in systematic reviews and their effects on information retrieval. *Journal of the Medical Library Association*, *107*(2), 210–221. https://doi.org/10.5195/jmla.2019.567

Sandino, J., Gonzalez, F., Mengersen, K., and Gaston, K. J. (2018). UAVs and Machine Learning Revolutionising Invasive Grass and Vegetation Surveys in Remote Arid Lands. *Sensors*, *18*(605). https://doi.org/10.3390/s18020605

Sandino, J., Pegg, G., Gonzalez, F., and Smith, G. (2018). Aerial mapping of forests affected by pathogens using UAVs, hyperspectral sensors, and artificial intelligence. *Sensors (Switzerland)*, *18*(4), 1–17. https://doi.org/10.3390/s18040944

Sarabandi, P., Yamazaki, F., Matsuoka, M., and Kiremidjian, A. (2004). Shadow detection and radiometric restoration in satellite high resolution images. *International Geoscience and Remote Sensing Symposium (IGARSS)*, *6*(1), 3744–3747. https://doi.org/10.1109/igarss.2004.1369936

Schirrmann, M., Giebel, A., Gleiniger, F., Pflanz, M., Lentschke, J., and Dammer, K.-H. (2016). Monitoring agronomic parameters of winter wheat crops with low-cost UAV imagery. *Remote Sensing*, *8*(9), 706.

Schmidt, K. S., and Skidmore, A. (2003). Hyperspectral remote sensing of vegetation species distribution in a saltmarsh. In *Natural Resources*. https://doi.org/ISBN 90-5808-830-8

Schut, Antonius. G. T. G. T., Traore, P. C. S., Blaes, X., and de By, R. A. (2018). Assessing yield and fertilizer response in heterogeneous smallholder fields with UAVs and satellites. *Field Crops Research*, *221*(February), 98–107. https://doi.org/10.1016/j.fcr.2018.02.018

Scoones, I., Marongwe, N., Mavedzenge, B., Murimbarimba, F., Mahenehene, J., and Sukume, C. (2011). Zimbabwe's land reform: Challenging the myths. *Journal of Peasant Studies*, *38*(5), 967–993. https://doi.org/10.1080/03066150.2011.622042

Senay, G. B., Lyon, J. G., Ward, A. D., and Nokes, S. E. (2000). Using high spatial resolution multispectral data to classify corn and soybean crops. *Photogrammetric Engineering and Remote Sensing*, *66*(3), 319–327. https://doi.org/0099-1112/00/6603-319$3.00/0

Sencaki, D. B., Grace, F. L. T., Gandharum, L., and Cahyaningtyas, I. F. (2019). Discrimination analysis of corn species using field hyperspectral data. *AGERS 2019 - 2nd IEEE Asia-Pacific Conference on Geoscience, Electronics and Remote Sensing Technology: Understanding and Forecasting the Dynamics of Land, Ocean and Maritime, Proceeding*, 37–42. https://doi.org/10.1109/AGERS48446.2019.9034340

Serra, J. (1986). Introduction to Mathematical Morphology. *Computer Vision, Graphics, and Image Processing*, *35*, 283–305. https://doi.org/10.1002/9781118600788.ch1

Shafian, S., Rajan, N., Schnell, R., Bagavathiannan, M., Valasek, J., Shi, Y., and Olsenholler, J. (2018). Unmanned aerial systems-based remote sensing for monitoring sorghum growth and development. *PloS One*, *13*(5), e0196605.

Shahbaz, P., Boz, I., and Haq, S. (2017). Determinants of Crop Diversification in Mixed Cropping Zone of Punjab Pakistan. *Direct Research Journal of Agriculture and Food Science*, *5*(11), 360–366. https://doi.org/10.1109/35.815456

Shao, G., Han, W., Zhang, H., Liu, S., Wang, Y., Zhang, L., and Cui, X. (2021). Mapping maize crop coefficient Kc using random forest algorithm based on leaf area index and UAV-based multispectral vegetation indices. *Agricultural Water Management*, *252*. https://doi.org/10.1016/j.agwat.2021.106906

Shi, Y., Thomasson, J. A., Murray, S. C., Pugh, N. A., Rooney, W. L., Shafian, S., Rajan, N., Rouze, G., Morgan, C. L. S., Neely, H. L., Rana, A., Bagavathiannan, M. V, Henrickson, J., Bowden, E., Valasek, J., Olsenholler, J., Bishop, M. P., Sheridan, R., Putman, E. B., … Yang, C. (2016). Unmanned Aerial Vehicles for High-Throughput Phenotyping and Agronomic Research. *PloS One*, *11*(7), e0159781.

Shoaib, M. (2023). Assessing the Potential of Sentinel-2 Imagery and NDVI Thresholds for the Development of Crop Phenology: A Case Study of Sahiwal District. The Pakistan Journal of Agricultural Sciences. https://doi.org/10.21162/pakjas/23.970

Shoko, C., Dube, T., Sibanda, M., and Gumindoga, W. (2015). In-depth analysis of the impacts of rural population growth on the natural environment: A GIS and remote sensing approach. *Transactions of the Royal Society of South Africa*, *70*(2), 149–153. https://doi.org/10.1080/0035919X.2015.1014877

Shu, M., Shen, M., Zuo, J., Yin, P., Wang, M., Xie, Z., Tang, J., Wang, R., Li, B., Yang, X., and Ma, Y. (2021). The application of UAV-based hyperspectral imaging to estimate crop traits in Maize inbred lines. *Plant Phenomics*, *2021*. https://doi.org/10.34133/2021/9890745

Sibanda, M., and Murwira, A. (2012). The use of multi-temporal MODIS images with ground data to distinguish cotton from maize and sorghum fields in smallholder agricultural landscapes of Southern Africa. *International Journal of Remote Sensing*, *33*(16), 4841–4855. https://doi.org/10.1080/01431161.2011.635715

Silva, G. F., Carneiro, G. B., Doth, R., Amaral, L. A., and Azevedo, D. F. G. De. (2018). Near real-time shadow detection and removal in aerial motion imagery application. *Journal of Photogrammetry and Remote Sensing*, *140*, 104–121. https://doi.org/10.1016/j.isprsjprs.2017.11.005

Singh, P., Srivastava, P. K., Shah, D., Pandey, M. K., and ... (2022). Crop type discrimination using Geo-Stat Endmember extraction and machine learning algorithms. *Advances in Space ...*, *73*(2), 1331–1348. https://doi.org/10.1016/j.asr.2022.08.031.Crop

Sishodia, R. P., Ray, R. L., and Singh, S. K. (2020). Applications of remote sensing in precision agriculture: A review. *Remote Sensing*, *12*(19), 1–31. https://doi.org/10.3390/rs12193136

Slingerland, M. (2000). *Mixed farming: scope and constraints in West African Savanna*.

Smith, A. M., & Blackshaw, R. E. (2017). Weed : Crop Discrimination Using Remote Sensing : A Detached Leaf Experiment Author ( s ): Anne M . Smith and Robert E . Blackshaw Published by : Weed Science Society of America and Allen Press Stable URL : http://www.jstor.org/stable/3989767 REFERENCES L. 17(4), 811–820.

Sodjinou, S. G., Mohammadi, V., Sanda Mahama, A. T., and Gouton, P. (2022). A deep semantic segmentation-based algorithm to segment crops and weeds in agronomic color images. *Information Processing in Agriculture*, *9*(3), 355–364. https://doi.org/10.1016/j.inpa.2021.08.003

Soria-Ruiz, J., and Fernandez-Ordonez, Y. M. (2017). Crop discrimination using remote sensing data in a region of high marginalization. *International Geoscience and Remote Sensing Symposium (IGARSS)*, *2017-July*(August), 3031–3034. https://doi.org/10.1109/IGARSS.2017.8127637

Stehr, N. J. (2015). Drones: The newest technology for precision agriculture. Natural Sciences Education, 44(1), 89–91

Stewart, E. L., Wiesner-Hanks, T., Kaczmar, N., DeChant, C., Wu, H., Lipson, H., Nelson, R. J., and Gore, M. A. (2019). Quantitative Phenotyping of Northern Leaf Blight in UAV Images

Using Deep Learning. *REMOTE SENSING*, *11*(19). https://doi.org/10.3390/rs11192209 WE - Science Citation Index Expanded (SCI-EXPANDED)

Stombaugh, T., Smith, S., and Thamann, M. (2017). The use of unmanned aircraft systems in agriculture. *Biosystems and Agricultural Engineering Update*, 1–6.

Stutsel, B., Johansen, K., Malbéteau, Y. M., and McCabe, M. F. (2021). Detecting Plant Stress Using Thermal and Optical Imagery From an Unoccupied Aerial Vehicle. *Frontiers in Plant Science*, *12*(October). https://doi.org/10.3389/fpls.2021.734944

Swain, K. C., Jayasuriya, H. P. W., and Salokhe, V. M. (2007). *Low-Altitude Remote Sensing with Unmanned Radio-Controlled Helicopter Platforms : A Potential Substitution to Satellite-based Systems for Precision Agriculture Adoption under Farming Conditions in Developing Countries*. *IX*(12), 1–16.

Sykas, D., Karathanassi, V., and Fountas, S. (2013). *A new methodology for the discrimination of plant species and their varieties using hyperspectral data: application on vetch and lentil*. *January 2014*, 879520. https://doi.org/10.1117/12.2027503

T. Ngongoni, N., Mapiye, C., Mwale, M., Mupeta, B., and Chimonyo, M. (2007). Potential of farm-produced crop residues as protein sources for small-medium yielding dairy cows. In *African Journal of Agricultural Research* (Vol. 2).

Tan, S., Liu, J., Lu, H., Lan, M., Yu, J., Liao, G., Wang, Y., Li, Z., Qi, L., and Ma, X. (2022). Machine Learning Approaches for Rice Seedling Growth Stages Detection. *Frontiers in Plant Science*, *13*(June), 1–15. https://doi.org/10.3389/fpls.2022.914771

Tan, Y., Gu, J., Lu, L., Zhang, L., Huang, J., Pan, L., Lv, Y., Wang, Y., and Chen, Y. (2025). Hyperspectral Band Selection for Crop Identification and Mapping of Agriculture. *Remote Sensing*, *17*(4). https://doi.org/10.3390/rs17040663

Tian, S., Lu, Q., and Wei, L. (2022). Multiscale Superpixel-Based Fine Classification of Crops in the UAV-Manned Hyperspectral Imagery. *Remote Sensing*, *14*(14), 0–21. https://doi.org/10.3390/rs14143292

Tian, Y., Yao, X., Yang, J., Cao, W., and Zhu, Y. (2011). Extracting Red Edge Position Parameters from Ground- and Space-Based Hyperspectral Data for Estimation of Canopy Leaf Nitrogen Concentration in Rice. *Plant Production Science*, *14*(3), 270–281. https://doi.org/10.1626/pps.14.270

Tikkiwal, G. C., and Khandelwal, A. (2012). Crop Acreage and Crop Production Estimates for Small Domains - Revisited. *Statistics in Transition*, *13*(1), 47–64.

Tripicchio, P., Satler, M., Dabisias, G., Ruffaldi, E., and Avizzano, C. A. (2015). Towards Smart Farming and Sustainable Agriculture with Drones. *Proceedings - 2015 International Conference on Intelligent Environments, IE 2015*, 140–143. https://doi.org/10.1109/IE.2015.29

Tsai, V. J. D. (2006). A comparative study on shadow compensation of color aerial images in invariant color models. *IEEE Transactions on Geoscience and Remote Sensing*, *44*(6), 1661–1671. https://doi.org/10.1109/TGRS.2006.869980

Tsoeleng, L. T., Odindi, J., and Mhangara, P. (2020). A comparison of two morphological techniques in the classification of urban land cover. *Remote Sensing*, *12*(7), 1–14. https://doi.org/10.3390/rs12071089

Tsouros, D. C., Bibi, S., and Sarigiannidis, P. G. (2019). A Review on UAV-Based Applications for Precision Agriculture †. *Mdpi*, *10*(349). https://doi.org/10.3390/info10110349

Ukaegbu, U. F., Tartibu, L. K., Okwu, M. O., and Olayode, I. O. (2021). Development of a Light-Weight Unmanned Aerial Vehicle for Precision Agriculture. *SENSORS*, *21*(13). https://doi.org/10.3390/s21134417 WE - Science Citation Index Expanded (SCI-EXPANDED)

Umamaheswari, S., and Jain, A. V. (2020). Encoder–Decoder Architecture for Crop-Weed Classification Using Pixel-Wise Labelling. *2020 International Conference on Artificial Intelligence and Signal Processing (AISP)*, 1–6.

UN, G. A. (1948). *Universal Declaration of Human Rights*. 217 A (III).

Vaiphasa, C., Skidmore, A. K., de Boer, W. F., and Vaiphasa, T. (2007). A hyperspectral band selector for plant species discrimination. *ISPRS Journal of Photogrammetry and Remote Sensing*, *62*(3), 225–235. https://doi.org/10.1016/j.isprsjprs.2007.05.006

Van De Vijver, R., Mertens, K., Heungens, K., Nuyttens, D., Wieme, J., Maes, W. H., Van Beek, J., Somers, B., and Saeys, W. (2022). Ultra-High-Resolution UAV-Based Detection of Alternaria solani Infections in Potato Fields. *Remote Sensing*, *14*(24). https://doi.org/10.3390/rs14246232

van der Merwe, D., Burchfield, D. R., Witt, T. D., Price, K. P., and Sharda, A. (2020). Drones in agriculture. *Advances in Agronomy*, *162*, 1–30. https://doi.org/10.1016/bs.agron.2020.03.001

van Tulder, M., Furlan, A., Bombardier, C., and Bouter, L. (2003). Updated Method Guidelines for Systematic Reviews in the Cochrane Collaboration Back Review Group. *Spine*, *28*(12), 1290–1299. https://doi.org/10.1097/01.brs.0000065484.95996.af

Varela, S., Dhodda, P. R., Hsu, W. H., Prasad, P. V, Assefa, Y., Peralta, N. R., Griffin, T., Sharda, A., Ferguson, A., and Ciampitti, I. A. (2018). Early-season stand count determination in Corn via integration of imagery from unmanned aerial systems (UAS) and supervised learning techniques. *Remote Sensing*, *10*(2), 343.

Vélez, S., Poblete-Echeverría, C., Rubio, J. A., Vacas, R., and Barajas, E. (2021). Estimation of leaf area index in vineyards by analysing projected shadows using uav imagery. *Oeno One*, *55*(4), 159–180. https://doi.org/10.20870/oeno-one.2021.55.4.4639

Velichko, A., Belyaev, M., Wagner, M. P., and Taravat, A. (2022). Entropy Approximation by Machine Learning Regression : Application for Irregularity Evaluation of Images in Remote Sensing. *Remote Sensing*, *14*(5983), 1–25.

Verrelst, J., Romijn, E., and Kooistra, L. (2012). Mapping vegetation density in a heterogeneous river floodplain ecosystem using pointable CHRIS/PROBA data. *Remote Sensing*, *4*(9), 2866–2889. https://doi.org/10.3390/rs4092866

Wagner, M. P., and Oppelt, N. (2020). Extracting Agricultural Fields From Remote Sensing Imagery Using Graph-Based Growing Contours. *Remote Sensing*. https://doi.org/10.3390/rs12071205

Wahab, I., Hall, O., and Jirström, M. (2018a). Remote sensing of yields: Application of uav imagery-derived ndvi for estimating maize vigor and yields in complex farming systems in sub-saharan africa. *Drones*, *2*(3), 28. https://doi.org/10.3390/drones2030028

Wahab, I., Hall, O., and Jirström, M. (2018b). Remote sensing of yields: Application of UAV imagery-derived ndvi for estimating maize vigor and yields in complex farming systems in Sub-Saharan Africa. *Drones*, *2*(3), 1–16. https://doi.org/10.3390/drones2030028

Wang, H., Lyu, S., and Ren, Y. (2021). Paddy rice imagery dataset for panicle segmentation. *Agronomy*, *11*(8). https://doi.org/10.3390/agronomy11081542

Wang, J., Zheng, Y., Wang, M., Shen, Q., and Huang, J. (2021). Object-Scale Adaptive Convolutional Neural Networks for High-Spatial Resolution Remote Sensing Image Classification. *Ieee Journal of Selected Topics in Applied Earth Observations and Remote Sensing*. https://doi.org/10.1109/jstars.2020.3041859

Wang, Y.-P., Chang, Y.-C., and Shen, Y. (2022). Estimation of nitrogen status of paddy rice at vegetative phase using unmanned aerial vehicle based multispectral imagery. *Precision Agriculture*, *23*(1). https://doi.org/10.1007/s11119-021-09823-w

Wang, Z., Nie, C., Wang, H., Ao, Y., Jin, X., Yu, X., Bai, Y., Liu, Y., Shao, M., Cheng, M., Liu, S., Wang, S., and Tuohuti, N. (2021). Detection and analysis of degree of maize lodging using uav-rgb image multi-feature factors and various classification methods. *ISPRS International Journal of Geo-Information*, *10*(5). https://doi.org/10.3390/ijgi10050309

Wang, Z., Zhao, Z., and Yin, C. (2022). Fine Crop Classification Based on UAV Hyperspectral Images and Random Forest. *ISPRS International Journal of Geo-Information*, *11*(4). https://doi.org/10.3390/ijgi11040252

Watts, A. C., Ambrosia, V. G., and Hinkley, E. A. (2012). Unmanned aircraft systems in remote sensing and scientific research: Classification and considerations of use. *Remote Sensing*, *4*(6), 1671–1692. https://doi.org/10.3390/rs4061671

Weiner, D. (2003). Community-integrated GIS for land reform in South Africa. *URISA Journal*, *15*, 61–73.

Woebbecke, D. M., Meyer, G. E., Von Bargen, K., and Mortensen, D. A. (1995). Color indices for weed identification under various soil, residue, and lighting conditions. *Transactions of the American Society of Agricultural Engineers*, *38*(1), 259–269.

Wolmer, W., and Scoones, I. (2000). The Royal African Society The Science of ’ Civilized ’ Agriculture : The Mixed Farming Discourse in Zimbabwe Author ( s ): William Wolmer and Ian Scoones Source : African Affairs , Vol . 99 , No . 397 ( Oct ., 2000 ), pp . 575-600 Published by : Oxford Un. *African Affairs*, *99*(397), 575–600.

Wulder, M. A., White, J. C., Coops, N. C., and Ortlepp, S. (2009). Remote Sensing for Studies of Vegetation Condition: Theory and Application. In T. A. Warner, M. D. Nellis, and G. M. Foody (Eds.), *The SAGE Handbook of Remote Sensing* (pp. 357–367). Sage Press, SAGE Publications Limited, London, United Kingdom, 504p. https://doi.org/10.4135/9780857021052

Xia, F., Quan, L., Lou, Z., Sun, D., Li, H., and Lv, X. (2022). Identification and Comprehensive Evaluation of Resistant Weeds Using Unmanned Aerial Vehicle-Based Multispectral Imagery. *Frontiers in Plant Science*, *13*. https://doi.org/10.3389/fpls.2022.938604

Yadav, A., Thakur, U., Saxena, R., Pal, V., Bhateja, V., and Lin, J. C.-W. (2022). AFD-Net: Apple Foliar Disease Multi Classification Using Deep Learning on Plant Pathology Dataset. *Plant and Soil*. https://doi.org/10.1007/s11104-022-05407-3

Yang, B., Hawthorne, T. L., Torres, H., and Feinman, M. (2019). Using Object-Oriented Classification for Coastal Management in the East Central Coast of Florida: A Quantitative Comparison between UAV, Satellite, and Aerial Data. *Drones*, *3*(3), 60. https://doi.org/10.3390/drones3030060

Yang, G., Liu, J., Zhao, C., Li, Z., Huang, Y., Yu, H., Xu, B., Yang, X., Zhu, D., Zhang, X., Zhang, R., Feng, H., Zhao, X., Li, Z., Li, H., and Yang, H. (2017). Unmanned aerial vehicle remote sensing for field-based crop phenotyping: Current status and perspectives. *Frontiers in Plant Science*, *8*, 1111. https://doi.org/10.3389/fpls.2017.01111

Yang, M.-D., Huang, K.-S., Kuo, Y.-H., Tsai, H. P., and Lin, L.-M. (2017). Spatial and spectral hybrid image classification for rice lodging assessment through UAV imagery. *Remote Sensing*, *9*(6). https://doi.org/10.3390/rs9060583

Yinka-Banjo, C., and Ajayi, O. (2020). Sky-Farmers: Applications of Unmanned Aerial Vehicles (UAV) in Agriculture. In *Autonomous Vehicles*. https://doi.org/10.5772/intechopen.89488

Yong, L., Tao, C., Yan, Z., Yongchao, T., Weixing, C., Xia, Y., Ni, W., Zheng, H., Zhou, X., Cheng, T., Yao, X., Tian, Y., Cao, W., and Zhu, Y. (2016). Comparative analysis of vegetation indices , non-parametric and physical retrieval methods for monitoring nitrogen in wheat using UAV-based multispectral imagery Yong Liu , Tao Cheng , Yan Zhu , Yongchao Tian , Weixing Cao , Xia Yao *, Ni Wang National En. *2016 IEEE International Geoscience and Remote Sensing Symposium (IGARSS)*, 7350–7353. https://doi.org/doi: 10.1109/IGARSS.2016.7730920

Zhang, H., Wang, Y., Shang, J., Liu, M., and Li, Q. (2021). Investigating the impact of classification features and classifiers on crop mapping performance in heterogeneous agricultural landscapes. *International Journal of Applied Earth Observation and Geoinformation*, *102*(May), 102388. https://doi.org/10.1016/j.jag.2021.102388

Zhang, J., Li, Y., Wan, G., Jiang, M., Huang, Z., Tao, X., Chen, J., and Chu, D. (2023). Small Target Detection Algorithm for UAV Based on Improved YOLOv5. *2023 8th International Conference on Signal and Image Processing, ICSIP 2023*, 78–82. https://doi.org/10.1109/ICSIP57908.2023.10270991

Zhang, L., Zhang, L., and Du, B. (2016). Deep learning for remote sensing data: A technical tutorial on the state of the art. *IEEE Geoscience and Remote Sensing Magazine*, *4*(2), 22–40. https://doi.org/10.1109/MGRS.2016.2540798

Zhang, W., Li, W., Wang, C., Yu, Q., Tang, H., and Wu, W. (2025). A novel index for mapping crop residue covered cropland using remote sensing data. *Computers and Electronics in Agriculture*, *231*(December 2024). https://doi.org/10.1016/j.compag.2025.109995

Zhao, L., Shi, Y., Liu, B., Hovis, C., Duan, Y., and Shi, Z. (2019). Finer classification of crops by fusing UAV images and sentinel-2A data. *Remote Sensing*, *11*(24). https://doi.org/10.3390/rs11243012

Zheng, H., Zhou, X., Cheng, T., Yao, X., Tian, Y., Cao, W., and Zhu, Y. (2016). Evaluation of a UAV-based hyperspectral frame camera for monitoring the leaf nitrogen concentration in rice. *2016 IEEE International Geoscience and Remote Sensing Symposium (IGARSS)*, 7350–7353.

Zhong, L. (2012). *Efficient crop type mapping based on remote sensing in the Central Valley, California*. University of California, Berkeley.

Zhu, C., Ding, J., Zhang, Z., Wang, J., Wang, Z., Chen, X., and Wang, J. (2022). SPAD monitoring of saline vegetation based on Gaussian mixture model and UAV hyperspectral image feature classification. *Computers and Electronics in Agriculture*, *200*(May), 107236. https://doi.org/10.1016/j.compag.2022.107236

Zigh, E., Belbachir, M. F., Kadiri, M., Djebbouri, M., and Kouninef, B. (2016). New shadow detection and removal approach to improve neural stereo correspondence of dense urban VHR remote sensing images. *European Journal of Remote Sensing*, *48*, 447–463. https://doi.org/10.5721/EuJRS2015482